



*Università degli Studi della Basilicata*  
*Scuola di Ingegneria*

Dottorato di Ricerca in  
Ingegneria per l'Innovazione e lo Sviluppo Sostenibile

***Exposure modelling and loss estimation  
for seismic risk assessment of residential buildings:  
innovative methods and applications***

Settori Scientifico-Disciplinari  
ICAR/09 - FIS/06

**Coordinatore del Dottorato**

Prof. Carmine Serio

**Relatore**

Prof. Angelo Masi

**Correlatori**

Dr. Massimiliano Pittore

Dr. Vincenzo Manfredi

**Dottorando**

Giuseppe Nicodemo

## PREFACE

The thesis is focused on some research activities developed during the three years of my PhD course attended at the School of Engineering of the University of Basilicata (Potenza, Italy). Main goal was the definition of new procedures aimed at supporting seismic risk assessment and reduction.

This thesis would have been impossible without the scholarship provided by the Basilicata region in the framework of the “agreement between the Basilicata region and the School of Engineering of the University of Basilicata for financing PhD scholarships on topics related to industrial development strategy (Industry 4.0)”. The results of the thesis contributed also to the achievement of the goals of ReLUIS-DPC 2019-2021 project funded by the Italian Department of Civil Protection (DPC). These supports are gratefully acknowledged.

Part of the content of this thesis has been already published on research journals, as reported in the following list.

- Masi A., Chiauzzi L., Nicodemo G., Manfredi V., 2020. *Correlations between macroseismic intensity estimations and ground motion measures of seismic events*. Bulletin of Earthquake Engineering, 18, 1899–1932 (2020). DOI 10.1007/s10518-019-00782-2
- Nicodemo G., Pittore M., Masi A., Manfredi V., 2020. *Modelling exposure and vulnerability from post-earthquake survey data with risk-oriented taxonomies: AeDES form, GEM taxonomy and EMS-98 typologies*. International Journal of Disaster Risk Reduction, 50, 101894. doi.org/10.1016/j.ijdr.2020.101894
- Masi A., Manfredi V., Nicodemo G., 2020. *Seismic rehabilitation of residential buildings: an action plan for the urban centers in Val d’Agri, Italy*. Bollettino di Geofisica Teorica ed Applicata (An International Journal of Earth Sciences). DOI 10.4430/bgta0333

## ACKNOWLEDGEMENTS

I would like to express deep gratitude to my tutor, Prof. Angelo Masi, for his advice and time. He taught me how hard work and critical thinking can make the difference in the research world.

I am very grateful to Dr. Massimiliano Pittore for his hospitality and scientific support during and after the activities at the GeoForschungsZentrum (GFZ).

I express my thanks to Dr. Iole Paradiso of the TeRN (Tecnologie per le Osservazioni della Terra e i Rischi Naturali) consortium for her availability and assistance.

Thanks to Dr. Vincenzo Manfredi for his significant support to the activities carried out in the three years of PhD course and for offering me precious suggestions.

Thanks also to all the research team members (Dr. Giuseppe Ventura, Dr. Andrea Digrisolo, Dr. Giuseppe Santarsiero); in these years, they often provided, in different ways, support and contribution to my research activities.

Finally, a very special acknowledgment to my family and Rossella for their patience, support and encouragement, without which I would not reach this objective.

Potenza, January 2021

Giuseppe Nicodemo

## ABSTRACT

Defining the seismic hazard, assessing the vulnerability of the main components of the built environment and, consequently, estimating the expected losses are key steps for setting up effective post-event emergency plans as well as medium-long term mitigation strategies. Despite the significant knowledge advancements achieved in the last years, several points need to be further developed. Among them the collection of reliable building inventories, the selection of appropriate measures of seismic intensity and the definition of accurate loss estimation models still propose some challenges for the scientific community.

The present PhD thesis aims at providing a contribution in this direction. After a comprehensive state of the art on seismic risk components along with a literature review focused on the main models to estimate the expected seismic losses, some new procedures related to hazard, exposure and loss estimation, have been proposed and applied.

Firstly, a model aimed at estimating the direct economic losses (i.e., building repair costs) has been developed by improving the models currently available in the literature. These models generally account for only the severity of damage (i.e., the maximum damage level), while damage extension and distribution, especially along the building height, are implicitly considered in the repair cost values. If on the one side, the assessment of safety condition depends essentially on damage severity, on the other side, damage extension strongly affects the estimation of economic impact. In this regard, the proposed model allows to explicitly consider both damage severity and distribution along the building height. The model is applicable to both Reinforced Concrete (RC) and masonry building types. It requires the determination of the more frequent damage distributions throughout the building height. At the current state, the procedure has been specifically implemented for existing Reinforced Concrete (RC) building types by performing Non-Linear Dynamic Analyses (NLDAs).

As for seismic hazard, correlations between macroseismic intensities and ground motion parameters have been derived processing data related to Italian earthquakes occurred in the last 40 years. Peak Ground Acceleration (PGA), Peak Ground Velocity (PGV) and Housner Intensity ( $I_H$ ) as instrumental measures, and European Macroseismic Scale (EMS-98) and Mercalli-Cancani-Sieberg (MCS) as macroseismic measures, have been considered. The correlations can be used both to adopt empirical damage estimation methods (e.g., Damage Probability Matrices) and to convert the macroseismic data of historical earthquakes into instrumental intensity values, more suitable to risk analyses and design practice.

Concerning exposure, an innovative methodology has been developed to convert the information on the typological characteristics collected through the AeDES form (currently used in Italy in post-



earthquake usability surveys) to recognized international standards such as the taxonomy proposed by the Global Earthquake Model (GEM) and the EMS-98 building types. The methodology allows to fully exploit the exposure and vulnerability data of post-earthquake surveys related to the Italian built environment and to define an exposure model in terms of risk-oriented classes more suitable for large-scale risk assessments.

Furthermore, an approach based on the integration of data collected with the CARTIS procedure (i.e., a protocol used in Italy for the typological-structural characterization of buildings at regional scale) and using the RRVS web-based platform (i.e., for a remote visual screening based on satellite images) has been proposed and specifically applied to the village of Calvello (Basilicata region, Southern Italy). This approach represents a useful tool for compiling residential building inventories in a quick and inexpensive way thus being very suitable in data-poor and economically developing countries.

To better illustrate the proposed methodological developments, some applications are provided in the last part of the thesis. The first one proposes a comparison among the results obtained applying some casualty estimation models available in the literature using the vulnerability and damage data collected in the L'Aquila urban area after the 2009 earthquake (data available on the Observed Damage Database Da.D.O. platform). After, by using the same data source, an exposure model in terms of EMS-98 types based on the 2009 post-earthquake data has been implemented for the residential buildings of L'Aquila town and the surrounding municipalities involved in the usability assessment surveys.

The third - expansive - application deals with the seismic risk assessment of the Val d'Agri area (Basilicata region, Southern Italy). This area has a strategic role for Italy due to the large quantities of oil extracted from local deposits, making available large resources deriving from royalties. Specifically, earthquake damage scenarios for the residential building stock of 19 villages have been prepared. Considering a seismic vulnerability distribution obtained from the integration of a building-by-building inventory and information collected with the CARTIS and RRVS approaches, the expected losses deriving from a seismic event with an exceedance probability of 10% in 50 years (475 years return period) have been determined. Finally, an action plan for the seismic risk mitigation, essentially based on the reduction of vulnerability of the building stock through a structural strengthening program, has been proposed and specifically applied to one of the villages in the area under study.

**Keywords** residential buildings, risk assessment, seismic hazard, exposure modelling, loss estimation

# TABLE OF CONTENTS

PREFACE .....	i
ACKNOWLEDGEMENTS .....	ii
ABSTRACT .....	iii
TABLE OF CONTENTS .....	v
LIST OF FIGURES .....	viii
LIST OF TABLES .....	xii
<b>Introduction .....</b>	<b>1</b>
<b>CHAPTER I</b>	
<b>Overview of seismic risk components.....</b>	<b>8</b>
Introduction .....	8
1.1 Seismic risk .....	9
1.2 Hazard component.....	11
1.3 Exposure component.....	17
1.4 Vulnerability component.....	22
References .....	26
<b>CHAPTER II</b>	
<b>Loss estimation models: literature review .....</b>	<b>31</b>
Introduction .....	31
2.1 Casualties .....	32
2.2 Direct economic losses.....	46
2.3 Unusability .....	55
References .....	60
<b>CHAPTER III</b>	
<b>Direct economic losses: a new model based on damage distribution .....</b>	<b>64</b>
Introduction .....	64
3.1 Background of economic loss models.....	65
3.2 Proposed model.....	66
3.3 Implementation for Reinforced Concrete building type .....	69
3.3.1 Description and modelling of building type.....	69
3.3.2 Damage combinations .....	71
3.3.3 Storey repair costs .....	76

3.3.4 Estimation of building repair cost and comparison with NRA-2018 values.....	81
Discussion .....	82
References .....	83

## CHAPTER IV

<b>Correlations between macroseismic and instrumental measures of seismic intensity.....</b>	<b>85</b>
Introduction .....	85
4.1 On the relationships available in literature.....	86
4.2 Methodology .....	88
4.2.1 Database .....	89
4.3 Proposed correlations .....	95
4.3.1 Direct relationships .....	95
4.3.2 Inverse relationships.....	102
4.4 Analysis of the proposed relationships.....	105
4.4.1 Comparison with other studies .....	106
Discussion .....	110
References .....	111

## CHAPTER V

<b>Building exposure modelling: definition of innovative approaches.....</b>	<b>113</b>
Introduction .....	113
5.1 Evaluation of exposure and vulnerability from post-earthquake data.....	114
5.1.1 Taxonomy description.....	116
5.1.1.1 AeDES form.....	116
5.1.1.2 GEM taxonomy.....	118
5.1.1.3 EMS-98 scale.....	119
5.1.2 Methodology .....	121
5.1.2.1 From AeDES form to GEM taxonomy.....	121
5.1.2.2 From GEM taxonomy to EMS-98 building types .....	123
5.2 An integrated approach for collecting exposure data of residential buildings.....	128
5.2.1 Methods .....	129
5.2.1.1 CARTIS format .....	129
5.2.1.2 RRVS platform.....	130
5.2.2 Implementation on the Calvello village .....	132
5.2.2.1 Analysis of the results and comparison with ISTAT data.....	137
Discussion .....	139
References .....	140

## **CHAPTER VI**

<b>Seismic risk assessment and reduction: applications.....</b>	<b>142</b>
Introduction .....	142
6.1 Comparison among casualty estimation models available in literature .....	143
6.2 Modelling exposure from the 2009 L’Aquila post-earthquake dataset.....	149
6.3 Seismic risk assessment and mitigation of the Val d’Agri area.....	156
6.3.1 Vulnerability assessment.....	157
6.3.2 Hazard analysis .....	161
6.3.3 Damage and loss assessment.....	164
6.3.4 Estimation of seismic strengthening costs.....	169
6.3.5 An application of mitigation strategy: the action plan for Viggiano village.....	172
6.3.6 Discussion .....	177
References .....	178

## **CHAPTER VII**

<b>Final remarks and future developments .....</b>	<b>181</b>
--	------------

APPENDIX .....	184
----------------	-----

# LIST OF FIGURES

## CHAPTER I

**Figure 1.1** Elements contributing to earthquake loss (Khater et al., 2003)

**Figure 1.2** Earthquake loss estimation methodology (HAZUS methodology)

**Figure 1.3** Comparison between macroseismic intensity scales (from Elnashai & Di Sarno, 2008)

**Figure 1.4** Hazard map of Italy: Peak Ground Acceleration (PGA) values (as a fraction of the gravity acceleration  $g$ ) with a 10% probability of exceedance in 50 years (475 years return period)

**Figure 1.5** Main tasks and related methodologies relevant for a global assessment of exposed assets (from Pittore et al., 2016)

**Figure 1.6** Example of fragility curve relevant to pre-1971 RC buildings (2 storeys-BF) developed in Masi et al. (2015)

## CHAPTER II

**Figure 2.1** M-parameters used in the estimation of the human casualties (Coburn and Spence, 2002)

**Figure 2.2** The average percentage of occupants trapped by collapse, M3 (Coburn and Spence, 2002)

**Figure 2.3** Injury distribution at the collapse, M4 (Coburn and Spence, 2002)

**Figure 2.4** The mortality post-collapse, M5 (Coburn and Spence, 2002)

**Figure 2.5** Modelling injury distributions within each damage state (Spence, 2007)

**Figure 2.6** Casualty rates for damage state D5 developed within LESSLOSS Project (Spence, 2007)

**Figure 2.7** Description of injury severity levels (HAZUS methodology)

**Figure 2.8** Event tree used for the estimation of casualties (HAZUS methodology)

**Figure 2.9** Default relationships for estimating population distribution (HAZUS methodology)

**Figure 2.10** a) Empirical fatality rates for Italy; b) Estimated and catalog recorded fatalities for Italy (Jaiswal and Wald, 2010)

**Figure 2.11** Building-Casualty Superclasses (SYNER-G project)

**Figure 2.12** Logic tree for calculation of direct economic losses (Kircher et al., 1997)

**Figure 2.13** Structural repair cost ratios in % of building replacement cost (HAZUS methodology)

**Figure 2.14** a) Fragility functions, b) consequence functions of a typical gypsum wall board (GWB) partition component (ATC-58 2012)

**Figure 2.15** a) Economic loss ratio for Italy; b) Estimated and catalog recorded historical earthquake losses (Jaiswal and Wald, 2011)

**Figure 2.16** Cumulative density function CDF of the relative repair cost (Dolce et al., 2006)

## CHAPTER III

**Figure 3.1.** Example of a damage combination for RC building with  $N_s=4$  and  $L_{dmax}=3$

**Figure 3.2** Floor plan (a) and three-dimensional view (b) of the building type with 4 storeys (from Ricci et al., 2019a)

**Figure 3.3.** Number of RC buildings (on the left) and DRCs (on the right) as a function of number of storeys for with usability rating B or C (in light grey) and E (in dark grey)

**Figure 3.4.** Best-fit linear regression between the direct repair cost of RC buildings (€/m<sup>2</sup>) and number of storeys for each damage level (Ld0, Ld1, Ld2, Ld3 and Ld4)

**Figure 3.5.** Comparison between the proposed building repair costs and the values adopted in the NRA (2018)

## CHAPTER IV

**Figure 4.1** Epicentral area of the selected earthquakes.

**Figure 4.2** Histogram of the selected earthquakes grouped according to local magnitude,  $M_l$  (on the left) with relative normal distribution. Magnitude versus distance, considering the Joyner Boore distance,  $R_{jb}$  (on the right). The  $R_{jb}$  distance axis is in logarithmic scale.

**Figure 4.3** Distribution of strong-motion data in terms of EMS-98 intensities (d) and the corresponding instrumental values PGA (a), PGV, (b) and  $I_H$  (c).

**Figure 4.4** Distribution of strong-motion data in terms of MCS intensities (d) and the corresponding instrumental values PGA (a), PGV, (b) and  $I_H$  (c).

**Figure 4.5** a) Best-fit linear regression between the MCS and EMS-98 values considering the areas in which both macroseismic values are available. The size of the circles is proportional to the number of data. b) Residual values obtained from the considered MCS data with respect to the linear regression reported in a)

**Figure 4.6** EMS-98 intensities versus the natural logarithm of PGA (a), PGV (b) and  $I_H$  (c) values. Single function (SF, dash-dot line), bilinear function (BF, L1 dashed line, L2 solid line) and the associated +/- one standard deviation (dotted lines) are also shown.

**Figure 4.7** Distribution of the correlation coefficients for PGA (a), PGV (b) and  $I_H$  (c) samples

**Figure 4.8** Macroseismic intensity (according to the EMS-98 scale) with respect to PGA (a), PGV (b) and  $I_H$  (c) values. The horizontal axis is in logarithmic scale.

**Figure 4.9** MCS intensities versus the natural logarithm of PGA (a), PGV (b) and  $I_H$  (c) values. Single function (SF, dash-dot line), bilinear function (BF, L1 dashed line, L2 solid line) and the associated +/- one standard deviation (dotted lines) are also shown

**Figure 4.10** Distribution of the correlation coefficients for PGA (a), PGV (b) and  $I_H$  (c) samples.

**Figure 4.11** Macroseismic intensity (according to the MCS scale) with respect to PGA (a), PGV (b) and  $I_H$  (c) values. The horizontal axis is in logarithmic scale

**Figure 4.12** Comparison between the proposed relationship between MCS intensity and PGA with the regressions of Faccioli & Cauzzi (2006) and Faenza & Michellini (2010). The PGA axes is in logarithmic scale

**Figure 4.13** Damage distribution for vulnerability class A according to DPMs defined by Zuccaro et al. (2000)

**Figure 4.14** Comparison between the proposed (inverse) relationship between PGA and MCS intensity with the regressions of Margottini et al. (1992), Faccioli & Cauzzi (2006) and Faenza & Michelini (2010). The PGA axes is in logarithmic scale.

## CHAPTER V

**Figure 5.1** Section 3 - Building typology of AeDES form

**Figure 5.2** Graphical representation of the class definitions for the EMS-98 scheme

**Figure 5.3** Section “0” of CARTIS form-Identification of the Town under study and the Town Compartments (TCs)

**Figure 5.4** Example of a building remotely inspected using the RRVs platform

**Figure 5.5** Territorial framework of Val d’Agri area (up) and built environment (down) of Calvello village

**Figure 5.6** Individuation of TCs for Calvello village

**Figure 5.7** Spatial distribution of the building stock of Calvello village in terms of building typology (a) and in terms of number of storeys (b)

**Figure 5.8** Overlapping of the Town Compartments (TCs) and Census sections (ISTAT 2011) of the urban area of Calvello village

## CHAPTER VI

**Figure 6.1** Distribution of the building stock of L’Aquila urban area in terms of building typologies (on the left) and in terms of vulnerability classes (on the right)

**Figure 6.2** Damage distribution in terms of EMS-98 levels for the building stock of L’Aquila urban area

**Figure 6.3** Distribution in terms of number of storeys for masonry and RC buildings of L’Aquila urban area

**Figure 6.4** Occupancy at time of earthquake (from Coburn and Spence, 2002)

**Figure 6.5** Comparison among the CEMs on the 2009 post-earthquake data of L’Aquila urban area

**Figure 6.6** Fatality rates (on the left) and number of casualties as a function of damage levels and building type (on the right) for NRA (2018) and Zuccaro and Cacace (2011) models

**Figure 6.7** Weight of the occupancy at time of earthquake on the casualty estimation

**Figure 6.8** Area stricken by 2009 L’Aquila earthquake with MCS macroseismic intensity values (on the left) and distribution of the buildings in terms of structural typology (on the right)

**Figure 6.9** Fuzzy compatibility scores of the observed building (see Table 6.3) with respect to the EMS-98 scheme. The solid and dashed segment represent the equivalent defuzzified values according to the mode, median or mean value of the TFNs.

**Figure 6.10** Exposure model using EMS-98 class definition schema

**Figure 6.11** Spatial distribution of EMS-98 building types: MAS1 (in red), RC2 (in blue), MAS3 (in green) and MAS5 (in purple). The colormap describes the number of surveyed buildings.

**Figure 6.12** Damage distribution for the EMS-98 building typologies with MCS intensity values assigned after the L’Aquila earthquake

**Figure 6.13**  $DI_{med}$  values (calculated when the number of observations is greater than 270) for the most widespread EMS-98 types (MAS1, RC2, MAS3 and MAS5) considering MCS intensity values. The EMS-98 building types are reported in decreasing order of seismic vulnerability (from MAS1 to RC2).

**Figure 6.14** On the left: map of the Agri valley area displaying the villages surveyed. On the right: summary of surveyed data.

**Figure 6.15** Distribution of the vulnerability classes in terms of buildings' number (a) and volume (b) for each considered village and summary table for all the villages

**Figure 6.16** On the left: Basilicata region and the considered villages (yellow area). On the right: seismic hazard map of Basilicata region according to OPCM3519/2006 for an exceedance probability of 10% in 50 years, soil class A

**Figure 6.17** View of the Viggiano village and the corresponding seismic microzonation map. The most populated area is highlighted.

**Figure 6.18** Expected damage levels in terms of number (on the left) and volume (on the right) of buildings. The damage distribution has been split into RC (in yellow) and masonry/other type (in red) buildings

**Figure 6.19** Direct economic losses for each considered vulnerability class, computed for each village

**Figure 6.20** Usability rating of the buildings surveyed after the 2009 L'Aquila earthquake for all vulnerability classes (a) and only for "A" and "B" classes (b).

**Figure 6.21** Built environment of Viggiano village.

**Figure 6.22** Distribution of Viggiano building stock for each vulnerability class.

**Figure 6.23** PGA median values for Damage State 3 obtained from the fragility curves provided by Lagomarsino and Cattari (2014)

**Figure 6.24** Vulnerability and economic loss reduction as a result of the action plan proposed for Viggiano.



# LIST OF TABLES

## CHAPTER I

**Table 1.1** Data sources and related approaches for building inventory (from Polese et al., 2019)

**Table 1.2** Damage Probability Matrix for buildings of vulnerability class D (from Dolce et al., 2003)

## CHAPTER II

**Table 2.1** Lethality rates (L4, L5) at damage levels, D4 and D5, for all vulnerability classes (So and Spence, 2013)

**Table 2.2** Casualty rates for reinforced concrete moment frame structures (HAZUS-MH)

**Table 2.3** Casualty rates for unreinforced masonry structures (HAZUS-HM)

**Table 2.4** Casualty percentage by damage level and building type (Zuccaro and Cacace, 2011)

**Table 2.5** Casualty Ratios (SYNER-G project)

**Table 2.6** Casualty percentage for computation of human losses (NRA, 2018)

**Table 2.7** Direct economic loss as a percentage of building replacement cost by damage state (HAZUS methodology)

**Table 2.8** Loss ratio corresponding to each damage (NERIES project)

**Table 2.9** Cost parameters used for computation of direct economic losses (IRMA platform)

**Table 2.10** Default values (HAZUS methodology)

**Table 2.11** Percentage of unusable buildings as function of damage level and vulnerability class (Chiauzzi et al., 2018)

**Table 2.12** Percentage of unsafe buildings as a function of damage level (Zuccaro and Cacace, 2011)

**Table 2.13** Usability ratios (SYNER-G project)

**Table 2.14** Percentages of usable and unsafe buildings (NRA, 2018)

## CHAPTER III

**Table 3.1** Cost parameters used for computation of direct economic losses

**Table 3.2** Assignment of damage levels Lds (EMS 98) on the basis of drift values,  $\Delta/L$

**Table 3.3** Damage combinations and their relative frequencies obtained from NLDAs for RC buildings with  $L_{dmax}=1$  and  $N_s = 2$  (a),  $N_s = 4$  (b) and  $N_s = 6$  (c)

**Table 3.4** Damage combinations and their relative frequencies obtained from NLDAs for RC buildings with  $L_{dmax}=2$  and  $N_s = 2$  (a),  $N_s = 4$  (b) and  $N_s = 6$  (c)

**Table 3.5** Damage combinations and their relative frequencies obtained from NLDAs for RC buildings with  $L_{dmax}=3$  and  $N_s = 2$  (a),  $N_s = 4$  (b) and  $N_s = 6$  (c)

**Table 3.6** Damage combinations and their relative frequencies obtained from NLDAs for RC buildings with  $L_{dmax}=4$  and  $N_s = 2$  (a),  $N_s = 4$  (b) and  $N_s = 6$  (c)

**Table 3.7** Usability distribution (A, B+C and E) conditional upon EMS-98 damage levels

**Table 3.8** Median DRCs as function of  $L_d$ s and  $N_s$

**Table 3.9** Storey Repair cost

**Table 3.10** Building repair costs as function of  $L_d$ s for RC types with  $N_s=2,4$  and 6

## CHAPTER IV

**Table 4.1** Main parameters of the selected earthquakes

**Table 4.2** Statistics concerning instrumental (PGA, PGV and  $I_H$ ) and macroseismic (MCS and EMS-98) data.

**Table 4.3** Statistical results for the proposed relationships (Eqs 4.11 - 4.16) in terms of correlation coefficient  $R$ , Mean Squared Error (MSE) and standard deviation ( $\sigma$ ) of the residuals

**Table 4.4** Statistical results for the proposed relationships (Eqs 4.21 – 4.26) in terms of correlation coefficient  $R$ , Mean Squared Error (MSE) and standard deviation ( $\sigma$ ) of the residuals.

**Table 4.5** Statistical results for the proposed inverse relationships (Eqs 4.27 – 4.38) in terms of Mean Squared Error (MSE) and standard deviation ( $\sigma$ ) of the residuals.

**Table 4.6** Ranges of PGA, PGV and  $I_H$  for EMS-98 intensities

**Table 4.7** Ranges of PGA, PGV and  $I_H$  for MCS intensities

**Table 4.8** Correlations between instrumental parameters (PGA, PGV and  $I_H$ ) and macroseismic intensity scales (MCS and EMS-98).

**Table 4.9** Relationships considered in the comparisons

**Table 4.10** MCS intensities provided by the considered relationship for PGA equal to 0.1g

## CHAPTER V

**Table 5.1** Events, record and form versions reported in Da.D.O. web-based platform

**Table 5.2** Attributes of the GEM taxonomy

**Table 5.3** EMS-98 structural types and corresponding range of vulnerability classes: the most likely class in red; the probable range in orange and less probable range (exceptional cases) in yellow

**Table 5.4** Correspondence between AeDES and GEM attributes

**Table 5.5** Set of the fuzzy compatibility levels for the attribute values of two EMS-98 building typologies. All attribute values not explicitly considered have been assigned a neutral score. LLRS stands for Lateral Load Resisting System.

**Table 5.6** Description of the GEM attribute values shown in Table 5.5 (adapted from Brzev et al., 2013)

**Table 5.7** Main characteristics of the BTs related to each TC

**Table 5.8** Description of the structural characteristics of each BT in TC1 with the corresponding percentages

**Table 5.9** Description of the structural characteristics of each BT in TC2 with the corresponding percentages

**Table 5.10** Comparison among data collected with CARTIS format and RRVS platform

**Table 5.11** Distribution in terms of material type and number of storeys for the buildings located in the 4 census sections (ISTAT 2011) overlapping to Town Compartments (TCs)

## CHAPTER VI

**Table 6.1** Factors influencing the Casualty Estimation Models (CEMs)

**Table 6.2** Criteria to assign vulnerability classes (from Chiauzzi et al., 2012)

**Table 6.3** Example of conversion of the attributes of a building surveyed through the AeDES form (id = 100) with the corresponding GEM taxonomic description

**Table 6.4** Weighting for the EMS-98 building schema

**Table 6.5** PGA and PGV values related to MCS intensities assigned after the L'Aquila earthquake

**Table 6.6** Mean damage index ( $DI_{med}$ ) for the EMS-98 building typologies considering MCS intensity values assigned after L'Aquila earthquake. The number of buildings considered in the  $DI_{med}$  calculation has been reported in round brackets and the  $DI_{med}$  values evaluated with a buildings number less than 270 have been highlighted in red.

**Table 6.7** Distribution of the vulnerability classes in terms of buildings' number and volume for each considered village

**Table 6.8** Values of PGA and  $I_H$  for  $T_R=475$  years and class B-T1 obtained from the Italian seismic hazard map, and EMS-98 macroseismic intensities

**Table 6.9** Damage Probability Matrices for buildings of vulnerability classes A, B, C and D and macroseismic intensity equal to VII and VIII (adapted from Dolce et al., 2003)

**Table 6.10** Number and percentage of the expected unusable buildings and homeless for each vulnerability class. Results from damage scenarios in terms of both number and volume of buildings are reported. For unusable buildings, the percentage related to each vulnerability class ( $\%V_C$ ) has been reported.

**Table 6.11** Distribution of mean damage index ( $DI_{med}$ ), number of unusable buildings, homeless and casualties for all 19 involved villages of the Agri valley area (damage scenario in terms of buildings' number).

**Table 6.12** Distribution of mean damage index ( $DI_{med}$ ), unusable volume, number of homeless and casualties for all 19 involved villages of the Agri valley area (damage scenario in terms of buildings' volume).

**Table 6.13** Seismic strengthening costs for each village and the mean value for each building with vulnerability class "A" and "B".

**Table 6.14** Vulnerability classes  $V_C$  and  $PGA_{LS}$  values for all masonry types considered by Lagomarsino and Cattari (2014). For each  $V_C$ , the mean values  $PGA_{LS,med}$  and the corresponding values of the ratio  $PGA_{LS,med}/PGA_{475y}$  (assuming  $PGA_{475y} = 0.29g$ ) are also reported

**Table 6.15** Expected losses for Viggiano before and after the strengthening program

## **APPENDIX**

**Table 4A** Macroseismic and instrumental data of the considered events

**Table 5A** Attribute values in terms of AeDES form and GEM taxonomy related to building position

**Table 5B** Attribute values in terms of AeDES form and GEM taxonomy related to building use

**Table 5C** Attribute values in terms of AeDES form and GEM taxonomy related to masonry buildings

**Table 5D** Attribute values in terms of AeDES form and GEM taxonomy related to other structures

**Table 5E** Attribute values in terms of AeDES form and GEM taxonomy related to building regularity

**Table 5F** Attribute values in terms of AeDES form and GEM taxonomy related to roof

## Introduction

Italy is one of the European countries with the highest seismicity, as indicated in the report of the Joint Research Center (JRC; Poljanšek et al., 2019), where is underlined that the damaging earthquakes for which the European Union Solidarity Fund (EUSF) intervened have occurred in the Italian peninsula.

The seismic activity is mainly concentrated in the central-southern part of the Apennine ridge and partly in the northern area. These territories were affected by some of the strongest and most destructive events, among which Irpinia-Basilicata 1980, Abruzzo 2009 and Central Italy 2016-2017. In the last 50 years, earthquakes caused about 5,000 victims and monetary losses for about 180 billion €. Moreover, they damaged and/or destroyed a significant amount of historical and artistic heritage. These disastrous consequences underlined the need for comprehensive seismic risk assessments aimed at defining prevention and mitigation strategies at national, regional and local level. In order to be effective, prevention activities should be based on three main elements (Oliveira et al., 2007): a) the assessment of the seismic hazard and the vulnerability of every component of the built environment; b) the evaluation of the consequences on the built environment; and c) the awareness of the importance of such assessments and of the practical implementation of efficient mitigation actions. A proper quantification of the human, social and economic losses due to future earthquakes is indeed crucial for planning actions relevant to both pre-event interventions and post-event emergency preparedness.

To this end, several national and international projects have been carried out in the last decades, such as HAZUS (FEMA, 2003), LESSLOSS (2004), RISK-UE (2006), NERA (2014), SYNER-G (Pitilakis et al., 2014a,b) and GEM (Silva et al., 2018). The last “National Risk Assessment” (NRA) for Italy, carried out by the Department of Civil Protection (DPC, 2018), provided an updated assessment of seismic risk on the basis of state-of-the-art methodologies and tools developed in the last years. Despite the enormous scientific advancements in several of the components underlying the estimation of seismic risk, e.g., in the vulnerability assessment as reported in the Italian NRA in which six different models were adopted (Dolce et al., 2020), some issues need to be further addressed in order to reduce the uncertainties associated with risk assessment, including, in particular:

- the collection of reliable building inventories to be associated with physical vulnerability models;
- the selection of instrumental intensity measures better correlated with the seismic response of buildings;
- the definition of more accurate loss estimation models.

Concerning exposure, several sources of information and approaches can be used for the assemblage of a building inventory (e.g., Polese et al., 2019). Several of the methods available in literature suggest

to consider information on the features of the buildings directly or indirectly related to their seismic vulnerability as, e.g., age of construction or type of lateral load-resisting system (e.g., Dolce et al., 2003). Such kind of information may be obtained with a building-by-building survey, but this is often difficult (if not feasible, for large scale assessment) due to time constraints and the significant economic and human resources needed. In fact, similar surveys are typically carried out only during post-earthquake survey campaigns or to integrate/verify data in spatially limited areas. Census data are the main source of information that can provide a comprehensive picture of the building stock over large areas, although this information is often limited and provided in aggregated form (over administrative boundaries). Innovative techniques based on satellite image processing are another important data source for building inventory but several features that are crucial for vulnerability assessment cannot be easily detected relying on remote sensing data alone.

The large amount of information from historical Italian earthquakes in terms of macroseismic intensity (Rovida et al., 2020) constitutes an important heritage for different scientific purposes, e.g., for the definition of the level of ground motion intensity in many towns where seismometric instruments are not available. Several empirical relationships between macroseismic intensity (usually, Mercalli-Cancani-Sieberg, MCS scale) and instrumental measures (usually, Peak Ground Acceleration, PGA, and Velocity, PGV) were developed in past studies (e.g., Margottini et al., 1992; Faenza and Michelini, 2010). However, a small number of relationships are based on the European Macroseismic Scale (EMS-98; Grünthal, 1998) and on the integral intensity parameters that are better correlated to the building response (Masi et al., 2015).

An accurate estimation of earthquake impact in terms of human, social and economic losses depends upon several different factors and their complex interdependencies. These losses are generally estimated based on specific parameters (e.g., structural damage, building typology). Direct economic loss models available in literature are generally based on correlations between a functional of physical damage, and the expected consequences in terms of repair and reconstruction cost (e.g., Dolce et al., 2006; DPC, 2018). The damage extension (along the building height) is neglected or implicitly considered in the repair cost values. If on the one side the safety condition depends mainly on the damage severity (i.e., maximum damage level) on structural members, on the other side the damage extension, also affecting non-structural elements, represents an important factor which can strongly affect the estimation of direct economic losses.

In this framework, the PhD thesis, organized in seven chapters, is dedicated to the development and application of new methods and tools for supporting seismic risk assessment and reduction. This Introduction, going over the seven chapters of the thesis, provides a general overview of the main research activities and results.

Chapter I provides the theoretical background on the seismic risk components and the approaches to evaluate them. The main concepts and procedures are briefly discussed to better understand the proposed methods and the achieved results.

Chapter II reports a comprehensive literature review of the principal approaches proposed to estimate the expected consequences in terms of casualties (deaths and injuries), social impact (unusable buildings) and direct economic losses (i.e., cost of repair or replacement of damaged buildings).

In Chapter III, starting from the procedures available in literature, a new model aimed at assessing the direct economic losses has been developed based explicitly on both the damage severity and distribution along the building height. The model has been implemented for the building prototypes representative of Reinforced Concrete (RC) structural types designed only for vertical loads in the 70's. An extensive campaign of Non-Linear Dynamic Analyses (NLDAs) has been performed to determine the expected damage distributions throughout the building, adopting a specific correlation function between seismic response and damage levels according to the EMS-98 scale (Masi et al., 2015).

In Chapter IV, correlations between macroseismic scales and ground motion parameters have been derived by selecting 179 ground-motion records belonging to 32 earthquake events occurred in Italy in the last 40 years. PGA, PGV and Housner Intensity ( $I_H$ ) as instrumental measures, and EMS-98 and MCS scale as macroseismic measures have been adopted in order to derive both direct (i.e., macroseismic intensity vs instrumental parameter) and inverse (i.e., instrumental parameter vs macroseismic intensity) relationships. The former (direct relationships) can be used to derive macroseismic input values in empirical building damage models, such as Damage Probability Matrices (e.g., Dolce et al., 2003), given an instrumental value of ground motion (i.e., PGA, PGV and  $I_H$ ). On the contrary, the inverse relationships allow macroseismic data of historical earthquakes to be converted, according to the scales currently used in Italy (i.e., MCS and EMS-98), into the instrumental intensity measures adopted in seismic risk analyses and design practice.

In Chapter V, two innovative approaches for modelling the exposure of residential building stock have been proposed. The first approach has been developed to convert the information on the typological characteristics collected during damage and usability surveys after Italian earthquakes according to recognized international standards. In order to reliably extract the exposure and vulnerability information specific to the Italian environmental conditions, the first step of the methodology allows to convert the typological-structural data collected through the AeDES form (Baggio et al., 2007), used in Italy since 1997 for post-earthquake usability surveys, in terms of the taxonomy proposed by the Global Earthquake Model (GEM, Brzev et al., 2013). Subsequently, using an attribute-based scoring methodology (Pittore et al., 2018), the most likely EMS-98 (Grünthal,

1998) building classes have been assigned based on the observed GEM attributes. In this way, an exposure model in terms of risk-oriented classes associated to specific fragility models can be implemented and, then, the information obtained from field surveys can be exploited for large-area risk assessments.

Furthermore, an approach combining interview-based surveys with the potential offered by a remote screening technique has been defined and applied to the village of Calvello (Basilicata region, Southern Italy) in order to define an inventory of typological features of residential buildings. It is based on the integration of the CARTIS format (Zuccaro et al., 2015) and the RRVS web-based platform (Pittore and Wieland 2013). The former is a rigorous procedure based on in situ inspections and aimed at collecting, in a quick way based on interview to local experts, useful information on the representative building typologies and their proportions in a selected country/region. On the other side, the RRVS platform allows to perform a remote building-by-building survey using panoramic (360°) images. The approach allows to reduce time, human and economic resources with respect to building-by-building surveys and to rapidly acquire data on building typologies more relevant than census. It could therefore be a useful tool for large-area assessments in data-poor or economically developing countries.

Chapter VI describes the application framework of the PhD thesis. Firstly, a comparison among different Casualty Estimation Models (CEMs) available in literature has been carried out in the L'Aquila urban area. In order to define the factors involved in each CEM and discuss the possible differences with respect to the real impact, the data related to 2009 L'Aquila earthquake have been considered.

Consequently, an exposure model has been defined basing on the post-earthquake data of the 2009 Mw 6.3 L'Aquila event available in the Observed Damage Database (Da.D.O.; Dolce et al., 2019) platform. Specifically, L'Aquila dataset related to the residential building stock of 137 municipalities has been converted in terms of GEM taxonomy and EMS-98 classes according to the approach proposed in Chapter V.

In conclusion, earthquake scenario studies focusing on a highly seismic area located in the South-West of the Basilicata region (Southern Italy), along the valley of the Agri river have been carried out. Starting from the seismic vulnerability assessment based on the building-by-building inventory defined in previous research activities carried out in 18 villages (Masi et al., 2014) together with the information on the Calvello village obtained from the approaches CARTIS and RRVS, the expected losses deriving from an earthquake scenario with an exceedance probability of 10% in 50 years (475 years return period) have been estimated. The Val d'Agri area has a strategic role because about 70% of the Italian oil extraction derives from local deposits. Large quantities of oil have been extracted



## *Introduction*

since the 1990s, making thus available large revenues deriving from royalties. These resources could be used for an extensive program of structural strengthening able to reduce the impact of future earthquakes. To this end, an action plan for the seismic risk mitigation of the residential building stock of the 19 villages located in the Agri Valley has been proposed, and applied to the village of Viggiano.

Finally, Chapter VII reports some final remarks on the main developments obtained in the research work, as well as on some future developments to be pursued in the field.

## References

- Baggio C., Bernardini A., Colozza R., Corazza L., Della Bella M., Di Pasquale G., Dolce M., Goretti A., Martinelli A., Orsini G., Papa F., Zuccaro G., (2007) Field manual for post-earthquake damage and safety assessment and short term countermeasures (AeDES). In: EUR 22868 EN – Joint Research Centre – Institute for the Protection and Security of the Citizen, Artur V.P., Taucer F. (Eds.), Luxembourg: Office for Official Publications of the European Communities 2007 – 100 pp.- Eur scientific and technical research series – ISSN 1018-5593
- Brzev S., Scawthorn C., Charleson A.W., Allen L., Greene M., Jaiswal K.S., et al. (2013) GEM Building Taxonomy Version 2.0. GEM Technical Report 2013-02 v1.0.0, GEM.
- Dolce M., Masi A., Marino M., Vona M., (2003) Earthquake damage scenarios of Potenza town (Southern Italy) including site effects. *Bulletin of Earthquake Engineering* 1(1):115–140
- Dolce M., Kappos A.J., Masi A., Penelis G., Vona M., (2006) Vulnerability assessment and earthquake scenarios of the building stock of Potenza (Southern Italy) using the Italian and Greek methodologies. *Engineering Structures* 28:357–371
- Dolce M., Speranza E., Giordano F., Borzi B., Bocchi F., Conte C., Di Meo A., Faravelli M., Pascale V. (2019) Observed damage database of past Italian earthquakes: the Da.D.O. WebGIS. *Bollettino di Geofisica Teorica ed Applicata* Vol. 60, DOI 10.4430/bgta0254
- Dolce, M., Prota, A., Borzi, B. et al. (2020) Seismic risk assessment of residential buildings in Italy. *Bull Earthquake Eng* (2020). <https://doi.org/10.1007/s10518-020-01009-5>
- DPC, (2018) National Civil Protection Department (ed), National risk assessment. Overview of the potential major disasters in Italy: seismic, volcanic, tsunamis, hydro-geological/hydraulic and extreme weather, droughts and forest fire risks
- Faenza L, Michelini A (2010) Regression analysis of MCS intensity and ground motion parameters in Italy and its application in ShakeMap. *Geophysical Journal International*, 180, 1138–1152
- FEMA, (2003) “HAZUS-MH-MR4 - Earthquake Model Technical Manual, Federal Emergency Management Agency, Washington, D.C.
- Grünthal G. (editor), (1998) European Macroseismic Scale 1998 (EMS-98). European Seismological Commission, sub commission on Engineering Seismology, working Group Macroseismic Scales. Conseil de l’Europe, Cahiers du Centre Européen de Géodynamique et de Séismologie, volume 15, Luxembourg
- LESSLOSS, (2004) European integrated project on risk mitigation for earthquakes and landslides, report 2004/02. In: Calvi GM, Pinho R., European School for Advanced Studies in Reduction of Seismic Risk (ROSE School), IUSS Press, Pavia, Italy
- Margottini C, Molin D, Serva L (1992) Intensity versus ground motion: a new approach using Italian data. *Engineering Geology* 33:45–58
- Masi A., Chiauzzi L., Samela C., Tosco L., Vona M., (2014) Survey of dwelling buildings for seismic loss assessment at urban scale: the case study of 18 villages in Val D’Agri, Italy. *Environmental Engineering and Management Journal*, February 2014, Vol.13, No. 2, 471-486.
- Masi A., Digrisolo A., Manfredi V., (2015) Fragility curves of gravity-load designed RC buildings with regularity in plan. *Earthquake Struct.*, 9, 1-27
- NERA, (2014) Network of European Research Infrastructures for Earthquake Risk Assessment and Mitigation. Final report. Available at web site <https://cordis.europa.eu/result/>
- Oliveira, C. S., Roca, A., & Goula, X. (Eds.). (2007). Assessing and managing earthquake risk: geo-scientific and engineering knowledge for earthquake risk mitigation: developments, tools, techniques (Vol. 2). Springer Science & Business Media.
- Pitilakis K., Crowley E., Kaynia A., (eds) (2014a) SYNER-G: typology definition and fragility functions for physical elements at seismic risk, vol 27. Geotechnical, geological and earthquake engineering. Springer, Heidelberg. ISBN 978-94-007-7872-6

## *Introduction*

Pitilakis K., Franchin P., Khazai B., Wenzel H, (2014b) SYNER-G: systemic seismic vulnerability and risk assessment of complex urban, utility, lifeline systems and critical facilities. Methodology and applications, geotechnical, geological and earthquake engineering. Springer, Heidelberg. ISBN 978-94-017- 8834-2

Pittore, M., and Wieland, M. (2013). Toward a rapid probabilistic seismic vulnerability assessment using satellite and ground-based remote sensing. *Nat. Hazards* 68, 115–145. doi: 10.1007/s11069-012-0475-z

Pittore M., Haas M., Megalooikonomou K.G., (2018) Risk-Oriented, Bottom-Up Modeling of Building Portfolios with Faceted Taxonomies. *Front. Built Environ.* 4:41. doi: 10.3389/fbuil.2018.00041

Polese M., Gaetani d’Aragona M., Prota A., (2019) Simplified approach for building inventory and seismic damage assessment at the territorial scale: an application for a town in southern Italy, *Soil dynamics and earthquake engineering*, 121 (2019) 405-420

Poljanšek, K., et al., 2019. Recommendations for National Risk Assessment for Disaster Risk Management in EU, EUR 29557 EN, Publications Office of the European Union, Luxembourg, 2019, ISBN 978-92-79-98366-5 (online), doi:10.2760/084707 (online), JRC114650.

RISK-UE, (2006) Mouroux P., Le Brun B., Risk-UE project: an advanced approach to earthquake risk scenarios with application to different European towns. In: Oliveira C.S., Roca A., Goula X. (Eds.), *Assessing and managing earthquake risk geo-scientific and engineering knowledge for earthquake risk mitigation: developments, tools, techniques*, Springer Netherlands Publisher, Netherlands, 479–508

Rovida, A., Locati, M., Camassi, R. et al. (2020) The Italian earthquake catalogue CPTI15. *Bull Earthquake Eng* 18, 2953–2984 (2020). <https://doi.org/10.1007/s10518-020-00818-y>

Silva V., Amo-Oduro D., Calderon A., Dabbeek J., Despotaki V., Martins L., Rao A., Simionato M., Viganò D., Yepes C., Acevedo A., Horspool N., Crowley H., Jaiswal K., Journeay M., Pittore M., (2018) Global earthquake model (GEM) seismic risk map (version 2018.1). <https://doi.org/10.13117/gem-global-seismic-risk-map-2018.1>

Zuccaro G., Dolce M., De Gregorio D., Speranza E., Moroni C., (2015) La scheda CARTIS per la caratterizzazione tipologico-strutturale dei comparti urbani costituiti da edifici ordinari. Valutazione dell’esposizione in analisi di rischio sismico. *Proceedings of GNGTS 2015* (in italian)

# CHAPTER I

## Overview of seismic risk components

### Introduction

Seismic risk is the potential impact caused by an earthquake and it is usually expressed in terms of a combination of the magnitude of the consequences and the likelihood of these consequences to occur. Natural phenomena, built environment and society are the main elements contributing to earthquake loss estimation (Figure 1.1). Seismic risk is normally determined by the convolution of the seismic hazard of the site or region, the exposed assets that may be affected by an earthquake and the vulnerability of those elements at risk. As an example, Italy has a medium-high seismic hazard (due to frequency and intensity of phenomena), a very high vulnerability (due to fragility of building, infrastructural, industrial, production and service assets) and an extremely high exposure (due to population density and its historical, artistic and monumental heritage). Hence, Italian peninsula has a high seismic risk in terms of damage, victims, social and economic losses expected after a strong earthquake.

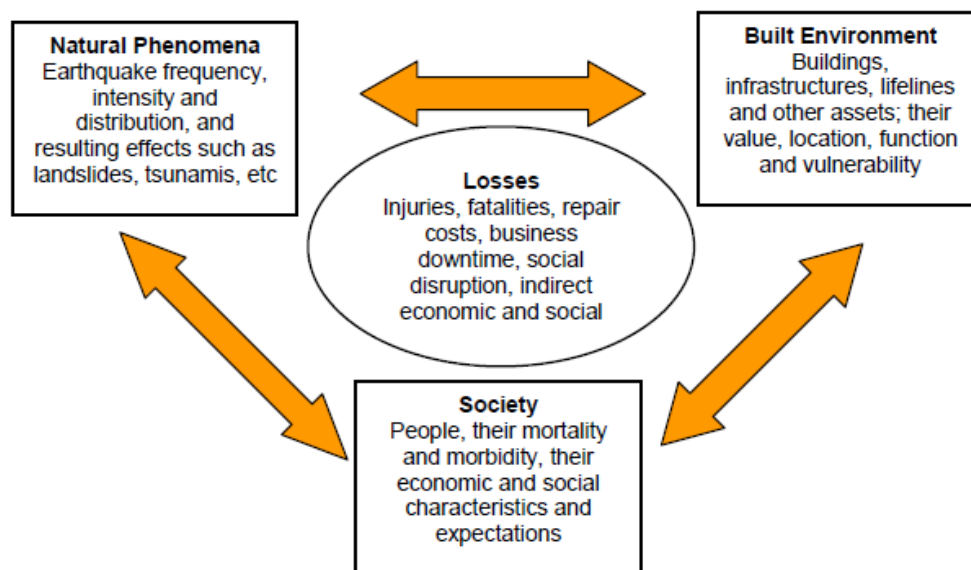


**Figure 1.1** Elements contributing to earthquake loss (Khater et al., 2003)

In this chapter, a global overview on the seismic risk and the main studies related to its assessment is provided with particular focus to the Italian territory. Furthermore, the main aspects of the seismic risk components are briefly discussed to better understand the proposed methodologies and the achieved results.

## **1.1 Seismic Risk**

Seismic risk can be defined as the expected value of human, economic, environmental and social losses, occurring in a certain time interval in a specific area due to one or more seismic events. Seismic risk assessment methodologies consider three main factors and their convolution relationship, that are seismic hazard, fragility/vulnerability of the system and inventory of physical and social elements exposed to hazard. Seismic hazard is a physical characteristic of the territory defined by the nature, frequency and intensity of earthquakes. Seismic exposure is defined as classification, organization and value of assets and activities in a territory, which can be affected by an earthquake in a direct or indirect way (i.e., buildings, infrastructures, networks, people, economic and productive activities). Seismic vulnerability is the proneness of buildings, infrastructures, people and so on to suffer damage due to earthquakes. It describes the amount of damage, induced by the seismic hazard, and expressed as a fraction of the value of the damaged assets under consideration. The components related to the earthquake risk assessment can be addressed by following the modular structure of the HAZUS methodology reported in Figure 1.2 (Whitman et al. 1997; Kircher et al. 2006; FEMA 2003).

Earthquake risk assessment can be carried out by means scenario studies for the quantification of the effects due to a single event, usually the maximum probable or maximum credible earthquake, or risk analyses for the evaluation of the probability of all potential losses in a specified period of time (e.g., one year) due to every likely event which might occur in the examined area. The results obtained from the scenario studies are useful for the civil protection emergency plans at local level, while the results of the risk analysis can be used for the preparation of prevision and prevention programs, therefore for the production of risk maps at national and regional scale.

In the past years, many efforts were put worldwide in the seismic risk assessment through the development of several tools and software. HAZUS (FEMA, 2003) is a standardized earthquake loss estimation methodology that provides quantitative estimates of expected losses in terms of casualties, social and economic impact. Global Earthquake Model (GEM) project performed remarkable advancements in the framework of risk assessment through a web-based platform, OpenQuake (Pagani et al., 2014), offering an integrated environment for modelling, viewing, exploring and managing earthquake risk (Silva et al., 2013). Numerous research projects dealing with the estimation of earthquake impact were funded by the European Union within the Framework Programmes for research and innovation (see JRC report; Poljanšek et al., 2019). In general, many authors performed nation-wide or urban level studies aimed at evaluating seismic risk and developing risk maps.

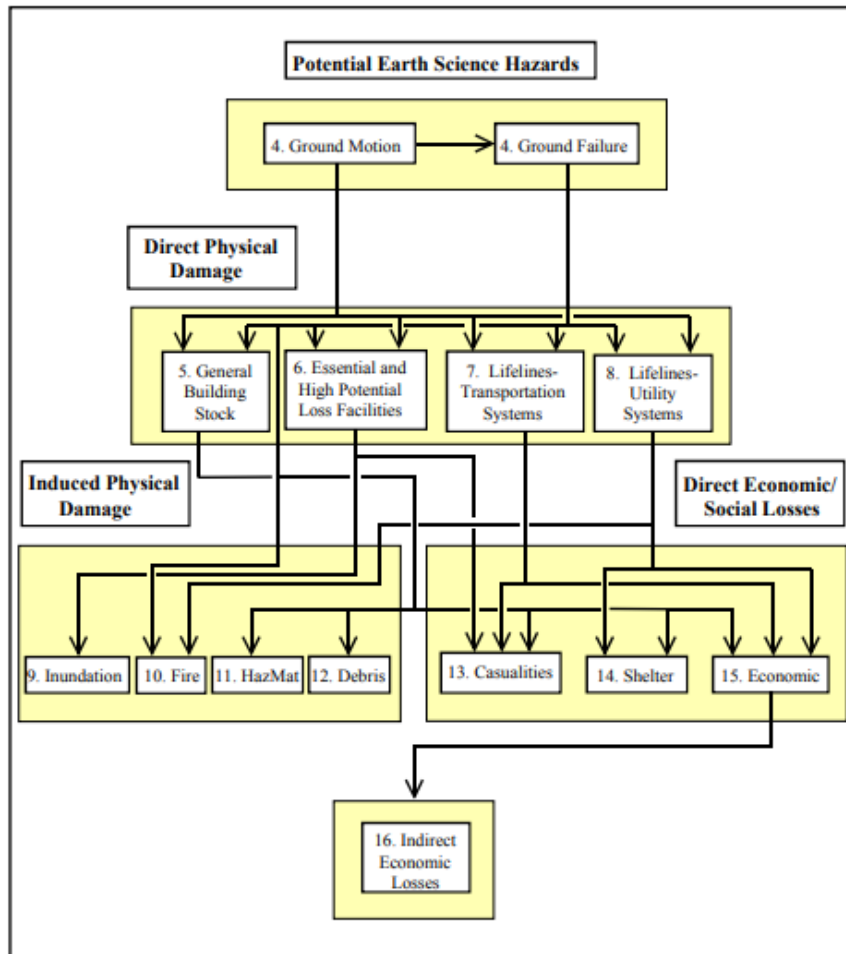


**Figure 1.2** Earthquake loss estimation methodology (HAZUS methodology)

As for Italy, the first maps of whole peninsula were prepared in 1996 by a Working Group set up by the Civil Protection Department (DPC). The aforementioned seismic risk maps were updated and presented in Lucantoni et al. (2001). A deep analysis of the proposed maps and a comparison with other studies (e.g., SAVE project; Zuccaro, 2004) was reported in Crowley et al. (2009). Considering the advancements made in the seismic hazard definition and in the vulnerability assessment methods, a new harmonized assessment was recently developed and defined in the last “National Risk Assessment” of the DPC (2018) with the support of ReLUIS (Network of university laboratories for seismic engineering) and Eucentre (European Centre for Training and Research in Earthquake Engineering). In this framework, a specific platform addressed to the scientific community, namely IRMA (Italian Risk MAPs), was developed in order to share data, methods and models for seismic risk assessments of Italian territory. Using the calculation engine OpenQuake, IRMA allows the upload of different vulnerability databases and different set of fragility curves used to perform damage/loss scenarios and produce risk maps (Dolce et al., 2020). It is worth also mentioning the risk assessment for Italy carried out by the GEM Foundation (Silva et al., 2018).

## 1.2 Hazard component

Earthquakes are geological phenomena, associated to a rupture in the solid exterior part of the earth (lithosphere), triggering relative displacements along active faults. The time, location and severity of earthquakes are unpredictable but the areas where they have occurred in the past and where active seismic faults exist, continue to be the most likely to be affected by earthquakes. In Italy, those zones are essentially in the central-southern part of the peninsula along the Apennine ridge and in some northern areas. Seismic hazard assessment aims at defining occurrence probability and severity of the future earthquakes.

Seismic severity can be defined using two different kinds of measures: *intensity* related to the effects of shaking at a given place and the *magnitude* related to the energy released by an earthquake at the source. Specifically, Magnitude is a quantitative measure of the event size and it is independent from the place of observation. It can be defined using Local or Richter Magnitude ( $M_L$ , 1952) else Moment Magnitude ( $M_w$ , Hanks and Kanamori, 1979). Conversely, Intensity is a local estimation of the earthquake severity, expressed by a measure of the strength of the ground motion at a particular location (i.e., depends on the stricken site).

In the last years, one of the main issues related to the seismic risk assessments is the selection of an appropriate earthquake Intensity Measure (IM) that characterizes the strong ground motion and best correlates with the response of buildings or other components (Pitilakis et al., 2014a). Each intensity measure may describe different characteristics of the motion, some of which may be more adverse for the structure or system under consideration. The use of a particular IM in seismic risk analysis should be guided by the correlation among the IM and the corresponding damage on the components of a system. Optimum intensity measures are defined in terms of practicality, efficiency, sufficiency, effectiveness, robustness and computability (Cornell et al. 2002; Mackie and Stojadinovic, 2005). Hence, the identification of the proper IM is determined from different constraints, which are first of all related to the adopted hazard model, but also to the element at risk under consideration and the availability of data and fragility functions for all different exposed assets.

It can be quantified by using two approaches: macroseismic and instrumental. The first one identifies the intensity of occurred earthquake through observations of the effects on buildings, environment and people over a limited area. The second one is based on quantitative parameters computed directly from instrumental time histories of recorded ground motion (i.e., the severity can be expressed as an analytical value measured by an instrument or computed from analysis of recorded accelerograms). Macroscopic intensity is defined after observing the effects and damage on humans, structures and nature. After seismic events, the degree of shaking is assigned during field surveys through intensity scales by considering visible consequences on the built environment and reports from those who

experienced the quake. There exist several intensity scales proposed worldwide, particularly in Europe and United States; most of which are modifications or adaptations of previous scales, and take their origins from the attempts of early seismologists to classify the effects of earthquake ground motion without instrumental recordings. Discrete scales based on ordinal degrees are used to quantify the macroseismic intensity providing a large description of earthquake effects. Some of the most common intensity scales are listed below:

- Mercalli-Cancani-Sieberg (MCS) scale (Sieberg, 1930) characterized by 12 levels and used in Southern Europe, especially in Italy, where it is currently used in the parametric earthquake catalogue (Rovida et al., 2019) and the macroseismic database (Locati et al., 2019);
- Modify Mercalli Intensity (MMI) scale characterized by 12-levels and used mainly in North America. It is the first scale in which the intensity for higher degrees is assigned considering also the vulnerability of buildings;
- Medvedev–Sponheuer–Karnik (MSK) scale characterized by 12-levels and used in several countries (Medvedev, 1977). This scale considers three vulnerability classes (A, B and C, being A the most vulnerable class) related to three building types (poor masonry buildings, good masonry buildings and reinforced concrete buildings, respectively);
- European Macroseismic Scale (EMS) characterized by 12-level and adopted mainly in Europe. The scale was issued in 1998 and referred to as EMS-98 (Grünthal, 1998). This scale considers six vulnerability classes related to different building typologies. The classes A, B and C are more or less similar to MSK classes while the other three ones refer to steel and wood buildings and, reinforced concrete buildings designed with earthquake reinforced techniques. . EMS-98 scale considers both environmental and human resentments and building damage. Three variables have been considered in the definition of macroseismic intensity degrees: the vulnerability of damaged buildings, the classification of damage levels and the definition of quantities.

A comparison between MCS, MMI, MSK and EMS scales is reported in Figure 1.3. It is worth noting that MSK and EMS scales return the same definition of intensity degrees while MCS and MMI scales return different range respect to the other definitions of macroseismic intensity. Some studies focused on relationships among the most adopted macroseismic intensity scales (e.g., Musson et al, 2010).

In the last Italian earthquakes, the macroseismic survey was performed by considering both MCS and EMS-98 scale, being the most used. The main advantage of using macroseismic intensity values is the huge availability of data provided by historical seismicity but it is not possible to directly use it as input data for the damage estimation by using structural analysis.



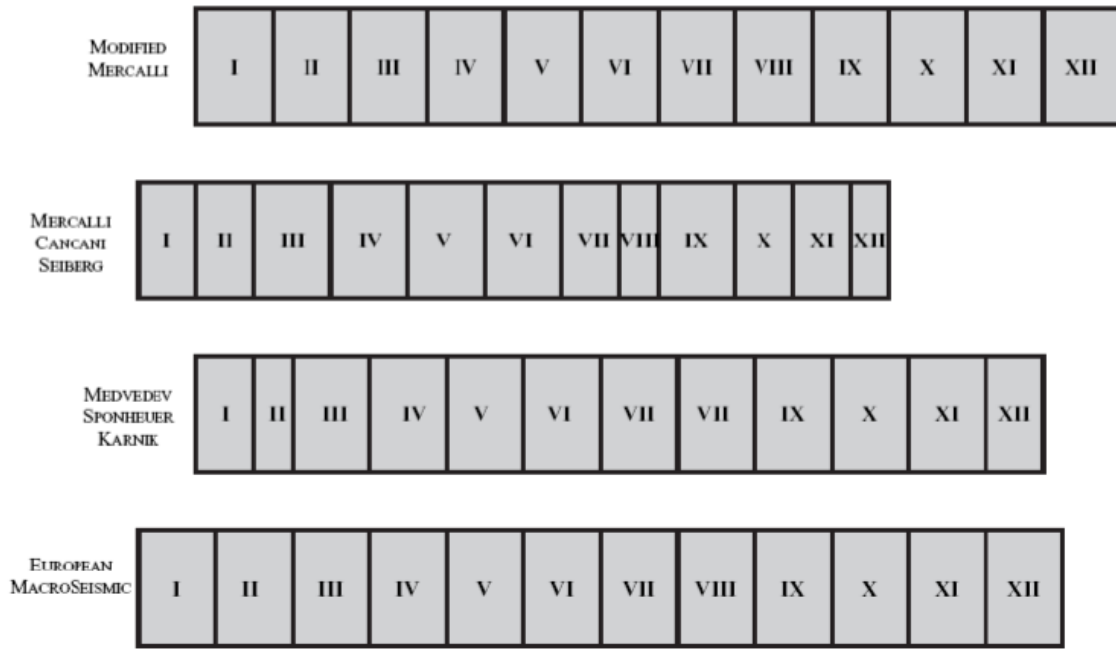


**Figure 1.3** Comparison between macroseismic intensity scales (from Elnashai & Di Sarno, 2008)

Instrumental intensity can be expressed by using different quantitative parameters calculated from time histories of ground motions recorded by accelerometers. The latter records the acceleration time history of an earthquake (i.e., accelerogram). The ground motion at a certain site can be generally described by different parameters expressing its acceleration, velocity, displacement and frequency content. Velocity and displacement can be derived from an accelerogram by means of integration and double integration, respectively. Many parameters can be used to describe and understand earthquake ground motion, among which peak or integral parameters (Cosenza and Manfredi, 2000). The peak parameters are Peak Ground Acceleration (PGA), Velocity (PGV) and Displacement (PGD), and peak motion ratios PGV/PGA and PGD/PGV. The values of PGA, PGV and PGD are computed as absolute maximum value of the recordings in terms of acceleration, velocity and displacement, respectively. The integral parameters are much more effective for measuring the energy content of a seismic event. Among these parameters, the Root Mean Square Acceleration (RMSA), Velocity (RMSV) and Displacement (RMSD) are defined as:

$$RMSX = \left[ \frac{1}{t_E} \int_0^{t_E} x^2(t) dt \right]^{1/2} \quad (1.1)$$

where  $x(t)$  is either the ground acceleration  $a_g(t)$ , velocity  $v_g(t)$  or displacement  $d_g(t)$  and  $t_E$  is the total duration of the earthquake. On the basis of RMSA, Arias intensity,  $I_A$  (Arias, 1970), adopted to quantified the energy in the accelerograms, is defined as follows

$$I_A = \frac{\pi}{2g} t_E RMSA^2 = \frac{\pi}{2g} \int_0^{t_E} a_g(t)^2 dt \quad (1.2)$$

Starting from  $I_A$ , the Saragoni Factor,  $P_D$  (Saragoni, 1990) is given by (1.3) in which  $v_0$  is the number of zero crossings of the record in the time unit.

$$P_D = \frac{I_A}{v_0^2} \quad (1.3)$$

Cosenza and Manfredi (1997) proposed a damage factor,  $I_D$ , related to the number of plastic cycles,  $n$ , and therefore, to the energy content of the earthquake according to the following expression:

$$I_D = \frac{2g}{\pi} \frac{I_A}{PGA \cdot PGV} \quad (1.4)$$

All the integral measures depend upon the duration of the earthquake which is a measure that cannot be predicted with any certainty and it largely influences the level of structural damage. About that, many authors proposed different definitions: for instance, Trifunac and Brady (1975) defined the effective duration,  $t_D$ , as the time elapsed between 5% and 95% of the RMSA; Kawashima and Aizawa (1989) introduced the bracketed duration,  $t_B$ , defined as elapsed time between the first and last acceleration being greater than a percentage of PGA or Trifunac and Novikova (1994) calculated  $t_D$  as the sum of the record intervals with a total amount of RMSA greater than 90%.

Other instruments related to seismic hazard description are the Response Spectra, that describe the maximum value of structural response to the excitation of strong motion, in terms of acceleration ( $S_a$ ), velocity ( $S_v$ ) and displacement ( $S_d$ ), experienced by a sample of Single Degree Of Freedom (SDOF) systems, having various natural periods (frequencies) and a specified level of equivalent viscous damping (for deepening see Chopra, 2012). Starting from Response Spectra, the Spectrum or Housner Intensity ( $I_H$ , Housner, 1952) is computed as the area under pseudo velocity response spectrum ( $S_v(T, \xi)$ ) by the following equation:

$$I_H = \int_{T_{min}}^{T_{max}} S_v(T, \xi) dT \quad (1.5)$$

where  $\xi$  is the fraction of critical damping,  $T$  is the fundamental period of vibration and ( $T_{min}$ ,  $T_{max}$ ) is the period range of integration.

This parameter can be interpreted as an integral measure of the energy demand. In this context, many authors proposed spectral parameters to be used as an intensity measure for risk assessments (e.g., Lin et al., 2013; Eads et al., 2015). Regarding the parameters described above, PGA is a basic measure of earthquake severity but is not totally reliable. Indeed, the past earthquakes with a large PGA produced not severe structural damage, while earthquakes with a low PGA produced a high level of destruction. Instead, PGV, as well as the integral parameters, seem to be a more representative measure of earthquake intensity as they are directly connected with energy demand.

Until the past century, earthquake severity was exclusively defined through macroseismic approach and, subsequently, recording networks have been placed worldwide. However, instrumental

recordings of local earthquake ground motions are not available in each town and stations are often placed far from epicenter. Then, only the estimation of macroseismic intensity returns an assessment of local resentments. For this reason, several relationships were developed in order to correlate the macroseismic intensity values and instrumental measures (e.g., Margottini et al., 1992; Faenza and Michelini, 2010; Chiauuzzi et al., 2012). This topic will be widely discussed in Chapter IV where new correlations have been proposed.

The approaches to seismic hazard assessment are based on characterizing the sources of hazard (size and spatial location of earthquakes) and the effect these sources would have on a particular location (earthquake ground motion). Seismic hazard can be evaluated using two different analyses:

- **Deterministic Seismic Hazard Analysis (DSHA)** based on the maximum probable or maximum credible earthquake (i.e., the largest earthquake that is reasonable to expect in a region) or modelling of fault rupture processes. Specifically, it is assumed that the future seismicity of a region shows a pattern which is similar to the one observed in the past; thus, no larger earthquakes are supposed to happen in the future. Deterministic values of ground-motion parameters are eventually obtained as a result. These approaches are strongly dependent on the availability of data;
- **Probabilistic Seismic Hazard Analysis (PSHA)** enables the association between a probability and a typically random phenomenon such as earthquake occurrence. The basic procedure of PSHA was first defined by Cornell (1968). PSHA makes use of historical and instrumental seismic records, seismogenic models, geological and geodetic data, time-dependent trends in earthquake recurrence and ground motion prediction equations. Moreover, PSHA provides a framework in which the uncertainties can be identified, quantified and combined in a rational manner (Silva, 2018). The results of a PSHA model are often represented in terms of curves or maps showing the value of a given ground motion parameter corresponding to an exceedance probability in a given period of time (e.g., 10% in 50 years) or to prescribed return period (e.g., 475 years). A hazard map is produced by carrying out assessments in a large number of locations within the region under study, showing the spatial variation. PSHA is an essential part of Probabilistic Seismic Risk Analysis (PSRA) in the Performance-Based Earthquake Engineering (PBEE) framework (Goulet et al. 2007; Ruiz-Garcia and Miranda 2007).

In Italy, the most recently issued seismic hazard model, named MPS04, was realized in 2004 by the National Institute of Geophysics and Volcanology (INGV) (Stucchi et al. 2004, 2011). It was the basis for the new seismic classification of the Italian territory and it was also incorporated in the Building Code, NTC-2008, and in the most recently approved, NTC-2018. Figure 1.4 shows the PSHA map relevant to a return period of 475 years, which reports the PGA in rigid soil condition

with horizontal surface. In Europe, the SHARE EU project released in 2013 a new seismic hazard model (Woessner et al. 2015), also with the contribution of the authors of the MPS04.

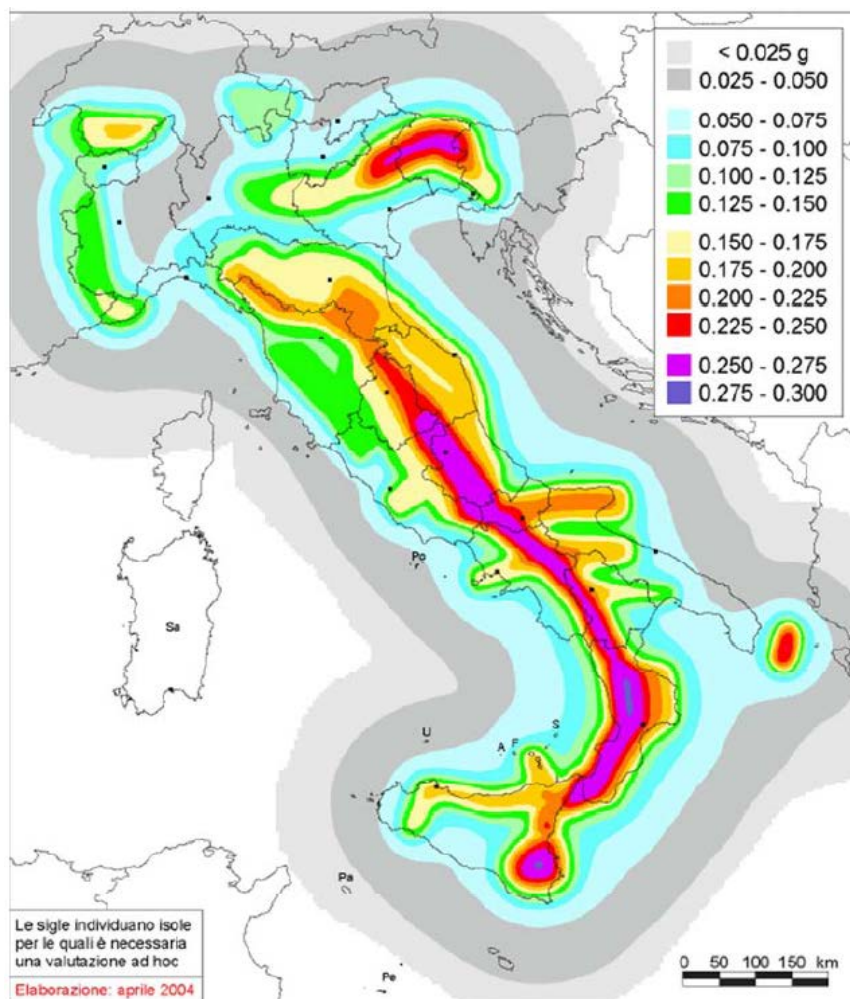


**Figure 1.4** Hazard map of Italy: Peak Ground Acceleration (PGA) values (as a fraction of the gravity acceleration  $g$ ) with a 10% probability of exceedance in 50 years (475 years return period)

Seismic hazard assessment is correlated to the definition of actions to be used in the design of new buildings and risk evaluation for civil protection purposes or insurance companies. Hazard studies serve also to produce maps of seismic zones that are included in design codes but are not effective for the design of new buildings. Seismic zones are only useful for the management and control of the building territory by relevant boards. On the basis of the MPS04 and the criteria provided by the Ordinances of the President of the Council of Ministers (OPCM 3274; 3519), Italian territory is subdivided into seismic zones, depending on the local hazard. In this framework, Seismic Microzonation (SM) is a useful support to implement an effective urban planning in relation to the basic hazard, the local amplification and the co-seismic effects. SM can be defined as “the assessment of local seismic hazards by identifying the zones of a given geographic area which have a homogeneous seismic behavior”.

### **1.3 Exposure component**

Exposure estimation refers to the identification of all the elements present in hazard zones that are potentially subject to losses. Assets that may be impacted by earthquakes include buildings, people, business and economic activities, basic services (health and educational facilities or emergency services), infrastructures (transportation, water, sewage, gas or communication), cultural heritage and the environment. Exposure is dynamic and characterized by continuous spatial and temporal changes due to urbanization, depopulation, changes in the settlements, modifications to building practices, variation of the building quality through seismic retrofitting, construction of temporary shelters and so on. (Brown et al., 2012; Aubrecht et al., 2013). Therefore, the collection and the update of exposure data for urban environments are crucial and challenging (Wieland et al. 2012). According to Pittore et al. (2016), main tasks and methodologies relevant for a global assessment of exposure component are: describing and storing, collecting, validating and communicating exposure data (Figure 1.5).

Buildings are a critical element in the characterization of the exposure in urban areas, since vulnerability and loss assessment models rely on the quantification of the exposed built environment. The definition of an adequate classification criterion for buildings and the development of a database to handle and store information are required to obtain a reliable exposure model.

Several international initiatives have been put efforts trying to find efficient methods to collect, organize and store exposure data on a global scale, while also accounting for its inherent spatial and temporal dynamics. In the framework of the Prompt Assessment of Global Earthquakes for Response (PAGER) system, a global building inventory was compiled based on harmonized data from various sources (Jaiswal et al., 2010). It provides fractions of building types present in urban and rural regions of each country by their functional use. The NERA project followed a similar procedure with focus on European countries (NERA, 2014). The GED4GEM (Dell'Acqua et al. 2013) project aimed to build an open homogenized database of global building stock and population distribution, containing spatial, structural and occupancy-related information at different scales as input to the GEM risk platform, OpenQuake (Pagani et al. 2014). Other databases that specifically provide physical exposure information are: LandScan (Bhaduri et al. 2007), WorldPop (WorldPop, 2015) initiatives or GEG-15 (De Bono and Chatenoux, 2015).

With regard to the classification criterion, the definition of a system (typology/taxonomy) for the characterization of the exposed building stock should be compatible with the fragility/vulnerability relationships considered in the risk assessment process. The preparation of the taxonomy involves the creation of a comprehensive and structured set of mutually exclusive and well-described attributes, which can be hierarchically structured or faceted and encoded in numeric or alphabetical codes (Hoffmann and Chamie, 2002). A taxonomy suitable for describing large-scale exposure should be

international, detailed, extendable, user friendly and capable of describing different types of exposed assets to match the requirements of related vulnerability models (Brzev et al., 2013).

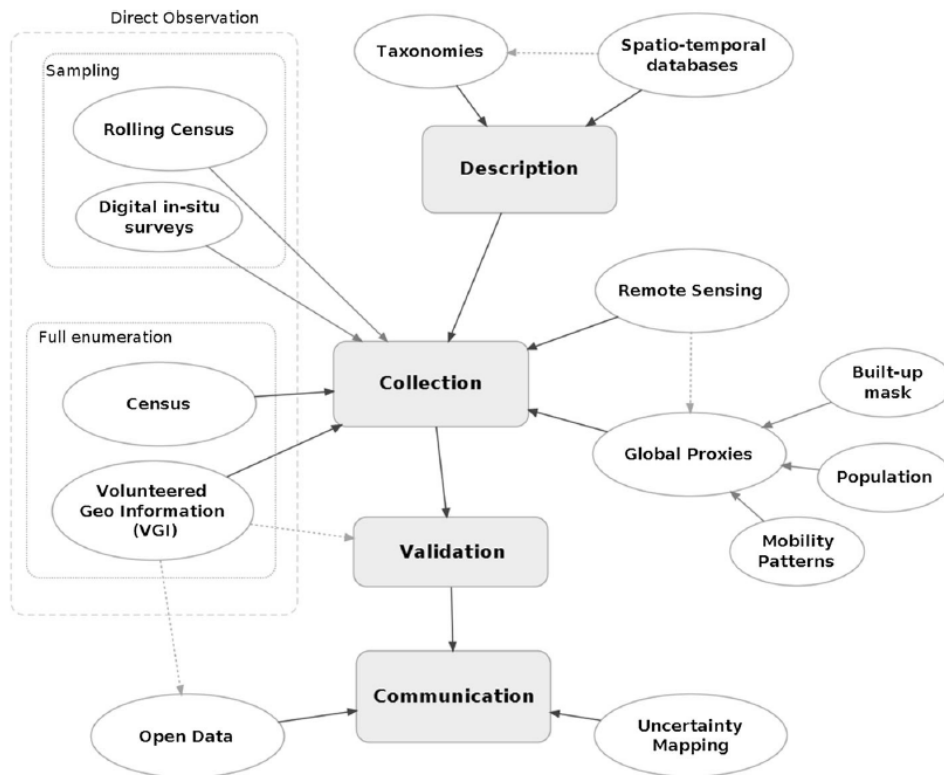


**Figure 1.5** Main tasks and related methodologies relevant for a global assessment of exposed assets (from Pittore et al., 2016)

Numerous taxonomies were developed in the world and in Europe in the field of earthquake engineering in order to classify and characterize building inventories in standardized and comparable ways. The taxonomies can be mainly classified as specific risk-oriented or the faceted (Pittore et al., 2018).

The first based on typological classes of buildings can be used for large-scale assessments. Each class consists of buildings with similar structural characteristics, since it is assumed that buildings of similar characteristics will have similar behaviors due to earthquakes. Risk-oriented taxonomies mainly describe and classify buildings based on their earthquake resistance and structural response to earthquakes. The use of these taxonomies is possible when the exposure models are based on in-situ data collection or combination of census data and expert judgment. The most comprehensive, risk-oriented classification of buildings globally is the PAGER-STR taxonomy (Jaiswal et al., 2010). The PAGER-STR taxonomy contains a total of 103 classes, in which buildings are varied with respect to wall material, height, lateral load resistance and earthquake design compliance. It was created by merging several pre-existing taxonomies and it was supplemented with building typologies collected through specific studies in several countries. The Federal Emergency Management Agency (FEMA) introduced the HAZUS taxonomy (FEMA, 2003) to quantitatively assess the impact of natural

phenomena on buildings in the United States. This taxonomy was based on the building classes that were proposed by a visual inspection with the aim of assessing their usable and safety characteristics and their occupancy. The HAZUS taxonomy contains 36 building typologies, mainly defined by different lateral resistance systems and with four levels of compliance with earthquake-resistant design regulations. In Europe, with the aim of recognizing the characteristics and variability of earthquake effects on the built environment, the EMS-98 scale (Grünthal, 1998) contains 15 different classes of buildings, which differ in the material used for the construction of walls and in different structural details pertaining to Earthquake-Resistant Design (ERD) levels.

On the contrary, the faceted taxonomies are made up of a set of taxonomies, and the task of each taxonomy is to describe a particular domain from a different facet (Tzitzikas, 2009). The hierarchy of classes is not fixed and, as a consequence, the taxonomy structure is flexible and it may be applicable to different hazards. In order to describe and classify buildings in Europe from the structural and functional point of view, a faceted taxonomy is proposed within the SYNER-G project (Pitilakis et al., 2014a), based on 15 aspects or a list of categories. The GEM project has developed a comprehensive faceted taxonomy to describe typical building typologies in the exposure models with global scope (Brzev et al., 2013). It is worth also mentioning the popular taxonomy targeting the description of structural components of buildings included in the World Housing Encyclopedia (World Housing Encyclopedia).

About collecting data on building stock and compiling an inventory, several approaches may be employed, that can be divided in two main categories: direct observation and remote sensing (Pittore et al., 2016). The latter is defined as the process of acquiring information about a building by means of use of Earth Observation Satellites (EOS) or other aerial sensor technologies (e.g., drones) without any physical contact. These observations offer the advantage of global coverage and temporal resolution adequate for identifying urban changes. In the last years, remote sensing is increasingly recognized as an important technique for deriving exposure characteristics of the built environment for rapid vulnerability assessments over various scales (Geiß and Taubenböck, 2013). Numerous studies emphasize the potential of remote sensing for collecting considerable amount of geo-spatial information, in a relatively short amount of time and with high repeatability (Borfecchia et al., 2010; Borzi et al., 2011; Wieland et al., 2012; Pinho, 2012; Geiß et al., 2015). The quality and the reliability of the exposure data collected by remote sensing techniques depend mainly on the image resolution. Medium-resolution satellite image data are used to derive proxies (land use/land cover) that can support an indirect characterization of exposure (built-up areas, population) over large areas. On the contrary, high resolution (HR) or very high resolution (VHR) earth observation data enable to extract exposure attributes on the level of individual buildings, among which building footprint, shape

irregularities, heights, roof materials, location (e.g., Sarabandi et al. 2008; Geiß et al. 2014; Wieland and Pittore 2014). However, studies using high-resolution images still show limitations in terms of covering large areas due to data availability, processing requirements or limited levels of process automation. Moreover, remote sensing approaches only provide exposure information that can be inferred from the top view. Considering the case of building stock, the analysis of the lateral structure and façades of buildings also has to be carried out. Therefore, some building features that are crucial for vulnerability assessment cannot be directly derived from remotely sensed data (e.g., structural type or building age).

On the contrary, direct observation refers to the manual collection of exposure information through in situ surveys (i.e., an expert physically moving closer to the structure to be examined) or remotely (e.g., exploiting high-resolution imagery from street-view cameras). Two strategies for direct observation can be distinguished: full enumeration (i.e., building-by-building survey) and statistical sampling. The first refers to the detection and definition of each building within a study area. It can therefore potentially achieve high levels of accuracy and detail. Usually, it requires a great deal of work and involves greater investment in terms of time and economic resources. It may in turn be subdivided into census methods, and so-called volunteered geographical information procedures. Census methods are the reference for national demographic data and the most known approach based on direct collection. Although being mostly concerned with the full enumeration of people and housing using great resources, National censuses have proved inefficient as the quality of the collected information is often scarce. On the other hand, statistical sampling has the advantage that only small subset areas need to be analyzed in detail to estimate preliminary statistics for a larger area of interest. Census methodologies are progressively changing from full enumeration to advanced sampling and statistical modelling (e.g., the rolling census). It is worth also mentioning that digital in situ data capturing systems have recently been proposed as time- and cost- effective supplements to commonly used in situ screening techniques (Bevington et al., 2012).

In general, the methods described above should be efficiently combined to obtain an accurate inventory of the building features without costly and time-consuming efforts. As an example, the building-by-building survey is often carried out on limited test sites and the results are extended on the basis of data collected using other information sources, such as census data (Crowley et al., 2009), cadastral maps (Lantada et al., 2009) or remote sensing surveys (Brown et al., 2012; Polli et al., 2009). These methods can be also combined adapting to local capabilities and availability of technical resources (Wieland et al. 2015; Gamba 2014): the joint use of remote sensing with ground-based in situ omnidirectional imaging (Wieland et al. 2012; Pittore and Wieland 2013) or with volunteered geographical information (Schauss 2015); the use of aerial images with census data and virtual



surveys (e.g., using Google StreetView; Osorio et al. 2015) or remote sensing data with volunteered geographic information from the OpenStreetMap project (Geiß et al., 2016). In Italy, an advancement towards compilation of regional scale inventories is provided by the CARTIS (CARatterizzazione TIpologica Strutturale; Zuccaro et al., 2015) approach. The CARTIS survey format allows to collect data on building typologies most widespread in a selected area, by interviewing one or more technicians that are local experts with deep knowledge of the construction characteristics in the area. Table 1.1 shows the main advantages and disadvantages and, the applicability scale related to the data sources and approaches for building inventory used mainly in Italy (i.e., census data; remote sensing; building-by-building survey and interview-based survey). In Chapter V, innovative approaches aimed at modelling exposure of residential buildings have been proposed.

Source	Building Features	Applicability scale	Advantage	Disadvantage
<b>Census data</b>	Spatial type features-basilar level (storey number) Attribute type features basilar level (age; material RC/Masonry/Other; state of preservation)	from town districts to regional or national scale	complete database for all the nation; information on both population and buildings; free or low-cost database	some countries have limited info by census returns; variable size of census unit; data are available in aggregated form at the census tract level for privacy reason; census forms compiled by non-experts
<b>Remote sensing (HR or VHR imagery)</b>	Spatial type features – intermediate level (building shape, position and height)	from town districts to regional, national or even larger scale	automatic and semi-automatic detection algorithms are being developed; geo-referenced spread data on potentially very large building stock; can be easily updated	requires processing massive data volumes; necessary the combination with other data sources (e.g., urban context information and/or local surveys on benchmark buildings) to derive attribute type building features (e.g., construction age, roof type)
<b>Interview based survey</b>	Detailed spatial and attribute type building features for building typologies and %	from town districts to regional or national scale	detailed info for building typologies; speed economic approach	data reliability depends on interviewed experience/ knowledge of the built environment
<b>Building by building</b>	Detailed spatial and attribute type building features	town districts	detailed info for single buildings in a district	costly and time consuming; difficulty of access to information for not visible features (e.g., horizontal system; strengthening interventions etc.)

**Table 1.1** Data sources and related approaches for building inventory (from Polese et al., 2019)

## 1.4 Vulnerability component

Vulnerability is the condition determined by physical, social, economic and environmental factors or processes which increase the susceptibility of an individual, a community, assets or systems to the impacts of hazards (UNISDR, 2016). Different kinds of vulnerability can be identified: (i) Social vulnerability is the susceptibility of a population or social system to harm from exposure to hazards (Alwang et al., 2001) and it depends to demographic and socio-economic factors; (ii) Physical vulnerability is related to the properties of structures determining their potential damage in case of a disaster (Ebert et al., 2008). The focus is on the physical vulnerability of structures such as buildings, which can collapse or suffer severe damage affecting the human, economic and social losses. The kind of damage depends on the building structure, age, materials, location, vicinity to other buildings and non-structural elements, and also on the duration and intensity of the earthquake.

Seismic vulnerability of a building can be described as its susceptibility to damage due to ground shaking of a given intensity. The aim of a vulnerability assessment is to obtain the probability of a given level of damage for a given building type due to an earthquake scenario. After an earthquake, the vulnerability of a building can be assessed inspecting the damage caused and associating it with the seismic intensity.

Vulnerability assessment before an earthquake can be performed through different existing methods based on (i) observation of damage due to past earthquakes (empirical approach), (ii) numerical analysis (analytical approach), and (iii) combination of such approaches (hybrid approach). The judgment of experts (expert approach) can be also considered. A comprehensive overview of the available methods for the assessment of building vulnerability is reported in Calvi et al. (2006). Specifically, the empirical (statistical) method is based on damage data obtained from observations after past earthquakes. These data are not always available and cannot be used to assess the vulnerability of individual buildings. The analytical (mechanical) method is based on numerical analyses of the structure through detailed time-history analysis or through simplified methods. Empirical and analytical approaches can be used in the framework of the hybrid methods (Kappos et al., 2016) that combine post-earthquake damage statistics with simulated and analytical data derived from a mathematical model of the building typology. Hybrid models can be particularly advantageous when there is a lack of damage data at certain intensity levels for the geographical area and they also allow calibration of the analytical model to be carried out. Furthermore, the use of observational data reduces the computational effort that would be required to produce a complete set of analytical vulnerability curves. The expert approach is based on expert opinions to assess the seismic behavior of given structural types or to identify the factors that determine the seismic vulnerability.

There are two ways of expressing the seismic vulnerability of a building or a type/category of buildings:

- 1) Damage Probability Matrices (DPMs) expressing in a discrete form the conditional probability of having a damage level  $L_d$ , due to an earthquake of intensity  $I$  and to the seismic vulnerability  $V$  according to the following expression:

$$DPM = P(L_d | I, V) \quad (1.6)$$

DPMs method is usually quantitative (i.e., provides numerical results), typological (i.e., evaluates the seismic behavior by assigning a structural typology identified by means of few basic features), statistical (i.e., the result is obtained from the statistical analysis) and direct (i.e., provides in a single step a measure of vulnerability). DPMs were traditionally derived using observed damage data. The basic concept of a DPM is that a given structural typology will have the same probability of being in a given damage state for a given earthquake intensity. On the basis of the data sustained in over 1600 buildings after the 1971 San Fernando earthquake, Whitman et al. (1973) proposed the use of DPMs for the probabilistic prediction of damage to buildings. One of the first European versions of a DPM was produced by Braga et al. (1982) based on data collected after the 1980 Irpinia earthquake. The approach involved the classification of buildings in three vulnerability classes (high A, medium B and low C) and the macroseismic intensity according to the MSK scale. In order to consider also the class D related to lower vulnerability, Dolce et al. (2003) developed the DPM relevant to this class (Table 1.2) by taking into account the information contained in the EMS-98 scale (Grünthal, 1998). Di Pasquale et al. (2005) changed the DPMs from the MSK to the MCS scale because the Italian seismic catalogue is based on this intensity, and the number of buildings is replaced by the number of dwellings. A macroseismic method was proposed by Lagomarsino and Giovinazzi (2006) that leads to the definition of damage probability functions based on the EMS-98 macroseismic scale (Grünthal, 1998). The limitation of the DPMs is due to the consideration of the individual buildings as fuzzy elements in the belonging class, no allowing a precise identification of the expected damage. Indeed, the result in numeric terms is distributed within the class. Furthermore, the results obtained so far show how the accuracy is strongly dependent on the availability of data.

Intensity	Damage Levels					
	0	1	2	3	4	5
VI	0.900	0.090	0.010	0.000	0.000	0.000
VII	0.715	0.248	0.035	0.002	0.000	0.000
VIII	0.401	0.402	0.161	0.032	0.003	0.000
IX	0.131	0.329	0.330	0.165	0.041	0.004
X	0.050	0.206	0.337	0.276	0.113	0.018

**Table 1.2** Damage Probability Matrix for buildings of vulnerability class D (from Dolce et al., 2003)

2) Fragility curves, which are continuous functions expressing typically the probability of exceeding a certain damage state (DS) for a given earthquake intensity. Adopting the lognormal cumulative density function, as commonly done in seismic fragility studies, and selecting PGA as the intensity parameter, the curve is given by (Kappos et al., 2016):

$$P[ds \geq ds_i[PGA]] = \Phi \left[ \frac{1}{\beta_{ds_i}} \ln \left( \frac{PGA}{PGA_{med, ds_i}} \right) \right] \quad (1.7)$$

where

- $PGA_{med, ds_i}$  is the median value of PGA at which the building reaches the threshold of DS,  $ds_i$ ;
- $\beta_{ds_i}$  is the standard deviation of the natural logarithm of PGA for DS  $ds_i$ ;
- $\Phi$  is the standard normal cumulative distribution function.

Fragility curves as well as the DPMs can be derived using different methods. Regarding the FCs derived through analytical/mechanical methods, they are based on computational analyses applied to a mechanical model of a given building. Analytical FCs were originally proposed in the HAZUS Technical Manual (FEMA & NIBS, 1999) for U.S. buildings and lifeline systems. In the HAZUS manual, FCs are described in terms of spectral displacements for four damage states involving both structural and non-structural components and the seismic response of the structure was calculated by non-linear static analysis (i.e., pushover analysis).

Afterwards, different intensity measures and methods of evaluating the building response were adopted in developing FCs. Regarding the methods adopted for the evaluation of seismic response, analytical FCs can be grouped into two main classes: FCs derived from either non-linear static-based approach or non-linear dynamic-based ones. About the intensity measures, two main categories can be defined: empirical, i.e., macroseismic intensity such as MCS or EMS-98 scale, and instrumental, i.e., peak (e.g., PGA, PGV), spectral (e.g.,  $S_a(T)$ ,  $S_d(T)$ ) or integral (e.g.,  $I_A$ ,  $I_H$ ) parameters.

As an example, Masi et al. (2015) developed fragility curves relevant to the Reinforced Concrete (RC) building types existing in most Italian and European villages, based on a similar approach to HAZUS. The methodology involves the following steps: selection of building types; simulated design of the selected building types; modelling the building types, involving masonry infills; nonlinear dynamic analyses; definition of the damage scale and set up fragility curves (Masi, 2003). In the definition of the FCs, a set of five damage levels according to the EMS-98 scale was considered whereas the intensity measure was described by adopting the Housner intensity ( $I_H$ ). Figure 1.6 shows fragility curves relevant to pre-1971 RC buildings (2 storeys-Bare Frame).

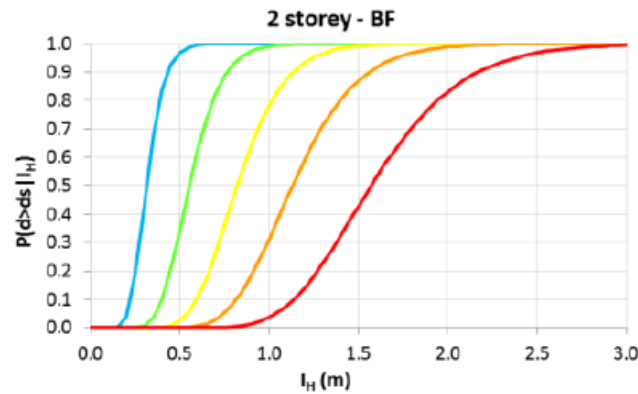


**Figure 1.6** Example of fragility curve relevant to pre-1971 RC buildings (2 storeys-BF) developed in Masi et al. (2015)

A collection of fragility functions for buildings, bridges, highway and railway infrastructure, harbor elements, health care facilities, electric power stations, gas and oil distribution networks, water and waste-water systems, may be found in Pitilakis et al. (2014a,b) in the context of SYNER-G project. Yepes et al. (2016) report the online database of physical vulnerability models (i.e., fragility and vulnerability curves, damage-to-loss models, and capacity curves for various types of structures) as part of the GEM initiative.

In the framework of the last “National Risk Assessment” (2018), six vulnerability models, four for masonry buildings and two for reinforced concrete buildings, were derived following different approaches (i.e., three models from empirical, two from analytical and one from hybrid heuristic approach; see Dolce et al., 2020).

## References

- Alwang, J., Siegel, P. B., & Jorgensen, S. L. (2001). Vulnerability: a view from different disciplines (Vol. 115). Social protection discussion paper series.
- Arias A. (1970) A measure of earthquake intensity. In: Seismic design of nuclear power plants. Cambridge, MA: MIT Press. 1970. 438–468.
- Aubrecht, C., Fuchs, S., & Neuhold, C. (2013). Spatio-temporal aspects and dimensions in integrated disaster risk management. *Natural Hazards*, 68(3), 1205-1216.
- Bevington J, Eguchi RT, Huyck CK et al (2012) Exposure data development for the global earthquake model. In: 15th world conference on earthquake engineering, Lisboa, 24–28 Sep 2012
- Bhaduri, B., Bright, E., Coleman, P., & Urban, M. L. (2007). LandScan USA: a high-resolution geospatial and temporal modeling approach for population distribution and dynamics. *GeoJournal*, 69(1-2), 103-117.
- Borfecchia, F., De Cecco, L., Pollino, M., La Porta, L., Lugari, A., Martini, S., ... & Pascale, C. (2010). Active and passive remote sensing for supporting the evaluation of the urban seismic vulnerability. *Italian Journal of Remote Sensing*, 42(3), 129-141.
- Borzi, B., Dell'Acqua, F., Faravelli, M., Gamba, P., Lisini, G., Onida, M., & Polli, D. (2011). Vulnerability study on a large industrial area using satellite remotely sensed images. *Bulletin of Earthquake Engineering*, 9(2), 675-690.
- Braga F., Dolce M., Liberatore D., (1982) A statistical Study on Damaged Buildings and Ensuing Review of the MSK-76 Scale. 8th ECEE, Atene, September 1982
- Brown, D., Saito, K., Liu, M., Spence, R., So, E., & Ramage, M. (2012). The use of remotely sensed data and ground survey tools to assess damage and monitor early recovery following the 12.5. 2008 Wenchuan earthquake in China. *Bulletin of Earthquake Engineering*, 10(3), 741-764.
- Brzev, S., Scawthorn, C., Charleson, A. W., Allen, L., Greene, M., Jaiswal, K., & Silva, V. (2013). GEM Building Taxonomy v2. 0. GEM Building Taxonomy Global Component, Global Earthquake Model, Pavia
- Calvi, G. M., Pinho, R., Magenes, G., Bommer, J. J., Restrepo-Vélez, L. F., & Crowley, H. (2006). Development of seismic vulnerability assessment methodologies over the past 30 years. *ISSET journal of Earthquake Technology*, 43(3), 75-104.
- Chiauzzi L., Masi A., Mucciarelli M., Vona M., Pacor F., Cultrera G., Gallovic F., Emolo A., (2012) Building damage scenarios based on exploitation of Housner intensity derived from finite faults ground motion simulations. *Bull Earthq Eng* 10:517–545
- Chopra Anil K., (2012) Dynamic of structures, theory and application to earthquake engineering. Prentice Hall, New Jersey.
- Cornell C.A. (1968) Engineering seismic risk analysis. *Bulletin of the Seismological Society of America* 58, 1583-1606.
- Cornell C.A., Jalayer F., Hamburger R.O., Foutch D.A. (2002) Probabilistic basis for 2000 SAC/FEMA steel moment frame guidelines. *J Struct Eng* 1284:26–533
- Cosenza E., Manfredi G. (1997) The improvement of the seismic-resistant design for existing and new structures using damage criteria. In: Fajfar P & Krawinkler H (eds) *Seismic design methodologies for the next generation of codes*. Rotterdam: Balkema. 1997. 119–130.
- Cosenza E., Manfredi G. (2000) Damage indices and damage measures. *Progress in Structural Engineering and Materials* 2000; 2:50 –59
- Crowley H., Colombi M., Borzi B., Faravelli M., Onida M., Lopez M., Polli D., Meroni F., Pinho R., (2009). A comparison of seismic risk maps for Italy, *Bull Earthq Eng* 7(1) 149–180.
- De Bono, A.; Chatenoux, B. (2015) *A Global Exposure Model for GAR 2015*, UNEP/GRID-Geneva; UNISDR: Geneva, Switzerland, 2015.
- Dell'Acqua, F., Gamba, P., & Jaiswal, K. (2013). Spatial aspects of building and population exposure data and their implications for global earthquake exposure modeling. *Natural hazards*, 68(3), 1291-1309

- Di Pasquale G., Orsini G., Romeo R.W., (2005) New Developments in Seismic Risk Assessment in Italy. *Bulletin of Earthquake Engineering*, 3:101–128-DOI 10.1007/s10518-005-0202-1
- Dolce M., Masi A., Marino M., Vona M., (2003) Earthquake damage scenarios of Potenza town (Southern Italy) including site effects. *Bulletin of Earthquake Engineering* 1(1):115–140
- Dolce, M., Prota, A., Borzi, B. et al. (2020) Seismic risk assessment of residential buildings in Italy. *Bull Earthquake Eng* (2020). <https://doi.org/10.1007/s10518-020-01009-5>
- DPC, (2018) National Civil Protection Department (ed), National risk assessment. Overview of the potential major disasters in Italy: seismic, volcanic, tsunami, hydro-geological/hydraulic and extreme weather, droughts and forest fire risks.
- Eads L, Miranda E, Lignos DG (2015) Average spectral acceleration as an intensity measure for collapse risk assessment. *Earthquake Eng Struct Dyn* 44(12):2057–2073
- Ebert, A., Kerle, N. (2008). Urban social vulnerability assessment using object-oriented analysis of remote sensing and GIS data. A case study for Tegucigalpa, Honduras. *The International Archives of the Photogrammetry, Remote Sensing and Spatial Information Sciences*, 37, 1307-1312.
- Elnashai A.S., Di Sarno L., (2008) *Fundamentals of Earthquake Engineering*. John Wiley & Sons.
- Faenza L, Micheli A (2010) Regression analysis of MCS intensity and ground motion parameters in Italy and its application in ShakeMap. *Geophysical Journal International*, 180, 1138–1152
- FEMA & NIBS, 1999 Earthquake loss estimation methodology – HAZUS 99. Federal Emergency Management Agency and National Institute of Buildings Sciences, Washington DC.
- FEMA, (2003) “HAZUS-MH-MR4 - Earthquake Model Technical Manual, Federal Emergency Management Agency, Washington, D.C.
- Gamba, P. (2014). Image and data fusion in remote sensing of urban areas: Status issues and research trends. *International Journal of Image and Data Fusion*, 5(1), 2-12.
- Geiß C, Taubenböck H (2013) Remote sensing contributing to assess earthquake risk: from a literature review towards a roadmap. *Nat Hazards* 68:7–48. doi:10.1007/s11069-012-0322
- Geiß C, Taubenböck H, Tyagunov S, Tisch A, Post J, Lakes T (2014) Assessment of seismic vulnerability from space. *Earthq Spectra*. doi:10.1193/121812EQS350M
- Geiß, C., Pelizari, P. A., Marconcini, M., Sengara, W., Edwards, M., Lakes, T., & Taubenböck, H. (2015). Estimation of seismic building structural types using multi-sensor remote sensing and machine learning techniques. *ISPRS Journal of Photogrammetry and Remote Sensing*, 104, 175-188.
- Geiß, C., Schauß, A., Riedlinger, T., Dech, S., Zelaya, C., Guzmán, N., ... & Taubenböck, H. (2016). Joint use of remote sensing data and volunteered geographic information for exposure estimation: evidence from Valparaíso, Chile. *Natural Hazards*, 1-25.
- Goulet C. A., Haselton C. B., Mitrani-Reiser, J., Beck J. L., Deierlein G. G., Porter K.A., Stewart, J. P., (2007) Evaluation of the seismic performance of a code-conforming reinforced concrete frame building from seismic hazard to collapse safety and economic losses. *Earthquake Engng Struct. Dyn.* 2007; 36:1973–1997.
- Grünthal G., (1998) *European Macroseismic Scale*. European Centre of Geodynamic & Seismology, Luxemburg, 15
- Hanks, T. C., H. Kanamori (1979). A moment magnitude scale, *J. Geophys. Res.* 84, 2348-2350
- Hoffmann, E., & Chamie, M. (2002). Standard statistical classifications: basic principles. *Statistical Journal of the United Nations Economic Commission for Europe*, 19(4), 223-241
- Housner G.W., (1952) Intensity of ground motion during strong earthquakes. Second technical report. August 1952, California Institute of Technology Pasadena, California
- Jaiswal, K.; Wald, D.; Porter, K. (2010) A global building inventory for earthquake loss estimation and risk management. *Earthq. Spect.* 2010, 26, 731–748.
- Kappos A.K., (2016) An overview of the development of the hybrid method for seismic vulnerability assessment of buildings, *Structure and Infrastructure Engineering*, 12:12, 1573-1584 (2016). <https://doi.org/10.1080/15732479.2016.1151448>

- Kawashima K., Aizawa K. (1989) Bracketed and normalized durations of earthquake ground acceleration. *Earthquake Engineering and Structural Dynamics* 1989; 18: 1041–1051.
- Khater M., Scawthorn C. and Johnson J.J., (2003) Loss Estimation, Chapter 31 in *Earthquake Engineering Handbook*, CRC Press.
- Kircher C.A., Whitman R.V., Holmes W.T., (2006) HAZUS earthquake loss estimation methods. *Nat Hazards Rev* 7(2):45–59
- Lagamarsino S. and Giovinazzi S., (2006) Macroseismic and mechanical models for the vulnerability and damage assessment of current buildings. *Bull. Earthq. Eng.* 4, 415–443. doi: 10.1007/s10518-006-9024-z
- Lantada N., Pujades L.G., Barbat A.H., (2009), Vulnerability index and capacity spectrum based methods for urban seismic risk evaluation. A comparison, *Natural Hazards*, 51, 501–524
- Lin T, Haselton CB, Baker JW. (2013) Conditional spectrum-based ground motion selection. Part I: Hazard consistency for risk-based assessments. *Earthquake Engineering and Structural Dynamics* 2013; 42(12):1847–1865. DOI:10.1002/eqe.2301.
- Locati M., Camassi R., Rovida A., Ercolani E., Bernardini F., Castelli V., Caracciolo C.H., Tertulliani A., Rossi A., Azzaro R., D'Amico S., Conte S., Rocchetti E. (2019) Italian Macroseismic Database (DBMI15), version 2.0. Istituto Nazionale di Geofisica e Vulcanologia (INGV) 2019. <https://doi.org/10.13127/DBMI/DBMI15.2>
- Lucantoni A., Bosi V., Brammerini F., De Marco R., Lo Presti T., Naso G., Sabetta F., (2001) Il rischio sismico in Italia. *SSN, Ingegneria Sismica*, XVIII-N. 1.
- Mackie K., Stojadinovic B. (2005) Fragility basis for California highway overpass bridge seismic decision making. PEER Report 2005/12, Pacific Earthquake Engineering Research Center, University of California, Berkeley, CA
- Margottini C, Molin D, Serva L (1992) Intensity versus ground motion: a new approach using Italian data. *Engineering Geology* 33:45–58
- Masi, A. (2003) Seismic Vulnerability Assessment of Gravity Load Designed R/C Frames, *Bulletin of Earthquake Engineering*, Vol. 1, No. 3, pp. 371-395.
- Masi A., Digrisolo A., Manfredi V., (2015) Fragility curves of gravity-load designed RC buildings with regularity in plan. *Earthquake Struct.*, 9, 1-27
- Medvedev SV (1977) Seismic intensity scale M.S.K.—76. *Publ Inst Geophys Pol Acad Sci A-6(117)*, Warsaw
- Musson R.M. W., Grünthal G. and Stucchi M. (2010) The comparison of macroseismic intensity scales, *J Seismol* (2010) 14:413-428 DOI 10.1007/s10950-009-9172-0
- NERA, (2014) Network of European Research Infrastructures for Earthquake Risk Assessment and Mitigation. Final report. Available at web site <https://cordis.europa.eu/result/>.
- NTC08 (2008), D.M. 14 gennaio 2008 - Norme tecniche per le costruzioni. Ministero delle Infrastrutture
- NTC18 (2018), D.M. 17 gennaio 2018 - Norme tecniche per le costruzioni. Ministero delle Infrastrutture
- OPCM 3274, (2003) Ordinanza del Consiglio dei Ministri n. 3274. Primi elementi in materia di criteri generali per la classificazione sismica del territorio nazionale e di normative tecniche per le costruzioni in zona sismica. GU n. 72 giugno 2003. Available at web site <http://www.cslp.it>
- OPCM, 3519 (28/04/2006) Ordinanza del Consiglio dei Ministri n. 3519. Criteri generali per l'individuazione delle zone sismiche e per la formazione e l'aggiornamento degli elenchi delle medesime zone. GU n.108 11/05/2006). Available at web site <http://www.cslp.it>
- Osorio, F. A., Acevedo, A. A., & Jaramillo, J. D. (2015). Methodology for the development of a seismic exposure model for Antioquia (Colombia). In *Memorias del VII Congreso Nacional de Ingeniería Sísmica*. Universidad de los Andes and Asociación Colombiana de Ingeniería Sísmica. Bogotá, Colombia.
- Pagani M., Monelli D., Weatherill G., Danciu L., Crowley H., Silva V., Henshaw P., Butler L., Nastasi M., Panzeri L., Simionato M., Vigano D., (2014) OpenQuake Engine: An Open Hazard (and Risk) Software for the Global Earthquake Model. *Seismological Research Letters*, Vol. 85, No. 3, pp. 1-13



- Pinho, R. (2012). GEM: a Participatory Framework for Open, State-of-the-Art Models and Tools for Earthquake Risk Assessment. In Proceedings of the 15th World Conference on Earthquake Engineering, Lisbon (pp. 24-28).
- Pitilakis K., Crowley E., Kaynia A., (eds) (2014a) SYNER-G: typology definition and fragility functions for physical elements at seismic risk, vol 27. Geotechnical, geological and earthquake engineering. Springer, Heidelberg. ISBN 978-94-007-7872-6
- Pitilakis K., Franchin P., Khazai B., Wenzel H, (2014b) SYNER-G: systemic seismic vulnerability and risk assessment of complex urban, utility, lifeline systems and critical facilities. Methodology and applications, geotechnical, geological and earthquake engineering. Springer, Heidelberg. ISBN 978-94-017- 8834-2
- Pittore, M., Wieland, M. (2013). Toward a rapid probabilistic seismic vulnerability assessment using satellite and ground-based remote sensing. *Natural hazards*, 68(1), 115-145.
- Pittore M., Wieland M., Fleming K., (2016) Perspectives on global dynamic exposure modelling for geo-risk assessment. *Nat Hazards* 86, 7–30 (2017). <https://doi.org/10.1007/s11069-016-2437-3>
- Pittore M., Haas M., Megalooikonomou K.G., (2018) Risk-Oriented, Bottom-Up Modeling of Building Portfolios with Faceted Taxonomies. *Front. Built Environ.* 4:41. doi: 10.3389/fbuil.2018.00041
- Polese M., Gaetani d’Aragona M., Prota A., (2019) Simplified approach for building inventory and seismic damage assessment at the territorial scale: an application for a town in southern Italy, *Soil dynamics and earthquake engineering*, 121 (2019) 405-420
- Poljanšek, K., et al., 2019. Recommendations for National Risk Assessment for Disaster Risk Management in EU, EUR 29557 EN, Publications Office of the European Union, Luxembourg, 2019, ISBN 978-92-79-98366-5 (online), doi:10.2760/084707 (online), JRC114650.
- Polli D., Dell’Acqua F., Gamba P., (2009) First steps towards a framework for earth observation (EO)-based seismic vulnerability evaluation, *Environmental Semeiotics*, 2, 16-30
- Rovida A., Locati M., Camassi R., Lolli B., Gasperini P. (2019) Italian Parametric Earthquake Catalogue (CPTI15), version 2.0. Istituto Nazionale di Geofisica e Vulcanologia (INGV) 2019. <https://doi.org/10.13127/CPTI/CPTI15.2>
- Ruiz-Garcia, J., Miranda, E., (2007) Probabilistic estimation of maximum inelastic displacement demands for performance-based design, *Earthquake Engineering and Structural Dynamics*, 36 :1235-1254.
- Sarabandi, P., Kiremidjian, A. S., Eguchi, R. T., & Adams, B. J. (2008). Building inventory compilation for disaster management: Application of remote sensing and statistical modeling. Technical Report Series MCEER-08-0025, MCEER: Buffalo.
- Saragoni GR. (1990) Response spectra and earthquake destructiveness. In: Proceedings 4th US National Conference on Earthquake Engineering, Palm Springs, USA, 20–24 May 1990. Berkeley, CA: Earthquake Engineering Research Institute (EERI). 1990. 35–43.
- Schauß, A. (2015). Joint Use of Remote Sensing and Volunteered Geographic Information for Exposure Estimation (Doctoral dissertation, Heidelberg University).
- Sieberg A (1930) Geologie der Erdbeben. *Handbuch der Geophysik* 2(4):550–555
- Silva V., Crowley H., Pagani M., Monelli D., Pinho R., (2013) Development of the OpenQuake engine, the global earthquake model’s open-source software for seismic risk assessment. *Nat Hazards*. doi:10. 1007/s11069-013-0618-x
- Silva V., (2018) Critical Issues on Probabilistic Earthquake Loss Assessment, *Journal of Earthquake Engineering*, 22:9, 1683-1709, DOI: 10.1080/13632469.2017.1297264
- Silva V., Amo-Oduro D., Calderon A., Dabbeek J., Despotaki V., Martins L., Rao A., Simionato M., Viganò D., Yepes C., Acevedo A., Horspool N., Crowley H., Jaiswal K., Journeay M., Pittore M., (2018) Global Earthquake Model (GEM) Seismic Risk Map (version 2018.1). doi: 10.13117/gem-globalseismic- risk-map-2018.1.
- Stucchi, M., Akinci, A., Faccioli, E., Gasperini, P., Malagnini, L., Meletti, C., Montaldo, V., Valensise, G., (2004) Mappa di Pericolosità sismica del territorio Nazionale [http://zonesismiche.mi.ingv.it/documenti/rapporto\\_conclusivo.pdf](http://zonesismiche.mi.ingv.it/documenti/rapporto_conclusivo.pdf) (in italian).
- Stucchi M, Meletti C, Montaldo V, Crowley H, Calvi GM, Boschi E (2011) Seismic hazard assessment (2003-2009) for the Italian building code. *Bulletin of the Seismological Society of America*, 101, 1885-1911.

- Trifunac M.D., Brady AG. (1975) A study on the duration of strong earthquake ground motion. *Bulletin of the Seismological Society of America* 1975:65(3): 581–626.
- Trifunac M.D., Novikova EI. (1994) Duration of strong ground motion in terms of earthquake magnitude epicentral distance, site conditions and site geometry. *Earthquake Engineering and Structural Dynamics* 1994: 23: 1023–1043.
- Tzitzikas Y., (2009) *Faceted Taxonomy-Based Sources*. Berlin; Heidelberg:Springer.
- UNISDR (2016) *Open-ended Intergovernmental Expert Working Group on Indicators and Terminology relating to Disaster Risk Reduction: Report of the Second Session (Informal and Formal)*, The United Nations Office for Disaster Risk Reduction, Geneva, Switzerland
- Whitman, R.V., Reed, J.W. and Hong, S.T. (1973). “Earthquake Damage Probability Matrices”, *Proceedings of the Fifth World Conference on Earthquake Engineering*, Rome, Italy, Vol. 2, pp. 2531-2540.
- Whitman R.V., Anagnos T., Kircher C.A., Lagorio H.J., Lawson R.S., Schneider P., (1997) Development of a national earthquake loss estimation methodology. *Earthquake Spectra*, 13(4), pp. 643-662.
- Wieland, M., Pittore, M., Parolai, S., & Zschau, J. (2012). Exposure estimation from multi-resolution optical satellite imagery for seismic risk assessment. *ISPRS International Journal of Geo-Information*, 1(1), 69-88.
- Wieland M, Pittore M (2014) Performance evaluation of machine learning algorithms for urban pattern recognition from multi-spectral satellite images. *Remote Sens* 6(4):2912–2939. doi:10.3390/rs6042912
- Wieland, M., Pittore, M., Parolai, S., Begaliev, U., Yasunov, P., Niyazov, J., ... & Abakanov, T. (2015). Towards a cross-border exposure model for the Earthquake Model Central Asia. *Ann. Geophys.*, 58, S0106.
- Woessner J, Danciu L, Giardini D, Crowley H, Cotton F, Grünthal G, Valensise G, Arvidsson R, Basili R, Demircioglu MB, Hiemer S, Meletti C, Musson R, Rovida A, Sesetyan K, Stucchi M, the SHARE consortium (2015) The 2013 European seismic hazard model: key components and results. *Bulletin of Earthquake Engineering*, 13, 3553-3596
- World Housing Encyclopedia. Available online: <http://www.world-housing.net/>.
- Worldpop (2015). Worldpop. <http://www.worldpop.org.uk/>
- Yepes C, Silva V, D'Ayala D, Rossetto T, Ioannou I, Meslen A, Crowley H (2016). The Global Earthquake Model Physical Vulnerability Database. *Earthquake Spectra*, 32(4):2567-2585
- Zuccaro G. (2004) *Inventory and vulnerability of the residential building stock at a national level, seismic risk and social/economic loss maps*. CD-ROM, Naples, Italy (in Italian)
- Zuccaro G., Dolce M., De Gregorio D., Speranza E., Moroni C., (2015) La scheda CARTIS per la caratterizzazione tipologico-strutturale dei comparti urbani costituiti da edifici ordinari. *Valutazione dell'esposizione in analisi di rischio sismico*. *Proceedings of GNGTS 2015* (in Italian)

## CHAPTER II

### Loss estimation models: literature review

#### Introduction

The main goal of a seismic risk assessment for a city, region or country is to calculate the seismic hazard and to convolve it with the vulnerability of the exposed building stock such that the damage of the buildings and losses (human, social and economic) can be predicted (Erdik, 2017). The latter are determined using specific loss estimation procedures based on different parameters (e.g., structural damage; building typology and so on). Estimates of expected losses are of great importance to: civil protection, relief and emergency services; physical and economic planning on different scales (local, national or international); management of facilities or public administration in earthquake-prone regions; insurance and reinsurance companies; drafting building regulations or codes of practice for constructions.

Several studies and projects were devoted to the development of methodologies and tools aimed at assessing seismic losses, among which RISK-UE (Mouroux and Le Brun, 2006), LESSLOSS (Calvi and Pinho, 2004; Spence, 2007), PAGER (Wald et al., 2010), NERIES (Erdik et al., 2010) and SYNER-G (Pitilakis et al., 2014a,b). One of the most used methodologies to estimate potential losses from natural hazards originates from HAZUS where, HAZUS-MH MR4 is a damage- and loss-estimation software developed by FEMA (2003). GEM initiative developed guidelines and software OpenQuake (Pagani et al., 2014) to carry out loss assessments (Silva et al., 2013; 2018).

Loss estimation methodologies can be categorized in two main types: *(i)* methodologies for regional loss estimation and *(ii)* methodologies for building-specific loss estimation. The latter ones allow to provide accurate estimates for individual buildings located at specific sites. About that, Performance-Based Earthquake Engineering (PBEE) approaches developed by the Pacific Earthquake Engineering Research (PEER, 2002) program are widely used in the last years (e.g., Porter, 2003; Aslani and Miranda, 2005). On the other side, regional loss estimation methods aim at estimating earthquake consequences for a large number of buildings within a geographical region (e.g., city or country).

In the following sections, an extensive deepening of the main literature studies and projects relating to models proposed to estimate the expected consequences in terms of casualties (deaths and injuries), direct economic losses (i.e., cost of repair or replacement of damaged buildings) and social impact (specially, unusable buildings) is reported. Furthermore, a comparison among different casualty estimation models is shown in Chapter VI.

## 2.1 Casualties

Loss estimation studies to be useful for earthquake protection need to include an assessment of human casualties, both deaths and injuries. The assessment of casualty levels is essential for medical and relief agencies to aid their preparedness. Despite its importance, assessing the number of casualties caused by a seismic event is a complex task due to the limited quality and quantity of information. An earthquake can cause deaths and injuries in many different ways: building collapse, infrastructure failures, heart attacks, triggered secondary hazards (e.g., landslides, mudflows and fires) and many other causes. According to past studies (Coburn and Spence, 1992; 2002), the number of the casualties is primarily related to building damage. In stronger events, casualties are highly affected by structural damage, especially by collapse instead, for smaller earthquakes, non-structural damages govern the estimation (Petal, 2004). The type and number of casualties vary with the characteristics of the earthquake and the building stock in the stricken area. Moreover, other factors such as different distribution of occupants in the day hours and year seasons, damage and building collapse mechanisms or effectiveness of rescue operations can affect the real impact.

Despite the above-mentioned uncertainties, several casualty estimates were performed using different approaches (NERIES Project, 2010; Jaiswal et al., 2011):

- *Empirical models* that, on the basis of fatality data statistics of past earthquakes, evaluate the casualties as function of earthquake severity in terms of macroseismic intensity (Jaiswal and Wald, 2010) or magnitude (Samardjieva and Badal, 2002) and population density;
- *Analytical models* that use building damage as input for the evaluation of casualties (e.g., Coburn and Spence, 2002; LESSLOSS, 2008). The approach requires the knowledge of building occupancy data and the probability of casualty levels for different building types with given damage states. This latter can be evaluated on the basis of past earthquake data or through the definition of the hazard, structural and damage analysis.

### From Coburn and Spence (1992) to So and Spence (2013)

The first model proposed by Coburn and Spence (1992) considers the following equation for estimating the number of casualties:

$$K = K_S + K' + K_2 \quad (2.1)$$

where

$K_S$  is the number of fatalities due to structural damage;

$K'$  is the number of fatalities from non-structural damage;

$K_2$  is the number of fatalities from follow-on hazards.

On the basis of the post-earthquake data of the last century, the contribution of  $K_S$  parameter is dominant (about 75% of casualties), particularly for strong shaking levels. The authors updated this approach to estimate the casualties by determining the “Lethality Ratio” (LR) for each class of damaged buildings. LR is defined as the ratio of the number of people killed to the number of occupants present in collapsed buildings. Considering the past earthquakes, LR is found to depend on different factors including building type and function, occupancy levels, type of collapse mechanism, ground motion characteristics, occupant behavior and Search And Rescue (SAR) effectiveness. LR for each building class is estimated using a set of M-parameters defining the expected proportions of occupants who are trapped, the proportion of those trapped who are subsequently rescued and the injury distribution in each group. The number of casualties derives from an estimate of the number of collapsed buildings and the LR for each class as reported in following equation:

$$K_S = D_5 * [M_1 * M_2 * M_3 * (M_4 + (1 - M_4) * M_5)] \quad (2.2)$$

where

$K_S$  is the number of casualties;

$D_5$  is the number of collapsed buildings;

$M_1$  is the average number of people in each collapsed building;

$M_2$  is percentage of occupants at time of earthquake (% of  $M_1$  indoors at onset of ground shaking and influenced by time of day and use of structures);

$M_3$  is the proportion of occupants trapped by collapse (% of  $M_2$  unable to escape);

$M_4$  is the mortality at collapse (% of  $M_3$  killed and injured at time zero after collapse);

$M_5$  is the mortality post-collapse (% of the trapped survivors that die before they can be rescued and it depends crucially on the effectiveness of SAR).

Figure 2.1 explains the specific meaning of M-parameters. Each building class has its own specific set of M-parameters that take into account the likely collapse characteristics and the SAR capability. Specifically, the proportion of occupants trapped by collapse ( $M_3$ ) is strongly influenced by building type, and increases with height.  $M_3$  is assumed to be smaller for events of lower intensity and affected by the type of ground motion (Figure 2.2).

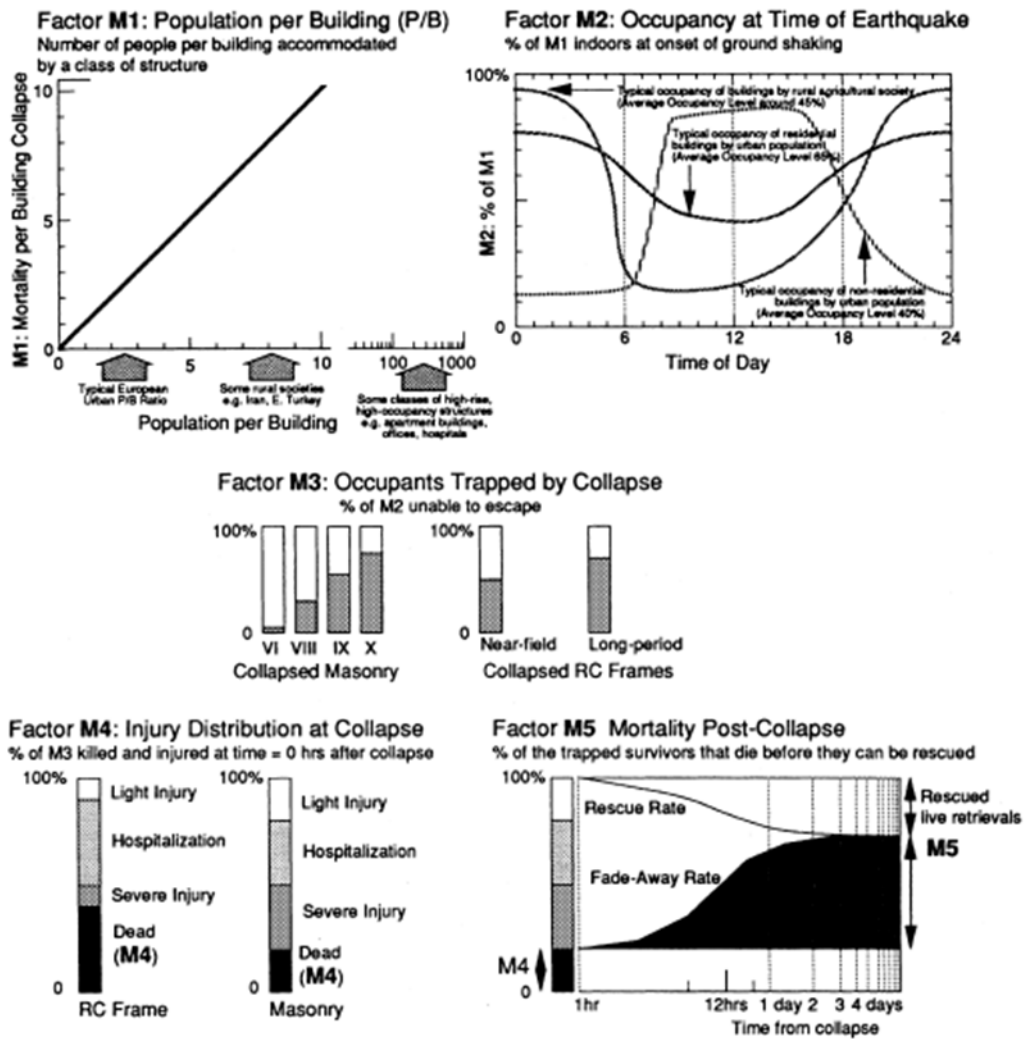


Figure 2.1 M-parameters used in the estimation of the human casualties (Coburn and Spence, 2002)

Collapsed masonry buildings (up to three storeys)				
Intensity	VII	VIII	IX	X
	5%	30%	60%	70%
Collapsed RC structures (3–5 storeys)				
Near-field, high-frequency ground motion:				70%
Distant, long-period ground motion:				50%

Figure 2.2 The average percentage of occupants trapped by collapse, M<sub>3</sub> (Coburn and Spence, 2002)

The proportion of occupants killed at collapse and the injured distribution (M<sub>4</sub>) are assumed to depend on building type (Figure 2.3). The mortality post-collapse (M<sub>5</sub>) depends crucially on the effectiveness of SAR, which varies considerably between countries (e.g., whether the rural or urban population is affected) and according to the earthquake severity, but depends also on the building type. Indeed, the rescue speed is slower for concrete and steel buildings for which heavy cutting and lifting equipment need to be deployed. On the contrary, in timber buildings, it is assumed that most of those trapped is quickly rescued (Figure 2.4).

Triage injury category	Masonry	RC
1. Dead or unsaveable	20	40
2. Life-threatening cases needing immediate medical attention	30	10
3. Injury requiring hospital treatment	30	40
4. Light injury not necessitating hospitalisation	20	10

Figure 2.3 Injury distribution at the collapse, M4 (Coburn and Spence, 2002)

Situation	Masonry	RC
Community incapacitated by high casualty rate	95	–
Community capable of organising rescue activities	60	90
Community + emergency squads after 12 hours	50	80
Community + emergency squads + SAR experts after 36 hours	45	70

Figure 2.4 The mortality post-collapse, M5 (Coburn and Spence, 2002)

A further update of the above-mentioned work was proposed by Spence (2007) in the framework of LESSELOSS project (2008) in which new casualty rates for three test cities (Istanbul, Thessaloniki and Lisbon) are defined. These casualty rates are based on the data obtained from past events such as 1995 Kobe, 1999 Chi-Chi, 1999 Kocaeli, 1994 Northridge and 1999 Athens and on the rates suggested by ATC-13 (1985), Coburn and Spence (1992) and FEMA&NIBS (1999).

The classification of M-parameters is modified to include an injury distribution at each damage state and not only account for injuries and deaths from trapped victims (i.e., damage state equal to 5). Indeed, buildings with a low damage level can also cause injuries and therefore need to be consider. The schema reported in Figure 2.5 shows the injury states added to the Coburn and Spence (2002) model (red box).

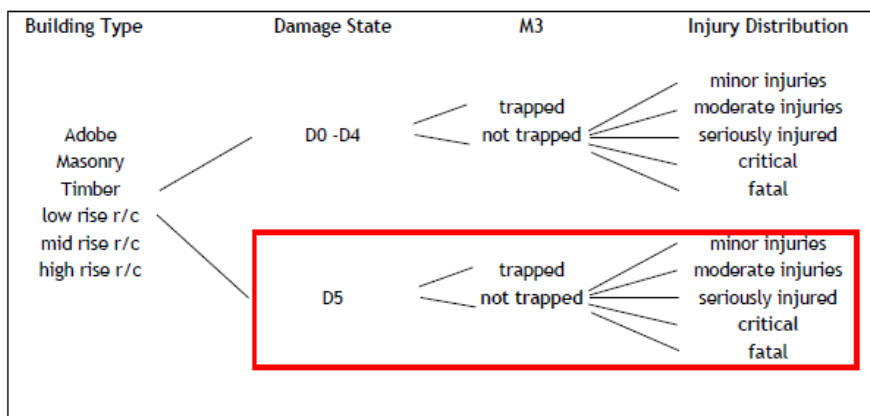


Figure 2.5 Modelling injury distributions within each damage state (Spence, 2007)

Considering the damage state D5, Figure 2.6 reports the casualty rates for different building types. The injury categories are uninjured (UI), slight injuries (I1), moderate injuries (I2), serious injuries (I3) critical injuries (I4) and deaths (I5). It is assumed that the number of killed and critically injured depends primarily on the partially or totally collapsed buildings (D4 and D5), and moderate and serious injuries depend on numbers of buildings with lower damage state.

	Damage State D5					
	UI	I <sub>1</sub>	I <sub>2</sub>	I <sub>3</sub>	I <sub>4</sub>	I <sub>5</sub>
Timber (1F)	45.7%	40.0%	12.0%	1.5%	0.1%	0.7%
Timber (2&3F)	43.9%	40.0%	12.5%	1.5%	0.1%	2.0%
Timber (>4F)	43.6%	40.0%	13.0%	2.0%	0.1%	1.3%
Masonry (1F)	23.6%	50.0%	12.0%	8.0%	0.4%	6.0%
Masonry (2&3F)	16.5%	50.0%	15.0%	10.0%	0.5%	8.0%
Masonry (>4F)	9.4%	50.0%	18.0%	12.0%	0.6%	10.0%
RC (1F)	32.9%	30.0%	19.0%	3.0%	0.2%	15.0%
RC (2&3F)	20.8%	30.0%	23.0%	4.0%	0.2%	22.0%
RC (>4F)	9.7%	30.0%	27.0%	5.0%	0.3%	28.0%
Steel (1F)	38.9%	30.0%	15.0%	2.0%	0.1%	14.0%
Steel (2&3F)	25.1%	30.0%	19.0%	3.0%	0.2%	22.8%
Steel (>4F)	10.0%	30.0%	23.0%	4.0%	0.2%	32.8%

Figure 2.6 Casualty rates for damage state D5 developed within LESSLOSS Project (Spence, 2007)

As could see in the new classification, in addition to the four original categories of injuries (lightly, moderately, seriously injured and deaths), a fifth division termed “critical” was introduced as probability of injuries resulting in severe disablement. This category is of particular concern in the sectors of health and insurance. For this purpose, a casualty severity list that included types of injuries and the relative assignment of Abbreviated Injury Severity (AIS) score was formulated on the basis of past earthquakes and medical literature, and monetary values assigned by US government agencies were associated with each AIS score. A further update of the present approach was reported in the works of So and Spence (2009; 2013) in which lethality rates for damage states D4 and D5 were defined according to different building vulnerability classes (Table 2.1).

<i>Vulnerability class</i>	<i>Description of class</i>	<i>Lethality rate for D4 (L4)</i>	<i>Lethality rate for D5 (L5)</i>
A	Weal masonry	0.05	0.200
B	Load-bearing masonry, unreinforced	0.0195	0.078
C	Structural masonry; pre-code reinforced concrete (RC) frame	0.0625	0.250
D*	Moderate code RC frame; concrete shear wall;	D1: 0.0625	D1: 0.250
	timber frame	D2:0.0034	D2: 0.013
E	Steel frame; high code RC	0.0695	0.278

\* Two subclasses, D1 and D2, were defined because the class D contains buildings with widely different lethality potential (RC frame and timber frame).

Table 2.1 Lethality rates (L4, L5) at damage levels, D4 and D5, for all vulnerability classes (So and Spence, 2013)



## HAZUS methodology

FEMA with the National Institute of Building Sciences (NIBS) developed the HAZUS software, that is a standardized earthquake loss estimation methodology. It consists of the main components of potential earth science hazard, direct physical damage, induced physical damage and direct economic/social loss. Starting from the first version (NIBS, 1997), several updates of the software were carried out regarding the estimation of earthquake impact, including both economic losses and population consequences (FEMA, 1999; 2003).

The latter version estimates losses at three levels of accuracy:

- Level 1, based solely on data from national databases;
- Level 2, based on professional judgment and detailed information on demographic data, buildings and other infrastructure at the local level;
- Level 3, based on detailed engineering input that develops a customized methodology designed to the specific conditions of a community.

HAZUS-MH MR4 model estimates casualties directly caused by structural or non-structural damage on the basis of four severity levels (Figure 2.7) to categorize injuries, from light injuries (Level 1) to death (Level 4). The casualty rates are obtained by revising those suggested in ATC-13 (1985) and by using limited post-earthquake fatality data. The casualty model is based on the studies of Coburn and Spence (1992), Murakami (1992) and Shiono et al. (1991) but, unlike the other approaches, the methodology is in event-tree format (Figure 2.8). In order to estimate the casualties from structural damage, the model considers a variety of inputs including the damage state probability and the building type with specific casualty rates provided for each damage state (D1-slight, D2 moderate, D3 Extensive, D4 complete without collapse, D4 complete with collapse) in combination with occupancy data and event time. The probability of suffering  $i$ -severity ( $i=1:4$ ) level for people involved in an earthquake is calculated by:

$$p_{SI} = \sum_{k=1}^5 w_{SI,k} p_k \quad (2.3)$$

where

- $p_{SI}$  is the probability to suffer an  $i$ -severity level ( $i=1:4$ );
- $p_k$  is the damage probability ( $k=1:5$ );
- $w_{SI,k}$  is the casualty rate considered for  $p_k$ .

The expected number of occupants in the  $i$  severity level ( $EN_i$ ) is calculated as the product among the number of occupants at the earthquake time ( $N_{occupants}$ ) and the probability suffering the  $i$  severity level ( $p_{SI}$ ). Casualty rates for each building typology are defined as function of severity level and damage state. As example, casualty rates for reinforced concrete moment frame structures and unreinforced masonry structures are reported in Tables 2.2-2.3 (HAZUS-HM), respectively.

Injury Severity Level	Injury Description
Severity 1	Injuries requiring basic medical aid that could be administered by paraprofessionals. These types of injuries would require bandages or observation. Some examples are: a sprain, a severe cut requiring stitches, a minor burn (first degree or second degree on a small part of the body), or a bump on the head without loss of consciousness. Injuries of lesser severity that could be self treated are not estimated by HAZUS.
Severity 2	Injuries requiring a greater degree of medical care and use of medical technology such as x-rays or surgery, but not expected to progress to a life threatening status. Some examples are third degree burns or second degree burns over large parts of the body, a bump on the head that causes loss of consciousness, fractured bone, dehydration or exposure.
Severity 3	Injuries that pose an immediate life threatening condition if not treated adequately and expeditiously. Some examples are: uncontrolled bleeding, punctured organ, other internal injuries, spinal column injuries, or crush syndrome.
Severity 4	Instantaneously killed or mortally injured

Figure 2.7 Description of injury severity levels (HAZUS methodology)

The methodology provides information for three moments of day: at 2:00 a.m. (night time scenario); at 2:00 p.m. (day time scenario) and at 5:00 p.m. (commute time scenario). The population is distributed into different occupancy categories. In Figure 2.9, there are two multipliers: the second indicates the fraction of population component present in an “occupancy” class for a particular time scenario and the first divides the population component into indoors and outdoors. Refer to FEMA (2003) for a detailed description of the variables in Figure 2.9.

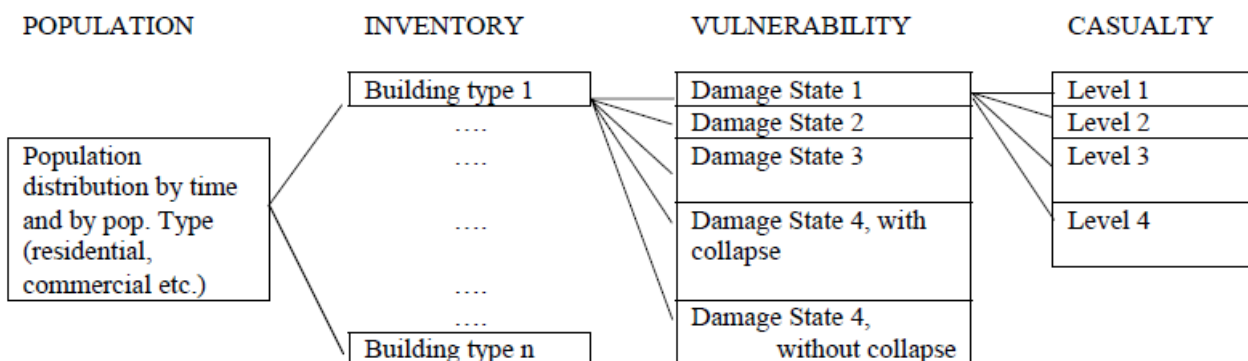


Figure 2.8 Event tree used for the estimation of casualties (HAZUS methodology)

Injury Severity	Slight damage	Moderate damage	Extensive damage	Complete damage
Severity 1	0.05	0.25	1	5* - 40**
Severity 2	-	0.03	0.1	1* - 20**
Severity 3	-	-	0.001	0.01* - 5**
Severity 4	-	-	0.001	0.01* - 10**

\*the smaller values are related with partial collapse of the buildings

\*\*the larger values are given for total collapse (the pancake type of collapse)

**Table 2.2** Casualty rates for reinforced concrete moment frame structures (HAZUS-MH)

Injury Severity	Slight damage	Moderate damage	Extensive damage	Complete damage
Severity 1	0.05	0.35	2	10* - 40**
Severity 2	-	0.04	0.2	2* - 20**
Severity 3	-	0.001	0.002	0.02* - 5**
Severity 4	-	0.001	0.002	0.02* - 10**

**Table 2.3** Casualty rates for unreinforced masonry structures (HAZUS-HM)

In the framework of "NEtwork of Research Infrastructures for European Seismology" (NERIES) project, the same methodology was applied in the ELER (Earthquake Loss Estimation Routine) software developed by Kandilli Observatory and Earthquake Research Institute (KOERI) of Bogazici University (Istanbul) and other researchers. However, the casualty rates given in HAZUS are not directly applicable to places other than USA, then alternative values for reinforced concrete and masonry buildings in Turkey were estimated by Erdik and Aydinoglu (2002) based on the casualty data from 1992 Erzincan and 1999 Kocaeli events.

Distribution of People in Census Tract			
Occupancy	2:00 a.m.	2:00 p.m.	5:00 p.m.
Indoors			
Residential	(0.999)0.99(NRES)	(0.70)0.75(DRES)	(0.70)0.5(NRES)
Commercial	(0.999)0.02(COMW)	(0.99)0.98(COMW) + (0.80)0.20(DRES) + 0.80(HOTEL) + 0.80(VISIT)	0.98[0.50(COMW) + 0.10(NRES) + 0.70(HOTEL)]
Educational		(0.90)0.80(GRADE) + 0.80(COLLEGE)	(0.80)0.50(COLLEGE)
Industrial	(0.999)0.10(INDW)	(0.90)0.80(INDW)	(0.90)0.50(INDW)
Hotels	0.999(HOTEL)	0.19(HOTEL)	0.299(HOTEL)
Outdoors			
Residential	(0.001)0.99(NRES)	(0.30)0.75(DRES)	(0.30)0.5(NRES)
Commercial	(0.001)0.02(COMW)	(0.01)0.98(COMW) + (0.20)0.20(DRES) + (0.20)VISIT + 0.50(1-PRFIL)0.05(POP)	0.02[0.50(COMW) + 0.10(NRES) + 0.70(HOTEL)] + 0.50(1-PRFIL) [0.05(POP) + 1.0(COMM)]
Educational		(0.10)0.80(GRADE) + 0.20(COLLEGE)	(0.20)0.50(COLLEGE)
Industrial	(0.001)0.10(INDW)	(0.10)0.80(INDW)	(0.10)0.50(INDW)
Hotels	0.001(HOTEL)	0.01(HOTEL)	0.001(HOTEL)
Commuting			
Commuting in cars	0.005(POP)	(PRFIL)0.05(POP)	(PRFIL)[0.05(POP) + 1.0(COMM)]
Commuting using other modes		0.50(1-PRFIL)0.05(POP)	0.50(1-PRFIL) [0.05(POP) + 1.0(COMM)]

**Figure 2.9** Default relationships for estimating population distribution (HAZUS methodology)

### “Human casualties in Earthquakes” book

A collection of studies on the estimation of human casualties was reported in Spence (2011). In the book organized into four parts, some existing casualty models such as Trendafiloski et al. (2009) for the “earthquake Loss Assessment for Response and Mitigation” (QLARM) project or Jaiswal and Wald (2010) for “Prompt Assessment of Global Earthquakes for Response” (PAGER) project were described. Moreover, significant new data and observations derived from studies relating to particular countries or regions were presented, including the work of Zuccaro and Cacace (2011).

#### Jaiswal and Wald (2010)

In the U.S. Geological Survey’s PAGER system, Jaiswal and Wald (2010) developed a country/region-specific empirical model for fatality estimation. The methodology consists of the development of fatality rate function in such a way that the total estimated deaths from all intensity levels matches the total recorded deaths. On the basis of a global catalogue of all significant worldwide earthquakes (from 1973 to 2007), a set of empirical vulnerability relationships able to provide a fatality rate as function of Modified Mercalli Intensity (MMI) is derived. The fatality rate is defined as the ratio of number of fatalities to the total population exposed at each level of shaking intensity (varies from 0 to 1). The expected number of fatalities  $E_i$  can be evaluated using the following equations:

$$E_i = \sum_j v_i(S_j)P_i(S_j) \quad (2.4)$$

$$v(S_j) = \Phi \left[ \frac{1}{\beta} \ln \left( \frac{S_j}{\theta} \right) \right] \quad (2.5)$$

where

- $S_j$  is a set of discrete values of shaking intensity at level  $j$  (e.g., 5.0; 5.5 of MMI);
- $v_i(S_j)$  is the fatality rate as function of shaking intensity  $S$  at level  $j$  for an event  $i$ ;
- $P_i(S_j)$  is the estimated population exposed to shaking intensity  $S$  at level  $j$  for an event  $i$ ;
- $\Phi$  is the standard normal cumulative distribution function;
- $\theta$  is the mean of the natural logarithm of the intensity measure;
- $\beta$  is the standard deviation of the natural logarithm of the intensity measure.

As can be seen in the (2.5), the fatality rate is expressed in terms of a two-parameter lognormal cumulative distribution ( $\beta$  and  $\theta$ ). For countries where fatality data related to historical earthquakes was available, the parameters of the distribution were obtained by minimizing the residual error (estimated vs recorded deaths) evaluated as square error (L2 norm), log-residual error (G norm) or

the combination of the previous two (L2G norm). For sake of simplicity, the expression to evaluate L2G norm is only reported:

$$\varepsilon_{3,k} = L2G \text{ norm} = \ln \left( \sqrt{\frac{1}{N} \sum_{i=1}^N (E_i - O_i)^2} \right) + \sqrt{\frac{1}{N} \sum_{i=1}^N [\ln(E_i - O_i)^2]} \quad (2.6)$$

where

- k indicates the country or a geographic location;
- N are the historical fatal earthquakes in the region k;
- $O_i$  is the number of recorded deaths for an earthquake i.

For countries where empirical data was lacking, a regionalization scheme that allows to aggregate fatal events on the basis of specific indicators able to associate countries with similar vulnerability was proposed. The scheme combines the information specific to geography, climatic similarities, building inventory and socioeconomic indicators (Jaiswal et al., 2009). Considering historical fatal earthquakes recorded between 1973 and 2007, empirical model parameters derived using country-specific or using regionalization scheme were proposed. As example, for Italy, Figure 2.10 reports the empirical fatality rates as function of MMI and the diagram showing estimated versus catalog recorded fatalities.

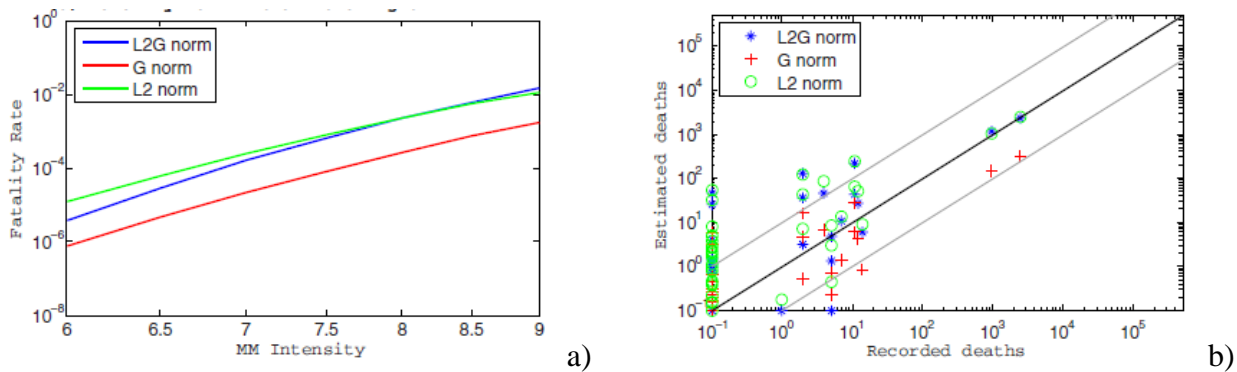


**Figure 2.10** a) Empirical fatality rates for Italy; b) Estimated and catalog recorded fatalities for Italy (Jaiswal and Wald, 2010)

Zuccaro and Cacace (2011)

The authors presented a model for the rapid estimation of casualties in Italy. Starting from the idea of Coburn and Spence (1992), a model for evaluating seismic casualties based on the data obtained from the National Institute of Statistics (ISTAT) was defined. The latter collected field data regarding the percentage of the victims per structural type and the lifestyle of the population.

In addition to the information about total population, the model is based on the evaluation of four fundamental parameters:

- mean of inhabitants by building type;
- occupancy rate by hour of the day and week;
- touristic index by town and period of the year;
- casualty percentage by building type and damage level.

On the basis of these parameters, the number of deaths ( $N_d$ ) and injured ( $N_i$ ) is then determined by the following expressions:

$$N_d = TI_c \sum_{t=1}^4 \sum_{j=1}^5 N_{t,j} NO_t QD_{t,j} \quad (2.7)$$

$$N_i = TI_c \sum_{t=1}^4 \sum_{j=1}^5 N_{t,j} NO_t QI_{t,j} \quad (2.8)$$

where

- $t$  is the building type ( $t = 1, \dots, 4$ );
- $j$  is the damage level ( $j = 1, \dots, 5$ );
- $N_{t,j}$  is the number of buildings of type  $t$  having damage level  $j$ ;
- $NO_t$  is the number of occupants (at the time of the event) by building type;
- $TI_c$  is the Touristic Index by city;
- $QD_{t,j}$  is the proportion of deaths by building type and damage level;
- $QI_{t,j}$  is the proportion of injured by building type and damage level.

The authors assumed that the number of injured and deaths is strictly correlated to the structural damage. The probability of injury or death of the building occupants is evaluated as a function of the damage levels D4 (i.e., very heavy damage) and D5 (i.e., destruction). On the basis of the observations of past events, the casualty evaluation considers also the structural typology, specifically distinguishing reinforced concrete or masonry. Table 2.4 reports the casualty percentage as a proportion of the occupants of the building, according to damage level and building structure type (“vertical structures”). As can be seen in Table 2.4, EMS-98 vulnerability classes (A, B, C, D according to Grünthal, 1998) are also considered.

Casualty percentage	Damage level						Vertical structure	Vulnerability class
	D0	D1	D2	D3	D4	D5		
QD	0	0	0	0	0.04	0.15	Masonry	A or B or C
QD	0	0	0	0	0.08	0.3	R.C.	C or D
QI	0	0	0	0	0.14	0.7	Masonry	A or B or C
QI	0	0	0	0	0.12	0.5	R.C.	C or D

**Table 2.4** Casualty percentage by damage level and building type (Zuccaro and Cacace, 2011)

The number of the occupants is dependent on the volume, the typology and the age of the building. In general, because of lack of information about the volume, the number of occupants is estimated considering the total population and the building typologies within the studied area. This estimation can vary strongly for buildings having different use classes (e.g., residential, school, industries). Because seismic casualties are dependent on the overall population density at the instant that event occurs, population mobility (i.e., from the satellite towns towards the larger urban settlements) and population variation during the month (long period), the day of the week and the hour (short period) are considered. In the paper, the investigation on “times of everyday life” performed by the ISTAT (2007) and the analysis carried out by Municipality and Province of Torino (2003) relating to main town and its satellite towns were used to evaluate population flows and the time in which the population is mainly at home or in other indoor. For the “long period” variation, it is generally seasonal due to tourist flows. Therefore, casualty estimations involving touristic villages need to consider specific information of the touristic presence through the year.

### **SYNER-G project**

Starting from the work of Coburn and Spence (1992), a model able to estimate the casualty number among the building occupants at the time of earthquake was developed in the framework of SYNER-G project (Khazai, 2013). The proposed methodology is composed of the following elements: building occupancy, damage probability matrices, seismic intensity, building-casualty type and casualty-damage ratios, that are combined as follows:

$$N_d = \sum_{t=1}^3 \sum_{d=1}^6 \sum_{i=1}^4 N_{t,d,i} CR_{t,d,i} NO_t \quad (2.9)$$

where

- $N_d$  is the number of deaths;
- $t$  is the building-casualty type;
- $d$  is the damage level (from D0 to D5);
- $i$  is the seismic intensity level;
- $N_{t,d,i}$  is the number of buildings of type  $t$  having damage level  $d$  at seismic intensity level  $i$ ;
- $CR_{t,d,i}$  is the proportion of deaths by building type, damage level and seismic intensity (i.e., Casualty Ratio);
- $NO_t$  is the number of occupants (at the time of the event) by building type  $t$

On the basis of casualty, damage and building type data collected for three large Italian earthquakes (1980 Irpinia; 1976 Friuli and 2009 L’Aquila), three “superclasses” of building typologies based on

their potential for producing casualties are defined (Figure 2.11). The Casualty Ratio (CR) is defined as the ratio of the number of people killed to the number of occupants present in collapsed buildings of a given class. Considering the data compiled from CATDAT (Daniell, 2011) for the three Italian earthquakes, Table 2.5 reports semi-empirical casualty ratios for each whole macroseismic intensity degree (from 6 to 9 of EMS-98 intensity scale), building-casualty type and damage level.

Casualty Potential	Superclass Category	Construction Typology	Description
very high	1-BC	Reinforced Concrete	Mid-rise and High-rise (> 3 story) reinforced concrete frame buildings; of in-situ reinforced filler slabs with ceramic plank fillers
high	2-BC	Stone, brick or block masonry walls with reinforced concrete floors/roofs	Field stone and Hewn stone walls; manufactured masonry units, concrete block, brick or hollow ceramic block, of three stories or more and have reinforced concrete floors. Also many of the traditional masonry buildings that have additional stories added in new materials without strengthening or supporting structure
moderate	3-BC	Stone, brick or block masonry walls with timber rubble masonry, timber or steel joist floors/roofs	Field stone and Hewn stone walls; manufactured masonry units, concrete block, brick or hollow ceramic block, of one to three stories and have reinforced concrete floors.

Figure 2.11 Building-Casualty Superclasses (SYNER-G project)

For a detailed description of the methodology used to evaluate the casualty ratios, refer to Khazai (2013). About the estimate of number of occupants, Coburn and Spence (2002) temporal occupancy model was used to obtain the population in different building types at the time of the earthquake. Furthermore, in order to take into account the variations of exposure over the day, the week and seasons, the analysis of Zuccaro and Cacace (2011) was considered for the Italian casualty model applications.

Intensity 6	D0	D1	D2	D3	D4	D5
1-BC	0	0	0	0.0011	0.0027	0.0067
2-BC	0	0	0	0.0005	0.0013	0.0033
3-BC	0	0	0	0	0.007	0.0017
Intensity 7	D0	D1	D2	D3	D4	D5
1-BC	0	0	0.009	0.0021	0.0053	0.0133
2-BC	0	0	0	0.0011	0.0027	0.0067
3-BC	0	0	0	0.0005	0.0013	0.0033
Intensity 8	D0	D1	D2	D3	D4	D5
1-BC	0	0.0009	0.0021	0.0053	0.0133	0.0333
2-BC	0	0	0.0011	0.0027	0.0067	0.0167
3-BC	0	0	0.0005	0.0013	0.0033	0.0083
Intensity 9	D0	D1	D2	D3	D4	D5
1-BC	0	0.0048	0.0073	0.0182	0.0454	0.1136
2-BC	0	0.0024	0.0036	0.091	0.0227	0.0568
3-BC	0	0.002	0.003	0.0076	0.0189	0.0473

Table 2.5 Casualty Ratios (SYNER-G project)



### “National Risk Assessment” report

In the last “National Risk Assessment” (NRA) of Italian Department of Civil Protection (DPC 2018), the probability of injuries or deaths among the building occupants is evaluated as a function of the EMS-98 damage level (Grünthal, 1998). It is assumed that the number of casualties is significant only for damage levels D4 and D5, independently from the building typology. The equations to calculate the expected number of deaths  $N_d$  or injured  $N_i$  are

$$N_d = \sum_{j=1}^n [(O_{Mj,D4} \cdot p_{d,D4} + O_{Mj,D5} \cdot p_{d,D5}) + (O_{RCj,D4} \cdot p_{d,D4} + O_{RCj,D5} \cdot p_{d,D5})] \quad (2.10)$$

$$N_i = \sum_{j=1}^n [(O_{Mj,D4} \cdot p_{i,D4} + O_{Mj,D5} \cdot p_{i,D5}) + (O_{RCj,D4} \cdot p_{i,D4} + O_{RCj,D5} \cdot p_{i,D5})] \quad (2.11)$$

where

- $n$  is the number of storey or class of storey;
- $O_{Mj,D4/D5}$ ,  $O_{RCj,D4/D5}$  is the number of occupants in building type (masonry or reinforced concrete) with number of storey equal to  $j$  or with a number of storey in the storey class  $j$  which experienced a damage level D4 or D5;
- $p_{d,D4}$ ,  $p_{d,D5}$  are the percentage of dead with respect to the occupants for D4 and D5;
- $p_{i,D4}$ ,  $p_{i,D5}$  are the percentage of injured with respect to the occupants for D4 and D5.

The percentages of dead and injured adopted in the NRA are reported in Table 2.6.

Expected Casualties	D4	D5
Dead $p_d$ (%)	1	10
Injured $p_i$ (%)	5	30

**Table 2.6** Casualty percentage for computation of human losses (NRA, 2018)

The same approach is also considered in the IRMA (Italian Risk Maps) platform, although different casualty percentages could be added by the user.

## 2.2 Direct economic losses

A proper quantification of the economic losses is of paramount importance for governments to define intervention priority for post-earthquake reconstruction phase or policies for disaster prevention and management.

Economic impact of earthquakes can be usually categorized in two main categories:

- loss caused by damage to buildings (direct loss);
- loss caused by interruption of economic activities (indirect loss).

Economic loss estimation can be performed using statistical techniques on data from past earthquakes to develop specific “Loss Functions”. Otherwise, because information about existing economic loss data is scarce, loss functions can be estimated by using analytical procedures (e.g., PBEE approaches). About the quantification of economic losses, many different measures in the framework of PBEE approaches can be used such as average economic loss for a given earthquake scenario; expected economic loss for a family of earthquake scenarios; expected annual loss; etc., (ATC, 2003). In Italy, the “Guidelines for the seismic risk classification of constructions” (D.M. 28/2/2017) consider Expected Annual Losses (EAL) to define risk classes of the buildings. Indeed, two indices are used in the seismic risk classification: the one associated to the Safety Index of the structure at the Limit State of Life Safety (SI-LS, according to the NTC-2018) and the one related to the EAL that estimates the building behavior in terms of expected economic annual losses. The latter index is evaluated as the area above the EAL curve obtained computing the performance of the structure for different earthquake intensities/return periods ( $T_r$ ), in the reference life of the construction (in terms of the mean annual frequency of exceedance,  $\lambda=1/T_r$ ) and the relevant repair costs, %RC and, connecting the points ( $\lambda$ , %RC) representative of each limit state (Cosenza et al., 2018). Large number of studies dealing with economic loss estimation were published at the building level (e.g., Welch et al., 2012; Cosenza et al., 2018;) or on a regional scale (e.g., Bal et al., 2008; Silva et al., 2013).

In the following, direct economic losses (i.e., the repair costs of building components) are mainly treated. These losses are, essentially, the translation of physical damage (e.g., EMS-98 damage states, Grünthal, 1998) into monetary values using local estimates of repair and reconstruction costs and they are generally quantified by the loss ratio (i.e., repair cost divided by replacement cost).

### HAZUS methodology

In the first version of FEMA & NIBS project, the process for direct economic loss estimation to all buildings in a region was defined according to the schema reported in Figure 2.12 (Kircher et al., 1997). Loss assessment depends on “building occupancy distribution” and “model building type”. The methodology provides values of building repair and replacement cost for each combination of model type and occupancy class. These values are defined for structural system, non-structural components divided in drift-sensitive (e.g., partitions, exterior walls and ornamentation) and acceleration-sensitive (e.g., ceilings, mechanical and electrical equipment, piping and elevators) and contents of the building. The costs for slight, moderate, extensive and complete damage states are defined as fraction of replacement cost of the building (Table 2.7) on the basis of Means data (Jackson, 1994). It is worth noting that only 50% of all contents is susceptible to damage (i.e., the percentage is halved than that related to other components).

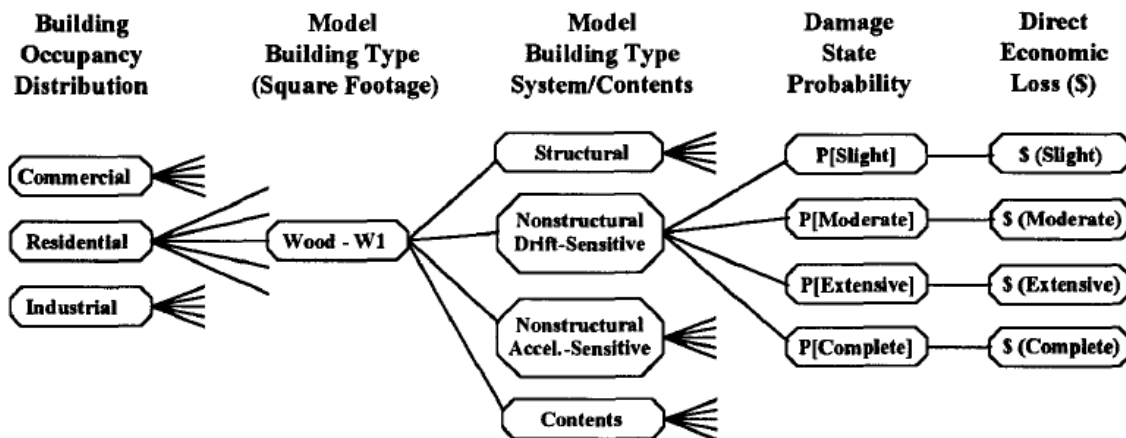


Figure 2.12 Logic tree for calculation of direct economic losses (Kircher et al., 1997)

The estimation of direct economic loss due to structural damage for a given building type is carried out according to the following equation:

$$\text{\$Loss}(\text{Structural}) = \sqrt{\sum_i^{\text{damage-states}} P_i[\text{SD}] \text{\$R}_i[\text{SD}]} \quad (2.12)$$

where

- $\text{\$R}_i[\text{SD}]$  are structural system loss rates for damage state  $i$ ;
- $P_i[\text{SD}]$  is the probability of structural damage for damage state  $i$ .

Similar equations are used to calculate losses due to non-structural components and contents. The total loss for a given building type and occupancy class is obtained from sum of structural, non-structural and contents losses. The total loss to all buildings is the sum of the individual losses to each type of buildings used for all occupancy classes.

Damage state	Structural system	Non structural (drift sensitive)	Non structural (acceleration sensitive)	Contents
<i>Slight</i>	2%	2%	2%	1%
<i>Moderate</i>	10%	10%	10%	5%
<i>Extensive</i>	50%	50%	50%	25%
<i>Complete</i>	100%	100%	100%	50%

**Table 2.7** Direct economic loss as a percentage of building replacement cost by damage state (HAZUS methodology)

In the updated version, HAZUS-HM MR4 (FEMA, 2003), different methodologies for the building loss estimation are provided considering the following elements:

- Building Repair and Replacement Costs (for structural and non-structural components);
- Building Contents Losses (e.g., furniture, computers and other supplies);
- Building Inventory Losses.

Regarding the first method, input data consist of direct physical damage estimates in terms of probabilities of being in each damage state, for each structural type and occupancy class. These damage state probabilities are then converted to monetary losses using inventory information and economic data. About the occupancy class, a 28-category occupancy classification (Figure 2.13) is defined. Then, for structural damage, losses are calculated as follows:

$$CS_{ds,i} = BRC_i \cdot \sum_{i=1}^{33} PMBTSTR_{ds,i} \cdot RCS_{ds,i} \quad (2.13)$$

$$CS_i = \sum_{ds=2}^5 CS_{ds,i} \quad (2.14)$$

where

- $CS_{ds,i}$  is the cost of structural damage (repair and replacement costs) for damage state  $ds$  and occupancy  $i$ ;
- $BRC_j$  is the building replacement cost of occupancy  $i$ ;
- $PMBTSTR_{ds,i}$  is the probability of occupancy  $i$  being in structural damage state  $ds$ ;
- $RCS_{ds,i}$  is the structural repair and replacement ratio for occupancy  $i$  in damage state  $ds$ .

The values of repair cost ratio for structural damage related to all occupancy classes are shown in Figure 2.13 (R.S. Means, 2002). For sake of simplicity, only structural component damage is considered but similar calculation is performed for non-structural damage. For a detailed description, refer to Chapter 15 of the FEMA (2003).

No.	Label	Occupancy Class	Structural Damage State			
			Slight	Moderate	Extensive	Complete
<b>Residential</b>						
1	RES1	Single Family Dwelling	0.5	2.3	11.7	23.4
2	RES2	Mobile Home	0.4	2.4	7.3	24.4
3-8	RES3a-f	Multi Family Dwelling	0.3	1.4	6.9	13.8
9	RES4	Temporary Lodging	0.2	1.4	6.8	13.6
10	RES5	Institutional Dormitory	0.4	1.9	9.4	18.8
11	RES6	Nursing Home	0.4	1.8	9.2	18.4
<b>Commercial</b>						
12	COM1	Retail Trade	0.6	2.9	14.7	29.4
13	COM2	Wholesale Trade	0.6	3.2	16.2	32.4
14	COM3	Personal and Repair Services	0.3	1.6	8.1	16.2
15	COM4	Professional/Technical/ Business Services	0.4	1.9	9.6	19.2
16	COM5	Banks/Financial Institutions	0.3	1.4	6.9	13.8
17	COM6	Hospital	0.2	1.4	7.0	14.0
18	COM7	Medical Office/Clinic	0.3	1.4	7.2	14.4
19	COM8	Entertainment & Recreation	0.2	1.0	5.0	10.0
20	COM9	Theaters	0.3	1.2	6.1	12.2
21	COM10	Parking	1.3	6.1	30.4	60.9
<b>Industrial</b>						
22	IND1	Heavy	0.4	1.6	7.8	15.7
23	IND2	Light	0.4	1.6	7.8	15.7
24	IND3	Food/Drugs/Chemicals	0.4	1.6	7.8	15.7
25	IND4	Metals/Minerals Processing	0.4	1.6	7.8	15.7
26	IND5	High Technology	0.4	1.6	7.8	15.7
27	IND6	Construction	0.4	1.6	7.8	15.7
<b>Agriculture</b>						
28	AGR1	Agriculture	0.8	4.6	23.1	46.2
<b>Religion/Non-Profit</b>						
29	REL1	Church/Membership Organization	0.3	2.0	9.9	19.8
<b>Government</b>						
30	GOV1	General Services	0.3	1.8	9.0	17.9
31	GOV2	Emergency Response	0.3	1.5	7.7	15.3
<b>Education</b>						
32	EDU1	Schools/Libraries	0.4	1.9	9.5	18.9
33	EDU2	Colleges/Universities	0.2	1.1	5.5	11.0

Figure 2.13 Structural repair cost ratios in % of building replacement cost (HAZUS methodology)

## ATC-58 2012

In the PBEE framework, a refined methodology to predict economic losses was developed by FEMA (ATC-58 2012a). In order to perform the practical implementation, a user-friendly software, called “Performance Assessment Calculation Tool” (PACT; ATC-58 2012b; Haselton and Baker, 2018) was included. This tool allows to capture building inventory data, input a given earthquake shaking probability or intensity, apply specific fragilities and consequences to each building component, and present the results in a defined format. The aim of FEMA P-58 project is the development of a methodology for seismic performance assessment of individual buildings that properly accounts for

uncertainty and communicates performance in accurate ways for the decision-making needs of stakeholders. FEMA P-58 reports a state-of-the-art seismic loss assessment method for buildings considering damage and loss of each type of component. It proposed a database of fragility functions and consequence functions for 764 types of components.

In the FEMA P-58 method, seismic loss is calculated by the following steps (e.g., Del Vecchio et al., 2018):

- Select proper ground motions as input. Subsequently, calculate the structural responses, including the peak interstorey drift ratios, peak floor accelerations, etc;
- Calculate the repair cost of each building component: first evaluate its damage state according to its fragility functions (Figure 2.14a) and, subsequently, calculate its repair cost using the corresponding consequence functions (Figure 2.14b) of the component;
- Obtain the total seismic loss of the entire building by summing the repair costs of all components. The total seismic loss considers the uncertainties of the structural responses, component fragility functions, and consequence functions by utilizing the Monte Carlo simulation.

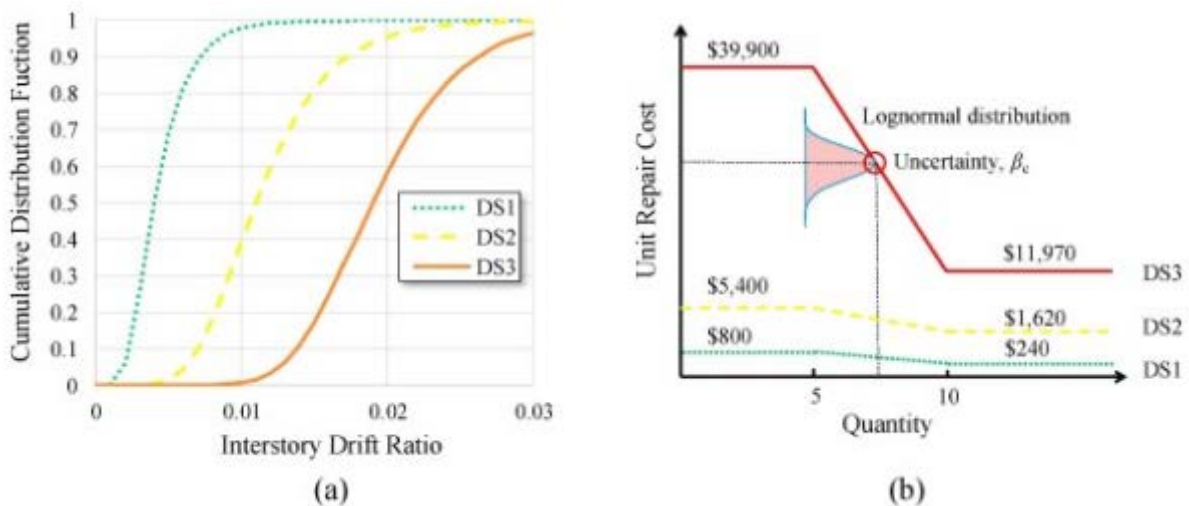


**Figure 2.14** a) Fragility functions, b) consequence functions of a typical gypsum wall board (GWB) partition component (ATC-58 2012)

### PAGER project

In PAGER project, economic losses are estimated on the basis of economic exposure at different levels of shaking intensity by considering data available for global earthquakes from 1980 to 2007 (Jaiswal and Wald, 2011). The procedure is similar to the empirical fatality estimation methodology reported in Section 2.1. Indeed, casualties are estimated using the total human exposure based on fatality rates and, in the same way, the development of a country or region-specific economic model is based on a loss ratio function to consider the economic exposure. The economic loss ratio  $r$  is defined as the economic loss normalized by the economic exposure and, as for the casualty estimation, is parameterized in terms of shaking intensity  $S$  using a two-parameter lognormal cumulative distribution function ( $\theta$  and  $\beta$ ):

$$r(S) = \Phi \left[ \frac{1}{\beta} \ln \left( \frac{S}{\theta} \right) \right] \quad (2.15)$$

The total economic exposure (*Eco.Exposure*) at a given intensity  $S$  can be computed as follows:

$$Eco.Exposure_S = \alpha_{region} \cdot Total\ GDP_{region,S} \quad (2.16)$$

where

- Total  $GDP_{region,S}$  is the total Gross Domestic Product (GDP) exposed at each shaking intensity  $S$  evaluated by multiplying the per-capita GDP of the country by the total population exposed at that shaking intensity level  $S$ ;
- $\alpha_{region}$  is an exposure correction factor (based on the ratio of per capita wealth to per capita GDP for each country).

The total expected economic loss caused by an earthquake is estimated by summing the product of total economic exposure and loss ratio at each shaking intensity level. In order to determine distribution parameters,  $\theta$  and  $\beta$ , for each country or region, the same procedure considered for casualty estimates is applied in which  $O_i$  is the recorded economic loss (in millions of USD taken from the Munich Re catalog; NatCatSERVICE, 2008) for the earthquake  $i$ . As example, for Italy, Figure 2.15 reports the economic loss ratio as function of MMI and diagram showing estimated versus catalog recorded historical earthquake losses.

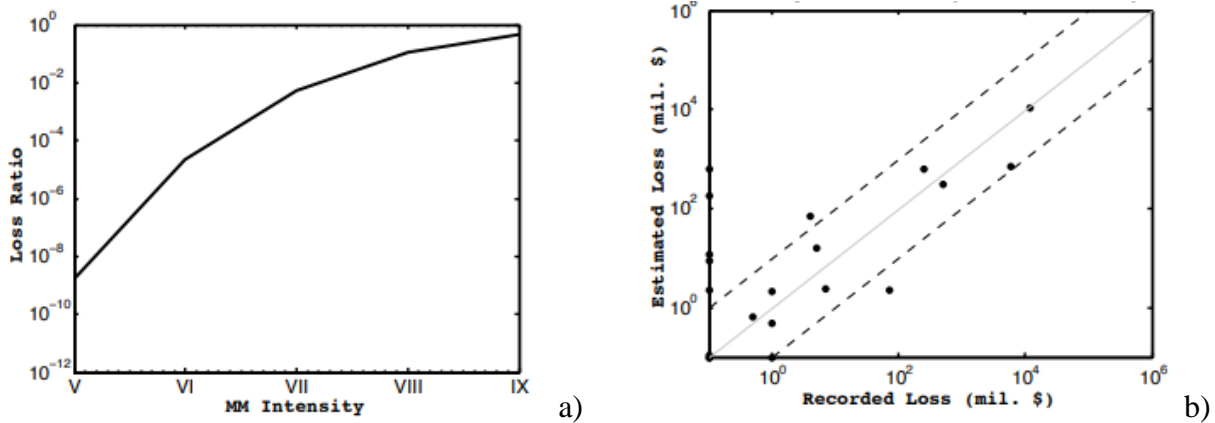


**Figure 2.15** a) Economic loss ratio for Italy; b) Estimated and catalog recorded historical earthquake losses (Jaiswal and Wald, 2011)

### KOERI method in the NERIES project

In the framework of NERIES project, a three-level methodology for the rapid estimation of earthquake shaking and losses in the Euro-Mediterranean region was developed using the ELER software (Erdik et al., 2010). In particular, the estimates of the direct economic losses are quantified in terms of Loss Ratios (LR) defined as the ratio between repair and reconstruction costs. EMS-98 damage states (from D1 to D5) are considered and the loss ratio is expressed in terms of percentage of the building replacement value (Table 2.8). ELER computes the monetary value of direct economic losses by multiplying the loss ratios with the total building cost for each building type (defined using RISK-UE, HAZUS or EMS-98 taxonomy), according to the following equation:

$$Loss(Btype, D_k) = LR(D_k) \times RC(Btype) \quad (2.17)$$

where

- LR is the loss ratio as function of the building's damage states,  $D_k$  ( $k=1-5$ );
- RC is the replacement cost defined for each building type (Btype) in the building database.

EMS-98 damage state	1	2	3	4	5
Loss ratio (LR)	5%	20%	50%	80%	100%

**Table 2.8** Loss ratio corresponding to each damage (NERIES project)



## ITALIAN APPROACHES

As for the Italian models, in the framework of the GEM project, the paper D’Ayala et al. (2015) reports some of the main studies based on past earthquake data, such as Milutinovic and Trendafiloski (2003), Goretti and Di Pasquale (2004), Di Pasquale et al. (2005) and Dolce et al. (2006). The latter developed a methodology for evaluating economic losses due to damage of the building stock. The authors combined the Damage Probability Matrices (DPM, Dolce et al., 2003) that give the probability to observe different damage levels  $L_d$  for each vulnerability class  $V$ , given a seismic intensity  $I$  with the probability of the relative repair cost ( $C_{r,r}$ ) relevant to the damage levels, according to the following expression:

$$\text{Prob}[C_{r,r} | I] = \sum_{L_d=1}^5 \sum_{V=A}^D \text{Prob}_{L_d}[C_{r,r} | L_d] \cdot \text{Prob}_V[L_d | V, I] \quad (2.18)$$

The expression allows to obtain the total probability for each considered value of repair cost  $C_{r,r}$ , given a macroseismic intensity  $I$ . EMS-98 damage levels (1-5) and vulnerability classes  $V$  (A,B,C,D) are considered. The economic damage index  $C_{r,r}$  (relative repair cost) is evaluated as the ratio of building repair and replacement cost, thus ranging between 0 and 1.  $C_{r,r}$  values were derived from the model of Masi et al. (2002), by considering the data (more than 50,000 buildings) collected after the 1997 Umbria-Marche and 1998 Pollino earthquake (Di Pasquale et al., 1998; Di Pasquale and Goretti, 2001). It is worth noting that Pasquale and Goretti (2001) proposed repair cost functions by assuming a standard normal distribution of  $C_{r,r}$ . On the contrary, Masi et al. (2002) and Dolce et al. (2006) developed curves of the  $C_{r,r}$ , by adopting the standard Beta distribution. Figure 2.16 shows the cumulative density function (CDF) of the relative repair cost, relevant to the damage levels. These curves indicate that  $C_{r,r}$  is dependent only on damage level, as reported also in Eq. (2.18).

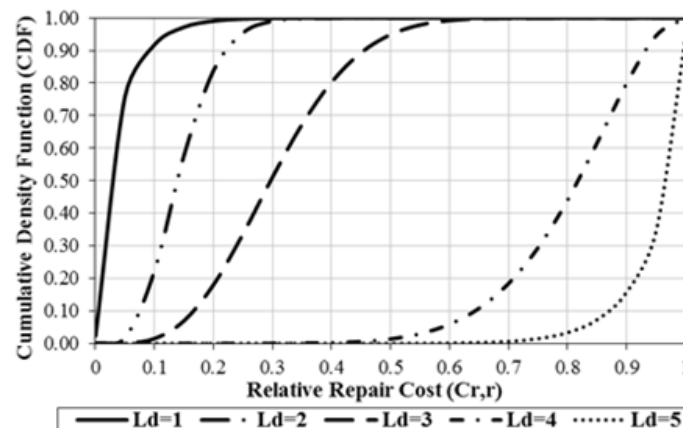


Figure 2.16 Cumulative density function CDF of the relative repair cost (Dolce et al., 2006)

In the last “National risk assessment” (DPC, 2018), the total direct economic losses are evaluated on the basis of loss parameters related to damage repair. The economic losses are a function of the damage level and the corresponding repair cost, according to the following equation:

$$L = CU \left( \sum_{j=1}^{np} \sum_{k=1}^5 A_{M,j} p_{M,k} c_k + \sum_{j=1}^{np} \sum_{k=1}^5 A_{RC,j} p_{RC,k} c_k \right) \quad (2.19)$$

where

- $n$  is the number of storey or class of storey;
- $CU$  is unitary cost of replacement of a building (Euro/m<sup>2</sup>), including technical expenses and VAT;
- $A_{M/RC,j}$  is the built area of a building type (Masonry or Reinforced Concrete) with number of stories equal to  $j$  or with a number of storey in the storey class  $j$ ;
- $P_{M/RC,k}$  is the damage probability of a building type (Masonry or Reinforced Concrete) to experience structural damage state  $k$ ;
- $c_k$  is the percentage cost of repair or replacement (with respect to  $CU$ ) for each structural damage state  $k$ .

On the basis of data collected during the reconstruction process following recent Italian earthquakes (e.g., Dolce and Manfredi, 2015; Dolce and Goretti 2015; Di Ludovico et al. 2017a, b), the percentages assumed for  $c_k$  for each damage level are reported in Table 2.9, considered also in IRMA platform.

CU	% cost	D1	D2	D3	D4	D5
1350	Default_Min	2	10	30	60	100
1350	Default_Max	5	20	45	80	100

**Table 2.9** Cost parameters used for computation of direct economic losses (IRMA platform)

Finally, many authors provided approaches for estimating the economic losses and percentages of the repair cost evaluated from observed data. An overview of the recent works carried out on the evaluation of economic impact is reported in the proceedings of the XVIII “L’Ingegneria Sismica in Italia” conference (ANIDIS, 2019). A special session “Loss-assessment and analysis of post-earthquake reconstruction costs” was devoted to the studies based on the comparison of available loss-assessment methodologies, the analysis of repair and replacement costs and other aspects. For instance, on the basis of the data collected on residential RC buildings damaged by 2009 L’Aquila earthquake, Di Ludovico et al. (2019) presented the repair costs (in terms of percentage of demolition and reconstruction cost) for different usability rating (specifically, B-C or E usability rating according to AeDES form; Baggio et al., 2007) and different damage states (EMS-98 scale).

## 2.3 Unusability

A further measure of the impact of earthquakes very useful for emergency planning and management is the number of unusable buildings. The estimation of expected unusability is fundamental to evaluate the number of homeless that need to short- or long- shelter. These quantities allow to evaluate the costs relevant to the temporary shelter and dwelling solutions. In fact, while the number of people seeking short-term shelter is important to emergency organization, the estimation of long-term homeless is of great concern to local governments. Generally, the number of unusable buildings is evaluated on the basis of data available from past earthquakes. After a seismic event, a field survey of building usability is carried out by expert technicians through the compilation of inspection forms to evaluate if the people can come back to their houses. In Italy, until the late '90, post-earthquake surveys were carried out using specific formats prepared by the National Group for the Defence against Earthquakes (GNDT). Later on, a specific survey tool was developed by the GNDT and the National Seismic Survey (SSN) for “damage assessment, short term countermeasures for damage limitation and evaluation of the post-earthquake usability of ordinary buildings”, referred to as AeDES form (Baggio et al., 2007). In addition to the usability evaluation, the form enables the collection of geometrical and structural information related to building vulnerability, and damage data. In other countries, the survey form considers only the observed damage and poor data are collected about the vulnerability. As an example, in Greece (Anagnostopoulos and Moretti, 2008) and Japan (Goretti and Inukai, 2002), post-earthquake usability considers two phases: one rapid aims at identifying buildings clearly usable or unusable for short-term use and one detailed is carried out on the remaining buildings requiring a more accurate survey for the long-term use. Refer to Masi et al. (2016) for a detailed overview of the survey forms adopted in several countries and the role of vulnerability in the final usability evaluation. Then, AeDES form represents a unique tool that allows to collect a great amount of information on the surveyed building stock. In this context, considering the large quantity of data available from past Italian earthquakes, a web-based platform Da.D.O. (Observed Damage Database) was developed by the DPC with the support of Eucentre Foundation in order to collect and catalog the information surveyed on the field (Dolce et al., 2019).

In this section, after the description of the HAZUS methodology (FEMA, 2003), the percentages of unusability proposed in the main Italian studies have been examined. These studies estimate the number of unusable buildings as function of damage level (generally, according to EMS-98 classification) and building typology.

## HAZUS methodology

The methodology developed by HAZUS considers the estimation of unusable buildings (called, “loss of habitability”) with the main objective to evaluate the number of displaced households (long-term shelter) and the number of people requiring only short-term shelter. The estimated number of uninhabitable dwelling units is calculated by combining the number of uninhabitable units due to actual structural damage, and the number of damaged units that are perceived to be uninhabitable by their occupants. Considering the residential occupancy inventory, building unusability is estimated directly from building damage and a distinction between single- and multi- family class is carried out. A different percentage of uninhabitable dwelling units need to be considered for single- and multi-family structures due to perception of people about home safety. Indeed, the renters of a multi-family structure perceive moderately damaged building as uninhabitable, instead those living in single-family homes tolerate much more damage and continue to live in their home. On the basis of previous work (Perkins, 1992), HAZUS proposed the following expressions to evaluate the number of unusable buildings:

$$\%SF = w_{SFM} \cdot \%SFM + w_{SFE} \cdot \%SFE + w_{SFC} \cdot \%SFC \quad (2.20)$$

$$\%MF = w_{MFM} \cdot \%MFM + w_{MFE} \cdot \%MFE + w_{MFC} \cdot \%MFC \quad (2.21)$$

where

- %SF is the percentage of unusability/uninhabitability for Single-Family Dwelling Units;
- %MF is the percentage of unusability/uninhabitability for Multi-Family Dwelling Units;
- %SFM, %SFE and %SFC is the damage state probability for moderate, extensive and complete structural damage in the single-family residential occupancy class, respectively;
- %MFM, %MFE and %MFC is the damage state probability for moderate, extensive and complete structural damage state in the multi-family residential occupancy class, respectively;
- $w_{SFM}$ ,  $w_{SFE}$  and  $w_{SFC}$  are the weight factor for moderate, extensive and complete structural damage state in the single-family residential occupancy class, respectively;
- $w_{MFM}$ ,  $w_{MFE}$  and  $w_{MFC}$  are the weight factor for moderate, extensive and complete structural damage state in the multi-family residential occupancy class, respectively.

The proposed methodology considers all dwelling units located in buildings with complete damage state to be uninhabitable. Table 2.10 reports default values that can be change by users. At this point, by applying an occupancy rate, the total number of displaced households can be calculated.

<b>Weigh Factor</b>	<b>Default Value</b>
WSFM	0.0
WSFE	0.0
WSFC	1.0
WMFM	0.0
WMFE	0.9
WMFC	1.0

**Table 2.10** Default values (HAZUS methodology)

## ITALIAN APPROACHES

### Lucantoni et al. (2001)

Starting from the indices reported in Bramerini et al. (1995) based on the statistics related to Italy, the authors proposed the following percentages related to unusable and collapsed buildings as a function of damage state:

- 40% of the buildings with damage state 3 and 100% of buildings with damage states 4 and 5 are considered unusable;
- 100 % of the buildings with damage state 5 is considered collapsed.

In the framework of the RISK-UE project (Monroux and LeBrun, 2006), Bramerini et al. (1995) considered the number of casualties and severely injured equal to 30% of the population living in collapsed buildings (i.e., with damage state 5) and the number of homeless equal to 100% of the population living in unusable buildings.

### Masi et al. (2006)

On the basis of the work of Di Pasquale and Goretti (2001) where data of past Italian earthquakes (among which 1980 Irpinia, 1984 Abruzzo, 1990 Sicilia, 1997 Umbria-Marche, 1998 Pollino, 2000 Monte Amiata) were analysed, the authors proposed an usability table (Table 2.11) aimed at taking into account both damage level and building type (according to the EMS-98 vulnerability classes) in the estimation of unusable buildings (Chiauzzi et al., 2018).

<b>Vulnerability Classes</b>	<b>Damage Level (EMS-98)</b>					
	<b>L<sub>d</sub>=0</b>	<b>L<sub>d</sub>=1</b>	<b>L<sub>d</sub>=2</b>	<b>L<sub>d</sub>=3</b>	<b>L<sub>d</sub>=4</b>	<b>L<sub>d</sub>=5</b>
<b>A</b>	0%	10%	30%	82%	100%	100%
<b>B</b>	0%	5%	23%	75%	100%	100%
<b>C, D (masonry buildings)</b>	0%	2%	18%	64%	100%	100%
<b>C, D (RC buildings)</b>	0%	0%	14%	38%	100%	100%

**Table 2.11** Percentage of unusable buildings as function of damage level and vulnerability class (Chiauzzi et al., 2018)

Zuccaro and Cacace (2011)

In the work related to the casualty model in Italy, Zuccaro and Cacace (2011) proposed the percentages to estimate the “unsafe” buildings for the following evaluation of homeless. Using the data of a wide sample of buildings surveyed after past Italian events, the authors considered that the probability of having unsafe buildings depends only on the building damage and not on the building typology (Table 2.12).

Damage level	0	1	2	3	4	5
% of unsafe buildings	2%	5%	10%	50%	100%	100%

**Table 2.12** Percentage of unsafe buildings as a function of damage level (Zuccaro and Cacace, 2011)

Cavalieri et al. (2012)

Within the research project SYNER-G (Khazai, 2013), the authors presented a model to evaluate social losses by integrating multiple infrastructural systems within a consistent computational framework. About the building usability, a simplified semi-empirical approach as a function of the severity of observed damage to structural and non-structural elements was developed on the basis of a detailed survey of 305 buildings in the Pettino after the 2009 L’Aquila earthquake (Elefante et al., 2011). In the proposed approach, the six usability classes (from A, usable buildings, to F, unusable building because of external risk) of AeDES form (Baggio et al., 2007) are reduced to three usability classes:

- buildings fully usable (FU) corresponding to AeDES rating A;
- buildings partially usable (PU) corresponding to AeDES ratings B and C;
- buildings immediately non-usable (NU) corresponding to AeDES ratings D, E and F.

Moreover, the six damage states (DS0-DS5) are reduced to three (None, Yield, Collapse). On the basis of the Pettino database, usability ratios (URs) for buildings are evaluated for each of the three usability classes as a function of the three damage states (Table 2.13).

UR	Damage state		
	None	Yield	Collapse
FU	0.87	0.22	0.00
PU	0.13	0.25	0.02
NU	0.00	0.53	0.98

**Table 2.13** Usability ratios (SYNER-G project)

In addition to the usability, the authors consider also the habitability of the buildings in order to evaluate the number of displaced people. Non-usable buildings are assumed to be non-habitable. Partially usable and fully usable buildings can be classified as non-habitable depending on the level of residual service in the utilities and the prevailing weather conditions at the time of impact.

“National risk assessment” report

In addition to casualties and economic losses reported in previous sections, the last “National risk assessment”, NRA (DPC, 2018) proposed also an estimation of the unusable and collapsed buildings (or dwellings). The number of unsafe buildings is evaluated on the basis of the damage distribution and building inventory. In particular, usable buildings (Us), among the damaged ones, are those affected by very slight damage, while unusable buildings are distinguished in two sub-categories, namely unusable buildings in the short term  $UnB_{st}$  (due to light or moderate damage) and unusable buildings in the long term  $UnB_{lt}$  (due to more severe damage). The equations to estimate unusable buildings are:

$$Us = \sum_{i=1}^5 (N_{Mi} u_{usk}) + \sum_{i=1}^5 (N_{RCi} u_{usk}) \quad (2.22)$$

$$UnB_{st} = \sum_{i=1}^5 (N_{Mi} u_{stk}) + \sum_{i=1}^5 (N_{RCi} u_{stk}) \quad (2.23)$$

$$UnB_{lt} = \sum_{i=1}^5 (N_{Mi} u_{ltk}) + \sum_{i=1}^5 (N_{RCi} u_{ltk}) \quad (2.24)$$

where

- $N_{M/RCi}$  is the number of masonry/RC buildings that experience structural damage level k;
- $u_{usk}$  is the percentage of usable buildings for each structural damage level k;
- $u_{stk}$  ( $u_{ltk}$ ) is the percentage of unsafe buildings in the short (long) term for each structural damage level k.

The percentages of usable and unsafe buildings as a function only of the damage level are reported in Table 2.14. In this approach, same percentages are adopted for different building typologies. The expected number of collapsed buildings is evaluated by considering 100% of buildings with damage state D5.

% Unsafe buildings	D1	D2	D3	D4	D5
$u_{us}$	100	60	0	0	0
$u_{st}$	0	40	40	0	0
$u_{lt}$	0	0	60	100	0

**Table 2.14** Percentages of usable and unsafe buildings (NRA, 2018)

## References

- Anagnostopoulos S.A. and Moretti M., (2008) Post-earthquake emergency assessment of building damage, safety and usability - Part 1: Organization. *Soil Dyn. Earthquake Eng.*, 28, 223-232.
- ANIDIS (2019) Atti del XVIII CONVEGNO ANIDIS “L’Ingegneria Sismica in Italia”. Ascoli Piceno
- Aslani H., and Miranda E., (2005) Probabilistic Earthquake Loss Estimation and Loss Disaggregation in Buildings, Report No. 157. Stanford, CA: John A. Blume Earthquake Engineering Center, Stanford University.
- ATC, (1985) Earthquake damage evaluation data for California. Applied Technology Council Report ATC-13, Redwood City, California, USA. 492p
- ATC, (2003) Procs. of FEMA-Funded Workshop on Communicating Earthquake Risk, Report ATC-58-1, Applied Technology Council, Redwood City, CA.
- ATC 58, (2012a) Seismic Performance Assessment of Buildings: Volume 1 (Methodology). Redwood City, California.
- ATC 58, (2012b) Seismic Performance Assessment of Buildings: Volume 2 (Implementation). Redwood City, California.
- Baggio C., Bernardini A., Colozza R., Corazza L., Della Bella M., Di Pasquale G., Dolce M., Goretti A., Martinelli A., Orsini G., Papa F., Zuccaro G., (2007) Field manual for post-earthquake damage and safety assessment and short term countermeasures (AeDES). In: EUR 22868 EN – Joint Research Centre – Institute for the Protection and Security of the Citizen, Artur V.P., Taucer F. (Eds.), Luxembourg: Office for Official Publications of the European Communities 2007 – 100 pp.- Eur scientific and technical research series – ISSN 1018-5593
- Bal I. E., Crowley H., Pinho R., (2008) Displacement-Based Earthquake Loss Assessment for an Earthquake Scenario in Istanbul. *Journal of Earthquake Engineering* 12(SUPPL. 2):12–22.
- Bramerini F., Di Pasquale G., Orsini G., Pugliese A., Romeo R., Sabetta F., (1995) Rischio sismico del territorio italiano. Proposta per una metodologia e risultati preliminari. SSN/RT/95/01. (In Italian).
- Calvi G.M., Pinho R., (2004) LESSLOSS-a European integrated project on risk mitigation for earthquakes and landslides. IUSS Press, Pavia
- Cavalieri F., Franchin P., Gehl P., Khazai B., (2012) Quantitative assessment of social losses based on physical damage and interaction with infrastructural systems *Earthquake Engineering & Structural Dynamics*, 41(11), 1569-1589.
- Chiauzzi L., Masi A., Samela C., Ventura G., (2018) Seismic risk assessment of residential buildings in Basilicata region (Southern Italy). *Structural 217 - maggio/giugno2018 - paper12 - ISSN 2282-3794 DELETTERA WP DOI 10.12917/STRU217.12* On lite at: <https://doi.org/10.12917/STRU217.12> (in Italian)
- Coburn A. and Spence R., (1992) *Earthquake Protection*. John Wiley & Sons Ltd., Chichester, England.
- Coburn, A. and Spence R., (2002) *Earthquake Protection (Second Edition)*, John Wiley and Sons Ltd., Chichester, England.
- Cosenza E., Del Vecchio C., Di Ludovico M., Dolce M., Moroni C., Prota A., Renzi E., ( 2018) The Italian Guidelines for Seismic Risk Classification of Constructions: Technical Principles and Validation. *Bulletin of Earthquake Engineering* 16:5905–5935 <https://doi.org/10.1007/s10518-018-0431-8>
- D.M. 28/02/2017, n. 58, integrato con il D.M. 07/03/2017, n. 65, Linee Guida per la classificazione del rischio sismico delle costruzioni.
- D’Ayala D., Meslem A., Vamvatsikos D., Porter K., Rossetto T., (2015) Guidelines for Analytical Vulnerability Assessment - Low/Mid-Rise, Vulnerability Global Component Project. <https://www.globalquakemodel.org/>
- Daniell J.E., (2011) Open source procedure for assessment of loss using global earthquake modelling software (OPAL). *Nat Hazards Earth Syst Sci* 11:1885–1900
- Del Vecchio C., Di Ludovico M., Pampanin S., Prota A., (2018) Repair Costs of Existing RC Buildings Damaged by the L’Aquila Earthquake and Comparison with FEMA P-58 Predictions. *Earthquake Spectra*, Volume 34, No. 1, pages 237–263, February 2018; © 2018, Earthquake Engineering Research Institute
- Di Ludovico M., Prota A., Moroni C., Manfredi G., Dolce M., (2017a) Reconstruction process of damaged residential buildings outside the historical centres after L’Aquila earthquake-part I: “light damage” reconstruction. *Bull Earthquake Eng.* doi:10.1007/s10518-016-9877-8.



- Di Ludovico M., Prota A., Moroni C., Manfredi G., Dolce M., (2017b) Reconstruction process of damaged residential buildings outside historical centres after the L'Aquila earthquake-part II: "heavy damage" reconstruction. *Bull Earthquake Eng.* doi:10.1007/s10518-016-9979-3.
- Di Ludovico M., De Martino G., Prota A., Manfredi G., (2019). Empirical damage and repair costs for the assesemnt of seismic loss scenarios. XVIII Conference Nazionale ANIDIS-Ascoli Piceno (in Italian)
- Di Pasquale G., Orsini G., Serra C., (1998) Assessment of the economic losses from the GNDT-DPC-SSN safety evaluation forms. In: Proc. of the international workshop on measures of seismic damage to masonry buildings.
- Di Pasquale G., Goretti A., (2001) Vulnerabilità funzionale ed economica degli edifici residenziali colpiti dai recenti eventi sismici italiana. X Congresso Nazionale ANIDIS-2001-Potenza-Matera
- Di Pasquale G., Orsini G., Romeo R.W., (2005) New Developments in Seismic Risk Assessment in Italy. *Bulletin of Earthquake Engineering*, 3:101–128-DOI 10.1007/s10518-005-0202-1
- Dolce M., Masi A., Marino M., Vona M., (2003) Earthquake damage scenarios of Potenza town (Southern Italy) including site effects. *Bulletin of Earthquake Engineering* 1(1):115–140
- Dolce M., Kappos A.J., Masi A., Penelis G., Vona M., (2006) Vulnerability assessment and earthquake scenarios of the building stock of Potenza (Southern Italy) using the Italian and Greek methodologies. *Engineering Structures* 28:357–371
- Dolce M., Goretti A., (2015) Building damage assessment after the 2009 Abruzzi earthquake. *Bulletin of Earthquake Engineering*, 13(8), 2241-2264.
- Dolce M., Manfredi G., (2015) Libro bianco sulla ricostruzione privata fuori dai centri storici nei comuni colpiti dal sisma dell'Abruzzo del 6 aprile 2009, Doppiavoce, Napoli, 153 pp.
- Dolce M., Speranza E., Giordano F., Borzi B., Bocchi F., Conte C., Di Meo A., Faravelli M., Pascale V. (2019) Observed damage database of past Italian earthquakes: the Da.D.O. WebGIS. *Bollettino di Geofisica Teorica ed Applicata* Vol. 60, DOI 10.4430/bgta0254
- DPC, (2018) National Civil Protection Department (ed), National risk assessment. Overview of the potential major disasters in Italy: seismic, volcanic, tsunamis, hydro-geological/hydraulic and extreme weather, droughts and forest fire risks.
- Elefante L., Esposito S., Iervolino I., (2011) Validation and benchmarking of socio-economic indicators using empirical data in the L'Aquila event. Tech Report D4.6 of the SYNER-G project, p. 265.
- Erdik M. and Aydinoglu N., (2002) Earthquake performance and vulnerability of buildings in Turkey. The World Bank Group Disaster Management Facility Report.
- Erdik M., Sesetyan K., Demircioglu M., Hancilar U., Zulfikar C., Cakti E., Kamer Y., Yenidogan C., Tuzun C., Cagnan Z., Harmandar E., (2010) Rapid earthquake hazard and loss assessment for Euro-Mediterranean region. *Acta Geophysica* 58(5):855-92
- Erdik M., (2017) Earthquake risk assessment. *Bull Earthquake Eng* 15:5055–5092 DOI 10.1007/s10518-017-0235-2
- FEMA & NIBS, 1999 Earthquake loss estimation methodology – HAZUS 99. Federal Emergency Management Agency and National Institute of Buildings Sciences, Washington DC.
- FEMA, (1999) "HAZUS99 user and technical manuals". Federal Emergency Management Agency Report: HAZUS 1999, Washington D.C.,USA.
- FEMA, (2003) "HAZUS-MH-MR4 - Earthquake Model Technical Manual, Federal Emergency Management Agency, Washington, D.C.
- Goretti A. and Inukai M., (2002) Post-earthquake usability and damage evaluation of reinforced concrete buildings designed not according to modern seismic codes. JSPS Short Term Fellowship, Final report, Servizio Sismico Nazionale, Dipartimento di Protezione Civile, Roma, Italy.
- Goretti A., Di Pasquale G., (2004) Building Inspection and Damage Data for the 2002 Molise, Italy, Earthquake. *Earthquake Spectra*, Volume 20, No. S1, pages S167–S190, July 2004; © 2004, Earthquake Engineering Research Institute
- Grünthal G., (1998) European Macroseismic Scale. European Centre of Geodynamic & Seismology, Luxemburg, 15

## Chapter II - Loss estimation models: literature review

Haselton C. B. and Baker J. W., (2018) Summary of findings from the benchmarking of FEMA P-58 seismic loss predictions versus HAZUS. Executive summary “SP3.”

ISTAT, Italian National Institute of Statistics. Italian population and housing census. On line at: [www.istat.it](http://www.istat.it)

Jackson, P.L., Editor, Means Square Foot Costs, (1994), R.S. Means Company, Inc., Kingston, MA.

Jaiswal K.S., Wald D.J., Hearne M., (2009) Estimating casualties for large earthquakes worldwide using an empirical approach. U.S Geological Survey OFR 2009-1136, p 78

Jaiswal K.S., and Wald D.J., (2010) An Empirical Model for Global Earthquake Fatality Estimation Earthquake Spectra, 26(4):1017-1037

Jaiswal K.S., Wald D.J., Earle P.S., Porter K.A., Hearne M., (2011) Earthquake Casualty Models Within the USGS Prompt Assessment of Global Earthquakes for Response (PAGER) System. In R Spence, E So, & C Scawthorn, Human Casualties in Earthquakes Progress in Modelling and Mitigation (pp. 171-184), Springer.

Jaiswal K.S., Wald D.J., (2011) Rapid estimation of the economic consequences of global earthquakes. U.S. Geological Survey Open-File Report 2011-1116

Khazai B., (eds). (2013) Guidelines for the consideration of socio-economic impacts in seismic risk analysis SYNER-G reference report 5, Publications Office of the European Union, Luxembourg. ISBN 978-92-79-28968-2. doi: 10.2788/43216

Kircher C.A., Reitherman R.K., Whitman R.V., Arnold C., (1997) Estimation of earthquake losses to buildings. Earthquake Spectra, 13(4): 703-720.

LESSLOSS (2008) Project for risk mitigation for earthquakes and landslides. Available at website: <https://cordis.europa.eu/project/rcn/74272/factsheet/en>

Lucantoni A., Bosi V., Brammerini F., De Marco R., Lo Presti T., Naso G., Sabetta F., (2001) Il rischio sismico in Italia. SSN, Ingegneria Sismica, XVIII-N. 1.

Masi A., Dolce M., Vona M., (2002) A procedure to estimate economic losses due to damage at residential buildings. In: Proc. DiSGG, no. 5

Masi A., Samela C., Santarsiero G., Vona M., (2006) Scenari di danno sismico per l'esercitazione nazionale di Protezione civile “Terremoto Val d’Agri 2006”. Convegno Nazionale ANIDIS-2007-Pisa

Masi A., Santarsiero G., Digrisolo A., Chiauzzi L., Manfredi V., (2016) Procedures and experiences in the post-earthquake usability evaluation of ordinary buildings. Bollettino di Geofisica Teorica ed Applicata Volume 57, Issue 2, 1 June 2016, Pages199-200

Milutinovic Z.V., Trendafiloski G.S., (2003) WP4 Vulnerability of current buildings. RISK-UE project (An advanced approach to earthquake risk scenarios with applications to different European towns.

Mouroux P., Le Brun B., (2006) Presentation of RISK-UE project. Bull Earthq Eng 4(4):323–339

Municipality of Torino (2003) Tempi e Orari della Città. [www.comune.torino.it/tempieorari](http://www.comune.torino.it/tempieorari)

Murakami H.O., (1992) A simulation model to estimate human loss for occupants of collapsed buildings in an earthquake In: The tenth world conference on earthquake engineering, vol.10, Spain, pp 5969-5974.

NatCatSERVICE, (2008) Natural catastrophes worldwide 1980 – 2008, Münchener Rückversicherungs Gesellschaft, Geo Risks Research (data made available through GEM Foundation, Pavia Italy).

NERIES Project (2010) Report “Development of ELER (Earthquake Loss Estimation Routine) Methodology: Vulnerability Relationships”. Deliverable D3

NIBS, National Institute of Building Science, (1997) Earthquake loss estimation methodology, HAZUS97: Technical manual. Report prepared for the Federal Emergency Management Agency, Washington D.C.

NTC18 (2018), D.M. 17 gennaio 2018 - Norme tecniche per le costruzioni. Ministero delle Infrastrutture

Pagani M., Monelli D., Weatherill G., Danciu L., Crowley H., Silva V., Henshaw P., Butler L., Nastasi M., Panzeri L., Simionato M., Vigano D., (2014) OpenQuake Engine: An Open Hazard (and Risk) Software for the Global Earthquake Model. Seismological Research Letters, Vol. 85, No. 3, pp. 1-13

PEER. (2002). Pacific Earthquake Engineering Research (PEER) Center. <https://peer.berkeley.edu/>

- Perkins J. B., (1992) Estimates of Uninhabitable Dwelling Units in Future Earthquakes Affecting the San Francisco Bay Region. ABAG: Oakland, California, 89 pp.
- Petal, M.A., (2004) Urban Disaster Mitigation and Preparedness: the 1999 Kocaeli Earthquake, Diss. Univ. of California, Los Angeles.
- Pitilakis K., Crowley E., Kaynia A., (eds) (2014a) SYNER-G: typology definition and fragility functions for physical elements at seismic risk, vol 27. Geotechnical, geological and earthquake engineering. Springer, Heidelberg. ISBN 978-94-007-7872-6
- Pitilakis K., Franchin P., Khazai B., Wenzel H, (2014b) SYNER-G: systemic seismic vulnerability and risk assessment of complex urban, utility, lifeline systems and critical facilities. Methodology and applications, geotechnical, geological and earthquake engineering. Springer, Heidelberg. ISBN 978-94-017- 8834-2
- Porter K.A., (2003) An overview of PEER's performance-based earthquake engineering methodology. 9<sup>th</sup> International conference on applications of probability and statistics in engineering, San Francisco, CA.
- Province of Torino (2003) Relazione Piano Territoriale di Coordinamento.
- Samardjieva, E. and Badal J., (2002) Estimation of the expected number of casualties caused by strong earthquakes. Bulletin of the Seismological Society of America, 92 (6), pp. 2310- 2322, Aug 2002.
- Shiono K., Krimgold K., Ohta Y., (1991) A method for the estimation of earthquake fatalities and its applicability to the global macro-zonation of human casualty risk. Proceedings of the Fourth International Conference Seismological Zonation, vol. 3. Stanford (CA), Aug 1991. p. 277–84.
- Silva V., Crowley H., Pagani M., Monelli D., Pinho R., (2013) Development of the OpenQuake engine, the global earthquake model's open-source software for seismic risk assessment. Nat Hazards. doi:10. 1007/s11069-013-0618-x
- Silva V., Amo-Oduro D., Calderon A., Dabbeek J., Despotaki V., Martins L., Rao A., Simionato M., Viganò D., Yepes C., Acevedo A., Horspool N., Crowley H., Jaiswal K., Journeay M., Pittore M., (2018) Global Earthquake Model (GEM) Seismic Risk Map (version 2018.1). doi: 10.13117/gem-globalseismic- risk-map-2018.1.
- So E., Spence R., (2009) Estimating shaking-induced casualties and building damage for global earthquake events. Final Technical Report, NEHRP Grant number 08HQGR0102
- So E., Spence R., (2013) “Estimating shaking-induced casualties and building damage for global earthquake events: a proposed modelling approach,” Bulletin of Earthquake Engineering, 11, 347-363
- Spence R., (ed) (2007) Earthquake disaster scenario predictions and loss modelling for urban areas. LessLoss Report 2007/07, July 2007, IUSS Press
- Spence R., So E., Scawthorn C., (2011) Human Casualties in Earthquakes Progress in Modelling and Mitigation. Cambridge, Springer.
- Trendafiloski G., Wyss M., Rosset Ph. (2009) Loss estimation module in the second generation software QLARM. In: Proceedings of the second international workshop on disaster casualties, Cambridge, June 2009 (Chapter 8 of this publication)
- Wald D.J., Jaiswal K.S., Marano K.D., Bausch D.B., Hearne M.G., (2010) PAGER—rapid assessment of an earthquake's impact. U.S. Geological Survey Fact Sheet 2010–3036, p 4
- Welch, D. P., J. Sullivan J.T., and Calvi G.M., (2012) Developing Direct Displacement Based Design and Assessment Procedures for Performance Based Earthquake Engineering. Pavia, Italy.
- Zuccaro, G., Cacace, F., (2011) Seismic Casualty Evaluation: The Italian Model, an Application to the L'Aquila 2009 Event. In R Spence, E So, & C Scawthorn, Human Casualties in Earthquakes Progress in Modelling and Mitigation (pp. 171-184), Springer.

## CHAPTER III

### Direct economic losses: a new model based on damage distribution

#### Introduction

A proper estimation of direct economic losses from future earthquakes is fundamental for decision-making at local, regional and national level in order to define adequate prevention policies. A large number of studies was published dealing with the estimation of direct economic impact as reported in Section 2.2 of Chapter II. Most of the models available in the literature generally provide specific loss functions that correlate the physical damage on the buildings with the economic consequences. The damage is usually defined according to the macroseismic classification (e.g., EMS-98 scale, Grünthal, 1998) referred to the maximum level observed on the entire building, while the economic losses are provided as building repair and reconstruction costs. The damage extension throughout the whole building is implicitly considered in the repair cost values associated with maximum damage level. If on the one side, the assessment of safety condition depends essentially on damage severity (i.e., the maximum damage level), on the other side, damage extension (along the building height) strongly affects the estimation of economic impact. In this framework, a new model for estimating direct economic losses which takes into account, in addition to the expected maximum damage, also the distribution of other damage levels along the building height, has been proposed. The model can be separately applied to different building types (e.g., masonry and Reinforced Concrete) with different elevation configurations (i.e., number of storeys or classes of storey). The damage levels at the building storeys (namely, *damage combination*) can be evaluated through empirical and observational sources or else numerical and analytical methods.

Specifically, a model for Reinforced Concrete (RC) building type designed in the 70's only for vertical loads has been implemented. The RC structural type with a number of storeys equal to 2, 4 and 6 has been considered. Non-Linear Dynamic Analyses (NLDAs) have been selected as method to determine the damage distributions by considering a specific correlation function between seismic response and damage levels (Masi et al., 2015). Furthermore, the data collected on residential RC buildings during the reconstruction process following the 2009 L'Aquila earthquake (Dolce and Manfredi, 2015; Di Ludovico et al. 2017a,b) have been analyzed in order to effectively set up the model.

### 3.1 Background of economic loss models

In the last years, economic losses are one of the key parameters to quantify the expected building performance in its reference life (Miranda and Aslani, 2003). The PBEE approaches (Porter, 2003; Haselton et al., 2008a; ATC 58, 2018) consider the expected annual loss as measure of seismic performance (i.e., decision variable). As for Italy, in addition of the Safety Index of the structure at the Limit State of Life Safety, Expected Annual Losses (EAL) are considered to define risk classes of the buildings (Cosenza et al., 2018). In the models available in literature (see Section 2.2 of Chapter II), the direct cost or loss ratio (i.e., repair cost divided by replacement cost) correlated to the physical damage of the buildings, are usually considered to quantify the direct economic losses. Regarding the Italian models, many studies were developed based on data of past earthquakes (e.g., Di Pasquale and Goretti, 2001; Milutinovic and Trendafiloski, 2003; Di Pasquale et al., 2005; Dolce et al., 2006 and DPC, 2018).

For sake of clarity, the methodology adopted in the last “National risk assessment” (NRA, 2018) has been further reported because it is the reference element for the proposed approach. Specifically, the direct economic losses are a function of the damage level (according to EMS-98 classification) and the corresponding repair cost, according to the following equation:

$$L = CU \left( \sum_{j=1}^n \sum_{k=1}^5 A_{M,j} p_{M,k} c_k + \sum_{j=1}^n \sum_{k=1}^5 A_{RC,j} p_{RC,k} c_k \right) \quad (3.1)$$

where  $n$  is the number of storey or class of storey,  $CU$  is the unitary cost of building replacement,  $A_{M/RC,j}$  is the built area of a building type (Masonry,  $M$ , or Reinforced Concrete,  $RC$ ) with number of stories equal to  $j$  or with a number of storey in the storey class  $j$ ,  $P_{M/RC,k}$  is the damage probability of a building type ( $M$  or  $RC$ ) to experience structural damage level  $k$  and  $c_k$  is the percentage cost of repair or replacement (with respect to  $CU$ ) for each structural damage level  $k$ . The percentages of  $c_k$  for each damage level considered in IRMA (Italian Risk MAs) platform are reported in Table 3.1.

% cost	D1	D2	D3	D4	D5
Min	2	10	30	60	100
Max	5	20	45	80	100

**Table 3.1** Cost parameters used for computation of direct economic losses

### 3.2 Proposed model

In this section, the proposed methodology for estimating direct economic losses has been defined. As discussed above, the models defined in literature studies are usually based only on the maximum level of physical damage for the entire building (generally according to the EMS-98 scale), sometimes also depending on the building type (i.e., the vulnerability class), while the damage extension is implicitly considered in the repair cost values related to the maximum damage.

Starting from the standard procedures reported in the literature, the proposed model explicitly takes into account both the damage severity (i.e., maximum damage level) and the damage distribution along the building height in order to provide a more accurate estimate of direct economic impact (Manfredi et al., 2019). In this way, the methodology allows to better underline the differences, in terms of damage distribution, related to the different seismic behavior of the buildings to vary the material (e.g., masonry and reinforced concrete), the type (e.g., number of storeys, regularity in plan and in elevation) or age of construction. However, the damage at the different building storeys is not easily and univocally determinable because it depends on several factors related to the typological-structural features of the building and the characteristics of the seismic input (e.g., Goulet et al., 2007). The proposed model is based on the assessment of the *damage combinations* (i.e., damage levels at the different building storeys). The damage combinations are a function of the number of storeys ( $N_s$ ) and the maximum damage level ( $Ld_{max}$ ). Each combination is composed by at least one  $Ld_{max}$  and the other damage levels ( $Ld_s$ ) at the building storeys are less or equal to  $Ld_{max}$ .

First of all, it should be noted that, for a building with a given  $N_s$  and  $Ld_{max}$ , the maximum number of possible damage combinations ( $N_{comb}$ ) can be evaluated through the following expression:

$$N_{comb} = (Ld_{max} + 1)^{N_s} - (Ld_{max})^{N_s} \quad (3.2)$$

An example of a possible damage combination with  $Ld_{max}=3$  and  $N_s=4$  is reported in Figure 3.1.

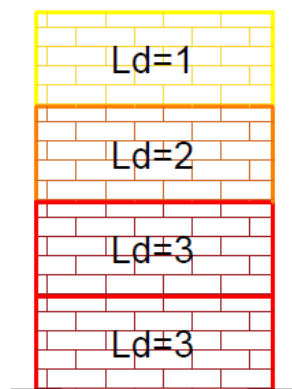


**Figure 3.1** Example of a damage combination for RC building with  $N_s=4$  and  $Ld_{max}=3$

However, as already mentioned, the damage combinations are not equally likely because, given the building characteristics, depend on the uncertainty of the seismic input. Hence, in order to evaluate the most likely damage combinations and the relative weight to be associated, empirical/observational sources or numerical/analytical methods can be considered.

Once defined the damage combinations, the following step of the methodology is the definition of the repair costs of each damage combination, assessed as sum of the repair costs associated with the damage at each building storey (“storey repair cost”).

Therefore, starting from the equation (3.1) adopted in the NRA (2018), the direct economic losses can be estimated using the following expression:

$$L = CU \cdot \left( \sum_{Ns=1}^n \sum_{Ld=1}^5 A_{Ns} \cdot p_{Ld} \cdot C_{Ld,Ns} \right) \quad (3.3)$$

where

- $CU$  is the reference unitary cost of construction of a building (Euro/m<sup>2</sup>), including technical expenses and VAT;
- $A_{Ns}$  is the built area of a building type with number of storeys equal to  $Ns$ ;
- $p_{Ld}$  is the damage probability of a building type to experience structural damage level  $Ld$ ;
- $C_{Ld,Ns}$  is the percentage of the building repair or replacement cost for each damage level  $Ld$  and for the building type with a number of storeys equal to  $Ns$ , that can be evaluated according to the following equation:

$$C_{Ld,Ns} = \sum_{i=1}^{N_{comb}} \sum_{j=1}^{Ns} W_i \cdot Cs(Ld_{i,j}) \quad (3.4)$$

where

- $N_{comb}$  is the number of the possible damage combinations obtained from equation 3.2, as function of  $Ld_{max}$  and  $Ns$ ;
- $W_i$  is the weight (or frequency) to be associated to the  $i$ -th damage combination;
- $Cs(Ld_{i,j})$  is the storey repair cost (defined as percentage of  $CU$ ), i.e., the repair cost related to a damage level  $Ld$  at the  $j$ -th storey for the  $i$ -th damage combination.

The equation (3.3) can be applied separately to different building types (e.g., Masonry and Reinforced Concrete).

The building repair cost (3.4) can be also expressed in matrix form through the following equation:

$$C_{Ld,Ns} = \cdot V_W^T \cdot V_C(M_{comb}) \quad (3.5)$$

The vector  $V_W$  (3.6) collects the weights ( $W_i$ ) related to the damage combinations. The vector  $V_C$  (3.7) considers the costs associated with the damage combinations. Specifically, each row of  $V_C$  refers to the cost of a single combination, calculated as the sum of the repair costs associated with the damage levels at the different building storeys. Therefore,  $V_C$  depends on the matrix of the damage combinations (having a number of rows equal to  $N_{comb}$  and a number of columns equal to  $N_s$ , see 3.8) and on the repair cost associated with each value of the matrix.

$$V_W = \begin{pmatrix} W_1 \\ \dots \\ W_i \\ \dots \\ W_{N_{comb}} \end{pmatrix} \quad (3.6)$$

$$V_C(M_{comb}) = \begin{pmatrix} \sum_{j=1}^{N_s} C(M_{comb}_{1,j}) & \dots & \dots & \dots & \dots \\ \sum_{j=1}^{N_s} C(M_{comb}_{i,j}) & \dots & \dots & \dots & \dots \\ \sum_{j=1}^{N_s} C(M_{comb}_{N_{comb},j}) & \dots & \dots & \dots & \dots \end{pmatrix} \quad (3.7)$$

$$M_{comb} = \begin{pmatrix} Ld_{1,1} & \dots & Ld_{1,j} & \dots & Ld_{1,N_s} \\ \dots & \dots & \dots & \dots & \dots \\ Ld_{i,1} & \dots & Ld_{i,j} & \dots & Ld_{i,N_s} \\ \dots & \dots & \dots & \dots & \dots \\ Ld_{N_{comb},1} & \dots & Ld_{N_{comb},j} & \dots & Ld_{N_{comb},N_s} \end{pmatrix} \quad (3.8)$$



### 3.3 Implementation for Reinforced Concrete building type

The proposed model has been implemented for the existing Reinforced Concrete (RC) building type designed during 70's by taking into account only vertical loads. Non-Linear Dynamic Analyses (NLDAs) have been considered to define damage combinations and relative weight (i.e., frequency of occurrence). Considering the seismic response of the building type evaluated by NLDAs, the damage levels according to the EMS-98 classification have been estimated using specific functions (i.e., assignation of damage levels based on interstorey drift, Masi et al., 2015). The wide set of accelerograms applied in the NLDAs has been appropriately selected in order to consider the uncertainties of the seismic input and to achieve the maximum damage levels (Iervolino et al., 2018; 2019). Furthermore, the data collected on residential RC buildings during the reconstruction process following the 2009 L'Aquila earthquake (Dolce and Manfredi, 2015; Di Ludovico et al. 2017a,b) have been considered in order to define the "storey repair cost".

#### 3.3.1 Description and modelling of building type

The RC structural type designed during 70's by taking into account only vertical loads (Gravity Load Designed, GLD) has been selected as representative of most of the existing residential RC buildings in Italy. In elevation, RC type with number of storeys equal to 2, 4 and 6 has been considered. The buildings have the same in-plan layout, with rectangular shape (total dimensions 21.4x11.8 m<sup>2</sup>), five bays along the X direction and three in the Y one. Inter-storey height is equal to 3.40 m for the first level and 3.05 for the others. Staircase substructure with knee beams is in symmetric position in relation to the Y direction. Infill configuration has been considered according to Infilled Frame (IF, infills uniformly distributed along the height). Regarding the lateral resisting configuration, coherently to usual design practice, the GLD type has frames in only one direction (i.e., orthogonal to the slab direction, Y). As an example, Figure 3.2 shows the plan and the three-dimensional view of the RC building type with 4 storeys (Ricci et al., 2019a). Section dimensions and reinforcement details have been evaluated by means of a simulated design (Masi, 2003) according to code prescriptions in force in Italy. As a result, cross-section dimensions of the interior flexible beams are 70x25 cm<sup>2</sup> and 100x25 cm<sup>2</sup>. Perimeter beams are rigid with section dimension equal to 30x50 cm<sup>2</sup>. Cross-section dimensions of columns are constant along the building height (30x30 cm<sup>2</sup>). Regarding concrete and steel mechanical properties, medium quality concrete, Rck250 (maximum allowable stress equal to 8.5 MPa) and deformed steel, FeB32k (maximum allowable stress equal to 1600 MPa) have been adopted, representing the most used during 1970s. The allowable stress method has been adopted in the safety verifications.

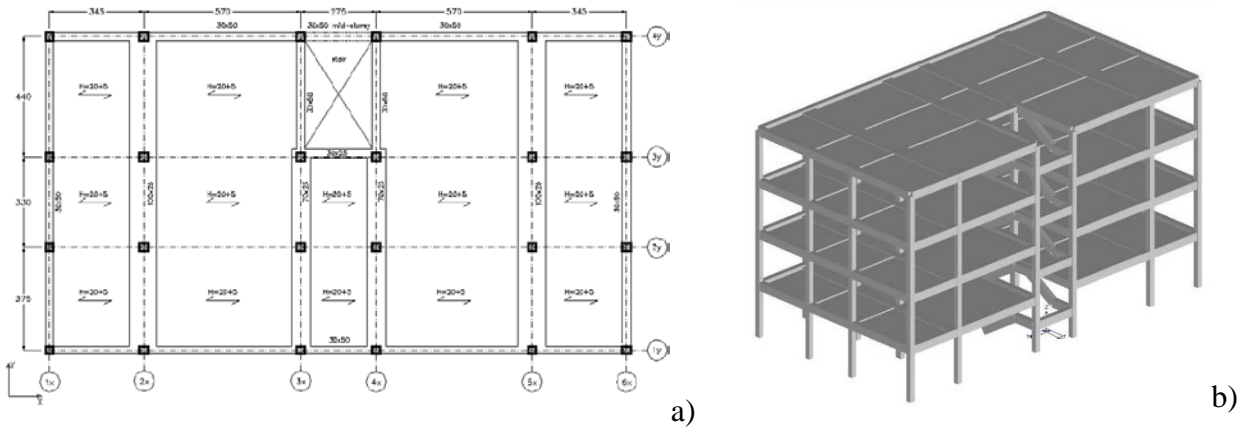


**Figure 3.2** Floor plan (a) and three-dimensional view (b) of the building type with 4 storeys (from Ricci et al., 2019a)

The RC building type has been analyzed with Non-Linear Dynamic Analysis (NLDAs). In this framework, a lumped plasticity approach has been adopted to model the nonlinear response of RC beam/column elements through the OpenSees software (McKenna, 2011). Moment-chord rotation springs are introduced at both ends of each beam/column elastic element. The modified Ibarra-Medina-Krawinkler (2005) deterioration model with peak-oriented hysteretic response based on parameters determined according to Haselton et al. (2008b) has been assigned to such springs. With respect to infills, consistent with the practice of the period, double-layer type with 8 cm (internal layer) and 12 cm (external layer) thick panels of hollow clay bricks and empty cavity (10 cm thick) has been considered. An equivalent concentric single-strut approach has been adopted to represent the infill panels (Decanini et al., 2014; Noh et al., 2017). Further details and considerations related to building modelling are reported in Ricci et al. (2019a,b).

NLDAs have been performed considering the wide set of accelerograms selected as part of the research project DPC-ReLUIIS "RINTC" (Iervolino et al., 2018; 2019). Seismic input selection for NLDAs is able to achieve all damage levels for the building type under study and to take into account the variability of the hazard characteristics related to different sites and subsoil categories.

### 3.3.2 Damage combinations


In this section, the damage combinations and the corresponding weights for the selected building type with a number of storeys  $N_s=2, 4$  and  $6$  have been determined by performing Non-Linear Dynamic Analyses (NLDAs). For each NLDA, the maximum value of the inter-storey drift (defined as ratio between the displacement,  $\Delta$ , and the inter-storey height,  $L$ ) of each storey has been determined. The damage (in terms of EMS-98 scale) has been associated as a function of the  $\Delta/L$  value of each building storey according to the relationship defined by Masi et al. (2015) and reported in Table 3.2.

$L_d$	0	1	2	3	4	5
$\Delta/L$ [%]	<0.1	0.1-0.25	0.25-0.5	0.5-1.0	1.0-2.5	>2.5

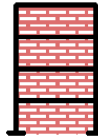
**Table 3.2** Assignment of damage levels (EMS 98) on the basis of drift values,  $\Delta/L$

Through this specific function, the expected damage level at each storey (i.e., *damage combination*) has been evaluated and the weight of each damage combination has been computed as frequency of occurrence. A limited number of damage combinations has been obtained from the NLDAs since the combinations are not equally likely, as discussed above. As an example, for  $L_{d_{max}}=1$ , the number of possible damage combinations ( $N_{comb}$ ) according to the (3.2) is equal to 3, 15 and 63 respectively for  $N_s = 2, 4$  and  $6$  while  $N_{comb}$  obtained from the NLDAs (i.e., with a frequency of occurrence greater than 0) is equal to 2, 4 and 11, respectively. It is worth also noting that, on the basis of EMS-98 definition related to  $L_{d5}$  (i.e., “Destruction-Very heavy structural damage) and assuming that  $L_{d5}$  at a single storey implies the building collapse, the proposed methodology for RC building type can be applied to  $L_d$  from 0 to 4. Tables 3.3-3.6 report the damage combinations and the corresponding frequency (i.e., weight) obtained from the NLDAs for  $N_s=2, 4$  and  $6$  and  $L_{d_{max}}=1-4$

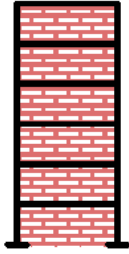
$Ld_{max}=1$

$N_s=2$	Damage level at each storey (Ncomb=2)	
	0	1
	1	1
<b>Frequency</b>	<b>54.9</b>	<b>45.1</b>

(a)

$N_s=4$	Damage level at each storey (Ncomb=4)			
	0	1	0	0
	1	1	0	0
	1	1	1	1
	1	1	0	1
<b>Frequency</b>	<b>60.9</b>	<b>32.6</b>	<b>4.3</b>	<b>2.2</b>


(b)

$N_s=6$	Damage level at each storey (Ncomb=11)										
	0	1	0	0	0	0	1	0	0	0	1
	1	1	1	0	0	1	1	1	1	0	1
	1	1	1	0	1	1	1	1	0	1	1
	1	1	1	1	1	0	1	1	1	1	1
	1	1	1	1	1	0	1	0	1	1	0
	1	1	0	0	1	0	0	0	0	0	0
<b>Frequency</b>	<b>25.6</b>	<b>20.9</b>	<b>18.6</b>	<b>11.6</b>	<b>4.7</b>	<b>4.7</b>	<b>4.7</b>	<b>2.3</b>	<b>2.3</b>	<b>2.3</b>	<b>2.3</b>

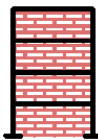
(c)

**Table 3.3** Damage combinations and their relative frequencies obtained from NLDAs for RC buildings with  $Ld_{max}=1$  and  $N_s = 2$  (a),  $N_s = 4$  (b) and  $N_s = 6$  (c)

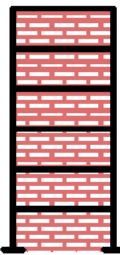
$$Ld_{max}=2$$

$N_s=2$	Damage level at each storey (Ncomb=2)	
	1	2
	2	2
<b>Frequency</b>	<b>87.2</b>	<b>12.8</b>

(a)

$N_s=4$	Damage level at each storey (Ncomb=7)						
	1	1	1	0	1	0	1
	2	1	1	1	2	1	1
	2	2	2	2	2	2	1
	2	2	1	1	1	2	2
<b>Frequency</b>	<b>38.2</b>	<b>23.5</b>	<b>11.8</b>	<b>8.8</b>	<b>8.8</b>	<b>5.9</b>	<b>2.9</b>


(b)

$N_s=6$	Damage level at each storey (Ncomb=15)														
	1	0	1	1	0	1	1	1	0	1	1	1	1	1	2
	2	1	1	1	1	1	1	1	1	2	2	2	2	2	2
	2	1	1	2	2	2	1	1	1	1	2	1	2	1	2
	2	2	2	2	2	2	1	2	2	2	2	1	2	1	2
	2	2	2	2	2	1	2	1	1	2	2	1	1	2	2
1	1	1	1	1	1	1	1	1	1	1	2	1	1	1	2
<b>Frequency</b>	<b>26.2</b>	<b>11.9</b>	<b>11.9</b>	<b>9.5</b>	<b>7.1</b>	<b>7.1</b>	<b>4.8</b>	<b>4.8</b>	<b>2.4</b>	<b>2.4</b>	<b>2.4</b>	<b>2.4</b>	<b>2.4</b>	<b>2.4</b>	<b>2.4</b>

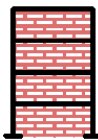
(c)

**Table 3.4** Damage combinations and their relative frequencies obtained from NLDAs for RC buildings with  $Ld_{max}=2$  and  $N_s = 2$  (a),  $N_s = 4$  (b) and  $N_s = 6$  (c)

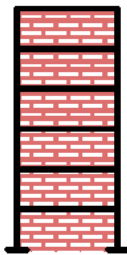
$$Ld_{max}=3$$

$Ns=2$	<b>Damage level at each storey (Ncomb=2)</b>	
	2 3	1 3
<b>Frequency</b>	<b>57.5</b>	<b>42.5</b>

(a)

$Ns=4$	<b>Damage level at each storey (Ncomb=12)</b>											
	1	1	1	2	1	0	1	1	1	2	1	2
	2	2	3	3	1	2	1	3	3	2	2	2
	3	3	3	3	3	3	3	3	2	3	2	3
	3	2	2	2	2	3	3	3	2	2	3	3
<b>Frequency</b>	<b>30.0</b>	<b>26.7</b>	<b>10.0</b>	<b>6.7</b>	<b>3.3</b>	<b>3.3</b>	<b>3.3</b>	<b>3.3</b>	<b>3.3</b>	<b>3.3</b>	<b>3.3</b>	<b>3.3</b>


(b)

$Ns=6$	<b>Damage level at each storey (Ncomb=17)</b>																
	1	1	1	2	1	0	0	1	1	1	1	2	2	2	2	1	1
	2	1	2	3	2	1	1	2	1	1	3	3	2	3	2	2	2
	2	2	3	3	3	1	2	2	3	2	3	2	2	3	3	2	2
	3	3	3	3	2	2	3	3	3	3	3	2	3	3	3	3	2
	3	3	3	3	2	3	3	2	2	2	3	2	3	2	3	2	3
	2	2	2	2	1	1	2	1	1	1	3	2	1	2	2	2	2
<b>Frequency</b>	<b>20.6</b>	<b>17.6</b>	<b>14.7</b>	<b>8.8</b>	<b>2.9</b>	<b>2.9</b>	<b>2.9</b>	<b>2.9</b>	<b>2.9</b>	<b>2.9</b>	<b>2.9</b>	<b>2.9</b>	<b>2.9</b>	<b>2.9</b>	<b>2.9</b>	<b>2.9</b>	<b>2.9</b>

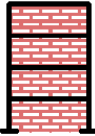
(c)

**Table 3.5** Damage combinations and their relative frequencies obtained from NLDAs for RC buildings with  $Ld_{max}=3$  and  $Ns = 2$  (a),  $Ns = 4$  (b) and  $Ns = 6$  (c)

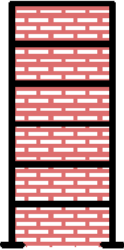
$$Ld_{max}=4$$

$N_s=2$	<b>Damage level at each storey (Ncomb=2)</b>	
	2 4	1 4
<b>Frequency</b>	<b>74.5</b>	<b>25.5</b>

(a)

$N_s=4$	<b>Damage level at each storey (Ncomb=14)</b>													
	1 3 4 3	1 2 4 4	2 3 4 4	1 3 4 4	2 3 4 3	2 4 4 4	1 2 4 3	1 2 3 4	1 4 4 3	1 3 3 4	2 4 3 3	2 2 4 4	2 4 4 3	2 2 3 4
<b>Frequency</b>	<b>16.4</b>	<b>16.4</b>	<b>14.5</b>	<b>10.9</b>	<b>9.1</b>	<b>9.1</b>	<b>7.3</b>	<b>5.5</b>	<b>1.8</b>	<b>1.8</b>	<b>1.8</b>	<b>1.8</b>	<b>1.8</b>	<b>1.8</b>

(b)

$N_s=6$	<b>Damage level at each storey (Ncomb=27)</b>																											
	2 3 4 4 4 3	1 2 4 4 4 3	1 2 3 4 4 4	1 2 3 4 4 2	1 2 3 4 4 2	1 3 4 4 4 3	1 2 3 4 4 3	2 2 3 4 4 3	2 3 3 4 4 3	1 2 2 4 4 2	2 3 3 4 3 2	1 3 3 4 3 2	1 1 2 4 3 2	1 1 3 4 3 2	1 3 3 4 3 2	2 3 4 4 3 2	2 2 3 4 3 2	1 2 4 4 4 4	2 3 4 4 4 3	1 4 3 4 4 3	1 3 3 4 4 2	1 2 3 3 4 3	1 2 3 3 4 3	2 2 3 3 4 3	2 3 3 4 4 3	1 3 3 4 4 3	2 3 3 4 4 3	
<b>Frequency</b>	<b>13.6</b>	<b>10.2</b>	<b>10.2</b>	<b>8.5</b>	<b>6.8</b>	<b>6.8</b>	<b>6.8</b>	<b>3.4</b>	<b>3.4</b>	<b>1.7</b>	<b>1.7</b>	<b>1.7</b>	<b>1.7</b>	<b>1.7</b>	<b>1.7</b>	<b>1.7</b>	<b>1.7</b>	<b>1.7</b>	<b>1.7</b>	<b>1.7</b>	<b>1.7</b>	<b>1.7</b>	<b>1.7</b>	<b>1.7</b>	<b>1.7</b>	<b>1.7</b>	<b>1.7</b>	<b>1.7</b>

(c)

**Table 3.6** Damage combinations and their relative frequencies obtained from NLDAs for RC buildings with  $Ld_{max}=4$  and  $N_s = 2$  (a),  $N_s = 4$  (b) and  $N_s = 6$  (c)

### 3.3.3 Storey repair costs

In order to define the building repair costs ( $C_{Ld,Ns}$ ) based on the damage distribution along the building height, the following step is the definition of the repair costs of each damage combination, assessed as sum of the repair costs associated to the damage at each building storey (“storey repair cost”). For such purpose, the Total Repair Costs (TRCs) of the RC buildings evaluated by Dolce and Manfredi (2015) and Di Ludovico et al. (2017a,b) for the reconstruction process following the 2009 L’Aquila earthquake have been considered. TRCs as a function of the number of storeys ( $N_s$ ) for the RC buildings with B-C (1460 bldgs.) and E (426 bldgs.) usability rating ( $U_R$ ) according to AeDES form (Baggio et al., 2007; Masi et al. 2016) were defined. TRC includes: building safety measures; demolition and removal including transportation costs and landfill disposal; repair interventions; repair and finishing works relevant to strengthening interventions (only for buildings with usability rating E according to AeDES form); testing of facilities; technical works for health and hygiene improvement; technical works to improve facilities; construction and safety costs; charges for the design and technical assistance of practitioners and furniture moving (De Martino et al., 2017).

In the paper Del Vecchio et al. (2020), the TRCs were divided into Direct Repair Costs (DRCs) and repair costs attributable to the strengthening interventions. Specifically, for the RC buildings with  $U_R=E$ , the percentage related to repair costs for strengthening interventions was estimated equal to about 15% of TRC. In order to define only DRCs consistent with the objectives of the present study (i.e., to estimate the direct economic losses), the median values of TRC for  $U_R=E$  estimated by Di Ludovico et al. (2017b) have been reduced to leave out the share attributable to strengthening interventions (15% of TRC). Figure 3.3 shows the number of RC buildings and the DRCs as a function of the  $N_s$  for buildings with  $U_R$  equal to B-C and E, indicated below as  $DRC(U_R, N_s)$ .

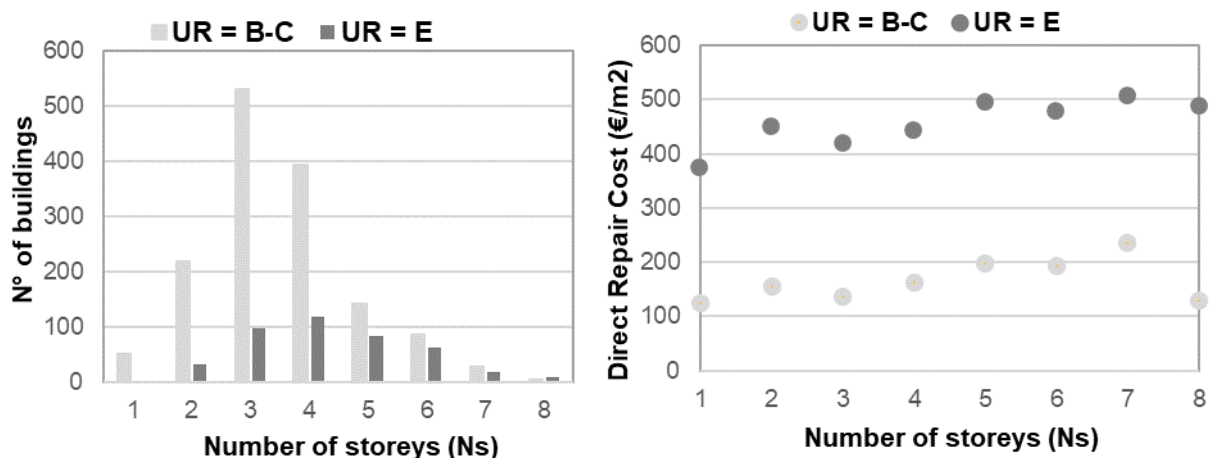


**Figure 3.3** Number of RC buildings (on the left) and DRCs (on the right) as a function of number of storeys for with usability rating B or C (in light grey) and E (in dark grey)

On the basis of the dataset related to the usability survey after L’Aquila earthquake (see Dolce and Goretti, 2015), the usability distribution conditional upon damage levels has been evaluated. In order



to convert the damage data collected through AeDES form in terms of EMS-98 damage levels ( $L_d$ s), the conversion schema for RC buildings reported in Del Gaudio et al. (2017) has been considered. The authors developed a schema between damage levels on vertical structures (VS) and infill-partitions (IP) according to the AeDES form and the six EMS-98  $L_d$ s. In the case of no damage information both to VS and IP, the building has not been considered in the current analyses. By considering a dataset of about 11,400 RC buildings, Table 3.7 shows the distribution of usability ratings (A, B-C and E) conditional upon EMS-98 damage levels in terms of frequency, indicated below as  $f(L_d, U_R)$ .

$U_R$	<i>Damage Level</i>					
	<b>0</b>	<b>1</b>	<b>2</b>	<b>3</b>	<b>4</b>	<b>5</b>
<b>A</b>	93.1	73.4	11.7	0.7	0.3	0.0
<b>B-C</b>	6.4	25.4	63.8	26.0	4.0	1.6
<b>E</b>	0.5	1.1	24.5	73.3	95.7	98.4

**Table 3.7** Usability distribution (A, B+C and E) conditional upon EMS-98 damage levels

At this point, the direct repair cost (DRC) as a function of the EMS-98 damage levels and the number of storeys can be evaluated according to the following equation:

$$DRC(L_d, N_s) = \sum_{U_R=A}^E DRC(U_R, N_s) \cdot f(L_d, U_R) \quad (3.9)$$

where

- $DRC(L_d, N_s)$  is the direct repair cost depending of EMS-98 damage level ( $L_d$ ) and the number of storeys ( $N_s$ );
- $U_R$  is the usability rating (i.e., A, B+C and E);
- $DRC(U_R, N_s)$  is the repair cost as function of usability rating,  $U_R$  (A, B+C and E) and  $N_s$  as reported in Figure 3.3. It is worth noting that DRC for  $U_R = "A"$  has been assumed equal to 0;
- $f(L_d, U_R)$  is the frequency of  $L_d$ s for the corresponding  $U_R$  as reported in Table 3.7.

It is worth underlining that the median DRCs have been computed assuming that the buildings under examination always underwent strengthening interventions and never demolition and reconstruction which is rather unlikely for  $L_d \geq 3$ . The demolished and reconstructed buildings were analyzed referring to the funding class “Edem” defined by Di Ludovico et al. (2017b). Because the costs related to the “Edem” class have not been included in the proposed approach, DRCs need to be re-evaluated by considering the expected share of demolished and reconstructed buildings after the L’Aquila earthquake. In order to consider the share addressing towards repair/strengthening (REP) and

demolition/reconstruction (DEM), the modified values of DRC can be calculated through the following expression:

$$DRC_{new}(Ld, Ns) = DRC(Ld, Ns) \cdot F(REP) + CU \cdot F(DEM) \quad (3.10)$$

where

- $DRC_{new}(Ld, Ns)$  is the direct repair cost as function of Ld and Ns, by considering also the demolition and reconstruction;
- $DRC(Ld, Ns)$  is the direct repair cost as function of Ld and Ns obtained from equation (3.9);
- $F(REP)$  and  $F(DEM)$  are the frequencies related to repair and strengthening or demolition and reconstruction, respectively;
- $CU$  is the mean unit cost for demolition and reconstruction set equal to €1213.4/m<sup>2</sup> (Del Vecchio et al., 2020) for RC buildings.

In this approach, it is assumed that the buildings with Ld3 always underwent repair/strengthening interventions, i.e.,  $F(REP)=100\%$ , while, for the buildings with Ld5, the frequency for DEM has been assumed equal to 100% (i.e., DRC for Ld5 is equal to CU). Regarding Ld4, the frequencies for REP and DEM have been assumed equal to 50% (i.e., 50% of the buildings were repaired and strengthened and 50% were demolished and reconstructed). These percentages have been determined on the basis of expert assessments related to damage combinations reported in Section 3.3.2. In order to distinguish the combinations related to REP or DEM and evaluate the corresponding frequency, a specific criterion based on the number of  $Ld_{max}$  in each combination ( $N_{Ld_{max}}$ ) has been defined. Specifically, the combinations with  $N_{Ld_{max}} \geq Ns/2$  are associated to DEM while those with  $N_{Ld_{max}} < Ns/2$  to REP. As an example, for buildings with  $Ns=4$  (see Table 3.6b), the first combination is associated to REP ( $N_{Ld_{max}} < 2$ ) while the second one is associated to DEM ( $N_{Ld_{max}} = 2$ ). At this point, the total frequency,  $F(REP)$  and  $F(DEM)$ , has been computed as sum of the frequencies of all the damage combinations related to REP and DEM, respectively. For  $Ns=4$ ,  $F(REP)$  and  $F(DEM)$  are equal to 0.44 and 0.56 while, for  $Ns=6$ , 0.53 and 0.47, respectively. It worth noting that, for  $Ns=2$ , the combinations have been associated to repair and strengthening. In order to define a single value for  $Ns=2, 4$  and  $6$ , the frequencies related to REP and DEM have been assumed equal to 50%.

Figure 3.4 shows the  $DRC_{new}$  (hereafter, only DRC) for RC buildings as a function of number of storeys (Ns) and damage levels (from Ld0 to Ld4) and the corresponding linear regression functions in order to obtain the related trend with the Ns. As discussed before, the repair cost for Ld5 has been assumed equal to CU and, then, it has not considered in the following analysis. It is worth noting that the DRCs for RC buildings with Ns equal to 8 defined by Di Ludovico et al. (2017a,b) have not been

considered because their evaluation was carried out on a dataset statistically not significant (i.e., 5 and 10 for  $U_R=B-C$  and E, respectively; see Figure 3.3).

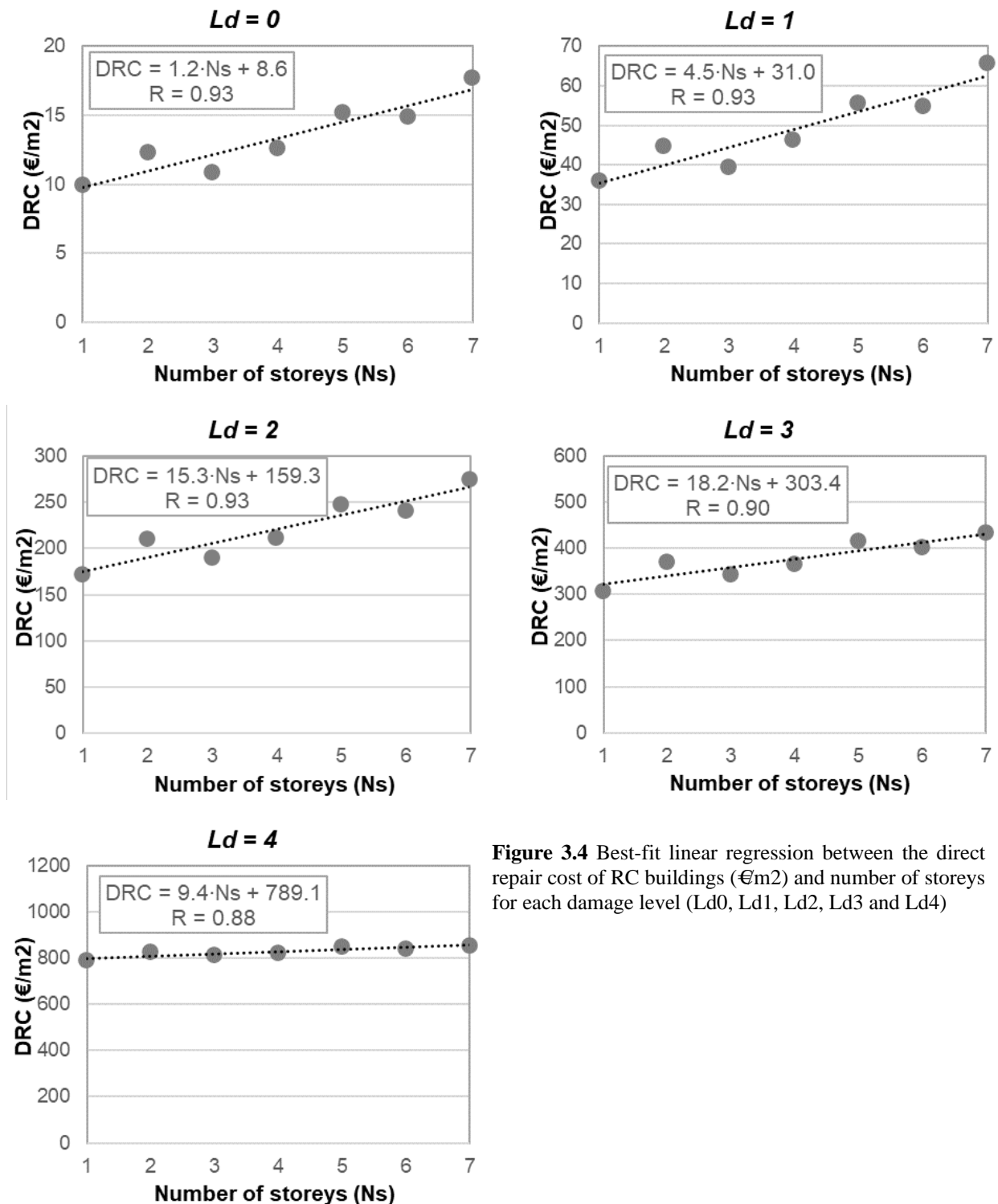


**Figure 3.4** Best-fit linear regression between the direct repair cost of RC buildings (€/m<sup>2</sup>) and number of storeys for each damage level (Ld0, Ld1, Ld2, Ld3 and Ld4)

In order to estimate the storey repair cost, it is assumed that the DRCs can be associated to the damage combinations obtained from NLDAs for RC buildings with  $N_s$  equal to 2, 4 and 6 (see Section 3.3.2). In this framework, Table 3.8 reports the DRCs (in terms of % of CU) for  $L_d=0-4$  and  $N_s=2, 4$  and 6 (obtained from the regressions shown in Figure 3.4). The damage combinations to be associated to

DRCs can be selected through specific criteria (for instance, the most frequent or a specific set of combinations). In the proposed approach, the combinations with the highest frequency related to Ld1-Ld4 for the RC type with N<sub>s</sub>=2, 4 and 6 have been considered. However, due to the large number of damage combinations and relative low frequency (less than 20%), the two most frequent combinations for Ld4 and N<sub>s</sub>=4 and 6 have been considered.

<i>DRC (% of CU)</i>					
<b>RC building type</b>	<b>Ld0</b>	<b>Ld1</b>	<b>Ld2</b>	<b>Ld3</b>	<b>Ld4</b>
N <sub>s</sub> =2	0.009	0.03	0.16	0.28	0.67
N <sub>s</sub> =4	0.011	0.04	0.18	0.31	0.68
N <sub>s</sub> =6	0.013	0.05	0.21	0.34	0.70

**Table 3.8** Median DRCs as function of Ld and N<sub>s</sub>

At this point, the storey repair cost (*C<sub>s</sub>*) related to different L<sub>d</sub>s and RC building type with N<sub>s</sub>= 2, 4 and 6 can be evaluated through the following expression:

$$C_s(L_d, N_s) = \frac{1}{N_{L_d}} \left[ DRC(L_d, N_s) - \sum_{k=0}^{L_d-1} N_k * C_s(k, N_s) \right] \quad (3.11)$$

where

- *C<sub>s</sub> (L<sub>d</sub>, N<sub>s</sub>)* is the storey repair cost as function of damage level (*L<sub>d</sub>*) and the number of storeys of a specific building type (*N<sub>s</sub>*);
- *DRC (L<sub>d</sub>, N<sub>s</sub>)* is the direct repair cost of the building as function of *L<sub>d</sub>* and *N<sub>s</sub>*;
- *N<sub>k</sub>* is the number of a specific damage level, *k*, in the damage combination (e.g., for the first combination with L<sub>d</sub><sub>max</sub>=3 and N<sub>s</sub>=4 in Table 3.5b, N<sub>L<sub>d</sub>=1</sub> = 1; N<sub>L<sub>d</sub>=2</sub> = 1 and N<sub>L<sub>d</sub>=3</sub> = 2);
- *C<sub>s</sub> (k, N<sub>s</sub>)* is the storey repair cost as function of a damage level, *k* and *N<sub>s</sub>*.

Once evaluated the storey repair cost for Ld0 as direct repair cost (DRC) divided by number of storeys (N<sub>s</sub>), the equation (3.11) must be coherently applied starting from the minimum (i.e., Ld1) to the maximum damage level (i.e., Ld4). It worth also underlining that, in the cases of two combinations (i.e., for Ld4 and N<sub>s</sub>=4 and 6), the average value of the storey repair costs has been considered.

Table 3.9 shows the values of the storey repair cost (*C<sub>s</sub>* in terms of percentage of CU) as function of the EMS-98 damage level and RC building type (N<sub>s</sub>=2, 4 and 6).

<i>Storey Repair Cost (% of CU)</i>					
<b>RC building type</b>	<b>Ld0</b>	<b>Ld1</b>	<b>Ld2</b>	<b>Ld3</b>	<b>Ld4</b>
N <sub>s</sub> =2	0.005	0.024	0.13	0.15	0.53
N <sub>s</sub> =4	0.003	0.010	0.06	0.12	0.37
N <sub>s</sub> =6	0.002	0.007	0.05	0.09	0.17

**Table 3.9** Storey Repair cost

### 3.3.4 Estimation of building repair cost and comparison with NRA-2018 values

On the basis of the storey repair costs evaluated in the previous section and the damage combinations with the relative weight obtained from NLDAs (Section 3.3.2), the building repair costs have been calculated according to the expression 3.4. Table 3.10 reports the building repair costs (in terms of percentage of CU) as function of the damage levels (Ld<sub>s</sub>) for RC building type with number of storeys (Ns) equal to 2, 4 and 6. As done in the “National Risk Assessment” (NRA, 2018), the percentage of the building repair cost associated to Ld0 has not defined while that for Ld5 is assumed equal to CU.

<i>Building repair cost (% of CU)</i>					
<b>RC building type</b>	<b>Ld1</b>	<b>Ld2</b>	<b>Ld3</b>	<b>Ld4</b>	<b>Ld5</b>
Ns=2	0.04	0.17	0.23	0.64	1.00
Ns=4	0.03	0.14	0.29	0.78	1.00
Ns=6	0.03	0.15	0.34	0.61	1.00

**Table 3.10** Building repair costs as function of Ld for RC types with Ns=2,4 and 6

Finally, a comparison between the proposed building repair costs and those adopted in the last NRA (DPC, 2018) and IRMA platform has been carried out. Specifically, the two sets of values reported in Table 3.1 have been considered. Regarding the proposed values, an average among the costs associated to the RC type with Ns=2, 4 and 6 has been derived. As can be seen in Figure 3.5, the proposed repair costs are intermediate among MIN and MAX values for all the damage levels, except for Ld3 for which the cost overlaps with the MIN value. This difference can be mainly due to the frequency associated to the repair/strengthening and demolition/reconstruction in the estimation of the storey repair costs (see Section 3.3.3).

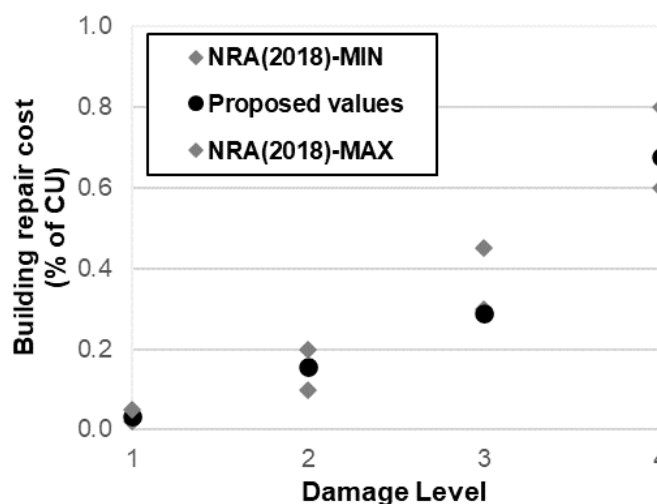


**Figure 3.5** Comparison between the proposed building repair costs and the values adopted in the NRA (2018)

## Discussion

A new model based on both damage severity (i.e., maximum damage level) and damage extension (i.e., distribution of the damage levels along the building height) has been defined to estimate the direct economic losses. The proposed model is based on the assessment of the *damage combinations* (i.e., damage levels at the different building storeys) and the definition of the repair costs of each damage combination, evaluated as sum of the costs associated with the damage at each building storey (*storey repair cost*). Although the damage extension does not strongly affect the structural safety assessment, its consideration represents a step forward for the estimation of the economic impact because it enables to explicitly highlight the differences related to seismic behavior of the buildings to vary material type and structural features. The proposed model can be developed and applied to different building types and the damage distribution can be evaluated through different methods.

Specifically, the model has been implemented for Reinforced Concrete (RC) building type designed in the 70's only for vertical loads with a number of storeys equal to 2, 4 and 6. Non-Linear Dynamic Analyses (NLDAs) have been selected as method to determine damage distributions by considering a specific correlation function between seismic response (i.e., interstorey drift) and damage levels (i.e., EMS-98 classification). Furthermore, the data collected on residential RC buildings during the reconstruction process following the 2009 L'Aquila earthquake have been analyzed in order to define the storey repair costs and, consequently, the building repair costs based on the damage distribution along the height. Results show that the costs (expressed as percentage of reconstruction cost) obtained from the proposed methodology are quite in agreement with the values adopted in the National Risk Assessment (2018).

In the outlook, the methodology should be extended to other building types (e.g., masonry) and further studies related to the storey repair cost estimation are required.

## References

- ATC 58, 2018. FEMA P-58-1, Seismic Performance Assessment of Buildings: Volume 1 (Methodology). Applied Technology Council, Redwood City, California.
- Baggio C., Bernardini A., Colozza R., Corazza L., Della Bella M., Di Pasquale G., Dolce M., Goretti A., Martinelli A., Orsini G., Papa F., Zuccaro G., (2007) Field manual for post-earthquake damage and safety assessment and short term countermeasures (AeDES). In: EUR 22868 EN – Joint Research Centre – Institute for the Protection and Security of the Citizen, Artur V.P., Taucer F. (Eds.), Luxembourg: Office for Official Publications of the European Communities 2007 – 100 pp.- Eur scientific and technical research series – ISSN 1018-5593
- Cosenza E., Del Vecchio C., Di Ludovico M., Dolce M., Moroni C., Prota A., Renzi E., ( 2018) The Italian Guidelines for Seismic Risk Classification of Constructions: Technical Principles and Validation. Bulletin of Earthquake Engineering 16:5905–5935 <https://doi.org/10.1007/s10518-018-0431-8>
- De Martino G., Di Ludovico M., Prota A., Moroni C., Manfredi G., Dolce M., (2017) Estimation of repair costs for RC and masonry residential buildings based on damage data collected by post-earthquake visual inspection. Bull Earthq Eng 15(4):1681–1706. <https://doi.org/10.1007/s10518-016-0039-9>
- Decanini L.D., Liberatore L., Mollaioli F., (2014) Strength and stiffness reduction factors for infilled frames with openings. Earthquake Engineering and Engineering Vibration, **13**(3), 437– 454, 2014.
- Del Gaudio C., De Martino G., Di Ludovico M., Ricci P., Verderame G.M., (2017) Empirical fragility curves from damage data on RC buildings after the 2009 L’Aquila earthquake. Bull Earthq Eng 15:1425. <https://doi.org/10.1007/s10518-016-0026-1>
- Del Vecchio C., Di Ludovico M., Prota A., (2020) Repair costs of reinforced concrete building components: from actual data analysis to calibrated consequence functions. Earthquake Spectra, Vol. 36(1) 353–377 DOI: 10.1177/8755293019878194
- Di Ludovico M., Prota A., Moroni C., Manfredi G., Dolce M., (2017a) Reconstruction process of damaged residential buildings outside the historical centres after L’Aquila earthquake-part I: ‘‘light damage’’ reconstruction. Bull Earthquake Eng. doi:10.1007/s10518-016-9877-8.
- Di Ludovico M., Prota A., Moroni C., Manfredi G., Dolce M., (2017b) Reconstruction process of damaged residential buildings outside historical centres after the L’Aquila earthquake-part II: ‘‘heavy damage’’ reconstruction. Bull Earthquake Eng. doi:10.1007/s10518-016-9979-3.
- Di Pasquale G., Goretti A., (2001) Vulnerabilità funzionale ed economica degli edifici residenziali colpiti dai recenti eventi sismici italiana. X Congresso Nazionale ANIDIS-2001-Potenza-Matera
- Di Pasquale G., Orsini G., Romeo R.W., (2005) New Developments in Seismic Risk Assessment in Italy. Bulletin of Earthquake Engineering, 3:101–128-DOI 10.1007/s10518-005-0202-1
- Dolce M., Kappos A.J., Masi A., Penelis G., Vona M., (2006) Vulnerability assessment and earthquake scenarios of the building stock of Potenza (Southern Italy) using the Italian and Greek methodologies. Engineering Structures 28:357–371
- Dolce M., Goretti A., (2015) Building damage assessment after the 2009 Abruzzi earthquake. Bulletin of Earthquake Engineering, 13(8), 2241-2264.
- Dolce M., Manfredi G., (2015) Libro bianco sulla ricostruzione privata fuori dai centri storici nei comuni colpiti dal sisma dell’Abruzzo del 6 aprile 2009, Doppiovoce, Napoli, 153 pp.
- DPC, (2018) National Civil Protection Department (ed), National risk assessment. Overview of the potential major disasters in Italy: seismic, volcanic, tsunamis, hydro-geological/hydraulic and extreme weather, droughts and forest fire risks.
- Goulet C. A., Haselton C. B., Mitrani-Reiser, J., Beck J. L., Deierlein G. G., Porter K.A., Stewart, J. P., (2007) Evaluation of the seismic performance of a code-conforming reinforced concrete frame building from seismic hazard to collapse safety and economic losses. Earthquake Engng Struct. Dyn. 2007; 36:1973–1997.
- Grünthal G., (1998) European Macroseismic Scale. European Centre of Geodynamic & Seismology, Luxemburg, 15

- Haselton C. B., Goulet C. A., Mitrani-Reiser J., Beck J. L., Deierlein G. G., Porter K. A., Stewart J. P., Taciroglu E., (2008a) An assessment to benchmark the seismic performance of a code-conforming reinforced concrete moment-frame building. Report 2007/12, Pacific Earthquake Engineering Research Center (PEER), Richmond, California.
- Haselton C.B., Liel A.B., Lange S.T., Deierlein G.G. (2008b) Beam-column element model calibrated for predicting flexural response leading to global collapse of RC frame buildings. Pacific Earthquake Engineering Research Center, Report 2007/03, Berkeley, California, USA, 2008.
- Ibarra, L.F., Medina, R.A., Krawinkler, H., (2005) Hysteretic models that incorporate strength and stiffness deterioration. *Earthquake engineering & structural dynamics*, 2005, 34(12), 1489-1511.
- Iervolino, I., Spillatura, A., Bazzurro, P., (2018) Seismic Reliability of Code-Conforming Italian Buildings, *Journal of Earthquake Engineering*, DOI: 10.1080/13632469.2018.1540372.
- Iervolino, I., Spillatura, A., Bazzurro, P., (2019) RINTC-e Project: Towards the Assessment of the Seismic Risk of Existing Buildings In Italy, *COMPdyn 201, 7<sup>th</sup> ECCOMAS Thematic Conference on Computational Methods in Structural Dynamics and Earthquake Engineering* M. Papadrakakis, M. Fragiadakis (eds.), Crete, Greece, 24–26 June 2019
- Manfredi V., Masi A., Nicodemo G., Digrisolo A., Santarsiero G., Ventura G., (2019) The role of damage extent in the estimation of direct economic losses of existing RC buildings XVIII Conference Nazionale ANIDIS-Ascoli Piceno (in Italian)
- Masi, A. (2003) Seismic vulnerability assessment of gravity load designed RC frames, *Bull. Earthq. Eng.*, 23 1(3), 371-395.
- Masi A., Digrisolo A., Manfredi V., (2015) Fragility curves of gravity-load designed RC buildings with regularity in plan. *Earthquake Struct.*, 9, 1-27
- Masi A., Santarsiero G., Digrisolo A., Chiauuzzi L., Manfredi V., (2016) Procedures and experiences in the post-earthquake usability evaluation of ordinary buildings. *Bollettino di Geofisica Teorica ed Applicata* Volume 57, Issue 2, 1 June 2016, Pages199-200
- McKenna, F. (2011) OpenSees: a framework for earthquake engineering simulation. *Computing in Science & Engineering*, 2011, Vol. 13, Issue 4, pp 58-66.
- Milutinovic Z.V., Trendafiloski G.S., (2003) WP4 Vulnerability of current buildings. RISK-UE project (An advanced approach to earthquake risk scenarios with applications to different European towns.
- Miranda E., Aslani H., (2003) Probabilistic response assessment for building-specific loss estimation. PEE Report 2003/03, University of California Berkeley.
- Noh N.M., Liberatore L., Mollaioli F., Tesfamariam S., (2017) Modelling of masonry infilled RC frames subjected to cyclic loads: State of the art review and modelling with OpenSees. *Engineering Structures* **150**, 599–621, 2017.
- NTC18 (2018), D.M. 17 gennaio 2018 - Norme tecniche per le costruzioni. Ministero delle Infrastrutture
- Porter K.A., (2003) An overview of PEER's performance-based earthquake engineering methodology. 9<sup>th</sup> International conference on applications of probability and statistics in engineering, San Francisco, CA.
- Ricci, P., Manfredi, V., Noto, F., Terrenzi, M., De Risi, M.T., Di Domenico, M., Camata, G., Franchin, P., Masi, A., Mollaioli, F., Spacone, E., Verderame, G.M., (2019a) RINTC-e: Towards seismic risk assessment of existing residential reinforced concrete buildings in Italy, *COMPdyn 2019, 7<sup>th</sup> ECCOMAS Thematic Conference on Computational Methods in Structural Dynamics and Earthquake Engineering*, M. Papadrakakis, M. Fragiadakis (eds.) Crete, Greece, 24–26 June 2019
- Ricci, P., Manfredi, V., Noto, F., Terrenzi, M., Petrone C., Celano F., De Risi, M.T., Camata, G., Franchin P., Magliulo G., Masi A., Mollaioli F., Spacone, E., Verderame, G.M., (2019b) Modeling and seismic response analysis of Italian code-conforming reinforced concrete buildings. *Journal of Earthquake Engineering*, **22**(S2), 105-139, 2018.



## CHAPTER IV

# Correlations between macroseismic and instrumental measures of seismic intensity

### Introduction

The estimation of macroseismic intensity of seismic events is usually carried out worldwide in order to quantify, through observations of the effects on buildings, the environment and people, the shaking pattern and the damage extent due to earthquakes. Macroseismic intensity is still often the only observed parameter to quantify the level of ground motion severity in many towns where seismometric instruments are not available. Moreover, macroseismic intensities are the only measures available for pre-instrumental historical earthquakes. With the advent of seismometric instruments and the availability of time-history records, many authors developed relationships between macroseismic intensity and instrumental measures in order to define the relevant values of ground motion parameters in the sites where only the macroseismic intensity was available or vice-versa. In this way, the large amount of information from historical earthquakes in terms of macroseismic intensity can be converted into terms of instrumental intensity in order to define the seismic hazard of an area. Further, starting from the shake maps in terms of instrumental intensity, macroseismic results can be used for post-earthquake analyses and immediate emergency plans.

Starting from the study of Chiauzzi et al. (2012), relationships between macroseismic scales and instrumental ground motion parameters have been derived by considering a large database of ground motion records. Three instrumental intensity measures (i.e., PGA, PGV and  $I_H$ ) and two macroseismic scales (i.e., MCS and EMS-98 scales) have been adopted in order to derive direct (i.e., macroseismic intensity *vs* instrumental parameter) and inverse relationships (i.e., instrumental parameter *vs* macroseismic intensity). These latter permit macroseismic data of historical earthquakes to be converted according to the scales mainly adopted in Italy (i.e., MCS) and in all European countries (i.e., EMS-98) into the three instrumental intensity measures most adopted in seismic risk analyses (i.e., PGA, PGV and  $I_H$ ). On the contrary, given an instrumental value of ground motion (i.e., PGA, PGV and  $I_H$ ), direct relationships can be used to derive seismic input values in empirical building damage models, such as Damage Probability Matrices (DPMs, Braga et al., 1982; Zuccaro et al., 2000; Dolce et al., 2003). It is worth noting that the available DPMs generally adopt either MSK or EMS-98 scales and only a small number of relationships (e.g., Chiauzzi et al., 2012) are able to generate macroseismic input for such models. As a consequence, the relationships represent an important tool in order to adopt DPMs in the framework of earthquake damage scenarios.

## 4.1 On the relationships available in literature

Several studies proposed relationships between different macroseismic intensity scales (e.g., Modified Mercalli Intensity, MMI; Mercalli-Cancani-Sieberg, MCS; Medvedev-Sponheuer-Karnik, MSK and European Macroseismic Scales, EMS-92; EMS-98) and ground motion parameters (e.g., Peak Ground Acceleration, PGA; Peak Ground Velocity, PGV; Arias Intensity,  $I_A$ ; Housner Intensity,  $I_H$ ). Other studies focused on relationships among the most adopted macroseismic intensity scales (e.g., Musson et al, 2010).

In Italy, the first relationships between instrumental parameters and macroseismic intensity scales were derived by Margottini et al. (1992). The authors defined some correlations between macroseismic intensity (i.e., MSK and MCS) and instrumental parameters (i.e., PGA and  $I_A$ ) starting from a database of 56 records related to 9 Italian earthquakes occurred between 1980 and 1990. Wald et al. (1999) developed regression relationships between MMI and PGA-PGV by comparing horizontal peak ground motions to observed intensities for 8 Californian earthquakes. A large amount of data deriving from California earthquakes was considered by Worden et al. (2012) to develop reversible relationships between MMI and three ground-motion parameters, such as PGA, PGV and pseudo-spectral acceleration (PSA). The proposed relationships were defined by adopting the Total Least Squares (TLS) method, which is able to account for uncertainty in both ground motion and macroseismic values. Starting from the database of Margottini et al. (1992), updated with additional earthquake data, Faccioli and Cauzzi (2006) defined new relationships between MCS and PGA-PGV. A complete overview of the works above described was developed by Gómez Capera et al. (2007), that also proposed a relationship between MCS intensity and PGA by adopting the Orthogonal Distance Technique (ODR). Considering the ODR technique, Faenza and Michelini (2010) determined relationships between MCS intensities and both PGA and PGV. In the literature, only a small number of relationships is defined in terms of EMS-98. Among them, Chiauzzi et al. (2012) correlated EMS-98 intensity and Housner intensity ( $I_H$ ), an integral parameter able to better represent the severity of seismic events (Masi et al. 2010, 2015), considering a sample of about sixty earthquake records.

The relationships reported above are generally linear regressions in which instrumental parameters are in terms of logarithm value. The main differences among them are related to the selected database, processing of data with different regression techniques and choice of macroseismic scale to be considered. With respect to the macroseismic scale, Chiauzzi et al. (2012) assumed as substantially coincident EMS-98, MSK-76 and EMS-92 scales. In fact, these scales take into account, in a simplified, even though sufficiently accurate way, building vulnerability and damage distributions in assigning macroseismic intensity values. On the contrary, MCS poorly takes building vulnerability

into account, even though in Faccioli and Cauzzi (2006), the equality among MSK and MCS was assumed. Concerning this matter, some authors (e.g., Codermatz et al., 2003) concluded that a substantial equality exists between MCS and the European definition of the macroseismic intensities (i.e., MSK-76, EMS-92 and EMS-98). On the contrary, other authors (e.g., Molin 1995) observed that, for higher intensities (i.e., VII degree), EMS and MCS scales may differ by one degree or more. Similarly, Braga et al. (1982) highlighted significant differences (up to 2 degrees) between the MSK and MCS scales during the huge damage survey of the 1980 Irpinia-Basilicata earthquake.

Regarding instrumental parameters, PGA is generally adopted in the available relationships due to its physical meaning and its large use in current seismic analyses. Nevertheless, Masi et al. (2003, 2011) highlighted the poor correlation between PGA and building damage compared with integral seismic parameters such as  $I_H$  and Arias Intensity, particularly in case of non-ductile existing buildings.

## 4.2 Methodology

In order to derive relationships between macroseismic and instrumental measures, a large database (179 items of data) consisting of both macroseismic data and accelerometric signals relevant to 32 seismic events has been considered. The selected events are characterized by ground motion records close to the area where macroseismic data is also available. This latter is in terms of EMS-98 and/or MCS scales, while PGA, PGV and Housner Intensity ( $I_H$ ) values have been computed from ground motion records. Specifically, for each accelerometric signal, the  $I_H$  value has been calculated using Equation 4.1 (by assuming the fraction of critical damping,  $\xi$ , equal to 5%):

$$I_H = \int_{0.1}^{2.5} S_V(T, \xi) dT \quad (4.1)$$

In the correlations with macroseismic data, the maximum value of PGA, PGV and  $I_H$  evaluated from the two horizontal components of the ground motion record has been considered.

Regression analyses have been performed by using the Total Least Squares (TLS) method, according to the procedure by Zaiontz (2019). According to the latter, the goal of the TLS method is to minimize the sum of the squared Euclidean distances  $d^2$  from the observed points  $y_i$  to the corresponding ones on the regression line (which is in the form  $y = a + bx$ ), as follows:

$$\min \left\{ \sum_{i=1}^n d_i^2 \right\} \quad (4.2)$$

that is equivalent to:

$$\min \left\{ \sum_{i=1}^n \frac{(y_i - y'_i)^2}{b^2 + 1} \right\} \quad (4.3)$$

where  $y_i$  and  $y'_i$  are the observed and the corresponding estimated data (along the vertical line), respectively, and  $b$  is given by:

$$b = \frac{w + \sqrt{w^2 + r^2}}{r} \quad (4.4)$$

where

$$w = \sum_{i=1}^n (y_i - y_m)^2 - \sum_{i=1}^n (x_i - x_m)^2 \quad (4.5)$$

and

$$r = 2 \sum_{i=1}^n (x_i - x_m) (y_i - y_m) \quad (4.6)$$

$x_m$  and  $y_m$  are the mean values of the  $x_i$  and  $y_i$  values, respectively. The intercept  $a$  can now be expressed as:

$$a = y_m - bx_m \quad (4.7)$$

An analogous procedure can be found also in Petráš and Bednářová (2010).

This statistical method allows the relationship between an independent (X) and a dependent variable (Y) to be estimated by minimizing the sum of the squares evaluated as the orthogonal distance between observed and predicted values. Consequently, it is a more appropriate technique in problems where both independent and dependent variables are affected by uncertainty. Use of the TLS technique also allows for inverting the relationships between macroseismic and instrumental intensity so that the calculated coefficients can be used to express instrumental values as function of macroseismic intensity.

#### 4.2.1 Database

In the present section the database used in the regression analyses is described and discussed. It consists of 179 accelerometric signals (each including both North-South and East-West components) derived from 32 earthquakes occurred in Italy in the last forty years. Figure 4.1 shows the epicentral area of the selected earthquakes, while Table 4.1 reports the main parameters of the earthquake events.

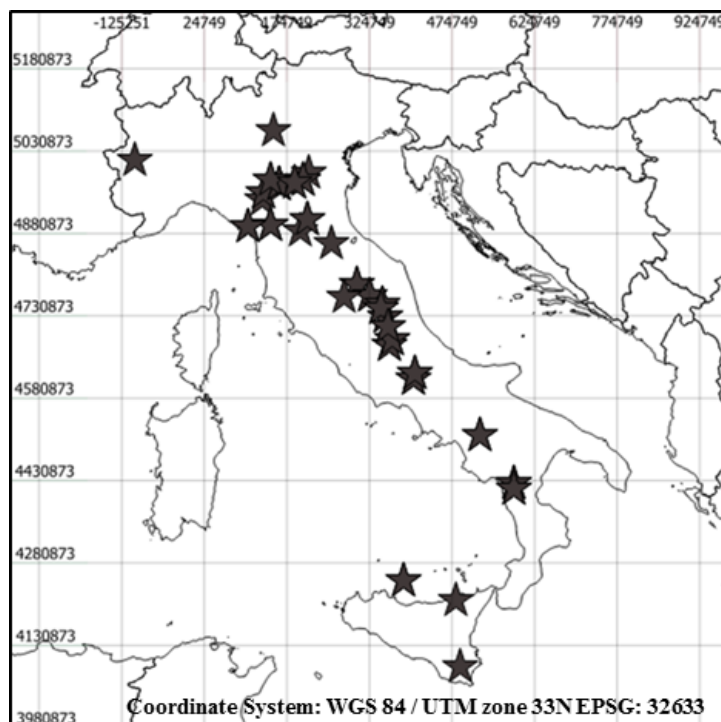


Figure 4.1 Epicentral area of the selected earthquakes.

The ground motion records are extracted from the Italian Accelerometric Archive (Working Group ITACA 2017). They were recorded by either the National Accelerometric Network (RAN) of the Italian Civil Protection Department (DPC) or the National Seismic Network operated by National Geophysics and Volcanology Institute (INGV), or other networks.

For each event, macroseismic data in terms of either EMS-98 or MCS scales or both are also available. Specifically, two subsets of data have been defined: the first contains EMS-98 data (139 records belonging to 28 earthquakes) while the second one regards MCS macroseismic intensity (157 records belonging to 27 earthquakes). For 23 earthquake events, both EMS-98 and MCS data are available.

<i>Epicentral area</i>	<i>Data</i>	<i>Latitude</i>	<i>Longitude</i>	<i>Depth (Km)</i>	<i>M<sub>L</sub></i>	<i>M<sub>W</sub></i>
Irpinia	23/11/1980	40.76	15.31	15.0	6.5	6.9
Parma	09/11/1983	44.65	10.37	28.1	5.0	5.0
Gubbio	29/04/1984	43.21	12.57	6.0	5.2	5.6
Lazio-Abruzzo	07/05/1984	41.70	13.86	20.5	5.9	5.9
Lazio-Abruzzo	11/05/1984	41.78	13.89	12.1	5.7	5.5
Garfagnana	23/01/1985	44.14	10.57	9.4	3.8	/
L'Aquila	20/05/1985	42.23	13.32	10.0	3.7	/
Reggio Emilia	24/04/1987	44.82	10.70	5.0	4.6	/
Reggio Emilia	02/05/1987	44.81	10.72	3.1	4.6	4.7
Umbria-Marche	26/09/1997	43.03	12.86	5.7	5.8	6.0
Basilicata	09/09/1998	39.98	16.03	7.4	5.5	5.6
Palermo	06/09/2002	38.38	13.70	5.0	5.6	5.8
Forlì	26/01/2003	43.88	11.96	6.5	4.3	4.7
Appennino Bolognese	14/09/2003	44.26	11.38	8.3	5.0	5.3
Lago di Garda	24/11/2004	45.69	10.52	5.4	5.2	5.0
Mugello	01/03/2008	44.06	11.25	3.8	4.4	4.7
Emilia Romagna	23/12/2008	44.54	10.35	22.9	5.2	5.5
L'Aquila	06/04/2009	42.34	13.38	8.3	5.9	6.1
Valle del Tevere	15/12/2009	43.01	12.27	8.8	4.3	4.2
Sicilia	24/06/2011	38.06	14.78	7.3	4.4	4.5
Pianura Padana	17/07/2011	45.01	11.37	2.4	4.8	4.8
Torino	25/07/2011	45.02	7.37	11.0	4.3	4.3
Pianura Padana	25/01/2012	44.87	10.51	29.0	5.0	5.0
Emilia	20/05/2012	44.90	11.26	9.5	5.9	6.1
Emilia	29/05/2012	44.84	11.07	8.1	5.8	6.0
Pollino	26/10/2012	39.88	16.02	9.7	5.0	5.2
Fivizzano	21/06/2013	44.13	10.14	7.0	5.2	5.1
Monti Iblei	08/02/2016	37.00	14.80	6.0	4.3	4.2
Accumoli	24/08/2016	42.70	13.23	8.1	6.0	6.0
Ussita	26/10/2016	42.91	13.13	7.5	5.9	5.9
Norcia	30/10/2016	42.83	13.11	9.2	6.1	6.5
Capitignano	18/01/2017	42.53	13.28	9.1	5.4	5.5

**Table 4.1** Main parameters of the selected earthquakes

Macroseismic intensities have been derived from two different sources: i) from past studies available in the literature (Margottini et al., 1992; Stucchi et al., 1998; Galli et al., 2001; Azzaro et al., 2004; Tertulliani et al., 2010; Chiauzzi et al., 2012), for seismic events occurred before 2002; ii) from post-earthquake surveys performed by QUEST (QUick Earthquake Survey Team by INGV), for seismic events occurred after 2002. The QUEST dataset, in particular, provides macroseismic data according to both the EMS-98 and MCS scales. It is worth underlining that earthquake events have been selected by considering only available macroseismic intensity values referred to village in which an accelerometric station (and the corresponding signal) was also located. The selected database is reported in Table 4A (in Appendix).

As shown in Figure 4.2a, the local magnitude values ( $M_I$ ) of the considered earthquake events have an almost normal distribution, with most of the data (55%) in the range  $5 \leq M_I \leq 6$ . Further, magnitude value refers to stations having a distance larger than 10 km (about 73% over the entire magnitude range), as shown in Figure 4.2b, where  $M_I$  vs distance values are plotted. To this purpose, the Joyner-Boore distance ( $R_{JB}$ ) was considered.  $R_{JB}$  values were calculated through the empirically calibrated model described in Montaldo et al. (2005) and Chioccarelli (2012), starting from the epicentral distance value.

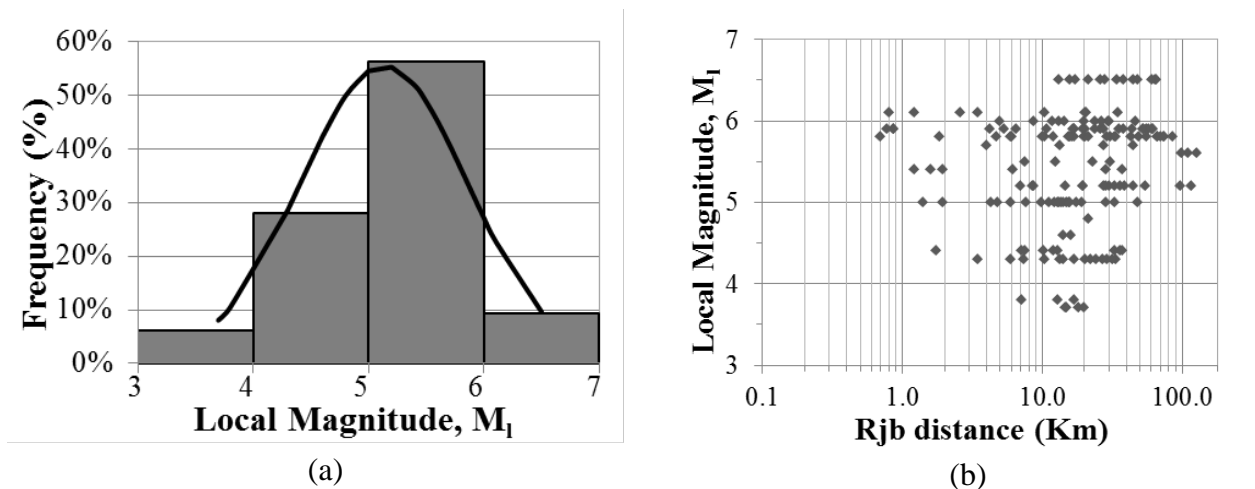


**Figure 4.2** Histogram of the selected earthquakes grouped according to local magnitude,  $M_I$  (on the left) with relative normal distribution. Magnitude versus distance, considering the Joyner Boore distance,  $R_{JB}$  (on the right). The Rjb distance axis is in logarithmic scale.

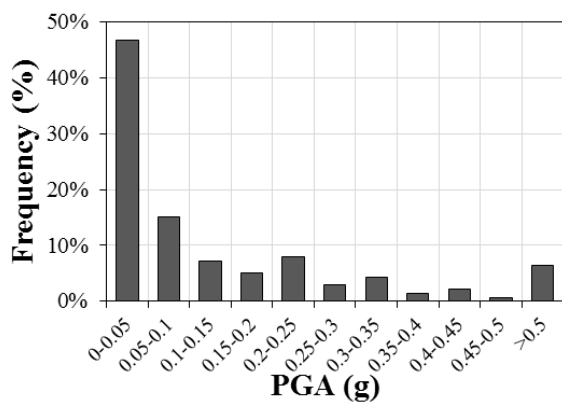
Regarding the database adopted in the regression analyses, Table 4.2 summarizes the main statistic parameters evaluated for both instrumental (PGA, PGV and  $I_H$ ) and macroseismic (MCS and EMS-98) intensities. Specifically, the mean and median values of PGA are 0.124g and 0.063g respectively, while they are 7.398 and 2.853cm/s for PGV, and 0.311m and 0.137m in terms of  $I_H$ . Considering the samples in terms of macroseismic intensity, the mean and median values are 5.79 and 5.5 for MCS, respectively; 5.55 and 5.0 for EMS-98. Large difference between mean and median values, in particular for instrumental parameters, is found. This is mainly because instrumental parameters are

lognormally distributed. Indeed, the mean and median of the sample in terms of logarithmic values are very close, that is -2.977 and -2.999 for PGA, 1.118 and 1.093 for PGV, and -2.399 and -2.255 for  $I_H$ , respectively.

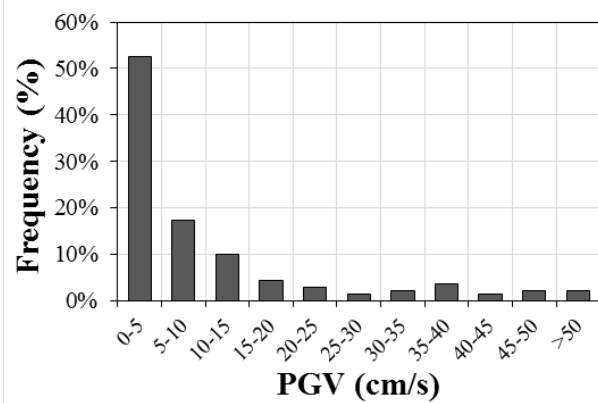
	PGA (g)	PGV (cm/s)	$I_H$ (m)	MCS	EMS-98
Sample size	179	179	179	157	139
Mean	0.124	9.573	0.311	5.79	5.55
Median	0.063	4.163	0.137	5.5	5
Minimum	0.002	0.045	0.002	4	4
Maximum	0.878	70.306	2.529	10.5	10
Standard Deviation	0.152	10.994	0.466	1.22	1.34
25 <sup>th</sup> Percentile	0.025	1.186	0.034	5	4.5
75 <sup>th</sup> Percentile	0.178	11.953	0.322	6	6

**Table 4.2** Statistics concerning instrumental (PGA, PGV and  $I_H$ ) and macroseismic (MCS and EMS-98) data.

Figures 4.3 and 4.4 show the mass distribution of the samples for the two subsets of data in terms of EMS-98 and MCS macroseismic intensities, respectively, and the corresponding instrumental values (in terms of PGA, PGV and  $I_H$ ). The EMS-98 data distribution (Figure 4.3d) is mainly characterized by low intensities, that is 4, 5 and 6 with a percentage of 18%, 28% and 15%, respectively. Similarly, in terms of ground motion parameters, about 50% of the values has very low intensity, i.e.,  $PGA \leq 0.05g$  (Figure 4.3a),  $PGV \leq 5cm/s$  (Figure 4.3b) and  $I_H \leq 0.1m$  (Figure 4.3c).



a)



b)



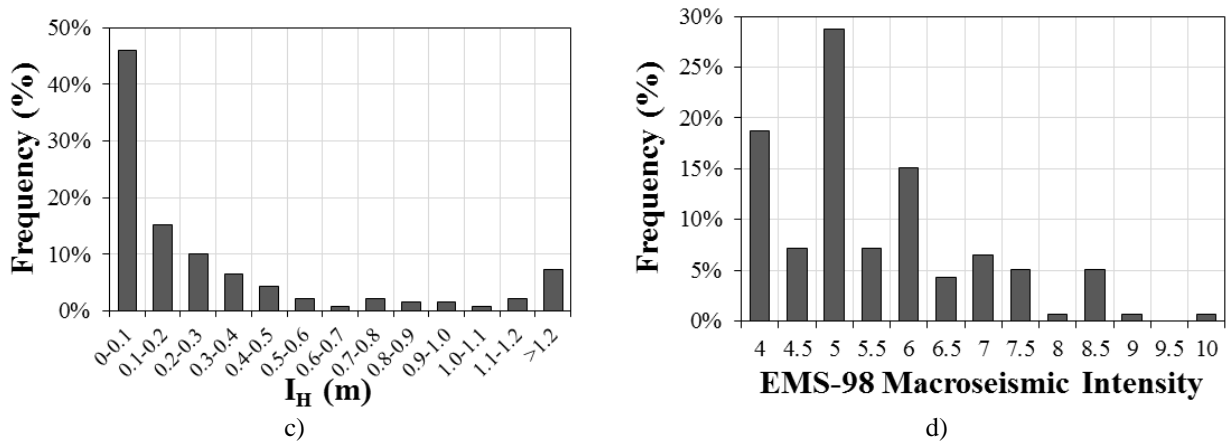


**Figure 4.3** Distribution of strong-motion data in terms of EMS-98 intensities (d) and the corresponding instrumental values PGA (a), PGV, (b) and  $I_H$  (c).

Similar results can also be found for the data subset in terms of MCS intensity, with frequencies of 24%, 17% and 18% for 5, 5.5 and 6 MCS intensity, respectively (Figure 4.4d). In terms of instrumental measures, lower values (i.e.,  $PGA \leq 0.05g$ ,  $PGV \leq 5cm/s$  and  $I_H \leq 0.1m$ ) include about 40% (50% for PGV) of the sample.

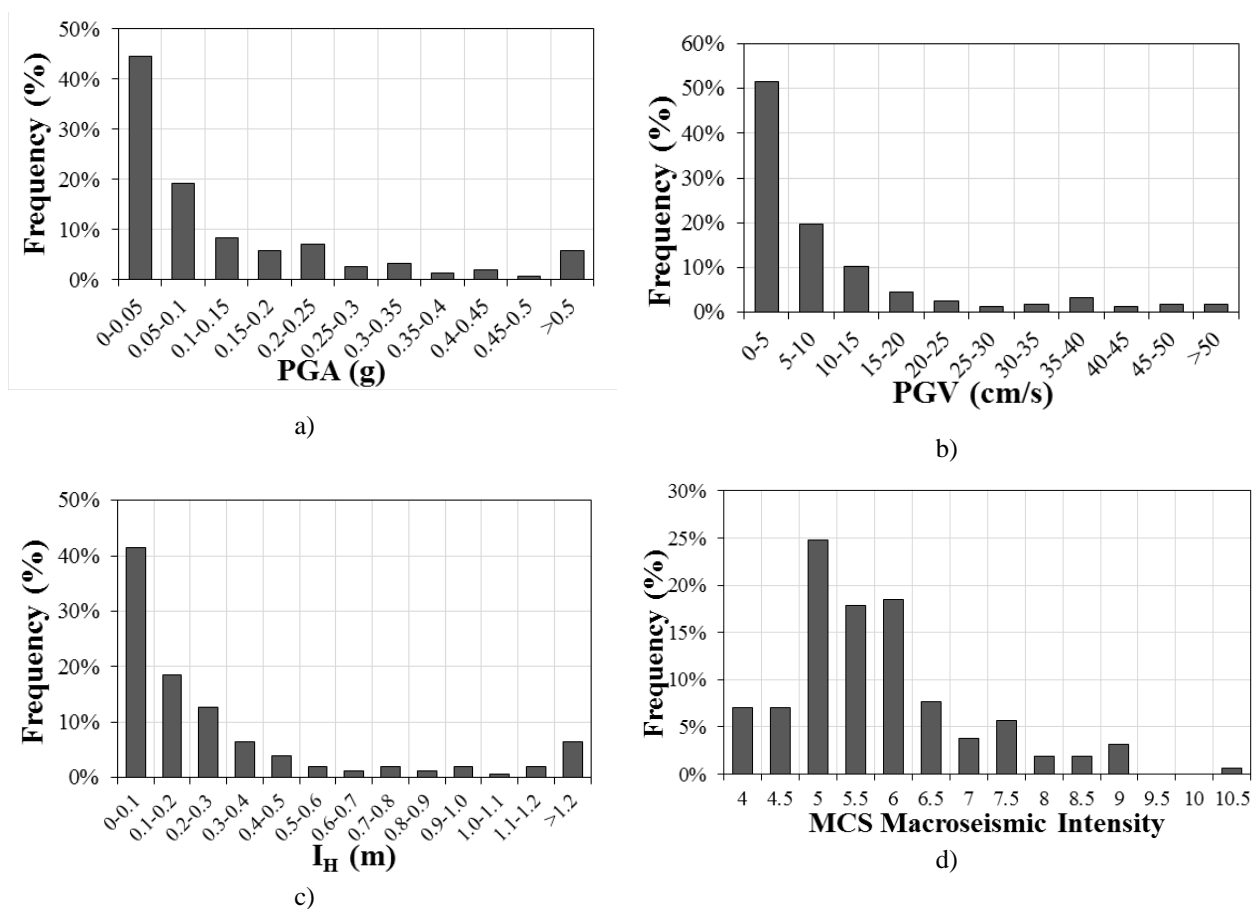


**Figure 4.4** Distribution of strong-motion data in terms of MCS intensities (d) and the corresponding instrumental values PGA (a), PGV, (b) and  $I_H$  (c).

Data related to earthquake events for which macroseismic intensities are available in both of the two considered scales (117 values) permit MCS and EMS-98 results to be compared. To this purpose, it is worth highlighting that for most of the data (about 70% of the sample, 78 values), MCS intensity is found equal to the EMS-98 one, while in about 30% of the sample (39 values), MCS intensity is higher (half or one degree) than the EMS-98 one. Figure 4.5a displays the linear regression function between MCS and EMS-98 intensity values ( $R=0.98$ ) while Figure 4.5b shows the residual values for MCS (observed minus estimated) and the corresponding trend.

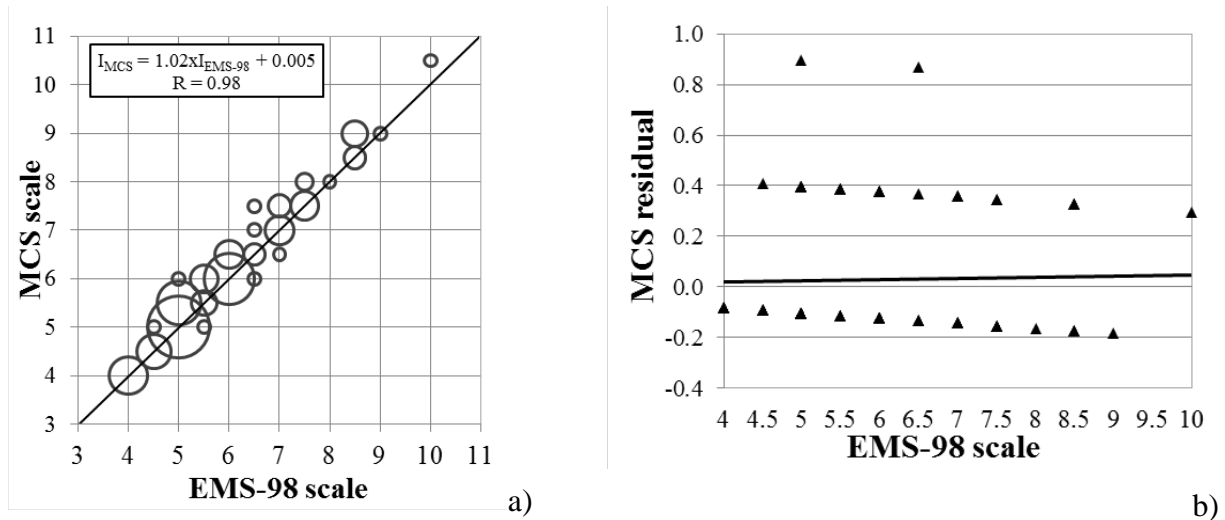


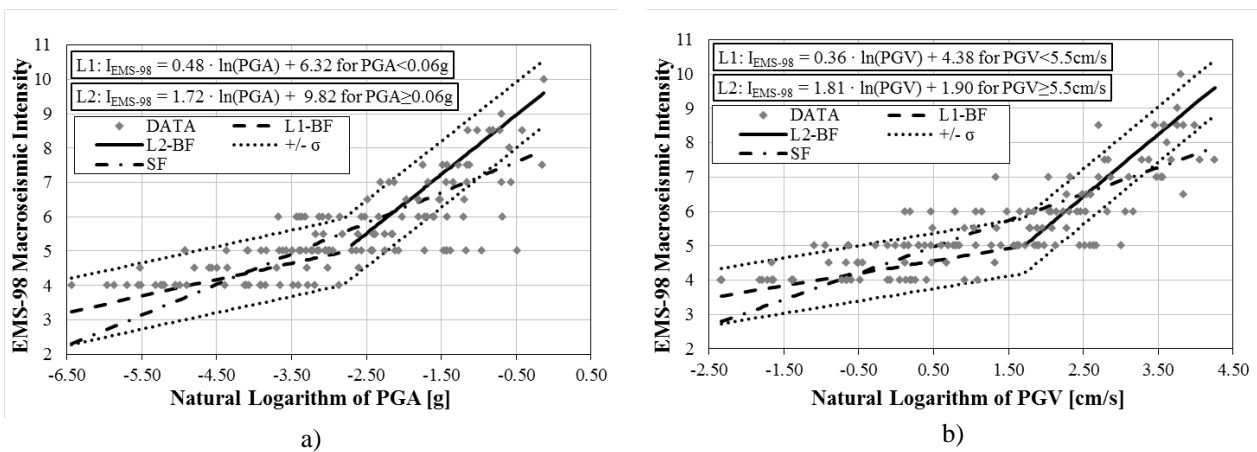
**Figure 4.5** a) Best-fit linear regression between the MCS and EMS-98 values considering the areas in which both macroseismic values are available. The size of the circles is proportional to the number of data. b) Residual values obtained from the considered MCS data with respect to the linear regression reported in a)

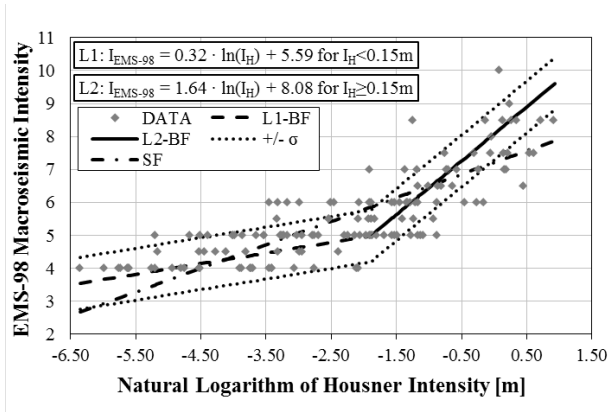
### 4.3 Proposed correlations

Starting from the above-described database, in this section statistical regressions by considering three instrumental parameters, i.e., PGA, PGV and Housner Intensity ( $I_H$ ), and two macroseismic intensity scales, i.e., EMS-98 and MCS, have been derived and analyzed. As previously said, they can be used in both direct (i.e., instrumental parameter is assumed as the independent variable and macroseismic intensity is the dependent one) and inverse direction (i.e., macroseismic intensity is assumed as the independent variable and instrumental parameter is the dependent one).

#### 4.3.1 Direct relationships

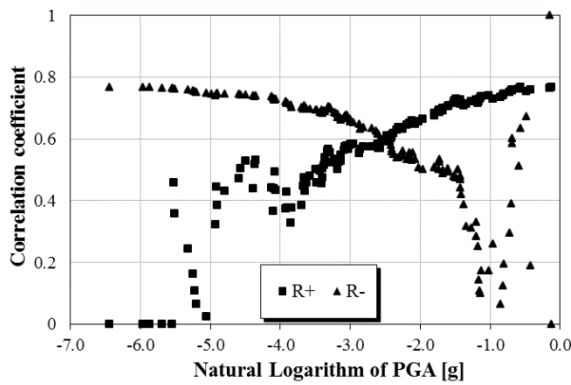
Figure 4.6 shows the EMS-98 macroseismic intensity values as a function of the natural logarithm of PGA (Fig. 4.6a), PGV (Fig. 4.6b) and  $I_H$  (Fig. 4.6c). First of all, the diagrams show that the data in terms of ground motion values are characterized by a larger variation in the range of intensities up to 6.0 EMS-98. As a matter of fact, for lower seismic intensities, building damage is generally absent and macroseismic intensities are mainly assigned on the basis of effects on people and objects. Therefore, a larger scatter of macroseismic data compared to instrumental data can be expected. On the contrary, for degrees higher than 6.0 EMS-98, building damage in terms of both distribution and severity becomes the key element in assigning of macroseismic intensity and, consequently, a lower variability can be found.



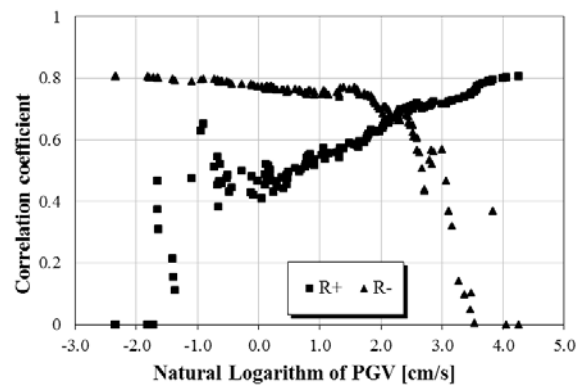


c)

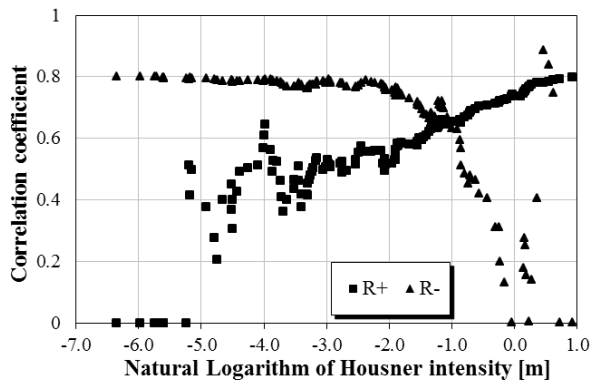
**Figure 4.6** EMS-98 intensities *versus* the natural logarithm of PGA (a), PGV (b) and  $I_H$  (c) values. Single function (SF, dash-dot line), bilinear function (BF, L1 dashed line, L2 solid line) and the associated +/- one standard deviation (dotted lines) are also shown.



a)



b)



c)

**Figure 4.7** Distribution of the correlation coefficients for PGA (a), PGV (b) and  $I_H$  (c) samples

Based on the above-described trend and in accordance with other studies on this topic (e.g., Faenza and Michelini, 2010; Worden et al., 2012), two types of functions have been considered in order to fit the data set, i.e., single (SF) and bilinear (BF) function, as shown in Figure 4.6 and reported in the following:

*Single functions*

$$I_{EMS-98} = 0.89 \cdot \ln(\text{PGA}) + 8.05 \quad (4.8)$$

$$I_{EMS-98} = 0.77 \cdot \ln(\text{PGV}) + 4.59 \quad (4.9)$$

$$I_{EMS-98} = 0.72 \cdot \ln(I_H) + 7.21 \quad (4.10)$$

*Bilinear functions*

$$I_{EMS-98} = 0.48 \cdot \ln(PGA) + 6.32 \quad PGA < 0.06g \quad (4.11)$$

$$I_{EMS-98} = 1.72 \cdot \ln(PGA) + 9.82 \quad PGA \geq 0.06g \quad (4.12)$$

$$I_{EMS-98} = 0.36 \cdot \ln(PGV) + 4.38 \quad PGV < 5.5cm/s \quad (4.13)$$

$$I_{EMS-98} = 1.81 \cdot \ln(PGV) + 1.90 \quad PGV \geq 5.5cm/s \quad (4.14)$$

$$I_{EMS-98} = 0.32 \cdot \ln(I_H) + 5.59 \quad I_H < 0.15m \quad (4.15)$$

$$I_{EMS-98} = 1.64 \cdot \ln(I_H) + 8.08 \quad I_H \geq 0.15m \quad (4.16)$$

For all the considered instrumental parameters, the best fit is found using the bilinear function (BF), as confirmed by adopting the Akaike Information Criterion (AIC) (Burnham and Anderson, 1998). Specifically, AIC values for BFs are 657, 633 and 627, respectively for PGA, PGV and  $I_H$  relationships; the corresponding values for SFs are 660, 640 and 648. As a result, only BFs are considered in the following.

The switch point values for BFs (equal to 0.06g, 5.5cm/s and 0.15m, respectively for PGA, PGV and  $I_H$  intensity measures) have been determined by sequentially adding (for R+ distribution) and removing (for R- one) a pair of data from opposite ends of PGA, PGV and  $I_H$  samples and, then, by evaluating the coefficient of correlation R. The switch point is the value at which R begins to simultaneously decrease (for R-) and increase (for R+). In order to detect the switch point value, an analytical procedure based on the difference between two consecutive R values (for both R+ and R- distributions) has been set up. According to the procedure, the switch point value is fixed when the above-mentioned difference exceeds a given tolerance. For example, with reference to  $I_H$  parameter (Fig. 4.7c), at a value equal to -1.9 (in terms of natural logarithm, equal to about 0.15m), the R- values tend to decrease (i.e., the difference with the previous R value exceeds the given tolerance) and the R+ values begin to increase as well (i.e., the difference with the previous R value exceeds the given tolerance). Consequently, for the  $I_H$  bilinear function, the switch point is equal to 0.15m.

Figures 4.7 show the trends of the R values for all the considered ground motion parameters.

For each relationship, Table 4.3 reports the statistical results in terms of correlation coefficient R, Mean Squared Error (MSE) and standard deviation ( $\sigma$ ) of the residuals. It is worth noting that the MSE values have been evaluated through the following expression:

$$MSE = \frac{1}{n} \sum_{i=1}^n (Y_i - \hat{Y}_i)^2 \quad (4.17)$$

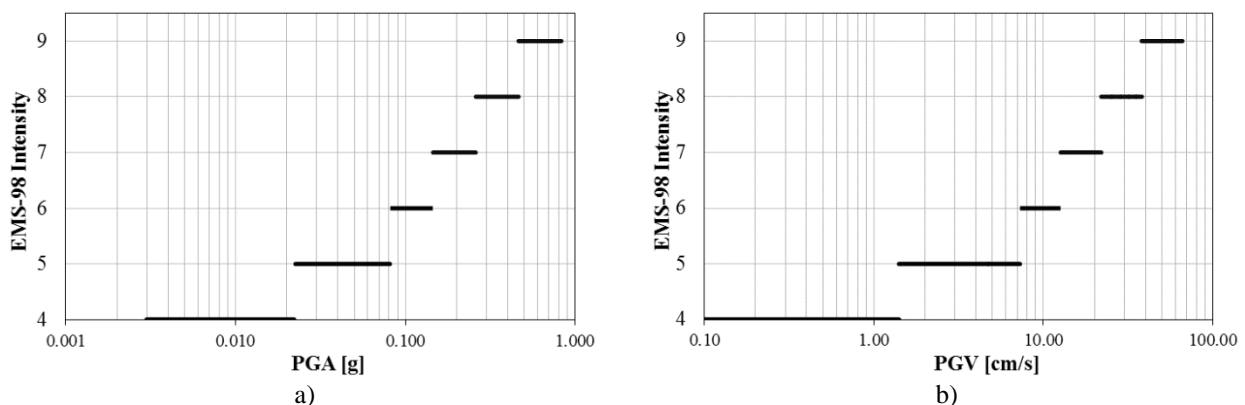
where  $Y$  are the observed data and  $\hat{Y}$  are the predicted one.

Eqs	R	MSE	$\sigma$
4.11	0.58	0.95	0.96
4.12	0.64		
4.13	0.59	0.65	0.81
4.14	0.75		
4.15	0.56	0.62	0.79
4.16	0.76		

**Table 4.3** Statistical results for the proposed relationships (Eqs 4.11 - 4.16) in terms of correlation coefficient R, Mean Squared Error (MSE) and standard deviation ( $\sigma$ ) of the residuals

Statistical analyses show that, for  $I_H$  values greater than 0.15m, a high correlation coefficient ( $R=0.76$ ) is found, which is close to the one obtained for  $PGV \geq 5.5\text{cm/s}$  ( $R=0.75$ ). On the contrary, a poor correlation ( $R=0.56$ ) characterizes the lower values of  $I_H$  (i.e.,  $I_H < 0.15\text{m}$ ), corresponding to medium-to-low values of EMS intensity. As already said, these results are expected because instrumental intensity measures such as  $I_H$  and  $PGV$  are well correlated to building damage which is generally experienced for higher values of seismic intensity (i.e.,  $I_H > 0.15\text{m}$ ,  $PGV \geq 5.5\text{cm/s}$ ). Similar results have been found also for  $PGA$ , where  $R$  is equal to 0.64 for  $PGA \geq 0.06\text{g}$ , while  $R=0.58$  is found for  $PGA < 0.06\text{g}$ . These results are also confirmed by both MSE and standard deviation values. In fact, the relationships in terms of  $PGA$  show both a greater error in the predicted values ( $MSE=0.95$ ) and a larger dispersion ( $\sigma=0.96$ ) than  $PGV$  and  $I_H$ , whose MSE values are equal to 0.65 and 0.62, while  $\sigma$  values are 0.81 and 0.79, respectively.

Considering that previous Eqs. 4.11-4.16 provide macroseismic values in a continuous form, a conversion into the discrete degrees of EMS-98 scale can be useful. To this purpose, Figure 4.8 shows the results obtained from Eqs. 4.11-4.16 for intensities ranging between 4 and 9, rounded to the nearest integer value. For ease of use, the horizontal axis, corresponding to the ground motion parameters (i.e.,  $PGA$ ,  $PGV$  and  $I_H$ ), is in base-10 logarithmic scale.



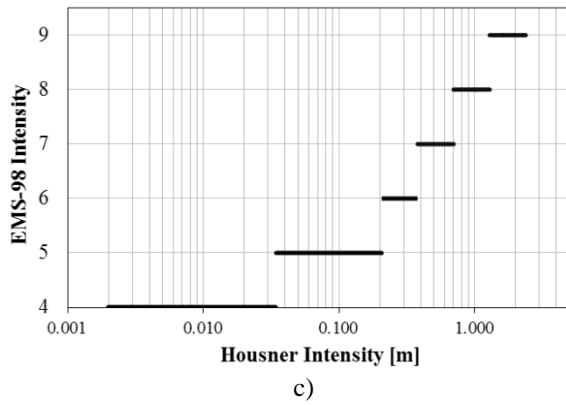
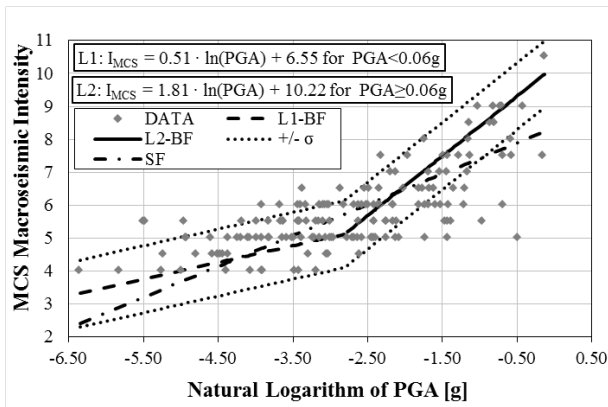
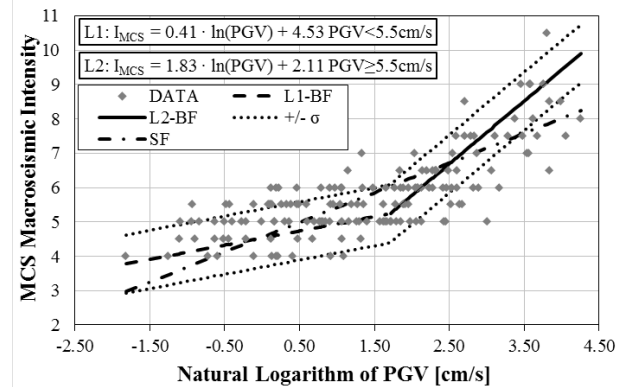


**Figure 4.8** Macroseismic intensity (according to the EMS-98 scale) with respect to PGA (a), PGV (b) and  $I_H$  (c) values. The horizontal axis is in logarithmic scale.

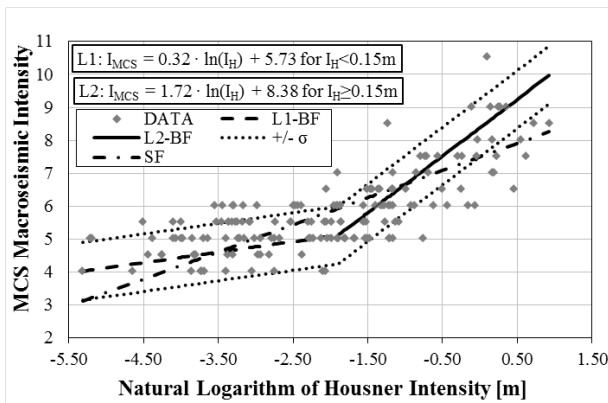
As a consequence of the strong correlation between the two macroseismic scales (MCS and EMS-98, see Figure 4.5), similar trends have been found in terms of MCS, as shown in Figures 4.9a, 4.9b and 4.9c, respectively for PGA, PGV and  $I_H$  intensity measures.



a)



b)



c)

**Figure 4.9** MCS intensities versus the natural logarithm of PGA (a), PGV (b) and  $I_H$  (c) values. Single function (SF, dash-dot line), bilinear function (BF, L1 dashed line, L2 solid line) and the associated +/- one standard deviation (dotted lines) are also shown

In the same Figures 4.9, both SFs and BFs are also shown and their analytical expressions are reported in the following:

*Single functions*

$$I_{MCS} = 0.94 \cdot \ln(PGA) + 8.36 \quad (4.18)$$

$$I_{MCS} = 0.87 \cdot \ln(PGV) + 4.55 \quad (4.19)$$

$$I_{MCS} = 0.83 \cdot \ln(I_H) + 7.50 \quad (4.20)$$

*Bilinear functions*

$$I_{MCS} = 0.51 \cdot \ln(PGA) + 6.55 \quad PGA < 0.06g \quad (4.21)$$

$$I_{MCS} = 1.81 \cdot \ln(PGA) + 10.22 \quad PGA \geq 0.06g \quad (4.22)$$

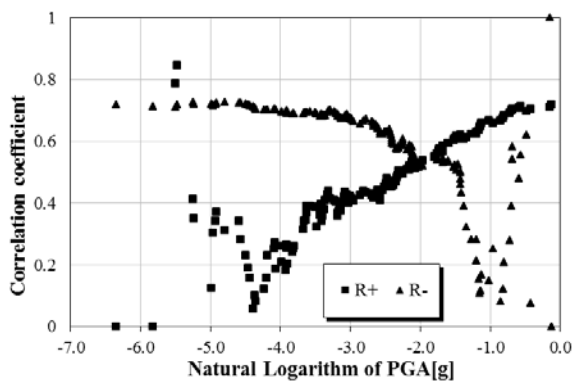
$$I_{MCS} = 0.41 \cdot \ln(PGV) + 4.53 \quad PGV < 5.5cm/s \quad (4.23)$$

$$I_{MCS} = 1.83 \cdot \ln(PGV) + 2.11 \quad PGV \geq 5.5cm/s \quad (4.24)$$

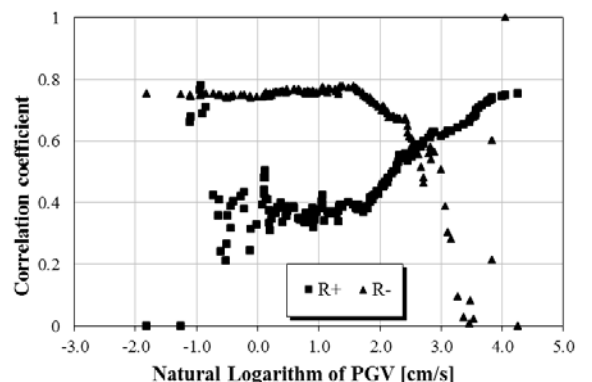
$$I_{MCS} = 0.32 \cdot \ln(I_H) + 5.73 \quad I_H < 0.15m \quad (4.25)$$

$$I_{MCS} = 1.72 \cdot \ln(I_H) + 8.38 \quad I_H \geq 0.15m \quad (4.26)$$

Similarly, to the relationships in terms of EMS-98, also for MCS data the best-fit is represented by the bilinear function. Specifically, AIC values for BFs are 762, 748 and 758, respectively for PGA, PGV and  $I_H$ ; the corresponding values for SFs are 771, 750 and 762. As a consequence, only BFs are considered in the following. The switch point values, equal to 0.06g for PGA, 5.5cm/s for PGV and 0.15m for  $I_H$ , are coincident with those ones for the EMS-98 scale. Figure 4.10 shows the trend of the correlation coefficients R.



a)



b)



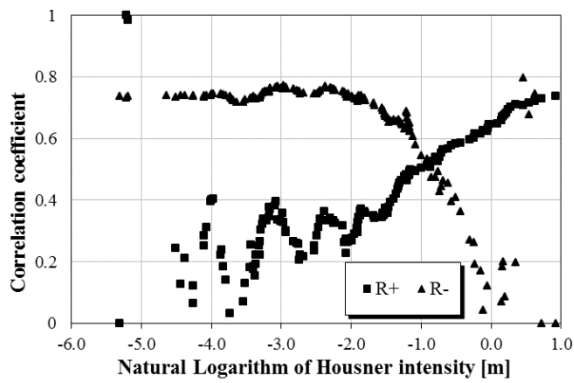


**Figure 4.10** Distribution of the correlation coefficients for PGA (a), PGV (b) and  $I_H$  (c) samples.

c)

For Equations 4.21-4.26, Table 4.4 reports the statistical results in terms of correlation coefficient  $R$ , Mean Squared Error (MSE, see Eq. 4.17) and standard deviation ( $\sigma$ ) of the residuals.

Eqs	R	MSE	$\sigma$
4.21	0.44	1.04	1.02
4.22	0.67		
4.23	0.38	0.71	0.85
4.24	0.76		
4.25	0.34	0.76	0.87
4.26	0.74		

**Table 4.4** Statistical results for the proposed relationships (Eqs 4.21 – 4.26) in terms of correlation coefficient  $R$ , Mean Squared Error (MSE) and standard deviation ( $\sigma$ ) of the residuals.

For the lower ranges of values of the considered instrumental parameter (i.e.,  $PGA < 0.06g$ ,  $PGV < 5.5cm/s$  and  $I_H < 0.15m$ , also corresponding to the L1 branch of the bilinear functions), statistical analyses provide the lower  $R$  values, that are equal to 0.44, 0.38 and 0.34, respectively. On the contrary, higher values have been found for the L2 branch (i.e., values higher than 0.06g for  $PGA$ , 5.5cm/s for  $PGV$  and 0.15m for  $I_H$ ), which are 0.67, 0.76 and 0.74 for the relationships in terms of  $PGA$ ,  $PGV$  and  $I_H$ , respectively.

In terms of error in the estimation and dispersion of results, the relationships relevant to  $PGA$  show the greater values of both MSE (1.04) and  $\sigma$  (1.02), while the lower ones are found for  $PGV$  (MSE=0.71,  $\sigma$ =0.85).

In order to provide a more useful representation of the proposed relationships, Figure 4.11 shows the results obtained from Eqs. 4.21-4.26 for discrete degrees of the MCS scale, respectively for  $PGA$ , (Fig. 4.11a),  $PGV$  (Fig. 4.11b) and  $I_H$  intensities (Fig. 4.11c). For ease of use, the horizontal axis, corresponding to the ground motion parameters (i.e.,  $PGA$ ,  $PGV$  and  $I_H$ ), is in base-10 logarithmic scale.

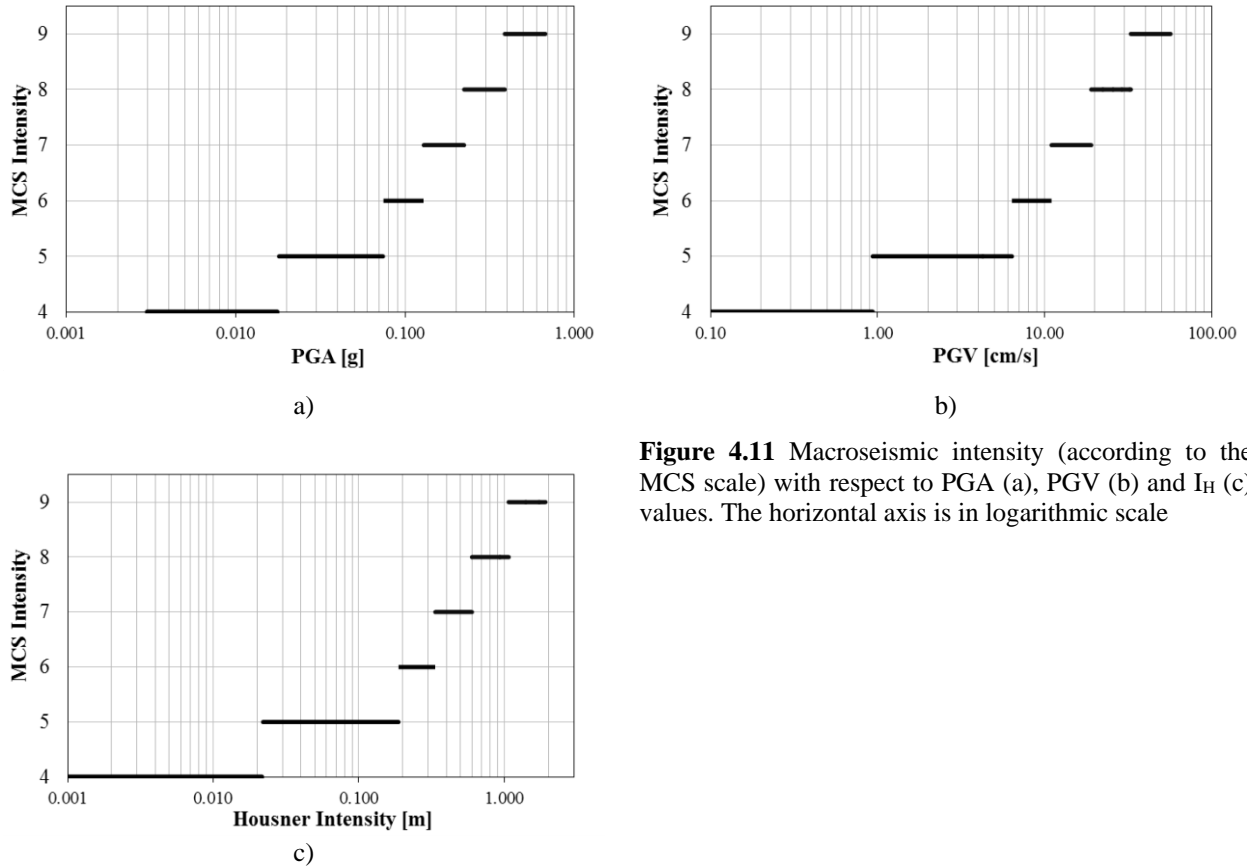


**Figure 4.11** Macroseismic intensity (according to the MCS scale) with respect to PGA (a), PGV (b) and  $I_H$  (c) values. The horizontal axis is in logarithmic scale

### 4.3.2 Inverse relationships

As a consequence of the adopted regression method (TLS), the above-described relationships can be easily inverted, i.e., using the same coefficients. In this way, known the macroseismic value as independent variable, the values of ground motion parameters (dependent variable) can be estimated, as follows:

*EMS-98 intensity measure*

$$PGA = e^{((I_{EMS-98} - 6.32)/0.48)} \quad I_{EMS-98} \leq 5 \quad (4.27)$$

$$PGA = e^{((I_{EMS-98} - 9.82)/1.72)} \quad I_{EMS-98} > 5 \quad (4.28)$$

$$PGV = e^{((I_{EMS-98} - 4.38)/0.36)} \quad I_{EMS-98} \leq 5 \quad (4.29)$$

$$PGV = e^{((I_{EMS-98} - 1.90)/1.81)} \quad I_{EMS-98} > 5 \quad (4.30)$$

$$I_H = e^{((I_{EMS-98} - 5.59)/0.32)} \quad I_{EMS-98} \leq 5 \quad (4.31)$$

$$I_H = e^{((I_{EMS-98} - 8.08)/1.64)} \quad I_{EMS-98} > 5 \quad (4.32)$$

MCS intensity measure

$$PGA = e^{((I_{MCS} - 6.55)/0.51)} \quad I_{MCS} \leq 5 \quad (4.33)$$

$$PGA = e^{((I_{MCS} - 10.22)/1.81)} \quad I_{MCS} > 5 \quad (4.34)$$

$$PGV = e^{((I_{MCS} - 4.53)/0.41)} \quad I_{MCS} \leq 5 \quad (4.35)$$

$$PGV = e^{((I_{MCS} - 2.11)/1.83)} \quad I_{MCS} > 5 \quad (4.36)$$

$$I_H = e^{((I_{MCS} - 5.73)/0.32)} \quad I_{MCS} \leq 5 \quad (4.37)$$

$$I_H = e^{((I_{MCS} - 8.38)/1.72)} \quad I_{MCS} > 5 \quad (4.38)$$

The switch point values of the above reported equations have been computed by solving Eqs 4.11-4.16 (for EMS-98) and Eqs 4.21-4.26 (for MCS) with the relevant corner values and rounding to the nearest integer value of the corresponding macroseismic intensity scales. As a result, for all ground-motion parameters (i.e., PGA, PGV and  $I_H$ ) and macroseismic scales (i.e., EMS-98 and MCS), the switch point values are set equal to 5.

Table 4.5 summarizes the statistical results in terms Mean Squared Error (MSE, see Eq. 4.17) and standard deviation ( $\sigma$ ) of the residuals.

	EMS-98		MCS	
	MSE	$\sigma$	MSE	$\sigma$
PGA (g)	0.01	0.11	0.01	0.11
PGV (cm/s)	80.17	8.98	117.01	10.16
$I_H$ (m)	0.11	0.34	0.12	0.34

**Table 4.5** Statistical results for the proposed inverse relationships (Eqs 4.27 – 4.38) in terms of Mean Squared Error (MSE) and standard deviation ( $\sigma$ ) of the residuals.

Starting from the above reported relationships, Table 4.6 provides the ranges of PGA, PGV and  $I_H$  values evaluated for some EMS-98 degrees. Note that the final values of each range refer to +/- half a degree of a given EMS-98 intensity. For example, the corner values of the first range in Table 4.6, i.e., 0.003-0.02g in PGA, have been evaluated by solving Eq. 4.27 with 3.5 and 4.5 EMS-98 intensities.

EMS-98 intensity	4	5	6	7	8	9
PGA (g)	0.003-0.02	0.02-0.08	0.08-0.15	0.15-0.26	0.26-0.46	0.46-0.83
PGV (cm/s)	0.09-1.40	1.4-7.3	7.3-12.6	12.6-22.0	22.0-38.1	38.1-66.2
Housner intensity (m)	0.002-0.03	0.03-0.21	0.21-0.38	0.38-0.70	0.70-1.29	1.29-2.38

**Table 4.6** Ranges of PGA, PGV and  $I_H$  for EMS-98 intensities

As for the EMS-98 inverse relationships, Table 4.7 provides the range values of PGA, PGV and  $I_H$  corresponding to each MCS intensity obtained from Eqs 4.33 and 4.38. The corner values of ranges refer to +/- half a degree of each MCS intensity.

MCS intensity	4	5	6	7	8	9
PGA (g)	0.003-0.02	0.02-0.07	0.07-0.13	0.13-0.22	0.22-0.39	0.39-0.67
PGV (cm/s)	0.08-1.0	1.0-6.4	6.4-11.0	11.0-19.0	19.0-32.8	32.8-56.6
Housner intensity (m)	0.001-0.02	0.02-0.19	0.19-0.34	0.34-0.60	0.60-1.07	1.07-1.91

**Table 4.7** Ranges of PGA, PGV and  $I_H$  for MCS intensities

### 4.4 Analysis of the proposed relationships

In this section, the proposed relationships have been analyzed and compared with some of the most prominent ones available in the technical literature.

For the sake of clarity, Table 4.8 summarizes the proposed regression relationships, separately for direct (i.e., for computing macroseismic intensity given a ground motion value, first column) and inverse functions (i.e., for estimating instrumental values starting from macroseismic intensities, second column).

First of all, the direct relationships proposed for higher instrumental values (i.e.,  $PGA \geq 0.06g$ ,  $PGV \geq 5.5cm/s$  and  $I_H \geq 0.15m$ ) generally provide higher values of the correlation coefficient (R) than those obtained for lower values ( $PGA < 0.06g$ ,  $PGV < 5.5cm/s$  and  $I_H < 0.15m$ ). These results are not startling because, on one hand, the considered instrumental parameter such as PGA, PGV and  $I_H$  are generally well correlated to the damage potential of seismic events and, on the other hand, macroseismic intensity assignment is affected by lower uncertainty when building damage increases.

<i>Direct relationships</i>	<i>Inverse relationships</i>
<b><math>I_{EMS-98} = f(PGA)</math></b>	<b><math>PGA = f(I_{EMS-98})</math></b>
$I_{EMS-98} = 0.48 \cdot \ln(PGA) + 6.32$ $PGA < 0.06g$ $I_{EMS-98} = 1.72 \cdot \ln(PGA) + 9.82$ $PGA \geq 0.06g$	$PGA = e^{((I_{EMS-98} - 6.32)/0.48)}$ $I_{EMS-98} \leq 5$ $PGA = e^{((I_{EMS-98} - 9.82)/1.72)}$ $I_{EMS-98} > 5$
<b><math>I_{MCS} = f(PGA)</math></b>	<b><math>PGA = f(I_{MCS})</math></b>
$I_{MCS} = 0.51 \cdot \ln(PGA) + 6.55$ $PGA < 0.06g$ $I_{MCS} = 1.81 \cdot \ln(PGA) + 10.22$ $PGA \geq 0.06g$	$PGA = e^{((I_{MCS} - 6.55)/0.51)}$ $I_{MCS} \leq 5$ $PGA = e^{((I_{MCS} - 10.22)/1.81)}$ $I_{MCS} > 5$
<b><math>I_{EMS-98} = f(PGV)</math></b>	<b><math>PGV = f(I_{EMS-98})</math></b>
$I_{EMS-98} = 0.36 \cdot \ln(PGV) + 4.38$ $PGV < 5.5cm/s$ $I_{EMS-98} = 1.81 \cdot \ln(PGV) + 1.90$ $PGV \geq 5.5cm/s$	$PGV = e^{((I_{EMS-98} - 4.38)/0.36)}$ $I_{EMS-98} \leq 5$ $PGV = e^{((I_{EMS-98} - 1.90)/1.81)}$ $I_{EMS-98} > 5$
<b><math>I_{MCS} = f(PGV)</math></b>	<b><math>PGV = f(I_{MCS})</math></b>
$I_{MCS} = 0.41 \cdot \ln(PGV) + 4.53$ $PGV < 5.5cm/s$ $I_{MCS} = 1.83 \cdot \ln(PGV) + 2.11$ $PGV \geq 5.5cm/s$	$PGV = e^{((I_{MCS} - 4.53)/0.41)}$ $I_{MCS} \leq 5$ $PGV = e^{((I_{MCS} - 2.11)/1.83)}$ $I_{MCS} > 5$
<b><math>I_{EMS-98} = f(I_H)</math></b>	<b><math>I_H = f(I_{EMS-98})</math></b>
$I_{EMS-98} = 0.32 \cdot \ln(I_H) + 5.59$ $I_H < 0.15m$ $I_{EMS-98} = 1.64 \cdot \ln(I_H) + 8.08$ $I_H \geq 0.15m$	$I_H = e^{((I_{EMS-98} - 5.59)/0.32)}$ $I_{EMS-98} \leq 5$ $I_H = e^{((I_{EMS-98} - 8.08)/1.64)}$ $I_{EMS-98} > 5$
<b><math>I_{MCS} = f(I_H)</math></b>	<b><math>I_H = f(I_{MCS})</math></b>
$I_{MCS} = 0.32 \cdot \ln(I_H) + 5.73$ $I_H < 0.15m$ $I_{MCS} = 1.72 \cdot \ln(I_H) + 8.38$ $I_H \geq 0.15m$	$I_H = e^{((I_{MCS} - 5.73)/0.32)}$ $I_{MCS} \leq 5$ $I_H = e^{((I_{MCS} - 8.38)/1.72)}$ $I_{MCS} > 5$

**Table 4.8** Correlations between instrumental parameters (PGA, PGV and  $I_H$ ) and macroseismic intensity scales (MCS and EMS-98).

On the contrary, for low seismic intensity (e.g.,  $PGA < 0.06g$ ,  $PGV < 5.5cm/s$  and  $I_H < 0.15m$ ), negligible damage on buildings is generally experienced and, therefore, macroseismic intensity is

mainly based on not physical effects (e.g., vibration felt by people) and/or poor information (e.g., swinging of objects). As a consequence, a larger scatter in the data distribution is expected

Comparing the R values obtained from the direct relationships in terms of the three instrumental measures also confirms the better correlation relevant to integral parameters, such as  $I_H$ , than peak intensity ones (i.e., PGA). In fact, R values related to  $I_H$  are 0.76 and 0.74 respectively for the relationships in terms of EMS-98 and MCS. On the contrary, in terms of PGA, R values equal to 0.64 and 0.67 are found, respectively for EMS-98 and MCS. For PGV, a similar value of R with respect to  $I_H$  has been found in the relationship for EMS-98 ( $R=0.75$ ) while it shows a slightly better correlation ( $R=0.76$ ) than  $I_H$  ( $R=0.74$ ) in case of fitting with MCS data.

The above reported results are also confirmed by the other statistical operators, such as the Mean Squared Error (MSE) and the standard deviation ( $\sigma$ ). Specifically, in the case of EMS-98, the values evaluated for  $I_H$  ( $MSE=0.62$ ,  $\sigma=0.79$ ) and PGV ( $MSE=0.65$ ,  $\sigma=0.81$ ) are lower than those referred to PGA ( $MSE=0.95$ ,  $\sigma=0.96$ ). Further, for the same instrumental intensity measure (i.e., PGA, PGV and  $I_H$ ), slightly higher R values have been found for the EMS-98 relationships compared to the MCS ones. In terms of MSE and standard deviation, EMS-98 relationships provide lower values with respect to MCS ones. This result can be clearly ascribed to the fact that, unlike MCS, the European scale takes into account both building vulnerability and observed damage distribution in assigning macroseismic intensities and, consequently, a better correlation to building damage is expected, especially for the higher intensity values.

#### 4.4.1 Comparison with other studies

Comparisons between the proposed relationships and those obtained in other studies have been carried out in order to discuss possible differences. As aforementioned, most of the available relationships in the technical literature consider PGA as instrumental measure and MCS as macroseismic scale. Therefore, in Figure 4.12, the proposed regression relationship for computing MCS macroseismic intensities given PGA values has been compared with those obtained by Faccioli & Cauzzi (2006) and Faenza & Michelini (2010). Table 4.9 reports the relationships derived by the authors and the adopted dataset. For the sake of clarity, the information related to the proposed relationship is also reported.

As for the computed MCS intensity, the differences among the considered relationships can be grouped with respect to three ranges of values. For  $PGA < 0.01g$ , the proposed relationship shows higher values than those obtained by Faenza & Michelini. In the range  $0.02g < PGA < 0.2g$  the proposed relationship underestimates the macroseismic intensities with respect to both Faccioli & Cauzzi and Faenza & Michelini. Finally, for  $PGA > 0.3g$ , the values obtained from the proposed relationship are greater than those obtained from the other considered relationships.

Reference	Direct relationships	Inverse relationships	Dataset
Margottini et al., (1992)	-----	$\log(PGA) = 0.525 + 0.22 \cdot I_{MCS}$	56 PGA-MCS data points from 9 Italian earthquakes
Faccioli & Cauzzi (2006)	$I_{MCS} = 1.96 \cdot \log(PGA) + 6.54$	$\log(PGA) = -1.33 + 0.2 \cdot I_{MCS}$	75 PGA-MCS data points from 26 earthquakes
Faenza & Michelini (2010)	$I_{MCS} = 2.58 \cdot \log(PGA) + 1.68$	$\log(PGA) = -0.65 + 0.39 \cdot I_{MCS}$	266 PGA-MCS data points from 87 Italian earthquakes
Proposed	$I_{MCS} = 0.51 \cdot \ln(PGA) + 6.55$ $PGA < 0.06g$ $I_{MCS} = 1.81 \cdot \ln(PGA) + 10.22$ $PGA \geq 0.06g$	$\ln(PGA) = (I_{MCS} - 6.55) / 0.51$ $I_{MCS} < 5$ $\ln(PGA) = (I_{MCS} - 10.22) / 1.81$ $I_{MCS} \geq 5$	157 PGA-MCS data points from 27 earthquakes

**Table 4.9** Relationships considered in the comparisons

In the comparison reported in Figure 4.12, it is worth noting that the Faccioli & Cauzzi relationship provides results limited to the range  $0.02g \leq PGA \leq 0.6g$ . For the lowest value ( $PGA=0.02g$ ), the Faccioli & Cauzzi relationship provides similar values to those obtained from both the proposed regression and the Faenza & Michelini regression, while, for PGA values around 0.6g, it provides lower macroseismic intensity values. Finally, the considered relationships are within the range obtained for the proposed regression +/- one standard deviation.

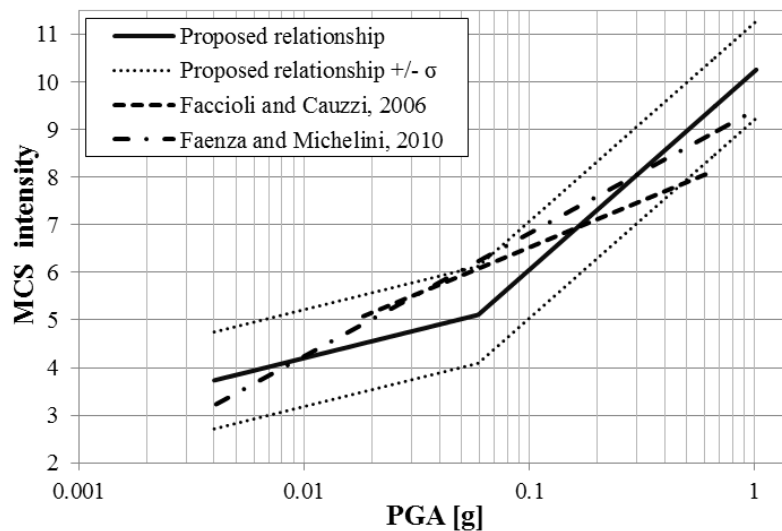


**Figure 4.12** Comparison between the proposed relationship between MCS intensity and PGA with the regressions of Faccioli & Cauzzi (2006) and Faenza & Michelini (2010). The PGA axes is in logarithmic scale

The differences found in the comparison are mainly due to the different adopted datasets and the bilinear form of the proposed relationship, as reported in Table 4.9. To this regard, it is worth noting that in the database used by Faenza & Michelini the low intensity values ( $PGA \leq 0.1g$ ) prevail differently from the database in this study. Specifically, the percentage of PGA values lower than 0.1g is 82%, while it is 62% for that considered in this study. Furthermore, other sources of differences can be also ascribed to both the regression technique and the criteria adopted for grouping different macroseismic scales.

In order to evaluate the influences of the above-described comparison in terms of predicted damage, an earthquake scenario is performed by using the DPMs defined by Zuccaro et al. (2000). As can be evaluated from Figure 4.12, for PGA equal to 0.1g, MCS intensities range from 6 (Proposed relationship) to 7 (Faenza and Michelini). All the results are reported in Table 4.10.

PGA (g)	PGA vs MCS relationships	MCS intensity
0.1	Proposed relationships	6
	Faccioli and Cauzzi, 2006	6.5
	Faenza and Michelini, 2010	7

**Table 4.10** MCS intensities provided by the considered relationship for PGA equal to 0.1g

These values, meant as seismic input for vulnerability class A, provide the damage distributions reported in Figure 4.13. In particular for damage level 3, the percentage of buildings ranges from about 12.3% (Proposed relationship) to about 16.1% (Faenza and Michelini). An intermediate value (about 14.2%) can be predicted by adopting the Faccioli and Cauzzi relationship.

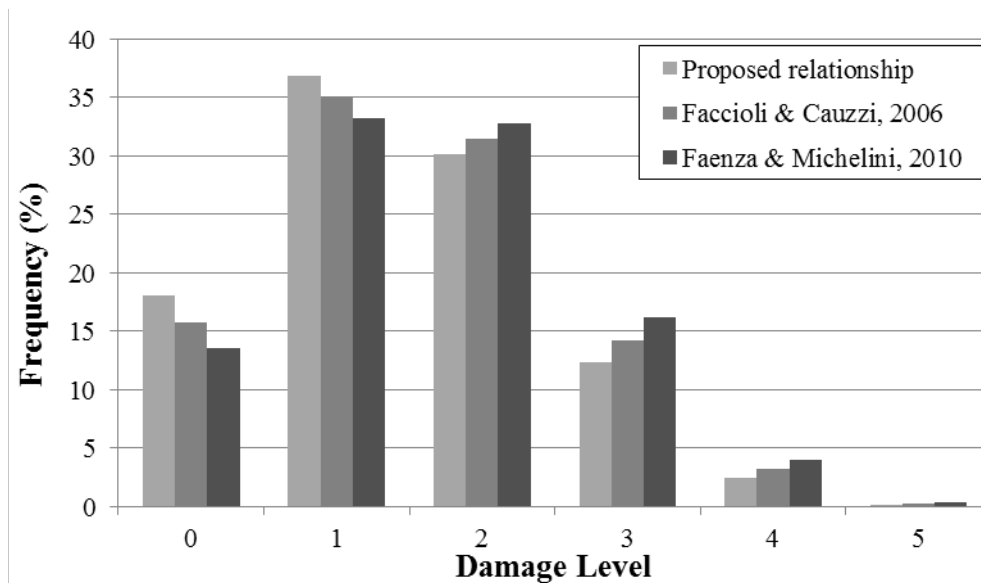


**Figure 4.13** Damage distribution for vulnerability class A according to DPMs defined by Zuccaro et al. (2000)

For the inverse relationships (i.e., PGA vs MCS), the proposed relationship has been compared with those obtained by Margottini et al., (1992), Faccioli & Cauzzi (2006) and Faenza & Michelini (2010), reported in Table 4.9. Figure 4.14 shows the values obtained from the considered relationships for discrete MCS values ranging from 4 to 9. Starting from a similar value estimated for  $I_{MCS} = 5$ , the proposed relationship provides lower values with respect to the other relationships for  $I_{MCS} < 5$ . On the contrary, in the range  $I_{MCS} \geq 5.5$ , the proposed regression provides greater values than all the considered relationships, although, for 8.5/9 MCS intensity, the Faenza & Michelini relationship provides a similar value (about 0.65g). It is worth noting that the Margottini et al. relationship cannot be applied for intensity greater than 8 MCS.



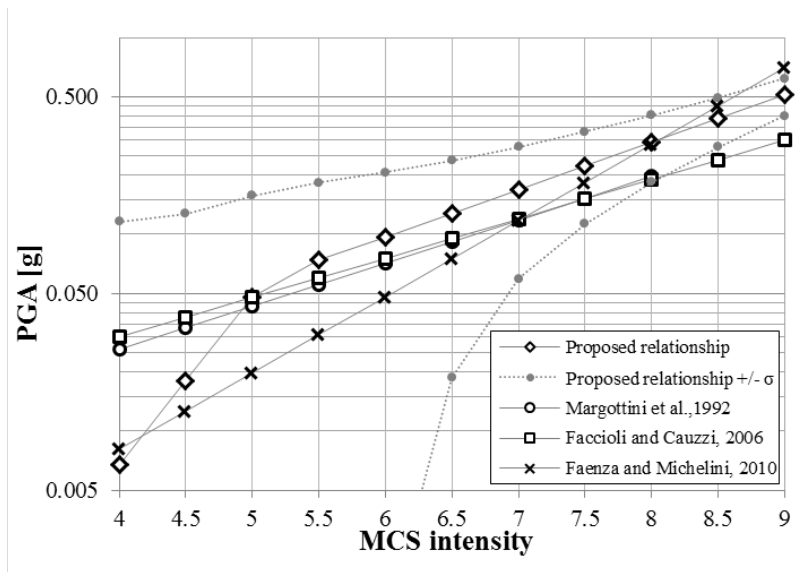


**Figure 4.14** Comparison between the proposed (inverse) relationship between PGA and MCS intensity with the regressions of Margottini et al. (1992), Faccioli & Cauzzi (2006) and Faenza & Michelini (2010). The PGA axes is in logarithmic scale.

## Discussion

Macroseismic data of historical earthquakes represent an essential source to improve knowledge on the seismic hazard of an area. In order to be considered in risk analyses, as well as in design practice, macroseismic intensities need to be converted into more suitable engineering parameters. In this framework, correlations between macroseismic intensities and ground motion parameters have been derived. Peak Ground Acceleration (PGA), Peak Ground Velocity (PGV) and Housner Intensity ( $I_H$ ) as instrumental measures, and European Macroseismic Scale (EMS-98) and Mercalli-Cancani-Sieberg scale (MCS) as macroseismic measures, have been considered. A large database containing 179 ground-motion records related to 32 earthquake events occurred in Italy in the last 40 years has been collected to derive reversible relationships (i.e., macroseismic vs instrumental intensity and vice-versa). For both EMS-98 and MCS data, the best-fit is a bilinear function with switch point at 0.06g, 5.5cm/s and 0.15m, respectively for PGA, PGV and  $I_H$ .

Statistical analysis results show that the higher correlation among instrumental and macroseismic data is generally found for the higher intensity values, for which building damage becomes the key parameter in assigning macroseismic intensity. For example, the correlation coefficient for the relationships in terms of EMS-98 scale is about 0.76 for  $I_H$ , 0.75 for PGV and 0.64 for PGA. Similar results are also found in terms of Mean Squared Error (MSE) and standard deviation ( $\sigma$ ) of the residual. In fact,  $I_H$  and PGV show lower values for both MSE (0.62 and 0.65, respectively) and  $\sigma$  (0.79 and 0.81, respectively) with respect to PGA (MSE=0.95,  $\sigma$ =0.96). These results also confirm the better capability of both  $I_H$  and PGV to represent the damage potential of ground motions with respect to PGA. Similar trend is found for the regressions in terms of MCS, although the statistical analysis results are generally poorer than EMS-98.

The comparison with other relationships available in the literature shows that the proposed relationship (in terms of MCS and PGA intensity measure) generally underestimates the macroseismic values for the lower intensities, while it provides higher values than those obtained from Faenza & Michelini for the higher intensities.

The proposed relationships actually provide useful tools in performing risk analyses and studies of earthquake scenarios. With respect to other relationships available in the literature, they provide instrumental vs macroseismic intensity relationships, and vice-versa, based on peak and integral parameters as for instrumental measures, and MCS and EMS-98 scales, as for macroseismic intensity. Further, they were derived on the basis of a larger dataset compared to other studies (e.g., Margottini, Wald et al., Faccioli & Cauzzi, Chiauzzi et al.) which, nevertheless, in the future needs to be extended by considering more earthquakes occurred in other countries.

## References

- Azzaro R, Barbano MS, Camassi R, D'Amico S, Mostaccio A, Piangiamore G, Scarfi L (2004) The earthquake of 6 September 2002 and the seismic history of Palermo (Northern Sicily, Italy): Implications for the seismic hazard assessment of the city. *Journal of Seismology* 8, 525–543.
- Braga F, Dolce M, Liberatore D (1982) A statistical study on damaged buildings and ensuing review of the MSK-76 Scale. In: 8th ECEE, Atene
- Burnham KP, Anderson DR (1998) *Model Selection and Multimodel Inference: A Practical Information-Theoretic Approach*, Springer-Verlag, Telos, Germany
- Chiauzzi L, Masi A, Mucciarelli M, Vona M, Pacor F, Cultrera G, Galovic F, Emolo A (2012) Building damage scenarios based on exploitation of Housner intensity derived from finite faults ground motion simulations. *Bulletin of Earthquake Engineering*. 10:517–545
- Chioccarelli E, De Luca F, Iervolino I (2012) Preliminary study of Emilia (May 20h 2012) earthquake ground motion records V2.11. Available at website <http://www.reluis.it>
- Codermatz R, Nicolich R, Slejko D (2003) Seismic risk assessments and GIS technology: applications to infrastructures in the Friuli–Venezia Giulia region (NE Italy). *Earthquake Engineering Structural Dynamics* 32:1677–1690.
- Dolce M, Masi A, Marino M, Vona M (2003) Earthquake damage scenarios of Potenza town (Southern Italy) including site effects. *Bulletin of Earthquake Engineering* 1(1):115–140
- Faccioli E, Cauzzi C (2006) Macroseismic intensities for seismic scenarios, estimated from instrumentally based correlations. In: European conference on earthquake engineering and seismology, Geneva, Switzerland, 3–8 September 2006
- Faenza L, Michelini A (2010) Regression analysis of MCS intensity and ground motion parameters in Italy and its application in ShakeMap. *Geophysical Journal International*, 180, 1138–1152
- Galli P, Molin D, Camassi R, Castelli V (2001). Il terremoto del 9 settembre 1998 nel quadro della sismicità storica del confine calabro-lucano. Possibili implicazioni sismotettoniche. *Il Quaternario - Italian Journal of Quaternary Sciences*, 14, 31-40.
- Gómez Capera AA, Albarello D, Gasperini P (2007) Aggiornamento relazioni fra l'intensità macrosismica e PGA, Technical report, Convenzione INGV-DPC 2004-2006.
- Margottini C, Molin D, Serva L (1992) Intensity versus ground motion: a new approach using Italian data. *Engineering Geology* 33:45–58
- Masi A (2003) Seismic vulnerability assessment of gravity load designed R/C frames. *Bulletin of Earthquake Engineering* 1(3):371–395
- Masi A, Chiauzzi L, Braga F, Mucciarelli M, Vona M, Ditommaso R (2010) Peak and integral seismic parameters of L'Aquila 2009 ground motions: observed vs code provision values. Special Issue L'Aquila Earthquake. *Bulletin of Earthquake Engineering*. DOI: 10.1007/s10518-010-9227-1.
- Masi A, Vona M, Mucciarelli M (2011) Selection of natural and synthetic accelerograms for seismic vulnerability studies on RC frames. *Journal of Structural Engineering ASCE Special Issue devoted to "Earthquake Ground Motion Selection and Modification for Nonlinear Dynamic Analysis of Structures"* 137(3):367–378
- Masi A, Digrisolo A, Manfredi V (2015) Fragility curves of gravity-load designed RC buildings with regularity in plan. *Earthquakes and Structures*, Vol. 9, No. 1 (2015) 1-27
- Molin D (1995) Consideration on the assessment of macroseismic intensity. *Ann Geophys* 38:805–810
- Montaldo V, Faccioli E, Zonno G, Akinci A, Malagnini L (2005) Treatment of ground-motion predictive relationships for the reference seismic hazard map of Italy. *Journal of Seismology*, 9, 295–316.
- Musson R.M. W., Grünthal G. and Stucchi M. (2010) The comparison of macroseismic intensity scales, *J Seismol* (2010) 14:413-428 DOI 10.1007/s10950-009-9172-0

Petráš I. and Bednárová D. (2010) Total Least Squares Approach to Modeling: A Matlab Toolbox. *Acta Montanistica Slovaca*, Ročník 15 (2010), číslo 2, 158-170

Stucchi M, Galadini F, Monachesi G (1998) The earthquakes of September/October 1997 in the frame of tectonics and long-term seismicity of the Umbria-Marche (Central Italy) Apennines. Available at website [http://emidius.mi.ingv.it/GNDT/T19970926\\_eng/](http://emidius.mi.ingv.it/GNDT/T19970926_eng/)

Tertulliani A, Arcoraci L, Berardi M, Bernardini F, Camassi R, Castellano C, Del Mese S, Ercolani M, Graziani L, Leschiutta I, Rossi A, Vecchi M (2010) An application of EMS 98 in a medium size city: the case of L'Aquila (Italy) after the April 6, 2009 Mw 6.3 earthquake. *Bulletin of Earthquake Engineering*. DOI: 10.1007/s10518-010-9188-4.

Wald DJ, Quitoriano V, Heaton TH, Kanamori H (1999) Relations between Peak Ground Acceleration, Peak Ground Velocity, and Modified Mercalli Intensity in California, *Earthquake Spectra*, 15, 3, 557-564

Worden, C.B., M.C. Gerstenberger, D.A. Rhoades, D.J. and Wald (2012) Probabilistic relationships between ground-motion parameters and Modified Mercalli intensity in California *Bull. Seism. Soc. Am.* 102(1), 204-221. DOI: <https://doi.org/10.1785/0120110156>.

Working Group ITACA (2017) Data base of the Italian strong motion data. Available at website <http://itaca.mi.ingv.it>

Zaiontz C. (2019) Real Statistics Using Excel, available on-line at [www.real-statistics.com](http://www.real-statistics.com)

Zuccaro G, Papa F, Baratta A (2000) Aggiornamento delle mappe a scala nazionale di vulnerabilità sismica delle strutture edilizie. In A. Bernardini A. (a cura di), *La vulnerabilità degli edifici: valutazione a scala nazionale della vulnerabilità sismica degli edifici*. Roma, CNR-GNDT, pp. 133-175

## CHAPTER V

### **Building exposure modelling: definition of innovative approaches**

#### **Introduction**

An accurate characterization of exposure component represents a key-element in the scope of seismic impact evaluation and risk reduction plans. As discussed in Chapter I, several data sources and related approaches are available for the assemblage of a building inventory (Polese et al., 2019a). In this regard, an exposure model based on a building-by-building survey is highly accurate and reliable, but it is often not feasible because time, economic and human resources needed are too great. Hence, alternative sources and approaches (e.g., census data or remote sensing) are used on their own or combined in order to obtain information on the typological-structural characteristics of the buildings, without elevated efforts in terms of time and costs. In this framework, two innovative approaches for modelling the exposure of residential building stock have been proposed.

The first approach allows to exploit the data collected during the post-earthquake inspections in order to define an exposure model of residential buildings. Specifically, the information on the typological characteristics surveyed with the AeDES form (Baggio et al., 2007) has been firstly described according to the faceted taxonomy proposed by the Global Earthquake Model (GEM; Brzev et al., 2013). In a subsequent processing step, employing an attribute-based scoring methodology, the EMS-98 building classes (Grünthal, 1998) have been assigned based on the GEM attributes. In this way, an exposure model in terms of risk-oriented classes correlated to a specific fragility/vulnerability model can be defined and, then, the field data can be exploited for large-scale risk assessments. This approach, based on the concept of fuzzy compatibility score, allows for an extensive characterization of the uncertainties, by ensuring the reproducibility of the results.

The second approach is based on the combination of two methods aimed at collecting building data: CARTIS format and RRVS web-based platform. The first aims to collect, in a quick way based on interview to local experts, useful information on the building typologies most widespread in a selected area (Zuccaro et al., 2015). On the other side, RRVS (Rapid Remote Visual Screening) platform allows to perform a building-by-building survey using remote sensing images (Pittore and Wieland, 2013). The approach combining interview-based surveys with the potential offered by a remote screening technique allows to define an exposure model in quick and inexpensive way, that could be very useful in data-poor or economically developing countries.

## **5.1 Evaluation of exposure and vulnerability from post-earthquake data**

One of the first activities to be carried out after an earthquake is the damage and usability assessment. Post-earthquake damage and usability surveys represent a crucial moment for effectively managing the emergency phase in the aftermath of a strong seismic event in order to decide whether the people could safely return to their houses or be hosted in temporary shelters. The activities of post-earthquake survey are carried out by expert technicians through the compilation of inspection forms. In Italy, a specific survey tool for “damage assessment, short term countermeasures for damage limitation and evaluation of the post-earthquake usability of ordinary buildings”, referred to as AeDES form (Baggio et al., 2007) is currently used (see Section 2.3 of Chapter II). In addition to the damage and usability evaluation, this form allows for the collection of geometrical and structural attributes highly related to building vulnerability. In other countries such as Japan (Goretti and Inukai, 2002), Colombia (AIS, 2009), U.S. (ATC, 2005), New Zealand (NZSEE, 2009) and Greece (Anagnostopoulos and Moretti, 2008), similar survey forms consider only the observed damage and very limited data are collected related to the vulnerability of the structures (Masi et al., 2016). Hence, the AeDES form is a unique tool that enables the management of post-earthquake phase and a wide availability of building information very useful for Disaster Risk Reduction (DRR) and prevention activities. These data were collected for individual buildings in the order of many tens of thousands for recent Italian events. In this framework, most of the data collected during the post-earthquake inspections carried out over the last 50 years were recently organized in the “Observed Damage Database” platform (Da.D.O.; Dolce et al., 2019). The latter aims at collecting, cataloging and comparing data related to building features and seismic damage collected with different post-earthquake inspection forms during the most important Italian earthquakes (Table 5.1). With the development of the Da.D.O. platform, the information of the post-earthquake inspections has been harmonized and made freely available to the scientific community. These data represent a valuable source of exposure and vulnerability information and constitute an important heritage for different scientific purposes, including, e.g., the calibration of damage estimation models in terms of damage probability matrices (e.g., Dolce et al., 2003) or fragility curves (e.g., Lagomarsino and Giovinazzi, 2006) for damage scenarios and risk analysis. In this regard, some vulnerability models in the “National Risk Assessment” (DPC, 2018) were derived based on the actual damage data available in Da.D.O. However, to date, the Da.D.O. potential for seismic risk assessment has not been fully exploited, partly because the format specifications are very particular to the Italian environmental conditions and the collected attributes are not directly related to existing risk-oriented classifications (e.g., PAGER-STR taxonomy (Jaiswal et al., 2010), HAZUS taxonomy (Kircker et al., 2006) or EMS-98 building types (Grünthal, 1998). In fact, the AeDES data are not immediately suitable for wide-scale risk assessment applications dealing

with hundreds of thousands of buildings. Usually, in risk analysis applications, small sets of MECE (Mutually Exclusive, Collectively Exhaustive) typological classes are used, with each class grouping structures with similar structural features and, therefore, expected comparable seismic performance.

<b>Event</b>	<b>Record</b>	<b>Form version</b>
Friuli 1976	41582	Friuli `76
Irpinia 1980	38079	Irpinia `80
Abruzzo 1984	51817	Abruzzo `84
Umbria Marche 1997	48525	AeDES 09/97
Pollino 1998	17442	AeDES 06/98
Molise-Puglia 2002	24141	AeDES 05/2000
Emilia 2003	1011	AeDES 05/2000
L'Aquila 2009	74049	AeDES 06/2008
Emilia 2012	22554	AeDES 06/2008
Garfagnana-Lunigiana 2013	3258	AeDES 06/2008

**Table 5.1** Events, record and form versions reported in Da.D.O. web-based platform

Therefore, in order to reliably extract the exposure and vulnerability information and match it according to recognized international standards, an innovative methodology has been developed to convert the information collected through the AeDES form to different formats more suitable for a large-scale risk evaluation and comparison. In the proposed approach, the information on the typological characteristics has been firstly described according to the faceted taxonomy proposed by Global Earthquake Model (GEM, v2.0; Brzev et al., 2013). The conversion process allows to harmonize the AeDES data, that are specific to the conditions to be found in Italy, in terms of a flexible taxonomy with a global scope. Moreover, this step enables to define an exposure model that is independent by the vulnerability/fragility component and could be also employed for the consideration of different, possibly concurrent hazards (multi-hazard analyses). However, the information in terms of GEM taxonomy (as well as the AeDES data) cannot be directly used for the large-scale seismic risk evaluations. Therefore, in a subsequent processing step, employing an attribute-based scoring methodology (Pittore et al., 2018), the EMS-98 building classes have been assigned based on the GEM attributes. In this way, an exposure model in terms of risk-oriented classes correlated to a specific fragility model (i.e., EMS-98 classes) can be defined and, then, the information based on field data (i.e., AeDES form) can be exploited for large-scale risk assessments. Therefore, the proposed approach allows to separately consider the data collection based on field observations and the exposure modelling (even vulnerability-based) by ensuring the reproducibility of the results. Furthermore, this methodology based on the concept of fuzzy compatibility score provides a transparent and sound characterization of the uncertainty underlying the class assignment process. In Chapter VI, the proposed approach has been exemplified with the data of the Mw 6.3 2009 L'Aquila earthquake by considering observed damage data and macroseismic intensity values as provided by the Da.D.O. platform.

### 5.1.1 Taxonomy description

The exposure component describes the collected data on the assets (buildings, infrastructure, lifelines) that are susceptible to be damaged by seismic events. As for buildings, two different taxonomy typologies can be used in order to describe the structural and non-structural characteristics, namely *risk-oriented* or *faceted taxonomies* (Pittore et al., 2018; see Section 1.3 of Chapter I). For large-scale applications, specific risk-oriented taxonomies are usually employed, among which PAGER-STR taxonomy (Jaiswal et al., 2010), HAZUS taxonomy (Kircker et al., 2006) or European Macroseismic Scale (Grünthal et al., 1998). The buildings belonging to each class have similar structural features and, therefore, are expected to show similar seismic behaviors during an earthquake. On the contrary, faceted taxonomies consider many different attributes to describe individual buildings at wide geographical scales (e.g., GEM taxonomy, Brzev et al., 2013). In large-scale applications, GEM taxonomy cannot be used as the risk-oriented ones because of different level of detail between the data collection and the risk assessment phase. The faceted taxonomies are independent by the fragility component and, hence, they cannot be directly employed to perform seismic risk assessment. In this context, the information collected through AeDES form during post-earthquake surveys can be regarded as an intermediate result because, although it is obtained from field surveys, some hints on the seismic vulnerability of the surveyed buildings can be extrapolated (see Section 5.1.1.1). Then, the data from the AeDES form represent a useful source in order to define exposure models both in terms of faceted taxonomies and risk-oriented classes. A description of the taxonomies considered in the proposed approach is reported below.

#### 5.1.1.1 AeDES form

The “post-earthquake damage and safety assessment and short-term countermeasures” form (AeDES; Baggio et al., 2007) is primarily focused on the usability evaluation for the short-term use of the buildings. However, in addition to damage data, the form includes the collection of dimensional and geometrical characteristics related to seismic vulnerability. In the last decades, the form was subjected to some modifications, until the current version was released in 2008.

The AeDES 06/2008 form (Masi et al., 2016) is composed of the following nine sections:

SECTION 1 - *Building identification* contains information about the identification of the survey and the building (location; position; denomination and use if it has a public or strategic function);

SECTION 2 - *Building description* collects the metrical data (i.e., the total number of storeys including basements; the number of basements; the average storey height and the average storey surface), the age with the period of construction and eventually of renovation and type of use and



exposure (i.e., type of use and relative number of units; utilization; number of occupants and type of property);

SECTION 3 – *Typology* provides the specific characteristics of masonry buildings, other structures (type and regularity) and roof (discussed below);

SECTION 4 - *Damage to structural elements and short-term countermeasures carried out* reports the damage level and the relative extension associated to five structural components, the pre-existent damage and the existing short-term countermeasures to quickly reduce the risk;

SECTION 5 - *Damage to non-structural elements and short-term countermeasures carried out* indicates the possible presence of damage to non-structural elements (e.g., plasters, chimneys or eaves) and the existing short-term countermeasures;

SECTION 6 - *External damage due to other constructions and short-term countermeasures carried out* indicates the risk (and the existing short-term countermeasures) induced by external components (adjacent buildings or distribution systems) and whether it affects directly the building, the entry road or the lateral road;

SECTION 7 - *Soil and foundations* individuates the site morphology and instabilities of the soil and/or foundation;

SECTION 8 - *Usability judgment* reports the building risk evaluation based on the previous sections, the usability rating (from A, usable building, to F, unusable building due to external risk), the survey accuracy, the suggested short-term countermeasures and the number of unusable building units, families and people to be evacuated;

SECTION 9 - *Other observations* reports possible surveyor's notes to clarify the contents of the other sections and the picture of the surveyed building.

In the following paragraphs, the sections 2 (“Building description”) and 3 (“Building Typology”) have been mainly referred. Figure 5.1 shows the section 3 of the AeDES form related to the building vulnerability indicators which may influence the seismic response. For masonry structures, the typological combination of vertical and horizontal characteristics is considered to describe the surveyed building. Regarding the vertical structural type, the quality (materials, mortar and construction quality) and the presence of tie beams or tie rods are considered instead, for horizontal structural types, different floor types (flexible, semirigid or rigid) can be defined. The presence of isolated RC, steel, masonry or wooden columns, mixed structures or possible strengthening interventions can be also surveyed. About other structures, the AeDES form considers reinforced concrete (frames or shear walls) and steel. Moreover, information on the shape irregularity both in plan and in elevation and, on the roof is reported. See Baggio et al. (2007) for a detailed description of the other sections. Although the data collected through the AeDES form are similar to a "faceted

taxonomy" specific for the Italian built environment, the different levels of grey color enable to indicate increasing levels of vulnerability on the basis of the seismic behavior observed in past earthquakes (Braga et al., 1982).

Vertical structures \ Horizontal Structures		Masonry buildings								Other structures		
		Unknown	Irregular layout or bad quality (rubble stones, pebbles,...)		Regular layout and good quality (Blocks, bricks, squared stone...)		Isolated columns	Mixed	Strengthened	REGULARITY		
			W/O tie rods or tie beams	With ties rods or tie beams	W/O tie rods or tie beams	With tie rods or tie beams				Irregular	Regular	
		A	B	C	D	E	F	G	H	A	B	
1	Not identified	○	□	□	□	□	SI	□	□			
2	Vaults without tie rods	□	□	□	□	□	○	G1	H1			
3	Vaults with tie rods	□	□	□	□	□		□	□			
4	Beams with <b>flexible</b> slab (wooden beams with a single layer of wooden planks, beams and shallow arch vaults,...)	□	□	□	□	□	NO	G2	H2			
5	Beams with <b>semirigid</b> slab (wooden beams with a double layer of wooden planks, beams and hollow flat blocks,...)	□	□	□	□	□	○	□	□			
6	Beams with <b>rigid</b> slab (r.c. floors, beams well connected to r.c. slabs,...)	□	□	□	□	□		G3	H3			

Other structures			
R.c. frames		□	
R.c. shear walls		□	
Steel frames		□	
REGULARITY	Irregular	Regular	
	A	B	
1	Plan and elevation	○	○
2	Infills distribution	○	○

Roof	
1	○ Thrusting heavy
2	○ Non thrusting heavy
3	○ Thrusting light
4	○ Non thrusting light

Figure 5.1 Section 3 - Building typology of AeDES form

### 5.1.1.2 GEM taxonomy

Within the Global Earthquake Model (GEM), a comprehensive faceted taxonomy (Tzitzikas, 2009) was introduced to provide a standardized description of buildings with a global scope which is independent on the geographical region and the specific hazard. The taxonomy scheme is organized as a series of tables, which contain information related to various building attributes. Each attribute corresponds to a specific characteristic of a single building or a building typology (class) that can affect its seismic performance. Table 5.2 reports the 13 different types of attributes with the relative attribute levels included in the GEM Building Taxonomy v2 (Brzev et al., 2013). As shown in Table 5.2, some attributes are complemented also by second- and third- level attributes. For each attribute level, an attribute value may be specified amongst a set of predefined values (Brzev et al., 2013). Then, the building can be described by a synthetic textual string related to the set of values. As an example, for the attribute type “Material of the Lateral Load-Resisting System” and the relative attribute level “Material Type (Level 1)”, 16 different attribute values are defined in order to effectively describe the building under study (e.g., Concrete, unreinforced “CU”; Steel “S”; Masonry, unreinforced “MUR”; etc.). The GEM taxonomy enables to characterize a wide variety of buildings, and can be also used to translate the descriptions associated to taxonomies such as PAGER-STR or HAZUS (see Brzev et al., 2013). Furthermore, the taxonomy can be a worthwhile tool in order to collect building information during the field surveys (e.g., Verrucci et al., 2014; Wieland et al., 2015

and Pittore et al., 2016). As indicated above, GEM taxonomy allows to define an exposure component independent by the fragility component but it cannot be used for a large-scale risk assessment.

TaxT Attribute Group	ID	Attribute type	Attribute levels
Structural system	1	Direction	Direction of the building
	2	Material of the Lateral Load-Resisting System	Material type (Level 1) Material technology (Level 2) Material properties (Level 3)
	3	Lateral Load-Resisting System	Type of lateral load-resisting system (Level 1) System ductility (Level 2)
Building information	4	Height	Height
	5	Date of construction or retrofit	Construction completed (year)
	6	Occupancy	Building occupancy class - general (Level 1) Building occupancy class - detail (Level 2)
Exterior attributes	7	Building Position within a block	Building Position within a block
	8	Shape of the building plan	Plan shape (footprint)
	9	Structural irregularity	Regular or irregular (Level 1) Plan irregularity or vertical irregularity (Level 2) Type of irregularity (Level 3)
	10	Exterior walls	Exterior walls
Roof/Floor/Foundation	11	Roof	Roof shape (Level 1) Roof covering (Level 2) Roof system material (Level 3) Roof system type (Level 4) Roof connections (Level 5)
	12	Floor	Floor system material (Level 1) Floor system type (Level 2) Floor connections (Level 3)
	13	Foundation system	Foundation system

**Table 5.2** Attributes of the GEM taxonomy

### 5.1.1.3 EMS-98 scale

The European Macroseismic Scale (Grünthal, 1998) is a discrete scale used to quantify the macroseismic intensity providing a large description of earthquake effects (Section 1.2 of Chapter I). Three aspects are considered in the definition of macroseismic intensity degrees: the vulnerability of damaged buildings, the classification of damage levels and the definition of quantities. Regarding the vulnerability, different building types predominantly accounting for wall materials but also considering different levels of Earthquake-Resistant Design (ERD) are defined. Each building type is correlated to an expected range of vulnerability classes (from “A” to “F” with “A” being the most vulnerable). Specifically, EMS-98 scale identifies a “*most likely vulnerability class*”, a “*probable range*” and a “*less probable range*” (exceptional cases) for each building type. For instance, the building type “MAS3” (i.e., buildings with very large/massive stones) is correlated to class “C” as most likely vulnerability class, to class “B” as probable range and to class “D” as less probable range. Table 5.3 reports the 15 building types and the corresponding range of vulnerability classes ( $V_C$ ) according to EMS-98 scale. These classes are representative of the building stock in Europe, although the scale is widely used also in other geographical areas (e.g., South America, Central and Oriental School of Engineering – University of Basilicata – Potenza (Italy)

Asia). The EMS-98 scale provides also a detailed description of the building types. For example, “MAS1” type is described as «...traditional constructions in which undressed stones are used as the basic building material, usually with poor quality mortar, leading to buildings which are heavy and have little resistance to lateral loading. Floors are typically of wood and provide no horizontal stiffening». Furthermore, a damage classification separately for masonry and reinforced concrete buildings considering six different levels from “0” (null damage) to “5” (destruction) is reported in EMS-98 scale.

Type of structures		I <sub>D</sub>	V <sub>C</sub>						
			A	B	C	D	E	F	
<b>Masonry</b>	Adobe (earth brick)	ADO							
	Rubble stone, fieldstone	MAS1							
	Simple stone	MAS2							
	Massive stone	MAS3							
	Unreinforced, with manufactured stone units	MAS4							
	Unreinforced, with RC floors	MAS5							
	Reinforced or confined	MR							
<b>Reinforced concrete</b>	Frame without earthquake-resistant design (ERD)	RC1							
	Frame with moderate level of ERD	RC2							
	Frame with high level of ERD	RC3							
	Walls without ERD	RC4							
	Walls with moderate level of ERD	RC5							
	Wall with high level of ERD	RC6							
<b>Steel</b>	Steel structures	STEEL							
<b>Wood</b>	Timber structures	WOOD							

**Table 5.3** EMS-98 structural types and corresponding range of vulnerability classes: the most likely class in red; the probable range in orange and less probable range (exceptional cases) in yellow

### 5.1.2 Methodology

In this section, the methodology developed to convert the information collected through AeDES form to different formats is reported. In the first step of the proposed approach, the information on the typological characteristics has been described according to the GEM taxonomy (Section 5.1.2.1). In a following processing step, using the score-based methodology proposed by Pittore et al. (2018), an EMS-98 building class has been assigned to each surveyed building based on its GEM attributes (Section 5.1.2.2). Therefore, starting from the AeDES data specific to the Italian built environment, the two steps enable to define: (i) an exposure model independent by the fragility component according to a taxonomy used worldwide (i.e., GEM taxonomy) and (ii) an exposure model in terms of risk-oriented classes correlated to a specific vulnerability model (i.e., EMS-98 classes) that can be employed for large-scale applications. Moreover, the proposed approach to exposure modelling exploits the potential of field-collected data within a transparent framework by allowing also an extensive characterization of the uncertainty related to the conversion process.

#### 5.1.2.1 From AeDES form to GEM taxonomy

The first step of the proposed method is the conversion of typological characteristics reported in AeDES form in terms of the attributes defined by the GEM taxonomy. The latest version (06/2008) of the AeDES form has been considered, although the same procedure can also be applied to the other versions or applied to different inspection templates. As described in the Section 5.1.1.2, the GEM taxonomy (v2, Brzev et al., 2013) considers 13 different *attributes types* with the relative *attribute levels* and, for each attribute level, an *attribute value* can be specified. Likewise, the AeDES form (Section 5.1.1.1) can be described according to different sections (“*AeDES section*”) with the relative attributes (“*AeDES attribute*”), and, for each attribute, a value (“*AeDES attribute value*”) can be associated (i.e., the specific option cell marked in the survey). For instance, considering Figure 5.1, the AeDES section is “Building typology” and the relative attributes are “Masonry buildings”, “Other structures”, “Regularity” and “Roof” with the specific attribute values (e.g., “R.C. frames”; “R.C. shear walls” or “Steel frames” for “Other structures” attribute). Hence, an individual building surveyed with AeDES form can be described through a set of different attribute values related to the specific cells of the form. On the basis of a comparative analysis of the attribute description reported in AeDES form and the GEM taxonomy, the AeDES attributes that are deemed relevant for estimating the seismic vulnerability and can be unambiguously associated to GEM attributes have been considered. Table 5.4 reports the sections and the attributes of AeDES form considered in the procedure (columns 1 and 2) and the corresponding attributes and attribute levels of GEM taxonomy (columns 3 and 4).

<b>AeDES section</b>	<b>AeDES attribute</b>	<b>GEM attribute</b>	<b>GEM attribute level</b>
Building identification	Building position	Building Position within a Block	Building Position within a Block (POSITION)
	Total number of storeys	Height	Number of storeys above ground (STORY_AG)
	No. of basements	Height	Number of storeys below ground (STORY_BG)
Building description	Construction and renovation age	Date of Construction or Retrofit	Date of Construction or Retrofit (YBET)
	Use	Occupancy	<ul style="list-style-type: none"> <li>• Building occupancy class-general (OCCUPCY)</li> <li>• Building occupancy class-detail (OCCUPCY_DT)</li> </ul>
Building typology	Masonry building	Material of the Lateral Load-Resisting System	<ul style="list-style-type: none"> <li>• Material type (Mat_type)</li> <li>• Material technology (Mat_tech)</li> <li>• Material properties (Mat_prop)</li> </ul>
		Floor	<ul style="list-style-type: none"> <li>• Floor system material (Floor_mat)</li> <li>• Floor system type (Floor_type)</li> <li>• Floor connections (Floor_conn)</li> </ul>
	Other structures and regularity	Material of the Lateral Load-Resisting System	Material type (Mat_type)
		Lateral Load-Resisting System	Type of lateral load-resisting system (LLRS)
		Structural Irregularity	Regular or irregular (STR_IRREG)
	Roof	Roof	<ul style="list-style-type: none"> <li>• Roof system material (ROOFSYSMAT)</li> <li>• Roof connections (ROOF_CONN)</li> </ul>

**Table 5.4** Correspondence between AeDES and GEM attributes

Most of the attribute types are categorical, and the corresponding attribute values are mutually exclusive and collectively exhaustive (MECE; Lee and Chen, 2018) for each considered attribute type. The specific conversion rules between AeDES form and GEM taxonomy for these attributes are reported in the Appendix (Tables 5A-5F). However, the taxonomic description also includes non-categorical types, namely the building age (ordinal), in terms of construction and renovation date, and the total number of storeys and the number of basements (numerical). In these cases, the following approach has been followed. As for the building age, since the AeDES form considers different ranges of the construction age (e.g.,  $\leq 1919$ ; 1919-1945; etc.), the corresponding GEM attribute “YBET” (i.e., “Upper and lower bound for the date of construction or retrofit”) has been employed in order to consider a range. It is worth remarking that the AeDES form considers both construction and renovation year through a possible double answer. Instead, the GEM taxonomy identifies only the year when the building construction was completed and does not distinguish between construction

and renovation age. For this reason, the renovation year (i.e., more recent year) has been considered. As for the number of storeys, the GEM taxonomy reports the building height above ground (STORY\_AG) in terms of number of storeys and number of storeys below ground (STORY\_BG). The AeDES form considers instead the total number of storeys and the total number of basements. Therefore, the number of storeys above ground has been calculated as difference between total number of storeys and number of basements.

#### 5.1.2.2 From GEM taxonomy to EMS-98 building types

The subsequent step of the proposed methodology consists in the assignation of EMS-98 building types (Section 5.1.1.3) based on the collected GEM attributes. In order to perform this step, the score-based methodology defined by Pittore et al. (2018) has been employed. The approach is based on a fuzzy-score and constraints system, which estimates the level of compatibility of a generic building, defined by its taxonomic description, with respect to one or more building classes defined within a specific MECE schema (e.g., PAGER-STR, HAZUS or EMS-98). GEM attributes as taxonomic description and the typological classes defined by the EMS-98 scale as the reference schema have been considered. The following steps have been followed:

- 1) Selection of the attributes “ $a_i$ ” to be considered for the class definition process, and their relative weight “ $W_i$ ”. The attributes describing the structural (and non-structural) features of the buildings most relevant for the discrimination of EMS-98 classes have been selected. The weights encode both the relative significance of the attribute types, and consider the potential uncertainty in the observation process;
- 2) For each attribute type “ $a_i$ ”, a set of compatibility scores has been associated to the corresponding attribute values “ $v_{ik}$ ” for each of the EMS-98 classes. Seven increasing levels of compatibility, from “---”: *highly incompatible*, to “+++”: *highly compatible*, have been considered, including a neutral “0” score. These are the semantic equivalent of a set of Triangular Fuzzy Numbers (TFN, Kaufmann and Gupta, 1985; Zhu et al., 1999). All possible attribute values have been initialized to the neutral compatibility level and only the attribute values which are expected to contribute to the overall compatibility score have been considered.

The weights and scores have been defined based on expert judgment, starting from the values originally proposed by Pittore et al. (2018). It is worth noting that the fuzzy formulation allows to frame the subjective judgment in the class assignment in a more transparent and formally consistent methodological approach, also ensuring the explicit consideration of the underlying uncertainties. Table 5.5 shows, for example, the two sets of compatibility levels for the significant attribute values

(“class descriptions”) for the building typologies “Simple stone” (MAS 2) and “Frame with moderate level of ERD” (RC 2) as defined by the EMS-98 scale. The description of the GEM attribute values shown in Table 5.5 is reported in Table 5.6

EMS-98 building class	GEM attribute							
	mat type	mat tech	mat prop	LLRS	year built	floor mat	floor type	floor conn
<b>Simple stone (MAS 2)</b>	MUR: +++						FW1: +++	
	M99: +						FM1: ++	
	MR: -	STRUB: +++	MOL: +++		<1919: +++		FM2: ++	
	CU: -		MOM: ++	LN: +++	1919-1945: +++	FW: +++	FM3: +	FWCN: +++
	C99: --	ST99: +++	MOCL: ++	LWAL: +		FC: +	FW2: +	
	CR: ---	STDRE: ++	MOC: +		1946-1961: ++	FM: +	FW3: +	
	SRC: ---	MUN99: +	MON: +				FW4: +	
	W: ---						FW99: +	
	MAT99: ---							
<b>Frame with moderate level of ERD (RC 2)</b>	CR: +++						FC2: +++	
	SRC: ++						FC3: ++	FWCP: +++
	C99: +				1972-1981: +++		FC1: +	
	MR: -	CIP: +++	MOC: +++	LFM: +++		FC: +++	FC4: +	
	M99: --	PC: +	MOCL: ++	LFINE: +	1962-1971: ++		FC99: +	
	MUR: ---				1982-1991: ++			
	W: ---							
	MAT99: ---							

**Table 5.5** Set of the fuzzy compatibility levels for the attribute values of two EMS-98 building typologies. All attribute values not explicitly considered have been assigned a neutral score. LLRS stands for Lateral Load Resisting System.

As shown in Table 5.5, eight GEM attributes have been selected. For the material type (*mat type*) both compatible and incompatible values have been specified, whereas for the other attributes only the positive compatible values have been defined. As reported in Section 5.1.1.3, the classes for RC buildings within the EMS-98 scale are defined according to their level of Earthquake-Resistant Design (ERD). Because such attribute is not reported in the current version of the GEM taxonomy and would be anyway very difficult to be assessed by a simple visual survey, the construction and renovation age has been used as a proxy to the expected ERD level. The compatibility score for the date of construction or retrofit has been estimated considering the evolution of Italian building codes. The set of assigned compatibility scores with respect to all building classes defines the overall EMS-98 conversion scheme, that can be graphically depicted as shown in Figure 5.2. With respect to the original schema from Pittore et al. (2018), the proposed schema considers a larger number of attribute values and the construction and renovation age has been used in place of the ductility to account for the ERD level. When information about the vertical structure (VS) is not available in the AeDES form, the GEM attribute value "MAT99" has been associated to attribute "mat type" (Table 5C in Appendix). Based on the latter assignation, for "mat type: MAT99" (see Figure 5.2), a “highly incompatible” score has been defined with respect to all EMS-98 classes because the information about VS is fundamental to evaluate the building typology.



<b>GEM taxonomy</b>		
<b>GEM attribute</b>	<b>GEM attribute value</b>	
	<b>ID</b>	<b>Description</b>
Material type (mat type)	MUR	Masonry, unreinforced
	M99	Masonry, unknown reinforcement
	MR	Masonry, reinforced
	CU	Concrete, unreinforced
	CR	Concrete, reinforced
	SRC	Concrete, composite with steel section
	W	Wood
	MAT99	Unknown material
	C99	Concrete, unknown reinforcement
Material technology (mat tech)	STRUB	Rubble (field stone) or semi-dressed stone
	ST99	Stone, unknown technology
	STDRE	Dressed stone
	MUN99	Masonry unit, unknown
	CIP	Cast-in-place concrete
	PC	Precast concrete
Material properties (mat prop)	MOL	Lime mortar
	MOM	Mud mortar
	MOCL	Cement: lime mortar
	MOC	Cement mortar
	MON	No mortar
Type of Lateral Load-Resisting System (LLRS)	LN	No lateral load-resisting system
	LWAL	Wall
	LFM	Moment frame
	LFINF	Infilled frame
Floor system material (floor mat)	FW	Wooden floor
	FC	Concrete floor
	FM	Masonry floor
Floor system type (floor type)	FW1	Wooden beams or trusses and joists supporting light flooring
	FM1	Vaulted masonry floor
	FM2	Shallow-arched masonry floor
	FM3	Composite cast-in-place reinforced concrete and masonry floor system
	FW2	Wooden beams or trusses and joists supporting heavy flooring
	FW3	Wood-based sheets on joists or beams
	FW4	Plywood panels or other light-weight panels for floor
	FW99	Wooden floor, unknown
	FC1	Cast-in-place beamless reinforced concrete floor
	FC2	Cast-in-place beam-supported reinforced concrete floor
	FC3	Precast concrete floor with reinforced concrete topping
	FC4	Precast concrete floor without reinforced concrete topping
	FC99	Concrete floor, unknown
Floor connections (floor conn)	FWCN	Floor-wall diaphragm connection not provided
	FWCP	Floor-wall diaphragm connection present

**Table 5.6** Description of the GEM attribute values shown in Table 5.5 (adapted from Brzev et al., 2013)

In order to assign an inspected building a specific EMS-98 building class, the overall compatibility score has been computed with respect to all available building classes according to the following equation (Pittore et al., 2018):

$$S_c(b) = \sum_{i=1}^n W_i \cdot \sum_{k=1}^{m_i} \delta_{ik}(b) s_{ik}^c \quad (5.1)$$

where

- $i$  is the  $i$ -th attribute,  $a_i$ , of GEM taxonomy;
- $k$  is the attribute value,  $v_{ik}$ , for each attribute,  $a_i$ ;
- $s_{ik}^c$  is the fuzzy score of the attribute value  $v_{ik}$  with respect to the building class (“c”) according to EMS-98 scale;
- $W_i$  is the weight associated to each attribute,  $a_i$ ;
- $\delta_{ik}$  indicates if the attribute value is considered in the taxonomic description,  $B(b)$ :

$$\delta_{ik}(b) \begin{cases} 1 & \text{if } v_{ik} \in B(b) \\ 0 & \text{otherwise} \end{cases}$$

The score is computed as a weighted combination of the individual (fuzzy) compatibility levels, and is itself defined by a TFN (Zhu et al., 1999). As an example, if the class “c” refers to “MAS2” typology as reported in Table 5.5, then the following defuzzified scores using the median values of the TFNs (Pittore et al., 2018) are assigned to the attribute values related to the attribute type `mat_type`:

$$S_{mat\_type} = \{MUR: +1, M99: +0.3, MR: -0.3, CU: -0.3, C99: -0.5, CR: -1, SRC: -1, W: -1, MAT99: -1\}$$

Particularly, if the attribute value “MUR” would be observed in a building, it contributes with a maximum score (+1, i.e., highly compatible) to the overall score with respect to the building class “MAS2” while the attribute values “W” with the minimum score (−1, i.e., highly incompatible). In order to compute the compatibility score  $S_c(b)$  with respect to a given class for each surveyed building, the same approach needs to be performed for each of the selected attribute types  $a_i$  with the assigned weight  $W_i$  (see Equation 5.1).

The formulation described above only considers categorical attributes. In order to account for non-categorical attributes, such as numerical values (e.g., number of stories), an additional *constraint* has been defined, which defines a specific condition to be satisfied (e.g., the number of storeys should be less than four for a given class). If the constraint is not satisfied, the total compatibility score of the considered building can be set to the minimum compatibility. In the proposed approach, one single constraint related to number of storeys (less than 2) for EMS-98 building type “ADO” has been defined. In order to assign a single, most suitable EMS-98 class to each building, the class with the

highest compatibility score has been selected using a fuzzy comparison and ranking approach (Bortolan and Degani, 1985, Dorohonceanu and Marin, 2002). A further threshold on the compatibility score can be introduced in order to filter out the cases where unreliable assignment may occur. In case no building class exceeds the threshold, the considered building is assigned to the special class OTH (Other) for later analysis.

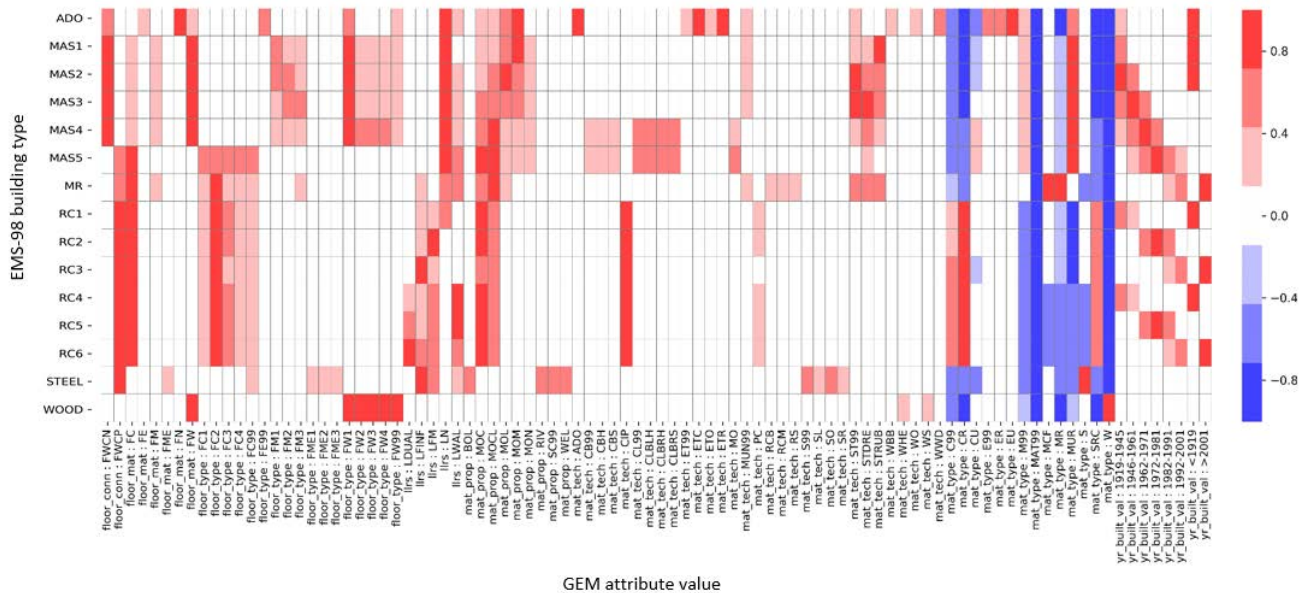


Figure 5.2 Graphical representation of the class definitions for the EMS-98 scheme

## **5.2 An integrated approach for collecting exposure data of residential buildings**

One of the main issues of the seismic loss assessments is the scarce reliability of existing building inventories in many areas of the world. Residential building inventory can be assembled employing different sources of information as discussed in Section 1.3 of Chapter I. Census data on population and houses are the primary source of information for providing a comprehensive picture of the building stock over a large scale. Considering European countries, the information on buildings from census returns is often limited to construction age and storey number. In Italy, ISTAT (Italian Institute of Statistics) provides data on construction age, building material, use and utilization, height and so on in aggregated form (i.e., over administrative boundaries). Building-by-building surveys are the most complete source providing detailed building features for single buildings in an investigated area. Given the elevated costs and time, this kind of survey is typically applied only during post-earthquake vulnerability and damage inspection campaigns or to integrate and/or verify data in spatially limited areas. Innovative techniques based on high resolution (HR) or very high resolution (VHR) satellite image processing are another important source for building inventory, allowing to rapidly gather spread geo-referenced information, such as footprint shape and size, number of storeys or height of storey. However, building features that are crucial for vulnerability assessment, such as the distinction of building materials or the building age, cannot be easily detected relying on earth observation data alone. In general, remote sensing should be efficiently combined with other methods (e.g., Wieland et al. 2012; Pittore and Wieland, 2013; Liuzzi et al., 2019). In order to perform the compilation of regional scale inventories, a new method based on interview to local technicians was developed in Italy, referred as CARTIS format (Zuccaro et al., 2015).

In this framework, an approach combining the CARTIS procedure with the potential offered by a remote screening technique, has been proposed. Specifically, the data collected with CARTIS format are integrated with the information surveyed through RRVS (Rapid Remote Visual Screening) web-based platform. The latter allows to perform a remote building-by-building survey using street-view images (Pittore and Wieland, 2013). The proposed approach enables to define an exposure model in a quicker and less expensive way than a building-by-building survey and also to rapidly acquire much more data on building typologies with respect to census returns (Polese et al., 2019a). It represents a useful tool especially for less developed areas of the world with high level of risk (Bilham, 2009). Furthermore, the data can be used for large-area risk assessments (e.g., Polese et al., 2019a). The proposed approach has been implemented for the village of Calvello located in the Agri Valley (Basilicata). As will be widely discussed in Chapter VI, the village and the entire area have a strategic economic role for Italy because of the oil extraction from local deposits.

### 5.2.1 Methods

A brief description of the methods aimed at collecting data on the building characteristics considered in the proposed approach is reported.

#### 5.2.1.1 CARTIS format

In the framework of ReLUIIS project, the CARTIS (CARatterizzazione Tipologica Strutturale) approach supports the compilation of regional scale inventories for the typological-structural characterization of Italian urban areas. The CARTIS form (Zuccaro et al., 2015) is normally compiled by an expert of the ReLUIIS Consortium for an entire town/country, suitably subdividing it in Town Compartments (TCs). For each TC, the form is filled by interviewing one or more technicians that are local experts with deep knowledge of the building stock characteristics in the area and collecting information on relevant Building Typologies (BTs) most widespread in each TC. Specifically, CARTIS form concerns the definition of homogeneous territorial zones (namely TCs) which consider buildings with the same age of construction and/or construction technique. On the basis of the AeDES survey tool (Baggio et al., 2007), the form is divided in the following four sections:

- (0) identification of the Town under study and the TCs identified in the Town;
- (1) identification of each prevailing typology inside the generic TC;
- (2) identification of the characteristics of each building typology (BT) identified in step (1);
- (3) characterization of the structural elements of each typology identified in step (1).

For each section, specific sub-forms are associated: a single form for the city (i.e., section 0; see Figure 5.3); one sub-form for each TC detected in the local territory (section 1) and one sub-form for each BT within each TC (sections 2 and 3). The classification of the BTs of each TC takes place by identifying the macro classes of buildings, first of all between reinforced concrete and masonry. After, for each identified typology, the main data needed to define the different seismic behavior are collected in the sections 2 and 3, including, e.g., total number of storeys, age of construction, characteristics of masonry and reinforced concrete structures, floor type, roof and so on.

The CARTIS form is widely used in Italy with about 300 towns investigated (Zuccaro et al., 2015) and all the data manually collected through the forms are uploaded on a web application and made freely available to the scientific community. Such information is more detailed with respect to the data available from census returns and supports effective use of more refined vulnerability models. Although referred to territorial units (i.e., TCs), the information collected on building typologies is disaggregated and it can be exploited to carry out vulnerability and risk assessments at different scales (Polese et al., 2019a,b).



 <b>PROTEZIONE CIVILE</b> Presidenza del Consiglio dei Ministri Dipartimento della Protezione Civile	 <b>RELUIS</b> Rete dei Laboratori Universitari di Ingegneria Sismica
<b>CARTIS 2014</b> SCHEDA DI 1° LIVELLO PER LA CARATTERIZZAZIONE TIPOLOGICO-STRUTTURALE DEI COMPARTI URBANI COSTITUITI DA EDIFICI ORDINARI	
<b>SEZIONE 0: Identificazione Comune e Comparti</b> <span style="float: right;"><b>PARTE A</b></span>	
DATA <input type="text"/> / <input type="text"/> / <input type="text"/>	
<b>a. DATI DI LOCALIZZAZIONE</b>	
Regione: _____	Codice ISTAT <input type="text"/>
Provincia: _____	Codice ISTAT <input type="text"/>
Comune: _____	Codice ISTAT <input type="text"/>
Municipalità/ Frazione/ Località (denominazione ISTAT) _____	
<b>b. DATI GENERALI COMUNE</b>	
Numero totale residenti del Comune <input type="text"/>	Piano Particolareggiato Centro Storico
Anno di prima classificazione sismica <input type="text"/>	<input type="radio"/> SI <input type="radio"/> NO
Anno di approvazione Piano Regolatore Generale <input type="text"/>	
Anno di approvazione Programma di fabbricazione <input type="text"/>	
Numero totale abitazioni	
Dato ISTAT <input type="text"/>	Dato rilevato <input type="text"/>
Numero totale edifici	
Dato ISTAT <input type="text"/>	Dato rilevato <input type="text"/>
<b>c. NUMERO ZONE OMOGENEE (COMPARTI)</b> <input type="text"/>	
<b>d. DATI IDENTIFICATIVI UNITÀ DI RICERCA (UR) RELUIS</b>	
Codice UR: <input type="text"/>	
Referente: _____	Mail: _____
Ente di appartenenza: _____	
Qualifica: _____	
Titolo di studio: _____	
Indirizzo: _____	
Tel. ufficio: _____	Cell.: _____
Compilatore: _____	Mail: _____
Firma del Compilatore: _____	
<b>e. DATI IDENTIFICATIVI TECNICO INTERVISTATO</b>	
Referente del Comune: _____ Tel./Cell.: _____	
Nominativo: _____	Nominativo: _____
Ente di appartenenza: _____	Ente di appartenenza: _____
Qualifica: _____	Qualifica: _____
Titolo di studio: _____	Titolo di studio: _____
Indirizzo: _____	Indirizzo: _____
Mail: _____	Mail: _____
Tel. ufficio: _____ Cell.: _____	Tel. ufficio: _____ Cell.: _____

Figure 5.3 Section “0” of CARTIS form-Identification of the Town under study and the Town Compartments (TCs)

### 5.2.1.2 RRVS platform

Remote sensing techniques are increasingly recognized as an important source for deriving exposure data related to the built environment. HR and VHR satellite image processing enables to rapidly gather information on building features, such as location and footprint, shape irregularities, heights and roof materials (e.g., Wieland and Pittore 2014). However, building data that are crucial for vulnerability assessment, such as the distinction of building materials (e.g., masonry/reinforced concrete) or the building age cannot directly be derived from remote sensing methods. In the last

years, digital in situ data capturing systems (e.g., coupling satellite and in situ images) have been proposed as supplements to field screening techniques or remote sensing methods.

In this framework, the Remote Rapid Visual Screening (RRVS) web-based platform was defined to perform remote building-by-building surveys (Pittore and Wieland 2013; Pittore et al., 2018). The platform enables to query for each selected building (identified through the own footprint) the omnidirectional images provided by the Google StreetView™ or Bing™ service. Several structural and nonstructural building features, such as material type, building height, vertical structural irregularities (in plan and in elevation) or roof type can be collected by following the GEM taxonomy (Brzev et al., 2013; see Section 5.1.1.2). The analysis of the image sequences can be performed manually through visual interpretation by the surveyor, trying to always fill the entries based on features clearly observable from satellite images. The main advantage consists that a large number of structures can be inspected in short time, also exploiting available ancillary information and providing an efficient first-level assessment of expected vulnerability. Figure 5.4 shows an example of a building remotely inspected using the RRVS web-based platform. The tab panel in the lower right side of the graphical interface includes the principal attributes of the GEM taxonomy. It is worth noting that the platform can also employ omnidirectional images captured with a mobile mapping system, where no suitable data is already available (Pittore and Wieland, 2013). For instance, mobile mapping systems such as omnidirectional cameras mounted on vehicles allow for automated compilation of georeferenced omnidirectional imagery according to predefined routing constrains (Wieland et al., 2012).

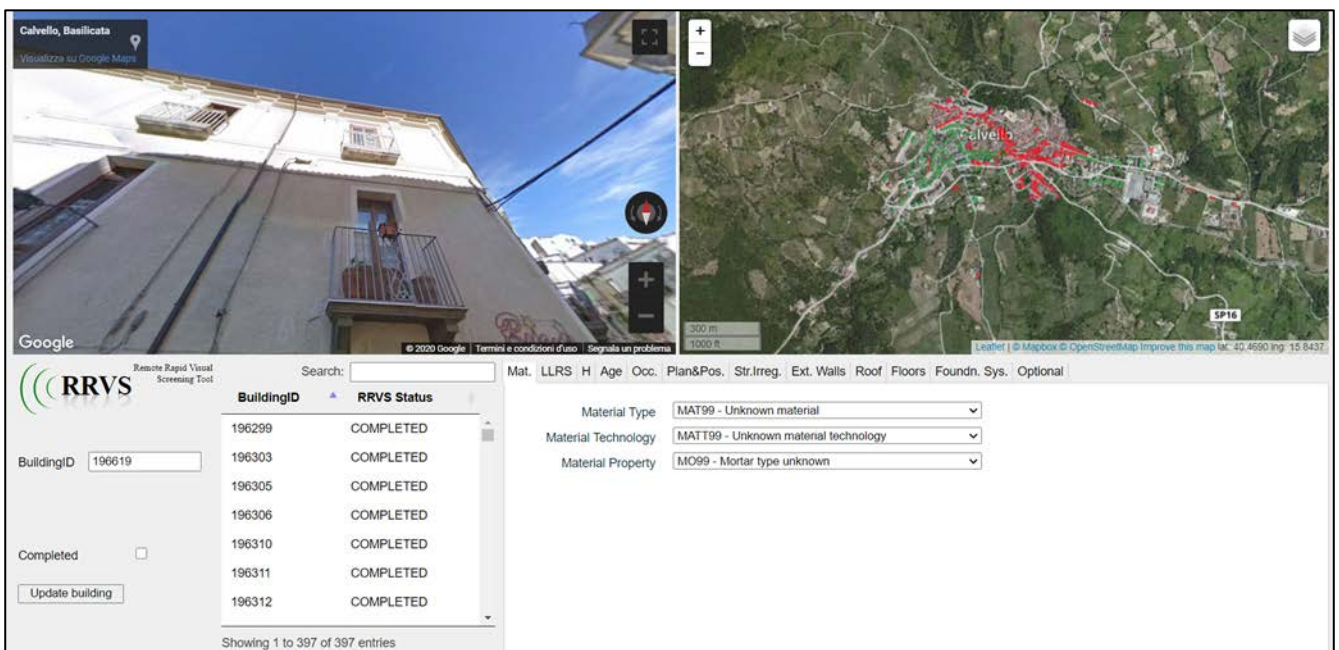
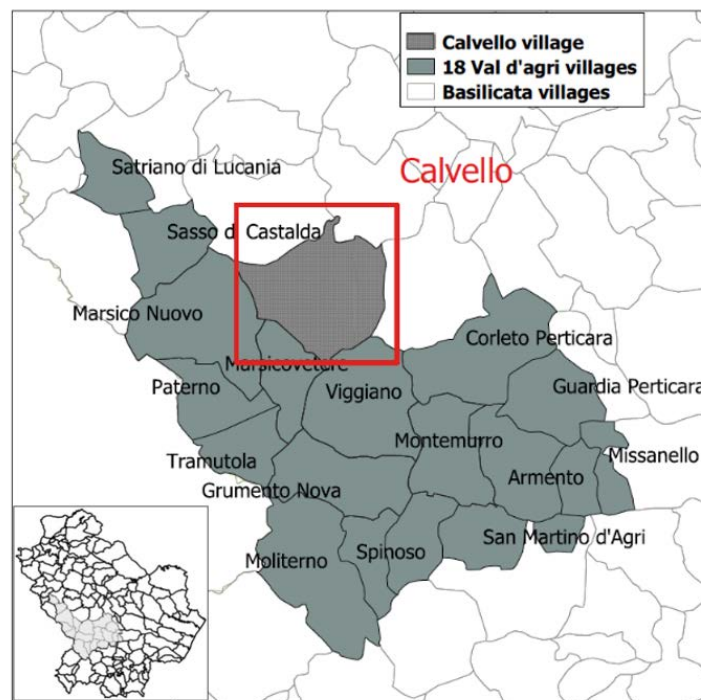


Figure 5.4 Example of a building remotely inspected using the RRVS platform



### 5.2.2 Implementation on the Calvello Village

The methods described in Section 5.2.1 have been applied to the village of Calvello (about 2'000 inhabitants; ISTAT 2011) located in the Agri Valley (Basilicata; Southern Italy). This area is characterized by high seismic risk and has a strategic role for Italy due to the presence of oil extraction plants, making available large resources deriving from royalties. Specifically, Calvello with other five villages (i.e., Grumento Nova, Marsico Nuovo, Marsicovetere, Montemurro and Viggiano) are referred as “OIL Villages”, in which the extraction of oil and the reinjection of the fluids are directly carried out. In the past, studies on 18 villages located in the Agri Valley, aimed at estimating the seismic vulnerability of residential buildings were carried out based on typological data deriving by a building-by-building survey (Masi et al., 2014). Although Calvello village is one of the six “OIL Villages”, it was not surveyed during the field inspection campaigns of the 18 Val d’Agri villages (Figure 5.5). In the scope of the definition of an earthquake damage scenario for the entire area (as will be discussed in Chapter VI), the proposed approach has been applied to collect data on residential building stock of the village of Calvello and, consequently, to evaluate the seismic vulnerability.



**Figure 5.5** Territorial framework of Val d’Agri area (up) and built environment (down) of Calvello village



Figure 5.6 shows the individuation of Town Compartments (TCs) for Calvello village in which different building typologies (BTs) have been individuated in each TC. By means of the CARTIS survey, the territory has been divided in two TCs: TC1 related to built-up area of the historical center (about 350 surveyed buildings) and TC2 related to expansion area (about 100 surveyed buildings). The main characteristics detected for the BTs in each TC are reported in Table 5.7: percentage of buildings, building position, number of storeys and age of construction. Table 5.7 reports that two BTs have been individuated for TC1 (i.e., MUR1 and MUR2) and four for TC2 (i.e., MUR1; CAR1; CAR2 and CAR3). Note that the BTs are denominated MUR for masonry buildings (MAS) and CAR for Reinforced Concrete buildings (RC). A brief description of structural features related to each BT (i.e., vertical and horizontal structure, roof type and structural regularity) is reported in Tables 5.8 (for TC1) and 5.9 (for TC2).

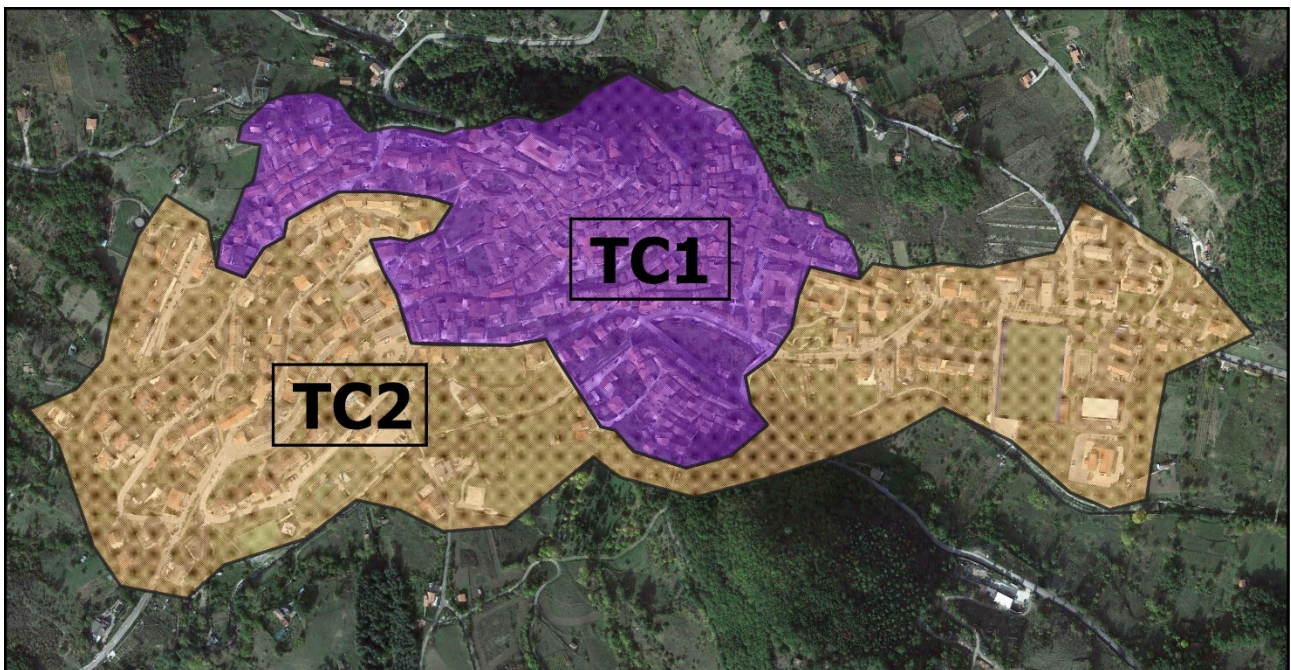




Figure 5.6 Individuation of TCs for Calvello village

TC	BT	% buildings for BT	% Building position		N° storeys	Age of construction
			Isolated	Aggregates		
TC1	MUR 1	70	0	100	2/3	<=1860/1861-1919
	MUR 2	30	30	70	2/3	<=1860/1861-1919
TC2	MUR 1	10	30	70	2/3	19-45/46-61
	CAR 1	40	100	0	3/4	87-91/97-01
	CAR 2	40	100	0	4/5	02-08/>2011
	CAR 3	10	100	0	2/3	92-96/02-08

Table 5.7 Main characteristics of the BTs related to each TC

<p style="text-align: center;"><b>TC1-MUR1</b></p> 	<p><u>Masonry characteristics</u> A1.1 Irregular-rounded stone-without brick courses- pebbles with irregular layout</p> <p><u>Horizontal structure</u></p> <ul style="list-style-type: none"> <li>• S1.2 Beams with flexible slab-wooden beams with a single layer of wooden planks (30%);</li> <li>• S3.2 Beams with rigid slab- RC floors with prefabricated joists (70%)</li> </ul> <p><u>Roof (shape-weight-material)</u> Pitched-light (70) and heavy (30)-wooden (70) and RC (30)</p> <p><u>Regularity in plan</u> Regular (80) and moderately regular (20)</p> <p><u>Regularity in elevation</u> Regular (80) and irregular (20)</p>
<p style="text-align: center;"><b>TC1-MUR2</b></p> 	<p><u>Masonry characteristics</u> A2.1 Irregular-rubble stone-without brick courses- rubble with irregular layout</p> <p><u>Horizontal structure</u></p> <ul style="list-style-type: none"> <li>• S2.1 Beams with semirigid slab-wooden beams with two perpendicular layers of wooden planks (30%);</li> <li>• S3.2 Beams with rigid slab- RC floors with prefabricated joists (70%)</li> </ul> <p><u>Roof (shape-weight-material)</u> Pitched-light (70) and heavy (30)-wooden (70) and RC (30)</p> <p><u>Regularity in plan</u> Regular (100)</p> <p><u>Regularity in elevation</u> Regular (80) and moderately regular (20)</p>

**Table 5.8** Description of the structural characteristics of each BT in TC1 with the corresponding percentages

After, a remote building-by-building survey through the RRVS platform has been performed by using the image sequences provided by Google StreetView™. In order to compare and integrate it with the data collected on the building stock with the CARTIS format, the RRVS survey has been carried out on the buildings located in TC2 in which four different BTs have been individuated. It is worth underlining that the RRVS platform represents a much more useful tool in heterogeneous areas (e.g., TC2) because it allows to effectively identify and distinguish the different typologies. Moreover, the application of the RRVS tool in the expansion areas (e.g., TC2) is easier and more effective than in the historical centers (e.g., TC1) because of the availability and quality of images.



<p style="text-align: center;"><b>TC2-MUR1</b></p> 	<p><u>Masonry characteristics</u> A2.1 Irregular-rubble stone-without brick courses- rubble with irregular layout</p> <p><u>Horizontal structure</u></p> <ul style="list-style-type: none"> <li>• S2.1 Beams with semirigid slab-wooden beams with two perpendicular layers of wooden planks (20%);</li> <li>• S3.2 Beams with rigid slab- RC floors with prefabricated joists (80%)</li> </ul> <p><u>Roof (shape-weight-material)</u> Pitched-light (70) and heavy (30)-wooden (70) and RC (30)</p> <p><u>Regularity in plan</u> Regular (100)</p> <p><u>Regularity in elevation</u> Regular (100)</p>
<p style="text-align: center;"><b>TC2-CAR1</b></p> 	<p><u>RC vertical and horizontal structure</u> D. Reinforced concrete frame structures with little consistent or absent infill panels-RC floors (high beams on the perimeter and flat beams inside)</p> <p><u>Roof (shape-weight-material-connection)</u> Pitched-heavy-RC-Non thrusting</p> <p><u>Regularity in plan</u> Regular (70) and irregular (30)</p> <p><u>Regularity in elevation</u> Regular (70) and moderately regular (30)</p> <p><u>Infill-Partitions at the ground storey</u> Regular layout</p>
<p style="text-align: center;"><b>TC2-CAR2</b></p> 	<p><u>RC vertical and horizontal structure</u> D. Reinforced concrete frame structures with little consistent or absent infill panels-RC floors (high beams on the perimeter and flat beams inside)</p> <p><u>Roof (shape-weight-material-connection)</u> Pitched-light (30) and heavy (70)- wooden (30) and RC (70)-Non thrusting</p> <p><u>Regularity in plan</u> Moderately regular (80) and irregular (20)</p> <p><u>Regularity in elevation</u> Regular (50) and moderately regular (50)</p> <p><u>Infill-Partitions at the ground storey</u> Irregular layout</p>
<p style="text-align: center;"><b>TC2-CAR3</b></p> 	<p><u>RC vertical and horizontal structure</u> D. Reinforced concrete frame structures with little consistent or absent infill panels-RC floors (high beams on the perimeter and flat beams inside)</p> <p><u>Roof (shape-weight-material-connection)</u> Pitched-heavy-RC-Non thrusting</p> <p><u>Regularity in plan</u> Regular (50) and moderately regular (50)</p> <p><u>Regularity in elevation</u> Regular (60) and irregular (40)</p> <p><u>Infill-Partitions at the ground storey</u> Not present</p>

**Table 5.9** Description of the structural characteristics of each BT in TC2 with the corresponding percentages



Several information related to building typology, number of storeys, building position and regularity in plan and in elevation has been surveyed on the TC2 buildings (135 bldgs.). Figure 5.7 shows the spatial distribution of the TC2 buildings in terms of building typology (i.e., Reinforced concrete, RC, or Masonry, MAS) and in terms of number of storeys. Most of the buildings inside the TC2 have RC structure (about 80% of the building stock) with a number of storeys higher or equal to 3 (about 80% of the RC buildings) while 20% of the building stock was built with MAS structure with a number of storeys less or equal to 3 (about 90%). In terms of regularity in plan, about 75% of the surveyed buildings can be classified as regular structures while the other ones can be classified as irregular. Moreover, the percentage of buildings with Pilotis Frame (PF) type (i.e., frames without masonry infills at the ground floor) is equal to about 20%.

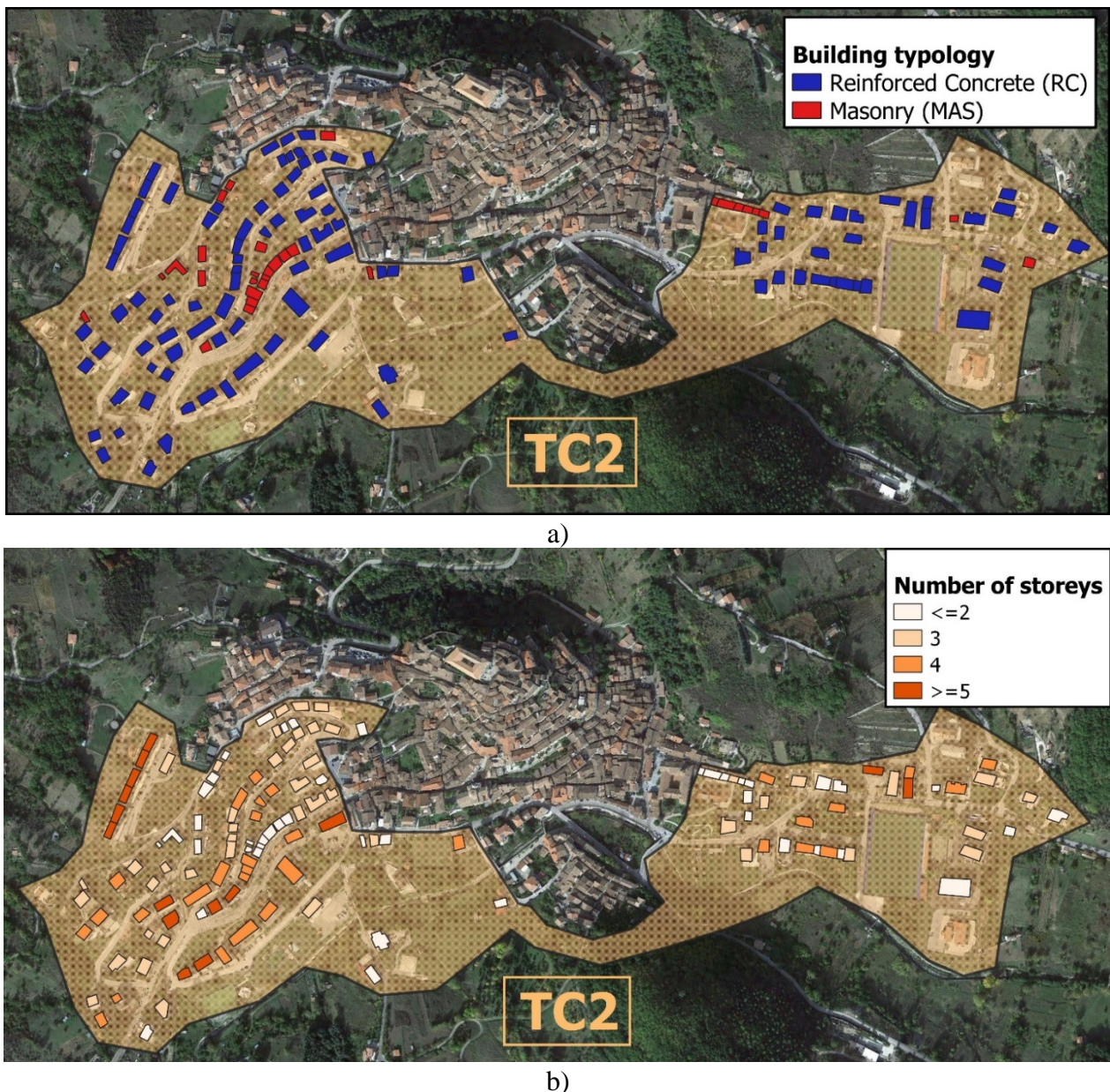


**Figure 5.7** Spatial distribution of the building stock of Calvello village in terms of building typology (a) and in terms of number of storeys (b)

5.2.2.1 Analysis of the results and comparison with ISTAT data

Firstly, a comparison among the data collected with CARTIS format and RRVS platform has been carried out as reported in Table 5.10. The information surveyed is fairly consistent in terms of building typology, number of storeys, regularity in plan and in elevation. However, the CARTIS format underestimates lightly the total number of buildings inside TC2 (100), the percentage related to masonry buildings (about 10%) and the percentage of PF buildings (about 10%).

<i>TC2</i>		
<i>Surveyed data</i>	<i>CARTIS</i>	<i>RRVS</i>
<i>N° buildings</i>	100	135
<i>% Masonry</i>	10	20
<i>% RC</i>	90	80
<i>% regular in plan</i>	80	75
<i>% irregular in plan</i>	20	25
<i>% PF buildings</i>	10	20

**Table 5.10** Comparison among data collected with CARTIS format and RRVS platform

Moreover, ISTAT dataset related to 2011 housing census has been considered and compared to the data collected through CARTIS and RRVS. The dataset contains useful information for the estimation of the distribution of buildings by construction type (RC, masonry or other types), use and utilization, age, height and so on. The data are provided in an aggregated form: for each attribute, the relevant number of buildings in the belonging census section is provided. Therefore, it is not possible to consider jointly different attributes such as structural type and number of storeys. Shapefiles containing census sections, represented by polygons, have been correlated to the attribute tables storing such data for each municipality. Specifically, the village of Calvello is divided in eight census sections but only four sections concern almost all the area related to the Town Compartments (TCs) identified with the CARTIS format (Figure 5.8). For these census sections, a summary of the main information related to material typology and building height (i.e., number of storeys) is reported in Table 5.11.

		<b>Census sections</b>				
		<i>1</i>	<i>2</i>	<i>3</i>	<i>4</i>	<i>Total</i>
<i>N° buildings</i>		189	203	719	9	1120
<i>N° residential buildings</i>		186	187	702	9	1084
<i>Material type of residential buildings</i>	<i>MUR</i>	164	132	669	4	969
	<i>CA</i>	7	28	31	2	68
	<i>OTHER (steel, wood)</i>	15	27	2	3	47
<i>Number of storeys of residential buildings</i>	<i>1</i>	37	20	166	1	224
	<i>2</i>	103	96	392	5	596
	<i>3</i>	39	49	139	1	228
	<i>≥ 4</i>	7	22	5	2	36

**Table 5.11** Distribution in terms of material type and number of storeys for the buildings located in the 4 census sections (ISTAT 2011) overlapping to Town Compartments (TCs)



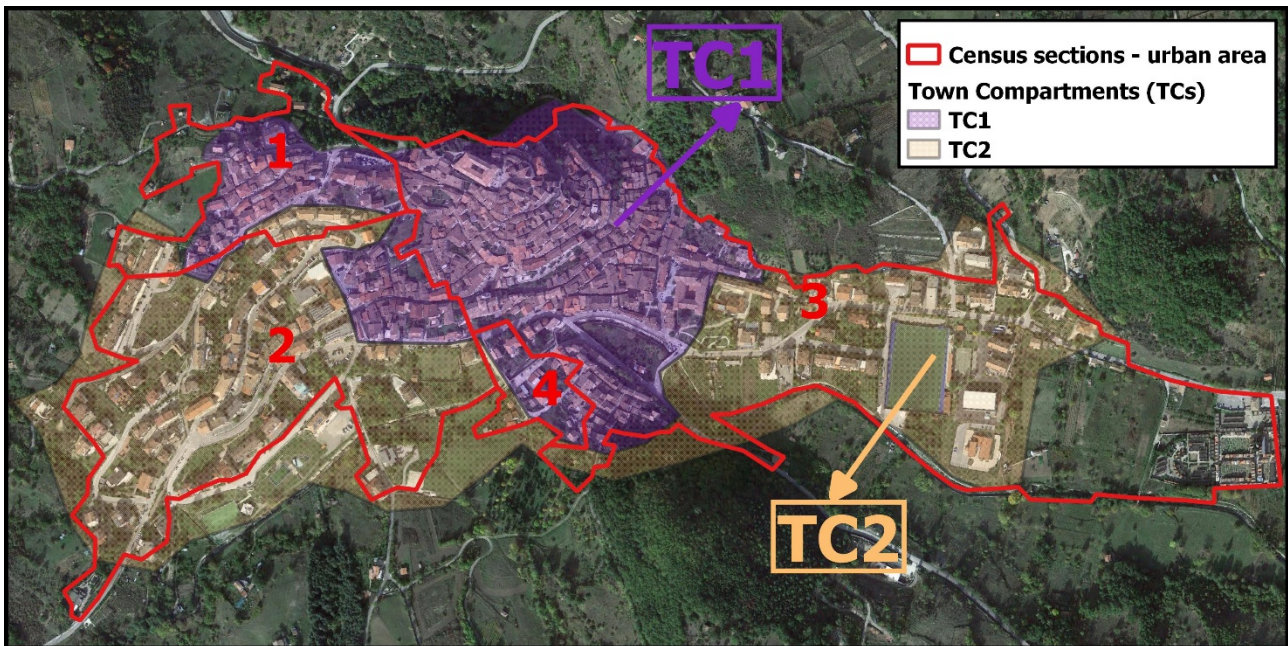


**Figure 5.8** Overlapping of the Town Compartments (TCs) and Census sections (ISTAT 2011) of the urban area of Calvello village

The number of buildings individuated by the ISTAT census (about 1000) is much greater than that estimated by CARTIS and RRVS approach (about 500). As underlined in past studies (e.g., Digrisolo et al., 2019), ISTAT data are not reliable due mainly to the misleading consideration of building aggregates. For instance, for census section 1, the number of buildings reported by ISTAT is equal to 189 but, by means of a survey with RRVS platform, the number of buildings is much less (about 70 bldgs.).

## **Discussion**

In order to perform a proper quantification of earthquake losses, building exposure modelling should be defined to be properly associated with vulnerability functions, however without becomes a costly and time-consuming process. In this regard, two approaches aimed at collecting data and defining inventories of the residential buildings have been proposed.

In order to fully exploit the scientific heritage of post-earthquake data organized on the Da.D.O. web-based platform, an innovative methodology has been developed to convert the information collected through the AeDES form to recognized international formats. The first step of the proposed approach allows to describe the information on the typological characteristics according to the faceted taxonomic description proposed by GEM. In a following step, a methodology based on the concept of fuzzy compatibility score has been employed in order to assign to each surveyed building a risk-oriented class (i.e., EMS-98 typologies). Starting from data specific to the Italian context, the first step enables to define an exposure model in terms of an international taxonomy that is independent by the vulnerability component and could be even employed for the consideration of multi-hazard modelling approaches. Through the second step, a building inventory in terms of risk-oriented classes (i.e., EMS-98 classes) correlated to specific fragility models can be obtained to be used for large-scale risk assessments. The fuzzy formulation of the methodology helps mitigating the impact of subjective, expert-based judgment in the class assignment and provides an extensive characterization of the underlying uncertainties, by ensuring the reproducibility of the results. As a result, the data collected through AeDES form represent a unique, invaluable source of information for scientific purposes and, through the proposed methodology, their potential for seismic risk assessments can be exploited at a much larger scale and considered even for different applications, including multi-hazard exposure and vulnerability evaluation. The proposed approach could be also implemented in the Da.D.O. platform in order to define (also spatially) an exposure model in terms of GEM taxonomy or EMS-98 classes for the building stock surveyed during the last Italian earthquakes.

Furthermore, the approach based on the integration of data collected with CARTIS format and RRVS web-based platform is a useful tool for defining residential building inventories. The approach has been applied to the Calvello village (Basilicata region) and a preliminary comparison with the ISTAT data has been carried out. The findings suggest that the proposed approach allows both to reduce time and resources with respect to building-by-building surveys and to rapidly acquire much more data on building typologies with respect to census returns. Moreover, the typological-structural data can be also used to assess the seismic vulnerability of the buildings. Finally, the RRVS platform could be also considered to evaluate the reliability of the data collected with the CARTIS format, widely used in Italy.

## References

- AIS, (2009) Guía técnica para inspección de edificaciones después de un sismo: manual de campo, 3d edition. Asociación Colombiana de Ingeniería Sísmica and FOPAE, Bogotá, Colombia, 54pp.
- Anagnostopoulos S.A. and Moretti M., (2008) Post-earthquake emergency assessment of building damage, safety and usability - Part 1: Organization. *Soil Dyn. Earthquake Eng.*, 28, 223-232.
- ATC, (2005) ATC-20-1. Field manual: post-earthquake safety evaluation of buildings, second edition. Applied Technology Council, Redwood City, CA.
- Baggio C., Bernardini A., Colozza R., Corazza L., Della Bella M., Di Pasquale G., Dolce M., Goretti A., Martinelli A., Orsini G., Papa F. and Zuccaro G., (2007) Field manual for post-earthquake damage and safety assessment and short-term countermeasures (AeDES). JRC Scientific and Technical Reports, European Commission, EUR22868 European Commission, EUR 22868 EN, Joint Research Centre, Institute for the Protection and Security of the Citizen, Luxembourg, 81pp., Luxembourg, 81pp.
- Bilham R., (2009) The seismic future of cities. *Bulletin of Earthquake Engineering*, 7, 839-887, DOI:10.1007/s10518-009-9147-0.
- Bortolan G. and Degani R., (1985) A review of some methods for ranking fuzzy subsets. *Fuzzy Sets Syst.* 15, 1–19. doi: 10.1016/0165-0114(85)90012-0
- Braga F., Dolce M., Liberatore D., (1982) A statistical study on damaged buildings and ensuing review of the MSK-76 Scale. In: 8th ECEE, Atene
- Brzev S., Scawthorn C., Charleson A.W., Allen L., Greene M., Jaiswal K.S., et al. (2013) GEM Building Taxonomy Version 2.0. GEM Technical Report 2013-02 v1.0.0, GEM.
- Digrisolo A., Masi A., Curcio I., Ventura G., Nicodemo G., (2019) Comparison among different methods aimed at collecting seismic vulnerability data for the preparation of building damage scenarios: experiences and applications. In Proceedings of the XVIII Italian Conference on Earthquake Engineering, Ascoli Piceno, Italy, 15-19 September 2019 (in Italian)
- Dolce M., Masi A., Marino M., Vona M., (2003) Earthquake damage scenarios of Potenza town (southern Italy) including site effects. *Bull. Earthquake Eng.*, 1, 115-140.
- Dolce M., Speranza E., Giordano F., Borzi B., Bocchi F., Conte C., Di Meo A., Faravelli M., Pascale V. (2019) Observed damage database of past Italian earthquakes: the Da.D.O. WebGIS. *Bollettino di Geofisica Teorica ed Applicata* Vol. 60, DOI 10.4430/bgta0254
- Dorohonceanu B. and Marin B., (2002) A simple method for comparing fuzzy numbers. CiteSeerX Scientific Literature Digital Library and Search Engine.
- DPC, (2018) National Civil Protection Department (ed), National risk assessment. Overview of the potential major disasters in Italy: seismic, volcanic, tsunami, hydro-geological/hydraulic and extreme weather, droughts and forest fire risks
- Goretti A. and Inukai M., (2002) Post-earthquake usability and damage evaluation of reinforced concrete buildings designed not according to modern seismic codes. JSPS Short Term Fellowship, Final report, Servizio Sismico Nazionale, Dipartimento di Protezione Civile, Roma, Italy.
- Grünthal G., (1998) European Macroseismic Scale 1998. Vol. 15. Centre Européen de Géodynamique et de Séismologie, Luxembourg.
- ISTAT, (2011) Italian National Institute of Statistics. Italian population and housing census. On line at: [www.istat.it](http://www.istat.it)
- Jaiswal K., Wald D., Porter, K., (2010) A global building inventory for earthquake loss estimation and risk management. *Earthq. Spect.* 26, 731–748. doi: 10.1193/1.3450316
- Kaufmann A. and Gupta M., (1985) Introduction to Fuzzy Arithmetic: Theory and Applications. Van Nostrand Reinhold Electrical/Computer Science and Engineering Series. Van Nostrand Reinhold Company



- Kircher C.A., Whitman, R.V., Holmes W.T., (2006) HAZUS earthquake loss estimation methods. *Nat. Hazards Rev.* 7, 45–59. doi: 10.1061/(ASCE)1527-6988(2006)7:2(45)
- Lagomarsino S. and Giovinazzi S., (2006) Macro seismic and mechanical models for the vulnerability and damage assessment of current buildings. *Bull. Earthq. Eng.* 4, 415–443. doi: 10.1007/s10518-006-9024-z
- Lee C. and Chen B., (2018) Mutually-exclusive-and-collectively-exhaustive feature selection scheme. *Appl. Soft Comp.* Volume 68, Pages 961-971
- Liuzzi M., Pelizari P.A., Geiß C., Masi A., Tramutoli V., Taubenböck H., (2019) A transferable remote sensing approach to classify building structural types for seismic risk analyses: the case of Val d'Agri area (Italy). *Bulletin of Earthquake Engineering*. <https://doi.org/10.1007/s10518-019-00648-7>
- Masi A., Chiauuzi L., Samela C., Tosco L., Vona M., (2014) Survey of dwelling buildings for seismic loss assessment at urban scale: the case study of 18 villages in Val D'Agri, Italy. *Environmental Engineering and Management Journal*, February 2014, Vol.13, No. 2, 471-486.
- Masi A., Santarsiero G., Digrisolo A., Chiauuzi L., Manfredi V., (2016) Procedures and experiences in the post-earthquake usability evaluation of ordinary buildings. *Bollettino di Geofisica Teorica ed Applicata* Volume 57, Issue 2, 1 June 2016, Pages199-200
- NZSEE, (2009) Building safety evaluation during a state of emergency guidelines for Territorial Authorities. New Zealand Society for Earthquake Engineering
- Pittore, M., and Wieland, M. (2013). Toward a rapid probabilistic seismic vulnerability assessment using satellite and ground-based remote sensing. *Nat. Hazards* 68, 115–145. doi: 10.1007/s11069-012-0475-z
- Pittore M., Wieland M., Fleming K., (2016) Perspectives on global dynamic exposure modelling for geo-risk assessment. *Nat Hazards* 86, 7–30 (2017). <https://doi.org/10.1007/s11069-016-2437-3>
- Pittore M., Haas M., Megalooikonomou K.G., (2018) Risk-Oriented, Bottom-Up Modeling of Building Portfolios with Faceted Taxonomies. *Front. Built Environ.* 4:41. doi: 10.3389/fbuil.2018.00041
- Polese M., Gaetani d'Aragona M., Prota A., (2019a) Simplified approach for building inventory and seismic damage assessment at the territorial scale: an application for a town in southern Italy, *Soil dynamics and earthquake engineering*, 121 (2019) 405-420
- Polese M., Di Ludovico M., Gaetani d'Aragona M., Prota A., Manfredi G. (2019b) Regional vulnerability and risk assessment accounting for local building typologies. *International Journal of Disaster Risk Reduction*, 43 (2020) 141400, DOI: 10.1016/j.ijdr.2019.101400
- Tzitzikas Y., (2009) *Faceted Taxonomy-Based Sources*. Berlin; Heidelberg:Springer.
- Verrucci E., Bevington J., Vicini A., (2014) Application of the GEM inventory data capture tools for dynamic vulnerability assessment and recovery modelling. *EGU General Assembly Conference Abstracts*, Volume 16 of EGU General Assembly Conference Abstracts, 15707.
- Wieland M., Pittore M., Parolai S., Zschau J., Moldobekov B., Begaliev U., (2012) Estimating building inventory for rapid seismic vulnerability assessment: Towards an integrated approach based on multi-source imaging. *Soil Dyn. Earthquake Eng.*, vol. 36, pp. 70–83, 2012
- Wieland M, Pittore M (2014) Performance evaluation of machine learning algorithms for urban pattern recognition from multi-spectral satellite images. *Remote Sens* 6(4):2912–2939. doi:10.3390/rs6042912
- Wieland M., Pittore M., Parolai S., Begaliev U., Yasunov P., Niyazov J., et al. (2015) Towards a cross-border exposure model for the Earthquake Model Central Asia. *Ann. Geophys.* 58, 1–8. doi: 10.4401/ag-6663
- Zhu K.J., Jing Y., Chang D.Y., (1999) A discussion on extent analysis method and applications of fuzzy AHP. *Eur. J. Operat. Res.* 116, 450–456. doi: 10.1016/S0377-2217(98)00331-2
- Zuccaro G., Dolce M., De Gregorio D., Speranza E., Moroni C., (2015) La scheda CARTIS per la caratterizzazione tipologico-strutturale dei comparti urbani costituiti da edifici ordinari. Valutazione dell'esposizione in analisi di rischio sismico. *Proceedings of GNGTS 2015 (in italian)*

## CHAPTER VI

### Seismic risk assessment and reduction: applications

#### Introduction

In this chapter, three specific applications have been developed to better illustrate the proposed methodological developments and their implications.

Firstly, a comparison among different Casualty Estimation Models (CEMs) available in literature and described in Chapter II, has been carried out in the L'Aquila urban area. In order to define the factors involved in each CEM and discuss the possible differences with respect to the real impact, the data related to 2009 L'Aquila earthquake have been considered.

Consequently, the methodology proposed in Chapter V (Section 5.1) has been exemplified with the data of the 2009 L'Aquila earthquake reported in the Observed Damage Database (Da.D.O.) platform. An exposure model has been implemented in terms of GEM taxonomy and EMS-98 building types basing on the post-earthquake data of residential buildings of 137 municipalities. The resulting model has been validated based on observed damage data from the same platform and the macroseismic intensity values officially estimated by the National Institute of Geophysics and Volcanology (INGV).

Finally, earthquake damage scenarios for 19 urban centers in the Val d'Agri area (Basilicata region, Southern Italy) have been prepared. This area is characterized by high seismic risk and has a strategic economic role for Italy due to the presence of oil extraction plants. Starting from the building-by-building inventory of typological characteristics collected during previous research activities related to 18 villages combined with the data obtained from the proposed approach for the village of Calvello (Section 5.2 of Chapter V), the seismic vulnerability of the whole building stock has been studied and the expected losses in terms of unusable buildings, human consequences and repair costs have been determined. Further, an action plan for the seismic risk mitigation based essentially on vulnerability reduction of the residential building stock of the villages located in the Agri valley has been defined, and specifically applied to the village of Viggiano.

## 6.1 Comparison among casualty estimation models available in literature

Many factors can affect the number of casualties during an earthquake. These factors can be mainly correlated to (i) vulnerability component (e.g., structural typology, building characteristics, structural and non-structural damage); (ii) exposure component (e.g., population in different building typologies, occupancy rates at the time of the event and use of the structures); (iii) hazard component (e.g., earthquake magnitude and macroseismic intensity) or (iv) other parameters (e.g., Search And Rescue (SAR) effectiveness). In the past years, several Casualty Estimation Models (CEMs) were defined based on the assessment of these factors in different ways, as described in Section 2.1 of Chapter II. For sake of clarity, Table 6.1 summarizes the factors and related criteria of each CEM, considered in the following comparison. As an example, for the CEM6 adopted in the National Risk Assessment, NRA (DPC, 2018), the probability of casualties among the building occupants (i.e., fatality rate) is evaluated as a function only of the EMS-98 damage levels, Ld4 and Ld5. The buildings are classified according to the structural typology, distinguishing masonry (MAS) and reinforced concrete (RC).

	DAMAGE LEVEL	BUILDING CLASSIFICATION	EARTHQUAKE INTENSITY	FATALITY RATE**	OCCUPANCY RATES	OTHER PARAMETERS
<b>CEM1</b> Coburn and Spence (2002)	Ld5	MAS-RC	Yes	Ld; BT; IM	Yes	SAR capability
<b>CEM2</b> So and Spence (2013)	Ld4-Ld5	Vc = A, B, C, D1, D2, E	-	Ld; BT	Yes	-
<b>CEM3</b> Jaiswal and Wald (2010)	-	-	Yes	***	-	Population exposed to shaking intensity
<b>CEM4</b> Zuccaro and Cacace (2011)	Ld4-Ld5	MAS-RC	-	Ld; BT	Yes	-
<b>CEM5</b> SYNER-G (2013)	Ld1-Ld5*	Superclass category (1-BC, 2-BC, 3-BC)	Yes	Ld; BT; IM	Yes	-
<b>CEM6</b> NRA (2018)	Ld4-Ld5	MAS-RC	-	Ld	-	-
* Depending on the macroseismic intensity values **Factors explicitly determining the fatality rates (Ld=Damage level; BT=Building Typology; IM=Macroseismic intensity) ***Fatality rate, defined as total killed divided by total population exposed at specific shaking intensity level, is expressed in terms of a two-parameter lognormal cumulative distribution function of shaking intensity						

**Table 6.1** Factors influencing the Casualty Estimation Models (CEMs)

In order to discuss possible differences among the CEMs and evaluate the factors that mainly affect the estimation of the casualties, the CEMs reported in Table 6.1 have been applied to the L'Aquila urban area. It is worth noting that HAZUS methodology based on America earthquake data has not been considered because it would be misleading to apply it to the Italian built environment.

The data related to the 2009 L’Aquila earthquake occurred on April 6 at 03:32:39 a.m. local time with a Mw equal to 6.3 have been considered. A value of macroseismic intensity equal to VIII-IX in terms of both MCS and EMS-98 scale has been assigned to the L’Aquila urban area (Galli and Camassi, 2009; Tertulliani et al., 2010). In order to obtain information related to building typology and damage, the dataset of the 2009 post-earthquake surveys reported in the Da.D.O. platform (Dolce et al., 2019) has been considered. Specifically, the dataset consists of about 11,300 buildings located in the L’Aquila urban area (about 40,000 inhabitants; extrapolation from ISTAT data).

As a first step, the distribution of the building stock in terms of structural typologies has been assessed (Table attached to Figure 6.1), underlining that about 83% of the buildings have masonry (43%) or RC (40%) structures. After, applying the criteria defined by Dolce et al. (2003) and Chiauzzi et al. (2012), and illustrated in Table 6.2, the seismic vulnerability according to the four classes,  $V_c$  (i.e., “A”, “B”, “C”, and “D” relevant to high, medium, medium-low, and low vulnerability, respectively) defined by EMS-98 scale (Grünthal, 1998) has been assigned to surveyed buildings. Specifically, the vulnerability of masonry buildings was assessed on the basis of the most important structural characteristics, that are horizontal and vertical structural type, period of construction and/or retrofitting. For RC buildings, medium-low vulnerability (i.e.,  $V_c$ =“C”) was assigned to structures without earthquake resistant design (i.e., built before 1980), while the lowest vulnerability class (i.e.,  $V_c$ =“D”) was assigned to buildings designed according to modern anti-seismic criteria (i.e., built or retrofitted after 1980).

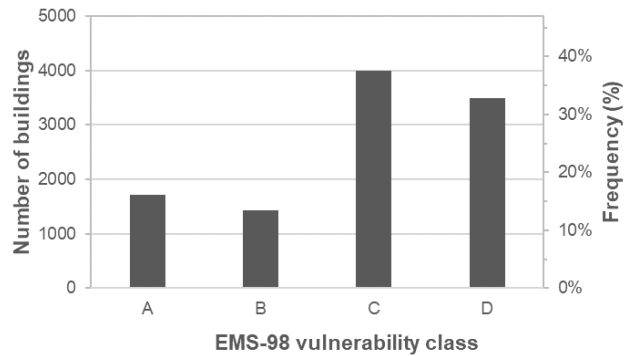
		Vertical Structure							
		Masonry Quality			Mixed	RC		Steel	Other
Horizontal Structures		Bad	Medium	Good		Frame	Wall		
Vaults	Without tie-beams	A	A	A	B	---	---	---	---
	With tie-beams	A	A	A	B	---	---	---	---
	Deformable	A	A	B	C	C	C	C	C
Floors	Semirigid	B	B	C	C	C	C	C	C
	Rigid, RC	B	C	C	C	C	C	C	C
<b>Buildings retrofitted after 1980</b>						D			
<b>Buildings built after 1980</b>						D			

Table 6.2 Criteria to assign vulnerability classes (from Chiauzzi et al., 2012)

Figure 6.1 reports the distribution of building vulnerability for the L’Aquila urban area. Results show that about 70% of the building stock is characterised by low and medium-low vulnerability classes. It should be noted that, for 650 buildings (6% of building stock), a vulnerability class cannot be assigned because no information on structural typology or construction/retrofitting age is available. Regarding the damage data, the CEMs take into account the damage levels according to the EMS-98 scale. The data relating to the 2009 L’Aquila event were collected with the AeDES 06/2008 form (Baggio et al., 2007), in which the structural damage of each building component (i.e., Vertical

structures, Floor, Stairs, Roof and Infills-Partitions) is defined for four damage levels (L<sub>d</sub>0, L<sub>d</sub>1, L<sub>d</sub>2-L<sub>d</sub>3, L<sub>d</sub>4-L<sub>d</sub>5) and three extension rates (<1/3; 1/3-2/3; >2/3). In order to assign a single EMS-98 damage level (from L<sub>d</sub>=0 to L<sub>d</sub>=5) to each building, the conversion schema proposed in Dolce et al. (2019) has been applied to damage related to only vertical structure (VS).

L'Aquila urban area		
Building typology	Number	Percentage
Masonry	4847	43%
R.C.	4486	40%
Steel	274	2%
Mixed (RC-Masonry)	774	7%
Undefined	930	8%
<b>Total</b>	<b>11311</b>	



**Figure 6.1** Distribution of the building stock of L'Aquila urban area in terms of building typologies (on the left) and in terms of vulnerability classes (on the right)

Figure 6.2 shows the distribution in terms of EMS-98 damage levels for the L'Aquila urban area. As can be seen, about 12% of the building stock was heavily damaged (i.e., L<sub>d</sub>4) and collapsed (i.e., L<sub>d</sub>5). It should be noted that no damage to VS for 40 buildings was assigned during the post-earthquake survey. Therefore, neglecting the buildings without information on vulnerability or damage, a dataset of about 10,600 buildings has been obtained. However, most of the models (e.g., CEM1, CEM4 and CEM6; see Table 6.1) were defined for masonry and RC structural typologies and, hence, a dataset of about 9,300 buildings has been considered in the comparison.

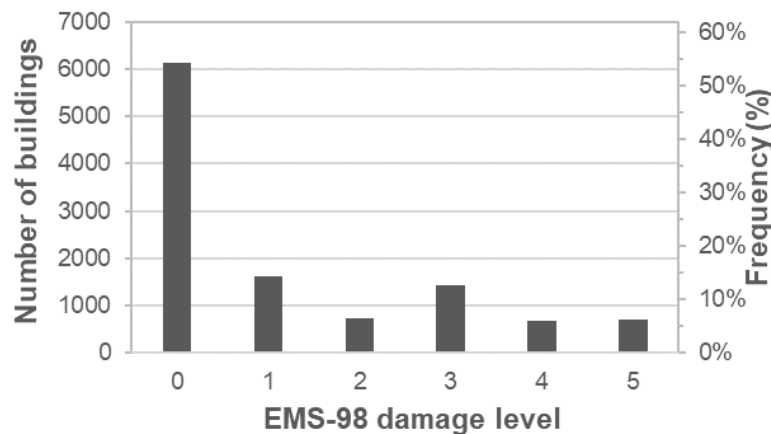


**Figure 6.2** Damage distribution in terms of EMS-98 levels for the building stock of L'Aquila urban area

In order to estimate the population in the different building typologies, the distribution in terms of number of storeys for RC and masonry (MAS) buildings has been obtained from Da.D.O. dataset, as reported in Figure 6.3. After, the mean value of people by building type, MAS or RC, has been estimated according to the following expression:

$$n^{\circ}_{MED} \frac{\text{people}}{\text{building}_{MAS/RC}} = n^{\circ}_{MED} \frac{\text{people}}{\text{storey}} \cdot n^{\circ}_{MED} \frac{\text{storeys}}{\text{building}_{MAS/RC}} \quad (6.1)$$

where

- $n^{\circ}_{MED} \frac{\text{people}}{\text{building}_{MAS/RC}}$  is the mean value of people by building type, MAS or RC;
- $n^{\circ}_{MED} \frac{\text{people}}{\text{storey}}$  is the mean value of people in each storey (obtained from Da.D.O. and ISTAT data);
- $n^{\circ}_{MED} \frac{\text{storeys}}{\text{building}_{MAS/RC}}$  is the mean value of storeys for single MAS and RC building (Figure 6.3).

As a result, the mean value of people by MAS and RC building type is equal to 3 and 4.5, respectively.

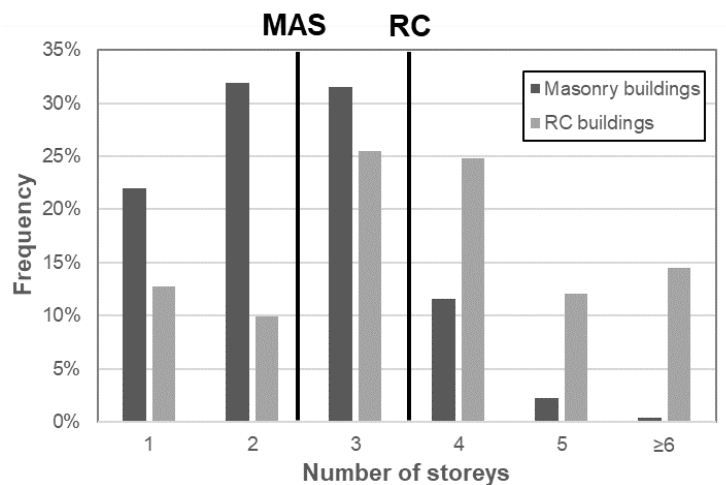


Figure 6.3 Distribution in terms of number of storeys for masonry and RC buildings of L’Aquila urban area

In order to estimate the occupancy rate at the time of the 2009 L’Aquila earthquake, the approach by Coburn and Spence (2002; Figure 6.4) has been considered with specific reference to the residential buildings (by urban population) and to the time of the earthquake (i.e., 03:32:39 a.m. local time). A value equal to about 72.5% has been obtained.

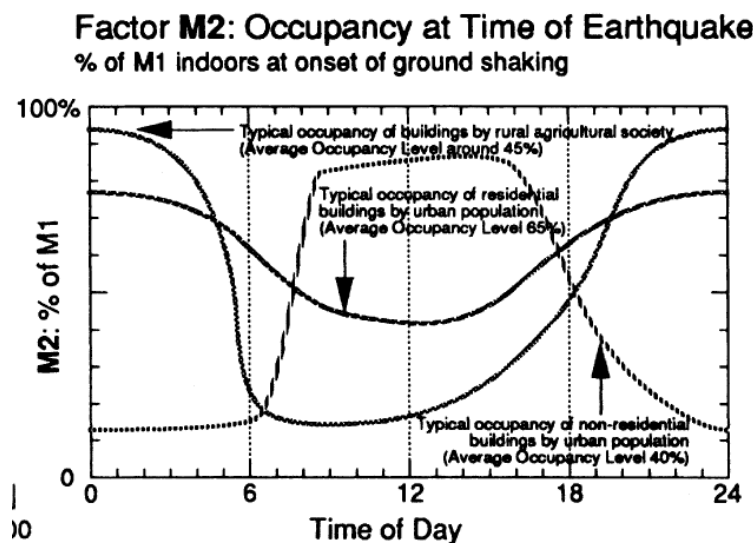
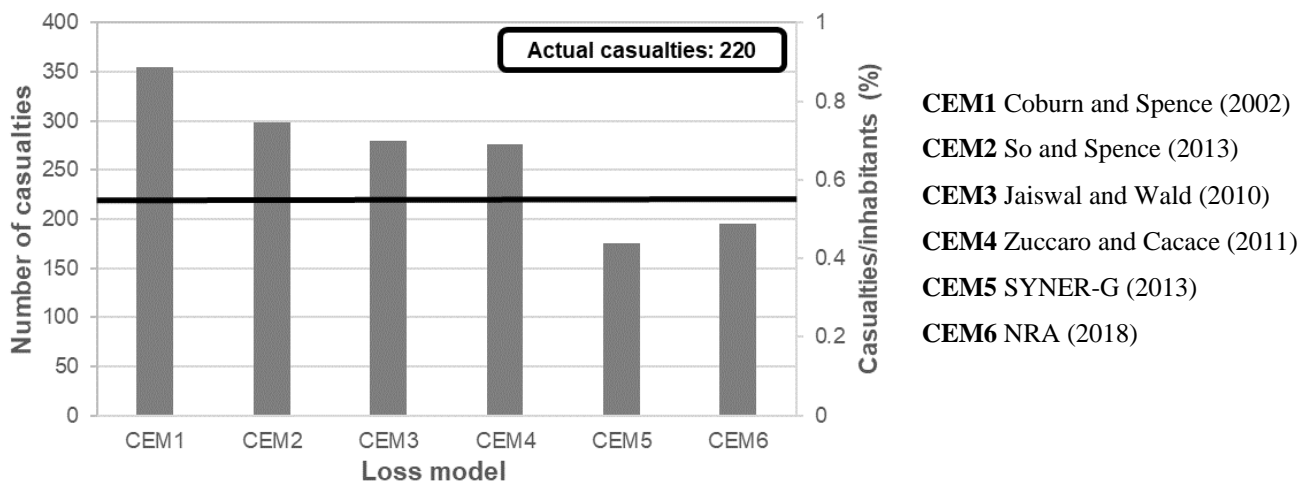


Figure 6.4 Occupancy at time of earthquake (from Coburn and Spence, 2002)

Therefore, based on the aforementioned parameters referring to the 2009 earthquake, the CEMs have been applied and the number of casualties for the L'Aquila urban area has been evaluated and reported in Figure 6.5. As for CEM3 (Jaiswal and Wald, 2010), the parameters ( $\theta$  and  $\beta$ ) are equal to respectively 13.23 and 0.18 and the population exposed to shaking intensity is equal to the number of inhabitants. Regarding the application of CEM1 (Coburn and Spence, 2002), M5 parameter (i.e., SAR capability) has been assumed equal to 0.45 for MAS and 0.7 for RC (Dolce, 2010).



**Figure 6.5** Comparison among the CEMs on the 2009 post-earthquake data of L'Aquila urban area

Figure 6.5 shows that the number of casualties varies from about 180 for CEM5 to about 350 for CEM1. With respect to the actual number of casualties (equal to 220; “Il Centro” newspaper), all the CEMs provide an overestimate, except for CEM5 and CEM6. The latter (NRA, 2018) provides the results most in agreement with the actual data. It is worth noting that the casualties deriving from non-structural damage, secondary effects (landslide, fire, etc.), infrastructure failures (viaducts, bridges, etc.) or simply panic have not been considered. The casualties from non-structural damage are relatively low because they are only dominant for low levels of ground shaking. The casualties deriving from the other causes (i.e., secondary effects; infrastructure failures or panic) rarely constitute a significant proportion of the total losses (such as for the 2009 earthquake).

In order to discuss the differences obtained between the CEMs, particular attention is devoted to CEM4 (Zuccaro and Cacace, 2011) and CEM6 (NRA, 2018). Although they are based on a similar approach, two main differences can be found related to the occupancy rate and the fatality rate. Specifically, for the CEM6 adopted in the NRA (2018), the fatality rates are independent from building typology and the occupancy rate at the time of the event is not explicitly considered (see Table 6.1). In order to evaluate the different weight of these parameters on the casualty estimation, the fatality rates adopted in the two models have been compared (Figure 6.6a) and the number of casualties as a function of damage level and building typology has been evaluated (Figure 6.6b). As can be seen in Figure 6.6a, despite being reduced by 72.5% to take into account the occupancy rate

at the time of the event, the fatality rates of Zuccaro and Cacace (2011) model are higher than those proposed by NRA (2018) which only vary with the damage levels. This aspect is one of the sources of discrepancy in the final estimation of the number of casualties (Figure 6.6b). Indeed, the percentage of casualties caused by buildings with Ld4 (for MAS and RC) and Ld5 (only for RC) is equal to about 18% for NRA (2018) and about 37% for Zuccaro and Cacace (2011).

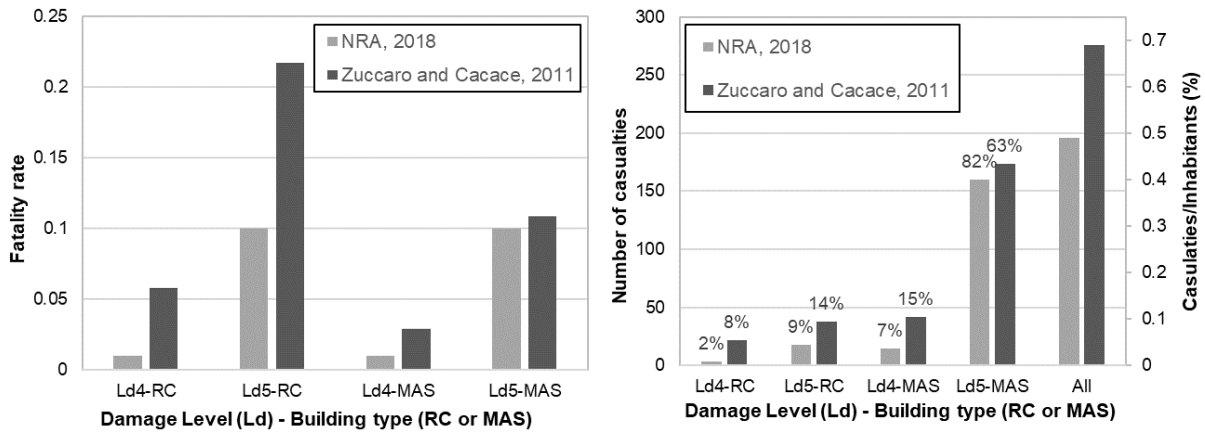


**Figure 6.6** Fatality rates (on the left) and number of casualties as a function of damage levels and building type (on the right) for NRA (2018) and Zuccaro and Cacace (2011) models

Furthermore, the weight of the occupancy rate at time of earthquake has been estimated considering three different scenarios related to residential building curve (Figure 6.4): (i) max occupancy rate (i.e., night time scenario) equal to 78%; (ii) min occupancy rate (i.e., day time scenario) equal to 45% and (iii) mean occupancy rate equal to 65%. The comparison (Figure 6.7) shows that the consideration of the occupancy rate provides important differences (about 45% among night and day time scenario).

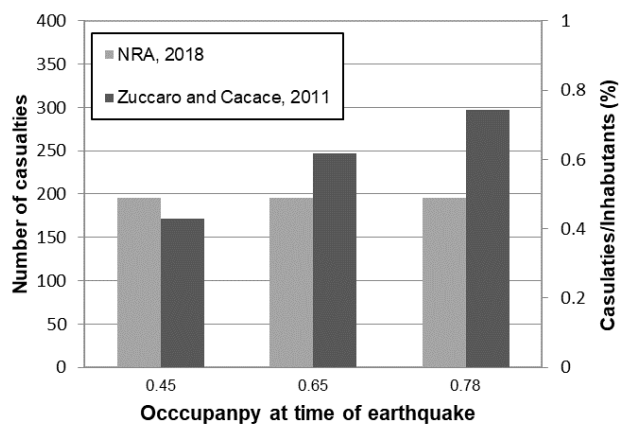
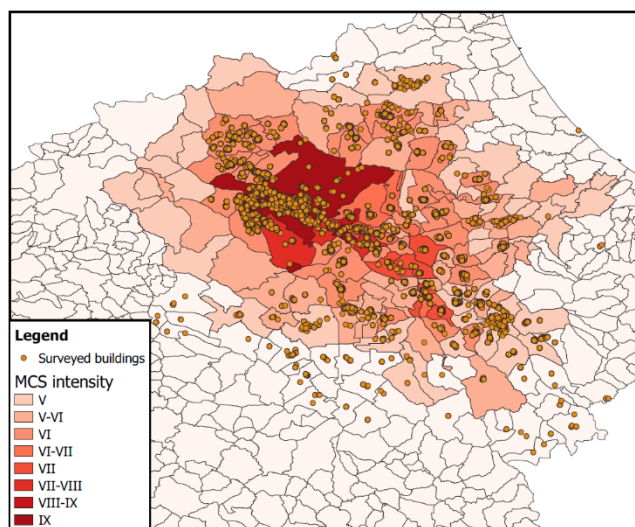


**Figure 6.7** Weight of the occupancy at time of earthquake on the casualty estimation



## 6.2 Modelling exposure from the 2009 L'Aquila post-earthquake dataset

The methodology for modelling building exposure based on post-earthquake data, described in the Section 5.1 of Chapter V, has been applied to the data of the 2009 L'Aquila earthquake (Tertulliani et al., 2010; Masi et al., 2011) as provided by the Da.D.O. platform. The earthquake caused heavy and extensive damage in several villages with MCS intensity values ranging from V to IX degree (Galli and Camassi, 2009). The macroseismic intensity values were reported also in Da.D.O. including 137 municipalities and 205 localities, thus forming the 'L'Aquila' database made up of about 74,000 records collected through the AeDES 06/2008 form. Figure 6.8 shows the area stricken by L'Aquila earthquake with macroseismic intensity values for the affected municipalities. Furthermore, the distribution of the surveyed buildings in terms of structural typologies is reported in the table attached to Figure 6.8. Most of the surveyed buildings have masonry structure (about 65%) while about 20% were built with RC structure. Small percentages equal to about 1% and 7% have steel or mixed structure, respectively. Finally, for about 8% of buildings, the structural typology was not assigned during the field survey.



Building typology	Number	Percentage
Masonry	49365	67%
R.C.	13047	18%
Steel	553	1%
Mixed (RC-Masonry)	5401	7%
Undefined	5683	8%
<b>Total</b>	<b>74049</b>	

**Figure 6.8** Area stricken by 2009 L'Aquila earthquake with MCS macroseismic intensity values (on the left) and distribution of the buildings in terms of structural typology (on the right)

L'Aquila database has been converted in terms of GEM taxonomy in accordance with the procedure described in Section 5.1.2.1. In the first phase, the mixed structures have not been considered in the analysis because GEM taxonomy does not consider this specific building typology. Therefore, the number of records considered is equal to 68,648.

Table 6.3 exemplifies the conversion process taking as example one of the surveyed buildings (id=100) with the attributes collected through the AeDES form and the corresponding attributes in terms of GEM taxonomy (only the attributes relevant for the classification are reported). On the basis of the approach reported in Section 5.1.2.2, the fuzzy compatibility score has been estimated for each

building in the L’Aquila database with respect to all EMS-98 classes. The compatibility score has been evaluated considering eight attributes and relative weighting reported in Table 6.4.

AeDES form		GEM taxonomy	
Attribute	Attribute value	Attribute type	Attribute value
Typology* <sup>1</sup>	C2 (masonry structure)	mat type	MUR
	<u>Vertical structure:</u>	mat tech	STRUB
	“Irregular layout or bad quality with tie rods or tie beams”	mat prop	MOL
		LLRS	L99
		floor mat	FM
	<u>Horizontal structure:</u>	floor type	FM1
	“Vaults without tie rods”	floor conn	FWCP
Construction and renovation	1982-1991	year built	1982-1991
Number of storeys* <sup>2</sup>	4	height (above ground)	4

\*<sup>1</sup> The attribute “Typology” considers both sections for masonry and other structures

\*<sup>2</sup> Difference between “total number of stories” and “number of basements”

**Table 6.3** Example of conversion of the attributes of a building surveyed through the AeDES form (id = 100) with the corresponding GEM taxonomic description

Attribute	Description	Weight
mat type	Material type	0,35
mat tech	Material technology	0,1
mat prop	Material property	0,05
LLRS	Type of lateral load-resisting system	0,2
year built	Date of Construction or Retrofit	0,1
floor mat	Floor system material	0,1
floor type	Floor system type	0,05
floor conn	Floor connections	0,05

**Table 6.4** Weighting for the EMS-98 building schema

Figure 6.9 shows the compatibility scores for the surveyed building (id = 100) described in Table 6.3. It can be noted that the class with the highest score in the EMS-98 schema is MAS1 but also other unreinforced masonry classes appear compatible with the considered building. By applying the same procedure to all buildings in the AeDES dataset, and assigning the class with the highest compatibility score, the exposure model shown in Figure 6.10 has been obtained. The buildings with (*defuzzified* median) compatibility score equal or less than zero have been assigned the OTH (Other) class. Moreover, Figure 6.11 shows the spatial distribution of four EMS-98 building types for the involved municipalities in the 2009 L’Aquila earthquake. The most widespread EMS-98 classes, MAS1, RC2, MAS3 and MAS5 (about 80% of L’Aquila database) have been considered. The administrative areas related to involved municipalities have been extrapolated by the website of Italian National Institute of Statistics (ISTAT). The representation reported in Figure 6.11 highlights the potential of the proposed approach also for spatial characterization of the exposure model.

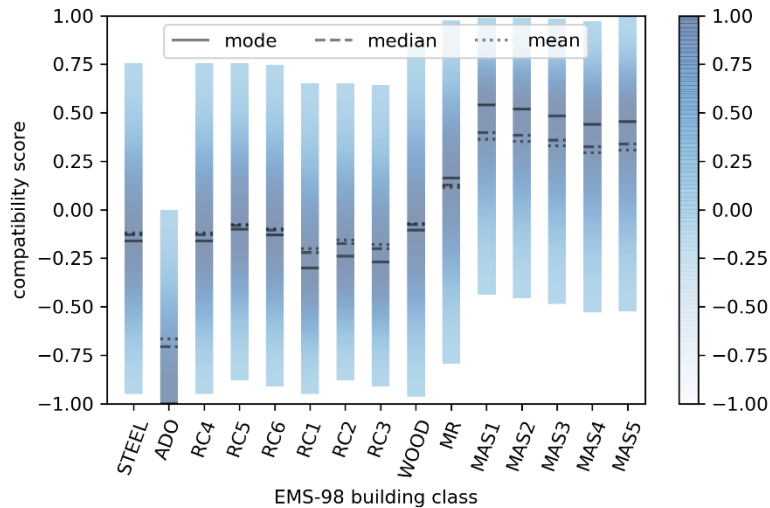


**Figure 6.9** Fuzzy compatibility scores of the observed building (see Table 6.3) with respect to the EMS-98 scheme. The solid and dashed segment represent the equivalent *defuzzified* values according to the mode, median or mean value of the TFNs.

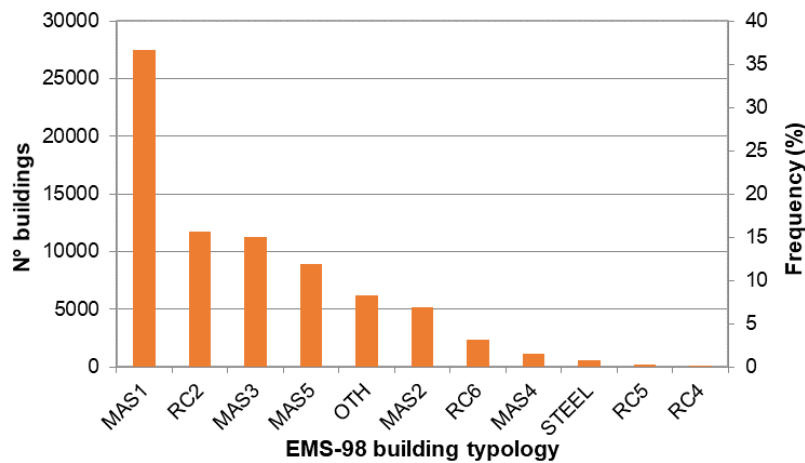


**Figure 6.10** Exposure model using EMS-98 class definition schema

The proposed methodology enables to define an exposure model correlated to a specific vulnerability model according to the EMS-98 definition. In order to validate the approach, the exposure model defined in terms of EMS-98 building types has been analysed considering also the damage data reported in the L’Aquila database. Specifically, a sanity check aimed at verifying if the observed damage distributions associated to the EMS-98 types comply with the vulnerability classification has been performed (i.e., the observed damage associated to EMS-98 types with high vulnerability should be more severe than that for types with low vulnerability). Therefore, each building defined by the EMS-98 type through the proposed methodology has been assigned to the corresponding damage level surveyed after the 2009 L’Aquila earthquake. As described in the previous section, the heuristic proposed in Dolce et al. (2019) has been applied to the damage data (in the Da.D.O. platform) related only to vertical structures (VS) in order to assign the EMS-98 damage level to each building.

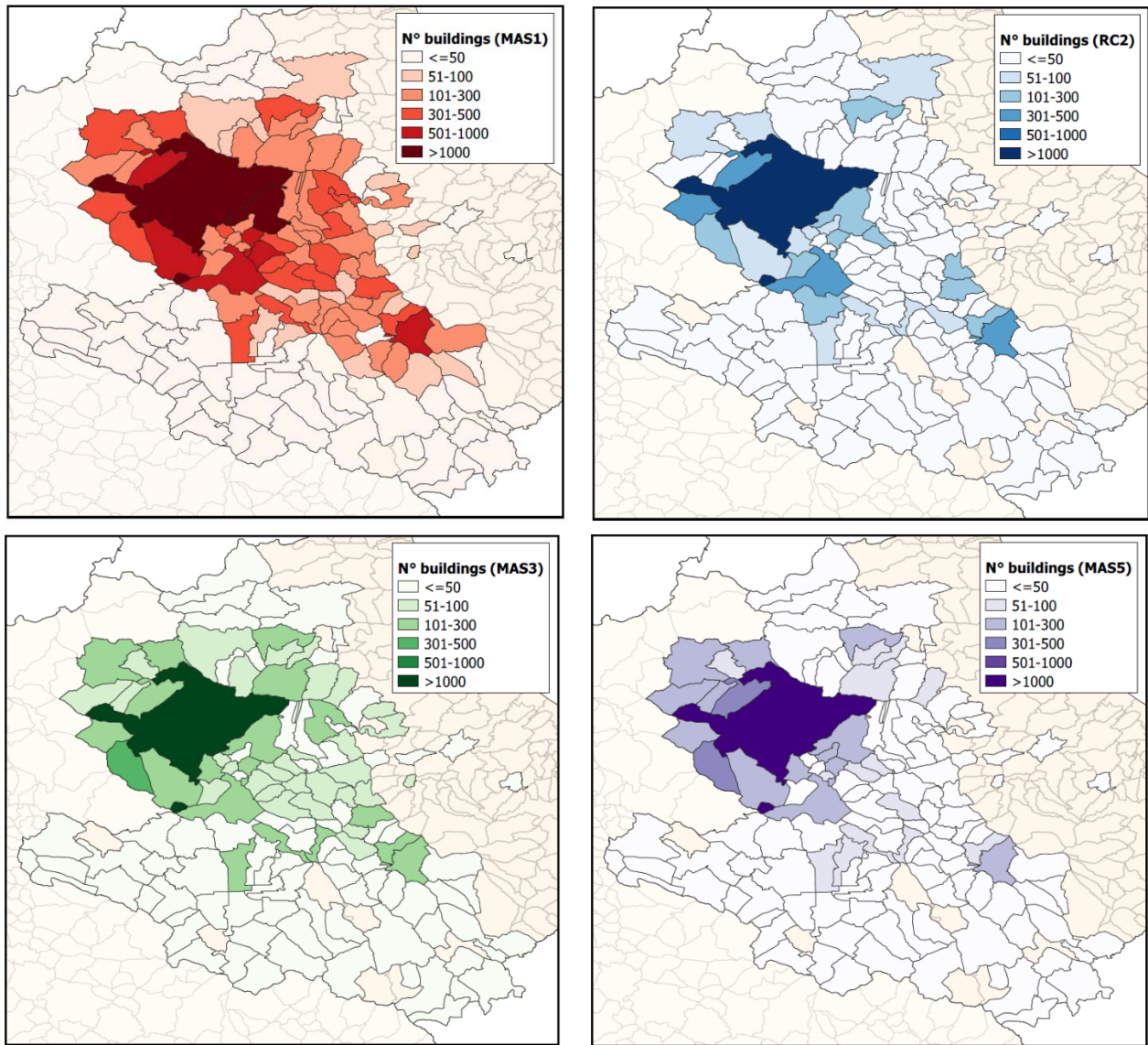


**Figure 6.11** Spatial distribution of EMS-98 building types: MAS1 (in red), RC2 (in blue), MAS3 (in green) and MAS5 (in purple). The colormap describes the number of surveyed buildings.

The observed damage has been associated to each EMS-98 building type, by taking into account also the macroseismic intensity (MCS) assigned after the L’Aquila earthquake to the involved municipalities (Figure 6.8). For each discrete value of MCS intensity (i.e., V, V-VI, VI, VI-VII, VII, VII-VIII, VIII-IX, IX), the observed damage distribution for all the considered typologies has been evaluated. Figure 6.12 reports the damage distribution related to the EMS-98 building typologies for all MCS intensity values. The class OTH has been neglected because this class cannot be assigned a seismic vulnerability. In order to provide an estimation of seismic intensity in terms of instrumental parameters, the bilinear correlations between macroseismic intensity and ground motion measures proposed in Chapter IV have been applied. Therefore, starting from the values of MCS intensity assigned after the L’Aquila earthquake in the area under study, Table 6.5 reports the corresponding values of Peak Ground Acceleration (PGA) and Velocity (PGV).

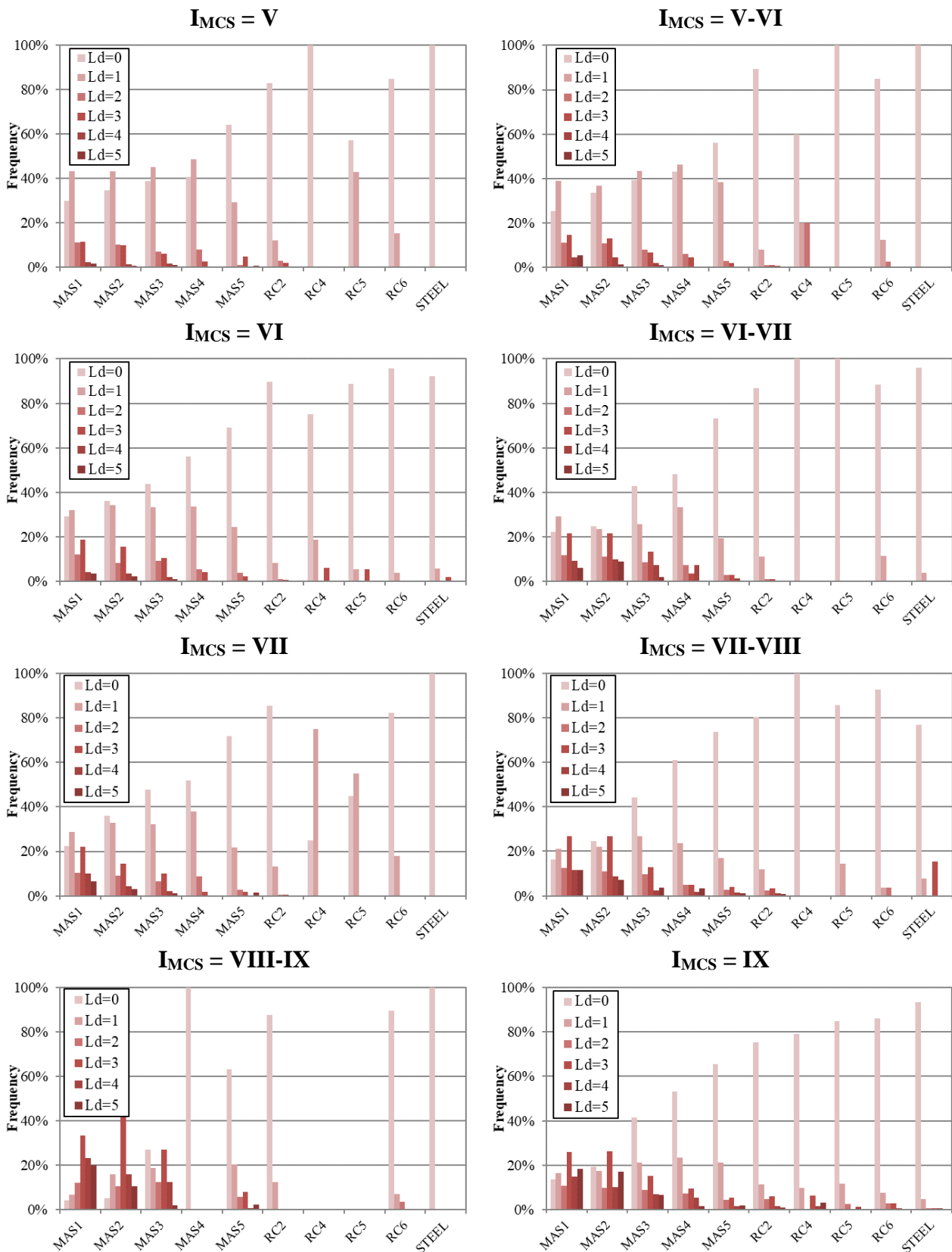


**Figure 6.12** Damage distribution for the EMS-98 building typologies with MCS intensity values assigned after the L'Aquila earthquake

MCS intensity	V	V-VI	VI	VI-VII	VII	VII-VIII	VIII-IX	IX
PGA (g)	0.05	0.07	0.1	0.13	0.17	0.22	0.39	0.50
PGV (cm/s)	3.2	6.4	8.4	11.0	14.5	19.0	32.8	43.2

**Table 6.5** PGA and PGV values related to MCS intensities assigned after the L’Aquila earthquake

The damage distribution for the EMS-98 typologies complies with the ranking of vulnerability classes (see Section 5.1.1.3 of Chapter V). For instance, for all MCS intensities, MAS1 related to most likely vulnerability class “A” provides an observed damage distribution more severe than MAS3 associated to class “C”. Furthermore, the mean damage index ( $DI_{med}$ ; Dolce et al., 2003) has been evaluated according to the following expression:

$$DI_{med} = \sum_i^n \frac{L_{di} f_i}{n} \quad (6.2)$$

where

- $L_{di}$  is the  $i$ -th damage level, varying between the first and fifth damage level of the EMS-98 scale;
- $n$  ( $= 5$ ) is the number of damage levels;
- $f_i$  ( $\in [0,1]$ ) is the observed frequency of occurrence.

$DI_{med}$  varies between 0 and 1, where  $DI_{med} = 0$  means total absence of damage and  $DI_{med} = 1$  means total destruction of the building set under examination. It provides a synthetic, aggregated estimation of different damage distributions, useful to compare them. Table 6.6 reports  $DI_{med}$  values related to EMS-98 building typologies for MCS intensity values, from VI to IX. The  $DI_{med}$  values referred to MCS intensity less to VI have not been considered because of the presumed lack of completeness of the survey. In fact, considering the municipalities for which MCS intensity values equal to V and V-VI were assigned, the comparison between the number of surveyed buildings (about 10,000) and the data extracted from the Italian housing census (ISTAT 2011) indicates that only about 35% (on average) of the building stock was inspected during the field survey. The number of buildings (included those with null damage) considered in the  $DI_{med}$  calculation has also been reported in Table 6.6. As can be noted, the number of buildings is quite variable (e.g., for  $I_{MCS} = VI$ ,  $DI_{med}$  value related to MAS1 and STEEL has been evaluated based on 8433 and 52 buildings, respectively). Therefore, in order to carry out a reliable comparison, the  $DI_{med}$  values calculated on a number of buildings less than 270 (namely, representative sample size evaluated by considering a margin of error equal to 5% and a confidence level equal to 90%; Bartlett et al., 2001) have been reported in Table 6.6 (highlighted in red) but have not been considered in the following analysis. The results show that the computed  $DI_{med}$  values meet adequately the EMS-98 vulnerability classification of classes and increase as expected with the MCS intensity values. As example, for  $I_{MCS} = VII$ , the  $DI_{med}$  decreases in accordance



to EMS-98 vulnerability classification with values equal to 0.38, 0.25, 0.18, 0.08 and 0.03 for MAS1, MAS2, MAS3, MAS5 and RC2, respectively.

<i>MCS</i> <i>intensity</i>	<i>EMS-98 building typology</i>									
	<i>MAS1</i>	<i>MAS2</i>	<i>MAS3</i>	<i>MAS4</i>	<i>MAS5</i>	<i>RC2</i>	<i>RC4</i>	<i>RC5</i>	<i>RC6</i>	<i>STEEL</i>
<i>VI</i>	0.29 (8433)	0.24 (1895)	0.19 (3777)	0.12 (356)	0.08 (2591)	0.03 (2548)	0.08 (16)	0.04 (18)	0.01 (508)	0.02 (52)
<i>VI-VII</i>	0.37 (1953)	0.39 (209)	0.25 (349)	0.18 (27)	0.08 (323)	0.03 (205)	0.00 (3)	0.00 (3)	0.02 (43)	0.01 (25)
<i>VII</i>	0.38 (2447)	0.25 (271)	0.18 (654)	0.12 (58)	0.08 (380)	0.03 (352)	0.15 (4)	0.11 (20)	0.04 (67)	0.00 (22)
<i>VII-VIII</i>	0.46 (1798)	0.39 (221)	0.23 (471)	0.15 (59)	0.09 (363)	0.07 (276)	0.00 (2)	0.03 (7)	0.02 (54)	0.11 (13)
<i>VIII-IX</i>	0.65 (189)	0.56 (19)	0.37 (48)	0.00 (4)	0.14 (138)	0.03 (72)	/ (0)	/ (0)	0.03 (28)	0.00 (5)
<i>IX</i>	0.53 (5830)	0.48 (1152)	0.29 (3388)	0.19 (401)	0.12 (3606)	0.10 (6109)	0.10 (62)	0.04 (85)	0.05 (1324)	0.02 (403)

**Table 6.6** Mean damage index ( $DI_{med}$ ) for the EMS-98 building typologies considering MCS intensity values assigned after L’Aquila earthquake. The number of buildings considered in the  $DI_{med}$  calculation has been reported in round brackets and the  $DI_{med}$  values evaluated with a buildings number less than 270 have been highlighted in red.

Moreover, Figure 6.13 shows the  $DI_{med}$  values calculated with a number of observations greater than 270 for the most widespread EMS-98 types (i.e., MAS1, RC2, MAS3 and MAS5; see Figures 6.10 and 6.11) as function of MCS intensity values. For a more intuitive interpretation of the results, the EMS-98 building typologies are reported in decreasing order of seismic vulnerability (from MAS1 to RC2). As already discussed above, the  $DI_{med}$  values increase as expected with the building vulnerability and with the seismic severity (from  $I_{MCS} = VI$  to  $I_{MCS} = IX$ ).

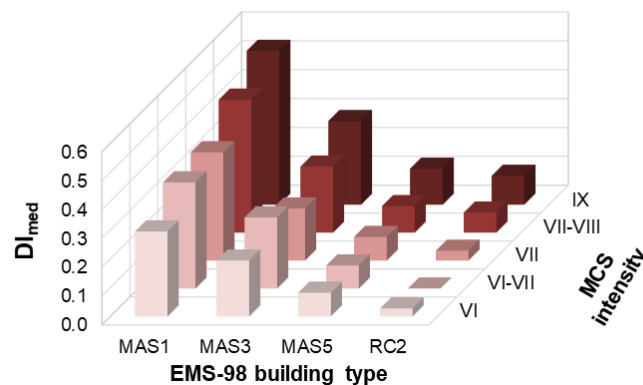


**Figure 6.13**  $DI_{med}$  values (calculated when the number of observations is greater than 270) for the most widespread EMS-98 types (MAS1, RC2, MAS3 and MAS5) considering MCS intensity values. The EMS-98 building types are reported in decreasing order of seismic vulnerability (from MAS1 to RC2).

Therefore, these results show that the EMS-98 types (mostly for masonry structures) with the relative observed damage comply with the ranking of vulnerability classes and their distribution is in line with what expected considering the respective MCS values. However, the low number of inspected RC and Steel buildings that can be associated to MCS values prevented a reliable comparison for these typologies, and further analysis on other datasets is required.

### 6.3 Seismic risk assessment and mitigation of the Val d'Agri area

Setting up of emergency plans to face the consequences of a damaging earthquake, development of methodologies aimed at assessing expected losses due to seismic events, and definition of sustainable solutions able to reduce the seismic vulnerability of residential buildings are crucial for medium-long term mitigation policies in urban areas. To this end, damage scenarios related to suitably selected events provide relevant data on the seismic risk of urban systems to support civil protection activities. A remarkable example of mitigation strategy in urban areas is the Community Action Plan for Seismic Safety (CAPSS) project developed by the Applied Technology Council (ATC) for the San Francisco Department of Building Inspection (ATC-52-2 report 2010). The project was created to support city agencies and policymakers with an action plan able to reduce the earthquake risk in existing privately-owned buildings, and also to develop repair and rebuilding guidelines aimed at accelerating recovery after an earthquake. Further, Yakut et al. (2012) proposed a study for the seismic risk prioritization at large scale of residential buildings in Istanbul with the objective of identifying the buildings that would be likely to sustain severe damage or suffer collapse during the expected Istanbul earthquake and, consequently, developing a rational risk reduction planning for minimizing losses. In this context, an action plan to reduce the seismic risk of 19 villages located in Basilicata region (Southern Italy) along the valley of the Agri river, has been defined. This area was struck by severe earthquakes in the past and has currently a strategic role for the entire country because about 70% (referring to the year 2017; DSG-UNMIG) of the Italian oil extraction derives from local deposits. Moreover, studies on the seismic risk of this area have gained increasing importance due to the highly debated question about earthquakes possibly induced or triggered by the oil extraction process. The topic of induced seismicity has caught greater attention in the last years, especially as a consequence of some cases of seismicity related to processes involving high-pressure injection of fluids (McGarr et al., 2002; Klose, 2013; Davies et al., 2013; Bommer et al., 2015). In the past, studies on the Agri valley aimed at estimating the seismic vulnerability of residential buildings were carried out (e.g., Masi et al., 2014). To this purpose, typological data deriving by a building-by-building survey were collected for 18 villages of the Agri valley. Starting from these data combined with the information collected for the village of Calvello (one of the six “OIL villages”; see Section 5.2 of Chapter V), an earthquake damage scenario by considering a seismic event with 475 years return period has been prepared. Results have been analyzed in terms of unusable buildings, human consequences (i.e., casualties) and repair costs. Further, a strategy essentially based on seismic vulnerability reduction has been proposed and related costs have been estimated on the basis of data reported in past studies (e.g., Di Ludovico et al., 2017a,b). Finally, an action plan has been specifically developed for the village of Viggiano in terms of needed costs for structural strengthening and consequent implementation timetables.



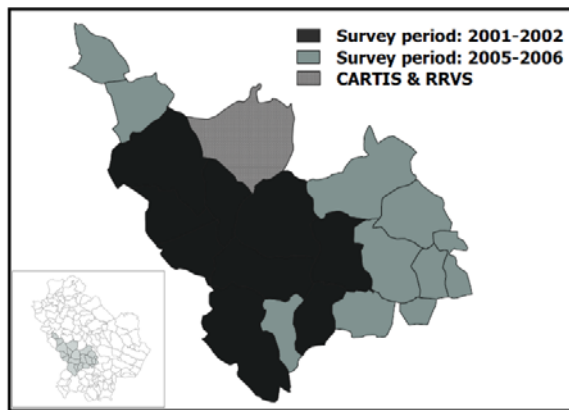
### **6.3.1 Vulnerability assessment**

The area under study is located along the valley of the Agri river (South-West of the Basilicata region) and has a population of about 40,000 inhabitants (ISTAT 2017; Figure 6.14). In the past, some studies were focused on the seismic risk of the Val d'Agri area, such as Masi et al. (2007) and Masi et al. (2014). The latter analysed the seismic vulnerability of the residential building stock belonging to 18 villages of the area on the basis of a building-by-building survey of typological characteristics. The survey was carried out by using a rapid inspection form named "Vulnerability Survey form in Peacetime" (VSP), derived from the post-earthquake inspection form AeDES (Baggio et al., 2007). The VSP form enabled the collection of building data such as identification (name, address, cadastral unit, photographs), geometrical dimensions (average plan surface, number of storeys, inter-storey height), use (property, function, percentage of use, number of dwellings and inhabitants), structural characteristics (materials, structural type, age of construction, strengthening interventions) and soil condition (geomorphology, landslide). The survey was carried out by trained technicians in two different periods, that are 2001-2002 and 2005-2006.

Most of the buildings of the surveyed villages have masonry structure (75% of the building stock) while only 20% were built with RC structure (other types amount to 5%). Instead, in terms of building volume a lower difference can be found, that is 42% and 51% for RC and masonry buildings, respectively. In terms of building height, about 77% of the surveyed buildings (65% in volume) can be classified as low-rise structures (i.e., buildings with a number of storeys in the range 1-3 for RC buildings and 1-2 for masonry and other types), while the other ones can be classified as mid-rise buildings (i.e., buildings with a number of storeys in the range 4-7 for RC buildings and 3-5 for masonry and other types). Very few buildings classified as high-rise structures are present in the area. About 60% of masonry buildings (45% in volume) were built before the Second World War (i.e., 1945), while RC buildings were built mostly after 1981 (15% and 30% in terms of number and volume, respectively), and therefore were designed using seismic criteria (the area under study was seismically classified after the 1980 Campania-Basilicata earthquake).

As discussed in Chapter V, the village of Calvello is one of the six "OIL Villages" of Agri Valley in which the extraction of oil and the reinjection of the fluids are directly carried out. However, the building stock of Calvello was not surveyed during the in-situ inspection campaigns carried out in 2001-2002 and 2005-2006. Therefore, the typological-structural characteristics of the building stock have been obtained from the application of the integrated approach, CARTIS and RRVS. The latter enabled the collection of information such as number of storeys, structural types, age of construction and so on. (Section 5.2 of Chapter V). As would be expected, the distribution of building stock of Calvello village (485 buildings) in terms of material, height and period of construction is consistent

with that of 18 villages described above. Specifically, most of the buildings have masonry structure (75% of the building stock) while 25% were built with RC structure. In terms of building height, about 78% of the buildings have a number of storeys equal to 2/3 (mainly, masonry buildings) while the other ones have 4/5 storeys (mainly, RC buildings). About 95% of masonry buildings were built before 1919 while RC buildings were built after 1987. Due to the lack of information on the volume of buildings, the average volume relevant to masonry and RC buildings of the 18 villages has been associated to the buildings of Calvello in order to prepare two seismic scenarios considering the building inventory in terms of number and volume (as will be explained later). Specifically, it is about 500m<sup>3</sup> for masonry buildings and about 1000 m<sup>3</sup> for RC ones. Therefore, the total volume for the building stock of Calvello village is equal to about 3.0x10<sup>5</sup> m<sup>3</sup>. A summary of the main collected data is reported in the table attached to Figure 6.14.

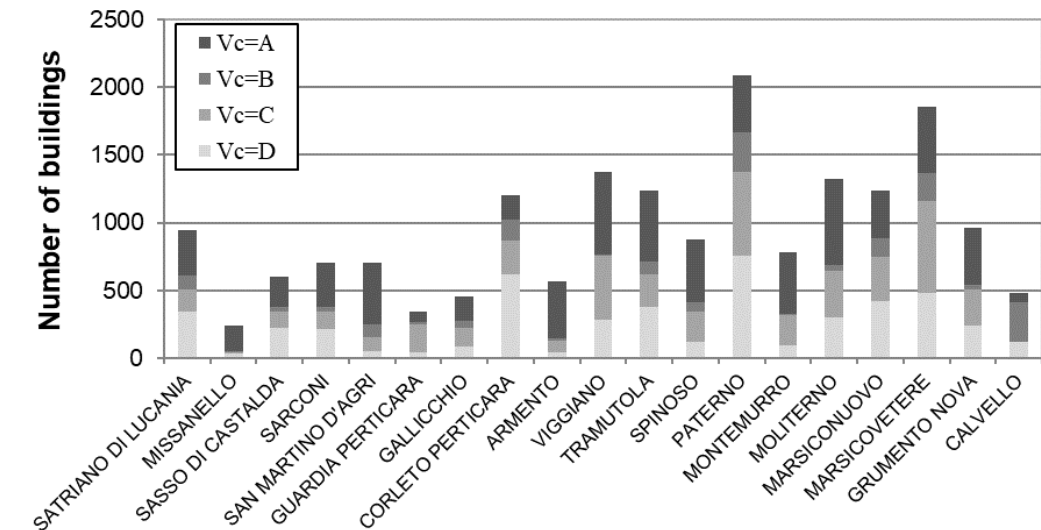


Number of villages	19
Number of buildings	18'000
Volume (m <sup>3</sup> ) of building stock	12 x 10 <sup>6</sup>
Number of retrofitted buildings	3'900
Percentage of retrofitted buildings	22%

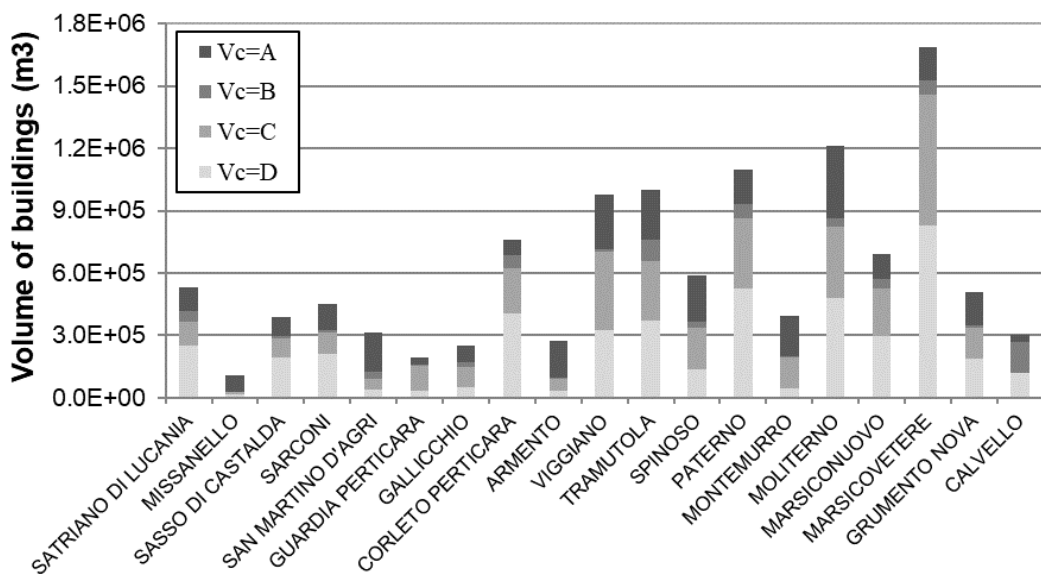
**Figure 6.14** On the left: map of the Agri valley area displaying the villages surveyed. On the right: summary of surveyed data.

Starting from the above-described typological data, Masi et al. (2014) assigned seismic vulnerability according to the four vulnerability classes,  $V_C$ , (i.e., “A”, “B”, “C”, and “D”) defined by EMS-98 scale (Grünthal, 1998). To this purpose, the criteria illustrated in Table 6.2 were adopted (Dolce et al., 2003; Chiauuzzi et al. 2012). Specifically, the vulnerability of masonry buildings was assessed on the basis of horizontal and vertical structural type, period of construction and/or retrofitting. For RC buildings, class “C” (i.e., medium-low vulnerability) was assigned to structures built before 1980 (i.e., without seismic criteria), while the class “D” (i.e., low vulnerability) was assigned to buildings (both masonry and RC structures) built or retrofitted after 1980 (i.e., designed according to modern anti-seismic criteria). The same criteria have been adopted for the building stock of Calvello village. Figure 6.15 reports the distribution of building vulnerability for all 19 villages and the attached table shows the data related to entire area under study (see also Table 6.7). Results show that the building stock is mainly characterized by low (class “D”) and medium-low (class “C”) vulnerability classes. Specifically, 39% of the building volume belongs to class “D” (27% in terms of number of buildings) while 30% belongs to class “C” (26% in terms of number). Nevertheless, it is worth highlighting that

the percentage of the highest vulnerability class (“A”) amounts to about 25% and 38% in terms of volume and number of buildings, respectively. The differences among vulnerability distributions in terms of volume and number of buildings are mainly due to the large difference in the average volume relevant to masonry buildings (i.e., about 500m<sup>3</sup>), which have generally higher vulnerability (i.e., V<sub>c</sub>=A or B), and RC buildings (i.e., about 1000m<sup>3</sup>), which have lower vulnerability (i.e., V<sub>c</sub>=C or D). As reported below, this result also influences loss scenarios.



a)



b)

	Number of buildings				Volume of buildings (m <sup>3</sup> )			
	Vulnerability Classes (EMS-98)				Vulnerability Classes (EMS-98)			
	A	B	C	D	A	B	C	D
<b>Total</b>	6841	1699	4608	4839	2.9E+06	7.4E+05	3.6E+06	4.6E+06
<b>%</b>	38	9	26	27	25	6	30	39

**Figure 6.15** Distribution of the vulnerability classes in terms of buildings’ number (a) and volume (b) for each considered village and summary table for all the villages

Village name	Number of buildings				Volume of buildings (m <sup>3</sup> )			
	Vulnerability Classes (EMS-98)				Vulnerability Classes (EMS-98)			
	A	B	C	D	A	B	C	D
Satriano di Lucania	332	110	158	346	1.2E+05	5.0E+04	1.2E+05	2.5E+05
Missanello	187	9	14	31	7.7E+04	3.8E+03	8.4E+03	1.8E+04
Sasso di Castalda	227	37	120	221	9.5E+04	1.0E+04	8.8E+04	2.0E+05
Sarconi	325	35	128	213	1.3E+05	1.3E+04	1.0E+05	2.1E+05
San Martino d'Agri	457	93	100	54	1.9E+05	3.2E+04	5.3E+04	3.8E+04
Guardia Perticara	82	13	208	44	3.9E+04	5.2E+03	1.2E+05	3.1E+04
Gallicchio	184	52	136	83	7.9E+04	2.7E+04	9.2E+04	5.3E+04
Corleto Perticara	185	148	256	615	8.0E+04	6.3E+04	2.2E+05	4.0E+05
Armento	423	20	87	39	1.8E+05	9.1E+03	5.8E+04	3.1E+04
Viggiano	612	11	474	281	2.7E+05	9.1E+03	3.8E+05	3.2E+05
Tramutola	520	95	237	382	2.4E+05	1.0E+05	2.8E+05	3.7E+05
Spinoso	458	72	227	117	2.3E+05	2.7E+04	2.0E+05	1.4E+05
Paterno	417	289	623	755	1.7E+05	6.9E+04	3.3E+05	5.3E+05
Montemurro	451	13	222	94	2.0E+05	5.8E+03	1.5E+05	4.6E+04
Moliterno	637	46	341	301	3.5E+05	4.2E+04	3.5E+05	4.8E+05
Marsico nuovo	351	135	328	421	1.2E+05	4.1E+04	2.3E+05	3.0E+05
Marsicovetere	495	204	678	481	1.6E+05	7.2E+04	6.3E+05	8.3E+05
Grumento nova	424	27	271	240	1.6E+05	1.0E+04	1.5E+05	1.9E+05
Calvello	74	290	-	121	3.7E+04	1.5E+05	-	1.2E+05

**Table 6.7** Distribution of the vulnerability classes in terms of buildings' number and volume for each considered village

### 6.3.2 Hazard analysis

The Italian seismic catalogue CPTI15 (Rovida et al., 2019) reports several events that struck the Agri valley in the past, the strongest one occurred on December 16, 1857, with epicentral intensity  $I_0 = XI$  MCS ( $M_w 7.1$ ). According to the Italian seismic map (OPCM 3519/2006) and adopted in the current Italian Building Code (NTC-2018), for the 18 villages located in the Agri valley, the expected values of Peak Ground Acceleration (PGA) for an event with 475 years return period (i.e., exceedance probability of 10% in 50 years) range between 0.143g and 0.262g on stiff soil ( $V_{s30} > 800\text{m/s}$ ; cat. A), as displayed in Figure 6.16.

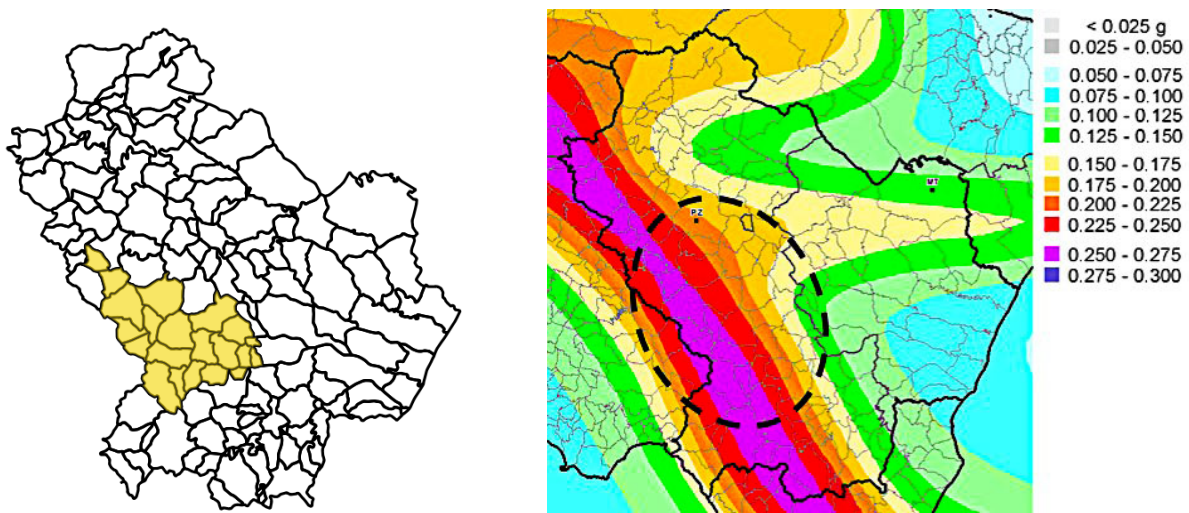


**Figure 6.16** On the left: Basilicata region and the considered villages (yellow area). On the right: seismic hazard map of Basilicata region according to OPCM3519/2006 for an exceedance probability of 10% in 50 years, soil class A

The above-mentioned hazard values referred to the Life Safety Limit State (SLV reported in NTC-2018 corresponding to Significant Damage limit state, SD, provided in EuroCode 8, part 3) have been adopted as seismic input. In order to take into account site effects, some results deriving from the seismic microzonation (SM) studies supported by the Basilicata region (MS-BAS) have been considered. In accordance with the criteria given in the Italian Guidelines for seismic microzonation (SM Working Group, 2015), three classes were qualitatively defined, that is “Stable zone”, “Stable zone - susceptible to local amplifications” and “Unstable zone”. Most of the Agri valley was classified as “Stable zone but susceptible to local amplification”, as specifically shown for the territory of Viggiano village in Figure 6.17. Further, specific studies on the local amplification effects in some villages of the Agri valley were carried out in the past within a research agreement between the Basilicata region and the University of Basilicata (Mucciarelli et al., 2005). According to the OPCM 3274/2003 code (also consistent with EC8 and NTC-2018), soil class B-T1 (i.e., “deposits of very dense sand, gravel, or very stiff clay, at least several tens of metres in thickness, characterised by a



gradual increase of mechanical properties with depth” and “no topographic amplification”) was mainly assigned. Therefore, based on the results from the two available studies, soil class B-T1 has been assumed for all villages under study.

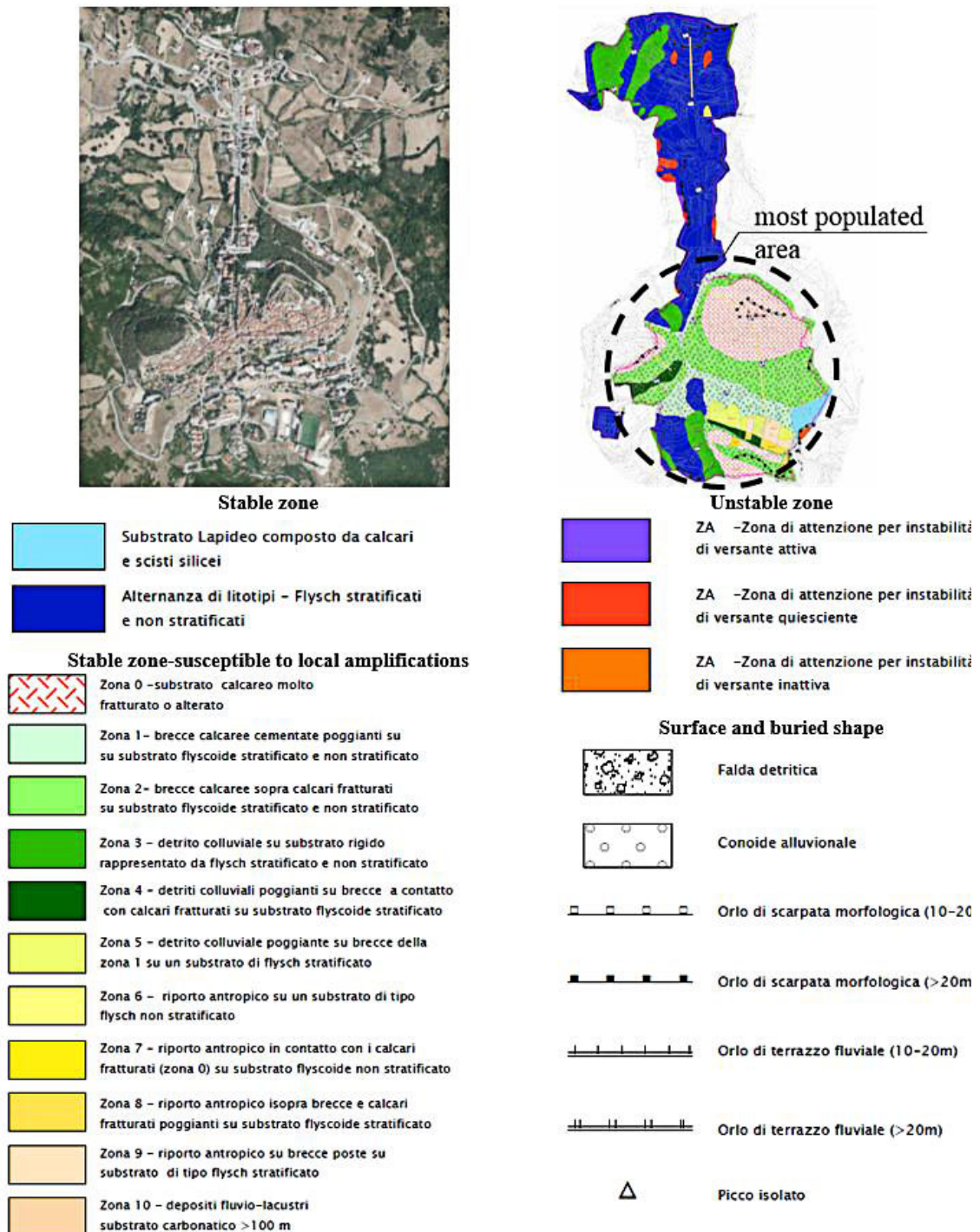


Figure 6.17 View of the Viggiano village and the corresponding seismic microzonation map. The most populated area is highlighted.

Damage Probability Matrices (DPMs - Braga et al., 1982; Dolce et al., 2003) have been adopted to compute seismic damage. Consequently, macroseismic intensities according to the EMS-98 scale (Grünthal, 1998) have to be evaluated to define the selected earthquake scenario. To this purpose, starting from the Italian seismic map and considering the greater capability of the Housner intensity,  $I_H$ , to represent seismic severity (e.g., Masi et al., 2015), the relationships developed in Chapter IV between  $I_{EMS-98}$  and  $I_H$  values have been considered and reported below:

$$I_{EMS-98} = 0.32 \cdot \ln(I_H) + 5.59 \quad I_H < 0.15m \quad (6.3)$$

$$I_{EMS-98} = 1.64 \cdot \ln(I_H) + 8.08 \quad I_H \geq 0.15m \quad (6.4)$$

For each village,  $I_H$  values have been computed on the basis of pseudo-velocity response spectrum according to the Italian seismic map (OPCM 3519/2006) and assuming the fraction of critical damping ( $\xi$ ) equal to 5%. For the considered event (i.e., exceedance probability of 10% in 50 years,  $T_R=475$  years, soil class B-T1), Table 6.8 reports the local values of PGA,  $I_H$  and  $I_{EMS-98}$ .

	Name of Villages	PGA (g)	$I_H$ (cm)	$I_{EMS-98}$
1	Armento	0.220	72	VIII
2	Calvello	0.274	84	VIII
3	Corleto Perticara	0.206	71	VII
4	Gallicchio	0.183	65	VII
5	Grumento Nova	0.300	93	VIII
6	Guardia Perticara	0.183	66	VII
7	Marsico Nuovo	0.300	90	VIII
8	Marsicovetere	0.297	89	VIII
9	Missanello	0.172	63	VII
10	Moliterno	0.304	91	VIII
11	Montemurro	0.270	82	VIII
12	Paterno	0.299	90	VIII
13	San Martino D'Agri	0.255	79	VIII
14	Sarconi	0.303	91	VIII
15	Sasso di Castalda	0.297	89	VIII
16	Satriano di Lucania	0.296	89	VIII
17	Spinoso	0.285	86	VIII
18	Tramutola	0.302	91	VIII
19	Viggiano	0.290	87	VIII

**Table 6.8** Values of PGA and  $I_H$  for  $T_R=475$  years and class B-T1 obtained from the Italian seismic hazard map, and EMS-98 macroseismic intensities

### 6.3.3 Damage and loss assessment

In this section, expected losses in terms of unusable buildings, homeless, casualties and repair costs have been estimated. To this purpose, two seismic scenarios have been prepared by considering the building inventory in terms of either number or volume of buildings.

Starting from the results of the building vulnerability assessment, for each village the number/volume of buildings suffering a certain damage level  $L_d$  due to the considered seismic input has been computed as follows:

$$N(L_d) = \sum_{V_C=A}^D [N_{V_C} \cdot DPM(L_d, V_C, I_{EMS})] \quad (6.5)$$

where  $L_d$  is the damage level as provided in EMS-98 scale, ranging between 0 and 5 ( $L_d=0$  means total absence of damage, while  $L_d=5$  means collapse),  $N_{V_C}$  is the number/volume of buildings for each vulnerability class  $V_C$  (i.e. “A”, “B”, “C” and “D”),  $DPM(L_d, V_C, I_{EMS})$  provides the probability of obtaining a damage level  $L_d$  given a macroseismic intensity  $I_{EMS}$  and a vulnerability class  $V_C$ . For sake of clarity, Table 6.9 reports the coefficients of the Damage Probability Matrices,  $DPM(L_d, V_C, I_{EMS})$ , for all the vulnerability classes and for the EMS-98 values VII and VIII considered in the proposed scenario (Dolce et al., 2003).

Vulnerability class ( $V_C$ )	Intensity ( $I_{EMS}$ )	Damage Level ( $L_d$ )					
		0	1	2	3	4	5
A	VII	0.064	0.234	0.344	0.252	0.092	0.014
	VIII	0.002	0.020	0.108	0.287	0.381	0.202
B	VII	0.188	0.373	0.296	0.117	0.023	0.002
	VIII	0.031	0.155	0.312	0.313	0.157	0.032
C	VII	0.401	0.402	0.161	0.032	0.003	0.000
	VIII	0.131	0.329	0.330	0.165	0.041	0.004
D	VII	0.715	0.248	0.035	0.002	0.000	0.000
	VIII	0.401	0.402	0.161	0.032	0.003	0.000

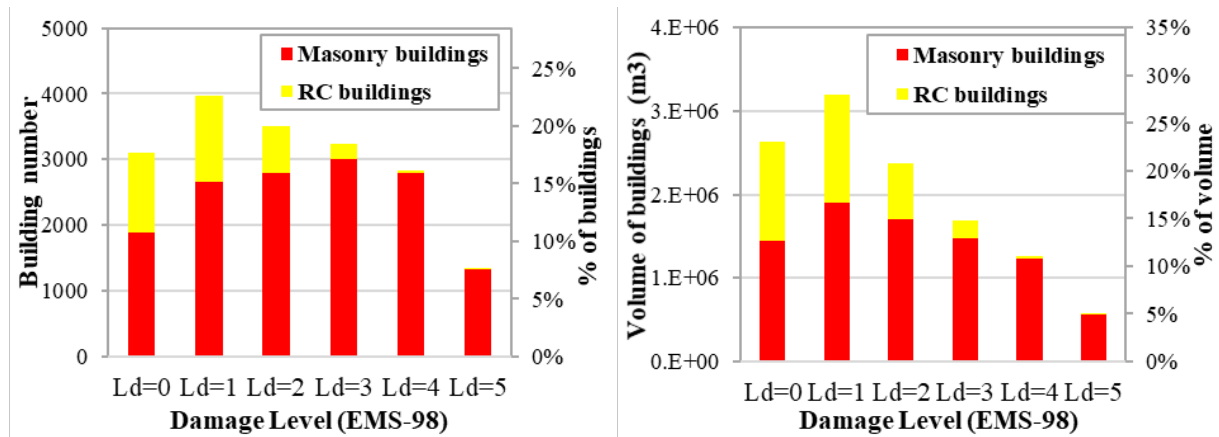
**Table 6.9** Damage Probability Matrices for buildings of vulnerability classes A, B, C and D and macroseismic intensity equal to VII and VIII (adapted from Dolce et al., 2003)

Figure 6.18 shows the expected damage distribution in terms of number (on the left) and volume (on the right) for each damage level (i.e., from  $L_d=0$  to  $L_d=5$ ). As can be seen, about 25% of the building stock (about 15% in terms of volume) would suffer a damage level  $L_d \geq 4$  (heavily damaged and collapsed buildings).

Results obtained from Eq. 6.5 have been also analyzed in order to evaluate unusable buildings, homeless and casualties. Specifically, unusable buildings have been calculated by using the percentages provided for the different vulnerability classes by Masi et al. (2007) and Chiauuzzi et al. (2018) on the basis of surveyed data after past earthquakes (see Section 2.3 of Chapter II). The



percentages of unusability refer to severely damaged buildings with rating “E” according to the AeDES form.



**Figure 6.18** Expected damage levels in terms of number (on the left) and volume (on the right) of buildings. The damage distribution has been split into RC (in yellow) and masonry/other type (in red) buildings

As for the homeless number, it has been estimated by multiplying the number/volume of unusable buildings and the average number of inhabitants per building/unit of volume. Possible differences in terms of average number of inhabitants per building located in the periphery with respect to the historic center have been neglected. Starting from the results reported in Figure 6.15 (i.e., distribution of the building vulnerability classes), Table 6.10 summarizes the number of unusable buildings and homeless for each vulnerability class as a function of both number and volume of buildings.

Vulnerability Classes $V_C$	Scenario in terms of number of buildings				Scenario in terms of building volume			
	Unusable buildings		Homeless		Unusable buildings		Homeless	
	Number	%	Number	%	Volume (m <sup>3</sup> )	%	Number	%
A	5575	31%	11775	30%	2.3E+06	20%	7610	20%
B	785	4%	1970	5%	3.4E+05	3%	1360	3%
C, D (masonry buildings)	840	5%	1880	5%	6.5E+05	5%	2170	5%
C, D (RC buildings)	205	1%	465	1%	2.0E+05	2%	675	2%
<b>All</b>	<b>7405</b>	<b>41%</b>	<b>16090</b>	<b>41%</b>	<b>3.5E+06</b>	<b>30%</b>	<b>11815</b>	<b>30%</b>

**Table 6.10** Number and percentage of the expected unusable buildings and homeless for each vulnerability class. Results from damage scenarios in terms of both number and volume of buildings are reported. For unusable buildings, the percentage related to each vulnerability class (%  $V_C$ ) has been reported.

In order to address a seismic intervention strategy, it is worth noting that the larger percentages refer to buildings with high vulnerability. Specifically, the percentage of unusable buildings with class “A” is equal to 31% of the whole building stock (20% in terms of volume), while the number of homeless amounts to 30% and 20% of inhabitants, respectively for scenario in terms of number and volume of buildings. The percentages of unusable buildings related to each vulnerability class are equal to about 81% (for  $V_c = “A”$ ), 46% (for “B”), 14% (for “C” and “D”, masonry buildings) and 5% (for “C” and “D”, RC buildings). With respect to casualties’ estimation, the approach proposed by Coburn and Spence (2002) and described in Section 2.1 of Chapter II has been adopted, whose parameters have been calibrated in order to calculate the minimum-maximum number of estimated victims.

Tables 6.11 and 6.12 summarize the expected losses for all villages of the Agri valley, respectively for the scenario in terms of number and volume of buildings. It is worth underlining that, as a consequence of the selected seismic input, the results have to be intended as the maximum expected losses for each single village, while it is very unlikely that they occur simultaneously.

In order to obtain a synthetic estimation of the global building damage, the mean damage index  $DI_{med}$  (which varies from 0 to 1) has been computed according to the equation 6.2 (Dolce et al., 2003).

Expected consequences (scenario in terms of number of buildings)						
Village	$DI_{med}$	Number of unusable buildings	% of unusable buildings	Number of homeless	% of homeless	Casualties
Satriano di Lucania	0.43	385	41%	955	41%	15-25
Missanello	0.36	85	35%	200	35%	0
Sasso di Castalda	0.43	245	40%	335	40%	5-10
Sarconi	0.47	330	47%	665	47%	15-25
San Martino d'Agri	0.60	460	65%	495	65%	10-20
Guardia Perticara	0.22	50	15%	80	15%	0
Gallicchio	0.27	100	22%	195	22%	0
Corleto Perticara	0.17	130	11%	270	11%	0
Armento	0.62	390	69%	415	69%	10-20
Viggiano	0.48	640	46%	1550	46%	30-55
Tramutola	0.46	555	45%	1365	45%	30-50
Spinoso	0.53	480	55%	780	55%	20-35
Paterno	0.37	660	32%	1055	32%	15-30
Montemurro	0.54	445	57%	685	57%	15-30
Moliterno	0.49	650	49%	1915	49%	40-75
Marsico nuovo	0.41	460	37%	1490	37%	15-30
Marsicovetere	0.41	680	37%	2020	37%	30-55
Grumento nova	0.47	445	46%	785	46%	15-25
Calvello	0.45	215	44%	835	44%	15-25
<b>All villages</b>	<b>0.43</b>	<b>7405</b>	<b>41%</b>	<b>16090</b>	<b>41%</b>	<b>280-510</b>

**Table 6.11** Distribution of mean damage index ( $DI_{med}$ ), number of unusable buildings, homeless and casualties for all 19 involved villages of the Agri valley area (damage scenario in terms of buildings’ number).

Considering the damage scenario in terms of number of buildings (Table 6.11), a mean value of  $DI_{med}$  equal to 0.43 has been computed for the whole area. Further, a total number of about 7,500 unusable

buildings (about 40% of the total building stock), about 16,000 homeless (about 40% of the inhabitants) and 280-510 casualties have been estimated. The scenario prepared in terms of volume (Table 6.12) reveals a lower percentage of expected losses. Specifically, a mean damage index equal to 0.36, about 12,000 homeless (about 30% of the total building stock) and 185-315 casualties have been evaluated. The differences among earthquake loss scenarios are mainly due to the different distributions of the seismic vulnerability in terms of volume and number of buildings. Specifically, as shown in Section 6.3.1, the building stock of the considered area is characterized by a large number of masonry buildings having higher vulnerability (mainly  $V_C=A$ ). On the contrary, in terms of volume, RC buildings (for which lower vulnerability classes have been assigned, i.e.,  $V_C=C$  or  $D$ ) prevail due to the higher average volume per building with respect to masonry ones. Therefore, the large number of buildings with high vulnerability (i.e., masonry buildings) inappropriately influences loss results when preparing the scenarios in terms of number of buildings. On the contrary, in case of scenarios in terms of volume, loss results reduce due to the higher volume of RC building stock having a lower vulnerability. In general, results from scenarios in terms of volume should be considered more accurate because building dimensions (such as volume and surface) are better correlated to both repair/reconstruction cost and exposure data.

**Expected consequences (scenario in terms of building volume)**

Village	$DI_{med}$	Unusable Volume (m <sup>3</sup> )	% of Unusable Volume	Number of Homeless	% of Homeless	Casualties
Satriano di Lucania	0.36	1.6E+05	30%	700	30%	10-15
Missanello	0.34	3.5E+04	33%	185	33%	0
Sasso di Castalda	0.35	1.1E+05	29%	240	29%	5-10
Sarconi	0.37	1.4E+05	31%	445	31%	10-15
San Martino d'Agri	0.57	1.9E+05	61%	460	61%	10-15
Guardia Perticara	0.20	2.6E+04	13%	70	13%	0
Gallicchio	0.24	4.6E+04	18%	165	18%	0
Corleto Perticara	0.15	6.4E+04	8%	215	8%	0
Armento	0.57	1.7E+05	62%	370	62%	10-15
Viggiano	0.39	3.2E+05	33%	1110	33%	20-35
Tramutola	0.38	3.3E+05	33%	1005	33%	15-30
Spinoso	0.45	2.5E+05	43%	610	43%	15-25
Paterno	0.32	2.7E+05	24%	810	24%	10-20
Montemurro	0.51	2.1E+05	52%	630	52%	15-25
Moliterno	0.39	4.1E+05	34%	1325	34%	25-45
Marsico nuovo	0.34	1.9E+05	27%	1090	27%	10-15
Marsicovetere	0.30	3.3E+05	20%	1090	20%	10-20
Grumento nova	0.40	1.8E+05	36%	610	36%	10-15
Calvello	0.40	1.1E+05	36%	685	36%	10-15
<b>All villages</b>	<b>0.36</b>	<b>3.5E+06</b>	<b>30%</b>	<b>11815</b>	<b>30%</b>	<b>185-315</b>

**Table 6.12** Distribution of mean damage index ( $DI_{med}$ ), unusable volume, number of homeless and casualties for all 19 involved villages of the Agri valley area (damage scenario in terms of buildings' volume).

Direct economic losses associated with repair of post-earthquake damage of residential buildings are one of the most important impact indicators to consider in planning seismic risk mitigation strategies. As discussed in Section 2.2 of Chapter II, different approaches can be used to estimate repair costs, frequently referred to data drawn from past earthquakes. The approach proposed by Dolce et al. (2006) has been applied in order to evaluate the total repair costs (direct economic losses) caused by the considered seismic scenario. Starting from the results obtained by Di Pasquale and Goretti (2001), the approach enables to compute the direct economic losses by convolving the DPMs (i.e., probability to observe different damage levels  $L_d$  for each vulnerability class  $V_c$ , given a seismic intensity  $I_{EMS}$ ) with the standard Beta distribution of the relative repair cost,  $C_{r,r}$ , (i.e., probability to observe a value of  $C_{r,r}$  for each damage level  $L_d$  according to the EMS-98 scale).

Specifically, by assuming an average reconstruction cost equal to 1,225 €/m<sup>2</sup> and a total volume of the building stock equal to about 12x10<sup>6</sup> m<sup>3</sup> (i.e., a total area equal to about 4x10<sup>6</sup> m<sup>2</sup>, assuming an average story height equal to 3.0m), the estimated value of total repair cost  $T_{Cr}$  is about 1,130 M€ (millions of euro). The considered reconstruction cost has been assumed on the basis of the Basilicata regional law DGR n.1942/2011, which provides a basic cost of 720 €/m<sup>2</sup> for new public housing, plus 55% for overheads and 10% for VAT. The costs are defined per square meter of the total gross area of the building. Figure 6.19 shows the direct economic losses related to each considered vulnerability class in all 19 villages. As expected, the higher percentage values of direct economic losses are related to the buildings with high vulnerability, i.e., class A, whose repair cost amounts to about 61% of the total repair cost. For Viggiano village, for which an action plan has been specifically defined as described below, the direct economic losses are about 103 M€

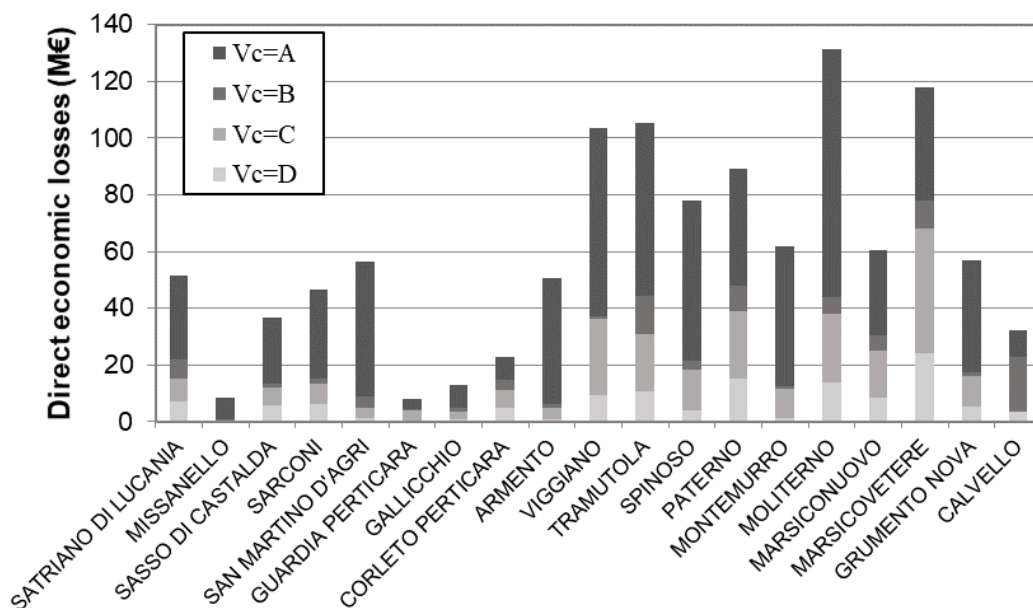


Figure 6.19 Direct economic losses for each considered vulnerability class, computed for each village

### 6.3.4 Estimation of seismic strengthening costs

In order to mitigate the seismic risk of the considered area, a strategy based on vulnerability reduction has been proposed and its relevant costs have been estimated. As reported in the previous sections, most of the expected losses are due to buildings having high- and mid-vulnerability. Therefore, strengthening interventions are primarily devoted at enhancing the seismic performance of buildings belonging to vulnerability classes “A” and “B”. As better discussed later, the seismic capacity of strengthened buildings has been set equal to 60% of the capacity currently required for new buildings (referred to the Life Safety limit state).

In order to assign the required strengthening costs, data from past studies on the reconstruction process after the 2009 L’Aquila earthquake have been considered (Dolce and Manfredi, 2015; Di Ludovico et al., 2017a,b; De Martino et al., 2017; Fico et al., 2019). This choice is based on the fact that the seismic hazard of L’Aquila area is comparable to the one under study and the target of the strengthening intervention adopted for the post-earthquake reconstruction is the same as mentioned above (i.e., at least 60% of the capacity required for the Life Safety limit state).

Specifically, the costs have been evaluated considering the two funding classes (FCs) defined by the Italian government in order to refund the “heavy damage” repair costs of unusable private buildings, that are:

- $FC_E$ , involving unusable buildings (i.e., with usability rating “ $UR_E$ ”) due to heavy structural and non-structural damage;
- $FC_{E-B}$ , involving unusable buildings (i.e., “ $UR_E$ ”) but having damage consistent with the usability rating “ $UR_B$ ” (i.e., temporarily unusable buildings, mainly due to heavy non-structural damage and slight structural damage).

A methodology has been properly defined in order to link the FCs to the considered vulnerability classes. First of all, on the basis of the data collected after the L’Aquila earthquake through the AeDES form (Masi et al., 2016) and adopting the criteria reported in Table 6.2 (Dolce et al., 2003; Chiauzzi et al. 2012), the distribution of the usability ratings as a function of the vulnerability classes has been analysed, as shown in Figure 6.20a. In order to better highlight the results for the two vulnerability classes considered in the strengthening strategy, Figure 6.20b shows the usability rating only for classes “A” and “B” (note also that the rating corresponding to the usable buildings, i.e., rating “ $UR_A$ ”, has been omitted).

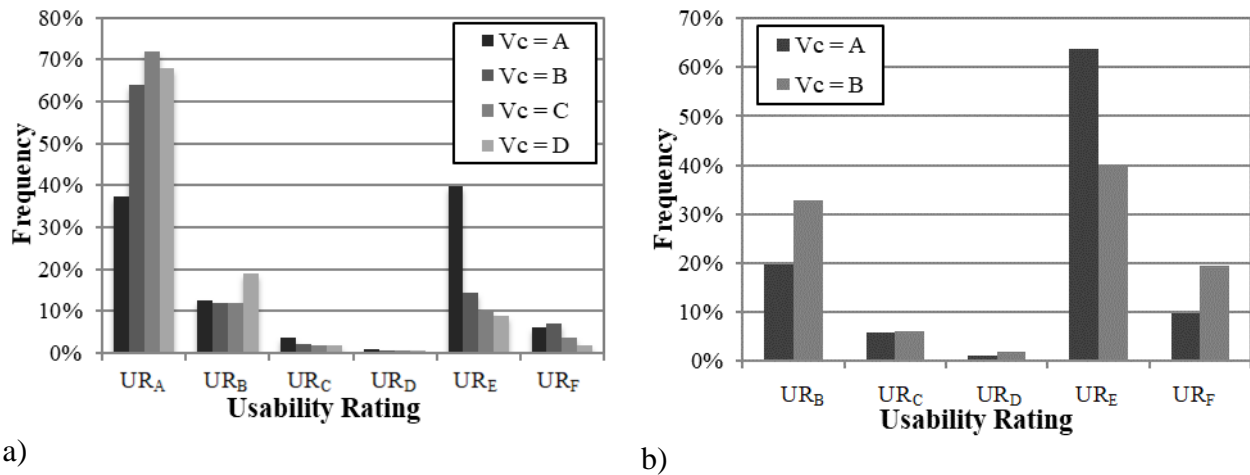


**Figure 6.20** Usability rating of the buildings surveyed after the 2009 L'Aquila earthquake for all vulnerability classes (a) and only for "A" and "B" classes (b)

Figure 6.20b shows that the usability rating "UR<sub>E</sub>" was assigned to most of buildings with vulnerability class "A" (about 65%). On the contrary, in case of the vulnerability class "B", the usability ratings "UR<sub>E</sub>" (about 40%) and "UR<sub>B</sub>" (about 32%) were mainly assigned. Therefore, the strengthening costs for the buildings with vulnerability class "A" have been derived from the ones of buildings having usability rating "UR<sub>E</sub>" and belonging to "FC<sub>E</sub>". As for buildings with vulnerability class "B", the costs have been obtained from the funding class of the unusable buildings having damage consistent with "UR<sub>B</sub>", i.e., "FC<sub>E-B</sub>". Specifically, the costs for buildings with vulnerability classes "A" and "B" have been estimated equal to 530 €/m<sup>2</sup> and 255 €/m<sup>2</sup>, respectively (VAT is equal to 10%). These values have been evaluated from the L'Aquila reconstruction process, as reported by Di Ludovico et al. (2017b). They originally take into account: (i) strengthening intervention (able to increase seismic capacity at least up to 60% of the New Buildings Standard, NBS), (ii) energy efficiency upgrading, (iii) structural/geotechnical tests, and (iv) damage repair. Regarding this latter cost, since it is a prevention strategy, no prior damage on the considered buildings has been assumed. Therefore, a rate equal to 20% of repair cost evaluated in the L'Aquila reconstruction process has been considered to take into account finishing works to be made as an unavoidable consequence of strengthening interventions (Del Vecchio et al., 2020).

It is also worth noting that, according to the L'Aquila "heavy damage" reconstruction process, the costs associated to "FC<sub>E-B</sub>" also derive from local strengthening interventions, for which no analyses related to the building safety reached after the intervention were required. For this reason, for types belonging to Vc=B (always masonry buildings), it has been assumed that local strengthening interventions are able to achieve the required safety level.

By considering the inventory of residential buildings (as reported in Figure 6.15 in terms of volume) and assuming an average height of dwellings equal to 3.0m, Table 6.13 reports the total strengthening costs estimated for each village and the mean values for building with Vc="A" and Vc="B". As can

be seen, the strengthening cost for the whole area is about 585 M€ while the mean value per single building is equal to about 76,000€ for vulnerability class “A” and 37,000€ for vulnerability class “B”. For each village, the mean values for single building have been evaluated as ratio between the total cost related to  $V_C=$ “A” and  $V_C=$ “B” and the corresponding number of buildings with  $V_C=$ “A” and  $V_C=$ “B” (see Table 6.7). Therefore, these mean values are dependent on the average volume of buildings with  $V_C=$ “A” and  $V_C=$ “B”.

Village	Estimated cost of seismic strengthening		
	Total cost (M€)	Mean value for building with $V_C=$ “A” (€)	Mean value for building with $V_C=$ “B” (€)
Satriano di Lucania	25	63,000	39,000
Missanello	14	74,000	36,000
Sasso di Castalda	18	75,000	24,000
Sarconi	24	70,000	31,000
San Martino d'Agri	37	75,000	29,000
Guardia Perticara	8	86,000	34,000
Gallicchio	16	77,000	44,000
Corleto Perticara	20	77,000	36,000
Armento	33	76,000	39,000
Viggiano	48	78,000	70,000
Tramutola	53	85,000	92,000
Spinoso	43	89,000	31,000
Paterno	36	71,000	20,000
Montemurro	36	79,000	38,000
Moliterno	67	99,000	78,000
Marsico nuovo	25	61,000	26,000
Marsicovetere	35	59,000	30,000
Grumento nova	29	67,000	32,000
Calvello	19	90,000	42,000
<b>All villages</b>	<b>586</b>	<b>76,000</b>	<b>37,000</b>

**Table 6.13** Seismic strengthening costs for each village and the mean value for each building with vulnerability class “A” and “B”.



### 6.3.5 An application of mitigation strategy: the action plan for Viggiano village

Based on the results described in the previous sections, an application is developed outlining a mitigation strategy on the building stock of Viggiano village (Figure 6.21). Specifically, an action plan aimed at the reduction of residential buildings' vulnerability has been defined in terms of costs and implementation timetable.



**Figure 6.21** Built environment of Viggiano village.

Viggiano was affected by several earthquakes in the past (Locati et al., 2019), particularly the December 16, 1857 earthquake (Mw 7.1; local intensity X MCS) and, more recently, the 1980 Irpinia earthquake (Mw 6.9; local intensity VI MCS). According to the Italian seismic zonation adopted in the OPCM 3274 (2003), Viggiano is classified as highly seismic zone (SZ 1). As reported in Table 6.8, for events with exceedance probability of 10% in 50 years (and soil class B-T1), the values of PGA,  $I_H$  and macroseismic intensity evaluated for Viggiano are equal to 0.29g, 87cm and VIII EMS, respectively. The building stock of Viggiano is made up of about 1,400 buildings, and  $10^6$  m<sup>3</sup> in terms of volume. Most of them (about 80% in terms of number of buildings and 56% in terms of volume) have masonry structure, while the other 20% (about 44% in terms of volume) are RC structures. As for building age, about 75% of buildings (about 52% in terms of volume) were built before 1945 (essentially masonry buildings), and only 17% (about 31% in terms of volume) after 1981 (mainly RC buildings) when the area was classified as seismic. According to the procedure described in Section 6.3.1, about 39% of volume of Viggiano buildings belongs to class “C” and 33% belongs to class “D”. The percentage of buildings with high vulnerability (class “A”) is equal to 27%, as shown in Figure 6.22.



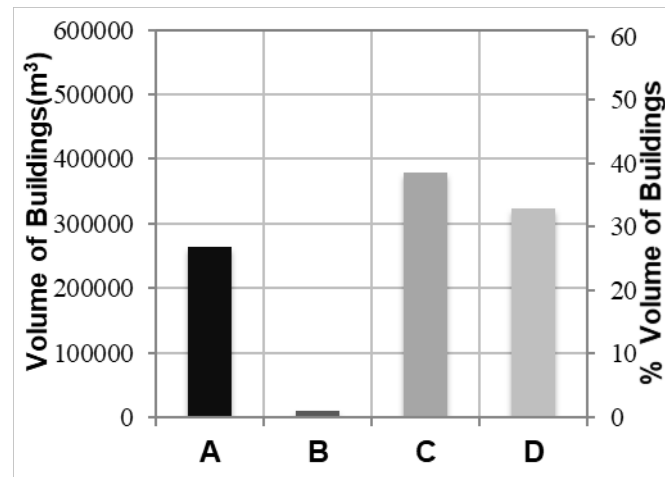


**Figure 6.22** Distribution of Viggiano building stock for each vulnerability class.

In the previous sections, expected losses for the considered scenario earthquake and strengthening costs (related to a seismic capacity able to reach at least  $NBS = 60\%$ ) have been determined for the vulnerability classes “A” and “B”. In order to perform a new damage scenario after the strengthening interventions, the vulnerability class of the retrofitted buildings (i.e., building with  $NBS = 60\%$ ) needs to be assessed. To this purpose, starting from the results obtained by Lagomarsino and Cattari (2014) on a wide set of masonry building types, the following step-by-step procedure has been set up:

- 1) according to the criteria reported in Table 6.2, the seismic vulnerability class of all 10 types considered by Lagomarsino and Cattari (2014) is assigned;
- 2) based on the fragility curves provided by Lagomarsino and Cattari (2014), the median PGA value (i.e., 50% of exceedance probability,  $PGA_{LS}$ ) is evaluated for each type with respect to Damage State 3 (Figure 6.23);
- 3) comparing the definitions of DS3 given in EMS98 and of Life Safety limit state given in EC8 and NTC-2018, DS3 is assumed as representative of a Life Safety condition;
- 4) for each vulnerability class evaluated at step 1, the mean value  $PGA_{LS,med}$  is calculated averaging the  $PGA_{LS}$  values referred to the related building types;
- 5) the ratio between  $PGA_{LS,med}$  and the value referred to the scenario event (i.e., 475y return period,  $PGA_{475y}$ ) is determined for each vulnerability class;
- 6) among all the vulnerability classes having  $PGA_{LS,med}/PGA_{475y}$  ratio values equal or greater than 0.6 (i.e. the threshold value of the strengthening intervention), the one with the lower  $PGA_{LS,med}/PGA_{475y}$  value is assumed as representative of the strengthened buildings.

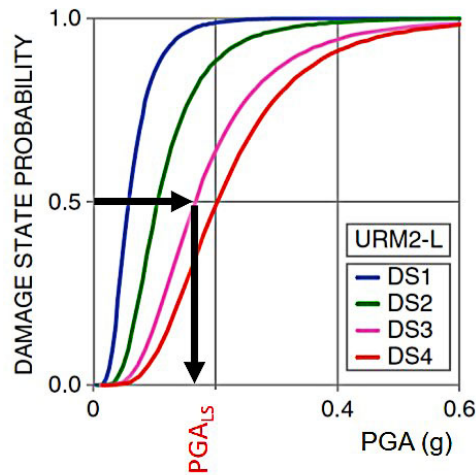


**Figure 6.23** PGA median values for Damage State 3 obtained from the fragility curves provided by Lagomarsino and Cattari (2014)

For all types considered in Lagomarsino and Cattari (2014) and described in detail in Appendix, Table 6.14 reports the corresponding vulnerability classes and  $PGA_{LS}$  values. For each vulnerability class, the mean  $PGA_{LS,med}$  value and the  $PGA_{LS,med}/PGA_{475y}$  ratio values are also reported (the  $PGA_{475y}$  value for Viggiano is equal to 0.29g). According to the above described procedure, the lower  $PGA_{LS,med}/PGA_{475y}$  value equal to 0.80 (among those equal or greater than 0.6) is referred to the vulnerability class “C”.

As a consequence, the buildings in Viggiano village having originally vulnerability class “A” or “B” after a strengthening intervention aimed at achieving at least  $NBS=60\%$  (requiring the costs estimated in Section 6.3.4) can be assigned vulnerability class “C” ( $PGA_{LS,med}/PGA_{475y} > 60\%$ ).

It is worth noting that this assumption is consistent with the results found by Di Ludovico et al. (2017b) for the L’Aquila reconstruction process. Specifically, for masonry buildings, the mean value of the capacity/demand ratio (with respect to the Life Safety limit state, SLV) after the strengthening intervention was found equal to about 70%.

Masonry building type	$V_C$	$PGA_{LS}$	$PGA_{LS,med}$	$PGA_{LS,med}/PGA_{475y}$
URM1-L	A	0.13	0.13	0.45
URM2-L	B	0.17		
URM2-M	B	0.14	0.16	0.52
URM3-M	C	0.25		
URM3-H	C	0.25		
URM3-M-IR	C	0.22		
URM3-H-IR	C	0.22	0.23	0.80
URM4-M	C	0.23		
URM4-H	C	0.23		
URM5-M	D	0.40	0.40	1.38

**Table 6.14** Vulnerability classes  $V_C$  and  $PGA_{LS}$  values for all masonry types considered by Lagomarsino and Cattari (2014). For each  $V_C$ , the mean values  $PGA_{LS,med}$  and the corresponding values of the ratio  $PGA_{LS,med}/PGA_{475y}$  (assuming  $PGA_{475y} = 0.29g$ ) are also reported

Finally, a damage scenario has been prepared considering the changes in the building vulnerability. Specifically, after the strengthening interventions, the percentage related to vulnerability class “C” increases from about 39% to 67%.

Table 6.15 summarizes the results of the new damage scenario. The unusable buildings (in terms of volume) decrease from  $3.2 \times 10^5$  to  $1.5 \times 10^5$ , while the expected casualties are in the range 0-5 instead of 20-35 (referred to the before strengthening condition). In terms of direct economic losses, the value decreases from 103 M€(before strengthening) to 55 M€(after intervention), with an economic loss reduction equal to 48 M€ which is practically coincident with the costs required for the adopted strengthening interventions (see Table 6.13).

<b>Expected loss</b>	<b>Before strengthening</b>	<b>After strengthening</b>
<i>Unusable buildings [m<sup>3</sup>]</i>	3.2E+05	1.5E+05
<i>Homeless</i>	1110	525
<i>Casualties</i>	20-35	0-5
<i>Direct economic losses (M€)</i>	103	55

**Table 6.15** Expected losses for Viggiano before and after the strengthening program

Accounting for the high number of buildings to be strengthened and the amount of the related costs, the action plan has been defined also in terms of implementation timetables. An annual financial investment equal to 5 M€ has been considered in order to reduce the seismic vulnerability of “A” and “B” classes, thus requiring a total implementation time of 10 years. This investment appears to be compatible with the amount of royalties annually assigned to Viggiano for the oil extraction activities. Indeed, in Italy, hydrocarbons deposits are public unavailable property and, consequently, private companies that produce hydrocarbons have to pay royalties to the State, the regions and the involved municipalities. From 2008 to 2018 an average value of royalties equal to about 110 M€/year was paid by Eni S.p.A and Shell Italia E&P S.p.A. to Basilicata region. In the same period, the municipality of Viggiano received an average value equal to 13 M€/year.

Figure 6.24 shows the trend of the expected direct economic losses as a function of the vulnerability reduction over ten years.

Despite the slight economic advantage deriving from the adopted strategy, it is worth highlighting the remarkable reduction in terms of both social and human losses (see Table 6.15), which appear as key elements in judging the benefits of a risk mitigation plan. Moreover, the indirect economic losses related to population assistance (Mannella et al., 2017) or business interruption (Benson and Clay, 2004) need to be strongly considered, even more in an area with a strategic role due to oil extraction.

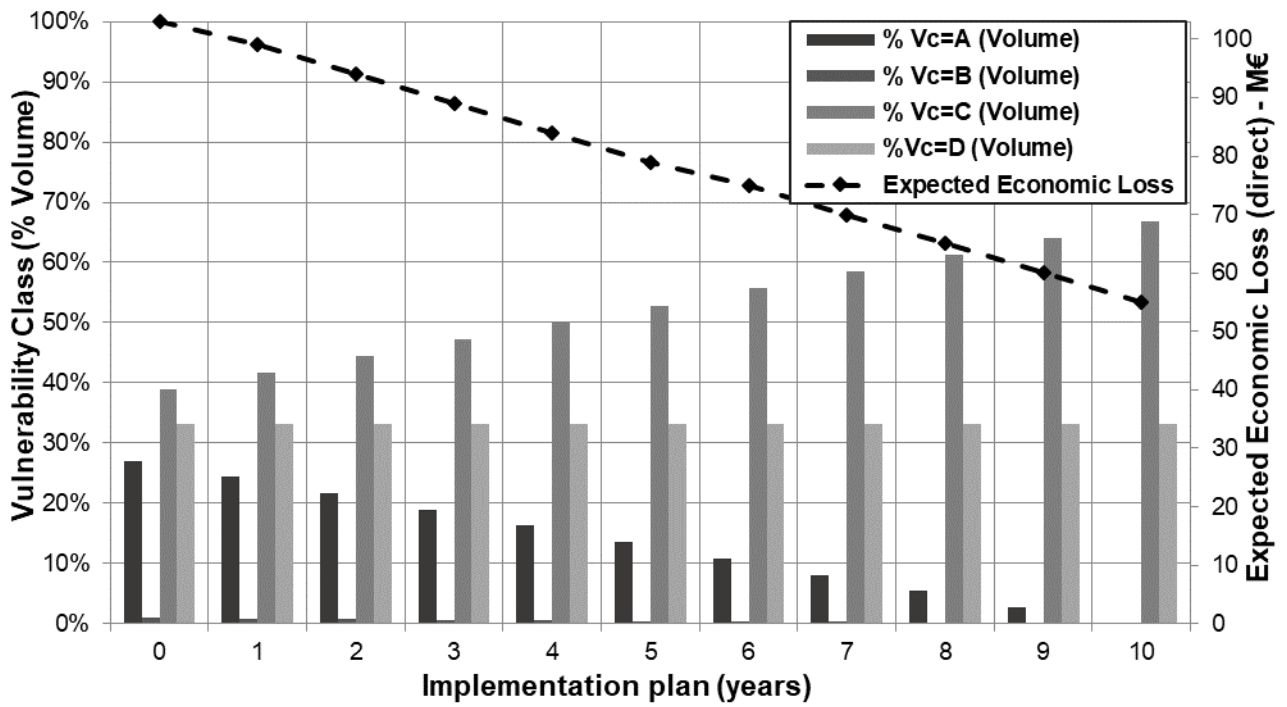


Figure 6.24 Vulnerability and economic loss reduction as a result of the action plan proposed for Viggiano.

### 6.3.6 Discussion

An earthquake damage scenario for the residential building stock of 19 villages located in the Agri valley has been prepared. A seismic event with an exceedance probability of 10% in 50 years (475 years return period) and a building vulnerability distribution based on an accurate building-by-building inventory for 18 villages and the data obtained from CARTIS and RRVS approach on Calvello village, have been considered. Heavy consequences in terms of human, social and economic losses, mainly due to masonry buildings with high and medium vulnerability (classes “A” and “B” according to EMS-98 scale), have been estimated. Specifically, about 7,500 unusable residential buildings (40% of the building stock), about 16,000 homeless (40% of the inhabitants) and 280-510 casualties have been estimated for the 19 villages. Moreover, the direct economic losses (i.e., the total repair cost) amount to about 1,130M€ A seismic risk mitigation strategy has been defined which aims to the seismic strengthening of the residential buildings with high- and medium-vulnerability (i.e., classes “A” and “B”) in order to reach a safety level essentially equivalent to a percentage of 60% of that one required by the Italian code for new buildings at the Life Safety limit state. In order to evaluate the strengthening costs, the data from the reconstruction programme after L’Aquila 2009 earthquake have been used. To this end, a methodology based on the usability ratings (and the corresponding funding classes) as a function of the vulnerability classes, has been purposely set up. An application to the village of Viggiano has been carried out to compare the expected consequences before and after the strengthening interventions. A new seismic scenario, where the vulnerability class of the strengthened buildings re-evaluated through an *ad-hoc* methodology based on studies available in the literature, has been prepared. Results show that a significant reduction of human, social and economic losses would derive from the strengthening program. Specifically, considering a total investment of 50 M€ over 10 years, the action plan defined for Viggiano village would allow about 50% reduction of the expected direct economic losses and, most importantly, a reduction of the expected number of casualties and homeless. As for the homeless reduction, it should be emphasized that applying the proposed risk mitigation plan would enable also to reduce the indirect economic losses related to population assistance and business disruption, which are generally important and even more crucial in an area with a strategic role on the Italian national energetic policy due to oil extraction. Moreover, the prevention strategy could contribute to prevent a negative phenomenon frequently detected in the aftermath of past Italian earthquakes, where a certain share of the affected population moves away from the stricken territory, also because of the long intervention times. Finally, regarding the financial backing, it is worth highlighting that Viggiano annually receives, for the oil extraction activities from deposits located in the area, an amount of royalties that could cover the entire cost of the seismic vulnerability reduction program.

## References

- ATC 2010, Here Today—Here Tomorrow: The Road to Earthquake Resilience in San Francisco: Potential Earthquake Impacts, ATC 52-2 Report, prepared for the San Francisco Department of Building Inspection by the Applied Technology Council, Redwood City, California
- Baggio C., Bernardini A., Colozza R., Corazza L., Della Bella M., Di Pasquale G., Dolce M., Goretti A., Martinelli A., Orsini G., Papa F., Zuccaro G., (2007) Field manual for post-earthquake damage and safety assessment and short term countermeasures (AeDES). In: EUR 22868 EN – Joint Research Centre – Institute for the Protection and Security of the Citizen, Artur V.P., Taucer F. (Eds.), Luxembourg: Office for Official Publications of the European Communities 2007 – 100 pp.- Eur scientific and technical research series – ISSN 1018-5593
- Bartlett J.E., Kotrlik J.W., Higgins C.C., (2001) Organizational Research: Determining Appropriate Sample Size in Survey Research. *Information Technology, Learning, and Performance Journal*, Vol. 19, No. 1, Spring 2001
- Benson C. and Clay E.J., (2004) Understanding the Economic and Financial Impacts of Natural Disasters. Disaster Risk Management series; 4. Washington, DC: World Bank. © World Bank. On line at: <https://openknowledge.worldbank.org/handle/10986/15025>
- Bommer J.J., Crowley H., Pinho R., (2015) A risk-mitigation approach to the management of induced seismicity. *Journal of Seismology*, 19(2), 623–646
- Braga F., Dolce M., Liberatore D., (1982) A statistical Study on Damaged Buildings and Ensuing Review of the MSK-76 Scale. 8th ECEE, Atene, September 1982
- Coburn A. and Spence R., (2002) Earthquake Protection, Second Edition. John Wiley & Sons, Ltd.
- Chiauzzi L., Masi A., Mucciarelli M., Vona M., Pacor F., Cultrera G., Galovic F. and Emolo A., (2012) Building damage scenarios based on exploitation of Housner intensity derived from finite faults ground motion simulations. *Bulletin of Earthquake Engineering*, 10(2), 517-545
- Chiauzzi L., Masi A., Samela C., Ventura G., (2018) Seismic risk assessment of residential buildings in Basilicata region (Southern Italy). *Structural 217 - maggio/giugno2018 - paper12* - ISSN 2282-3794 DELETTERA WP DOI 10.12917/STRU217.12 On lite at: <https://doi.org/10.12917/STRU217.12> (in Italian)
- Davies R., Foulger G., Bindley A., Styles P., (2013) Induced seismicity and hydraulic fracturing for the recovery of hydrocarbons. *Mar Pet Geol* 45:171–185
- De Martino G., Di Ludovico M., Prota A., Moroni C., Manfredi G., Dolce M., (2017) Estimation of repair costs for RC and masonry residential buildings based on damage data collected by post-earthquake visual inspection *Bull Earthquake Eng* 15:1681–1706 DOI 10.1007/s10518-016-0039-9
- Del Vecchio C., Di Ludovico M., Prota A., (2020) Repair costs of reinforced concrete building components: from actual data analysis to calibrated consequence functions. *Earthquake Spectra*, Vol. 36(1) 353–377 DOI: 10.1177/8755293019878194
- Di Ludovico M., Prota A., Moroni C., Manfredi G., Dolce M., (2017a) Reconstruction process of damaged residential buildings outside the historical centres after L’Aquila earthquake-part I: “light damage” reconstruction. *Bull Earthquake Eng*. doi:10.1007/s10518-016-9877-8
- Di Ludovico M., Prota A., Moroni C., Manfredi G., Dolce M., (2017b) Reconstruction process of damaged residential buildings outside historical centres after the L’quila earthquake-part II: “heavy damage” reconstruction. *Bull Earthquake Eng*. doi:10.1007/s10518-016-9979-3
- Di Pasquale G. and Goretti A., (2001) Economic and functional vulnerability of residential buildings stricken by Italian recent seismic events. In: 10th Anidis conference, Potenza, Italy, 9–13 September 2001 (in Italian)
- Dolce M., Masi A., Marino M., Vona M., (2003) Earthquake damage scenarios of Potenza town (Southern Italy) including site effects. *Bulletin of Earthquake Engineering* 1(1):115–140
- Dolce M., Kappos A.J., Masi A., Penelis G., Vona M., (2006) Vulnerability assessment and earthquake scenarios of the building stock of Potenza (Southern Italy) using the Italian and Greek methodologies. *Engineering Structures* 28:357–371

- Dolce M., (2010) Emergency and post-emergency management of the Abruzzi earthquake. In: 14th European conference on earthquake engineering, Ohrid, Macedonia, 3–8 September 2010, published in MGarevski, A Ansal (eds) Earthquake engineering in Europe, Springer. doi:10.1007/978-90-481-9544-2\_19
- Dolce M. and Manfredi G., (2015) “Libro bianco sulla ricostruzione privata fuori dai centri storici nei comuni colpiti dal sisma dell’Abruzzo del 6 aprile 2009”, Doppiavoce, Napoli, 153 pp. (in Italian)
- Dolce M., Speranza E., Giordano F., Borzi B., Bocchi F., Conte C., Di Meo A., Faravelli M., Pascale V. (2019) Observed damage database of past Italian earthquakes: the Da.D.O. WebGIS. Bollettino di Geofisica Teorica ed Applicata Vol. 60, DOI 10.4430/bgta0254
- DPC, (2018) National Civil Protection Department (ed), National risk assessment. Overview of the potential major disasters in Italy: seismic, volcanic, tsunami, hydro-geological/hydraulic and extreme weather, droughts and forest fire risks.
- DSG-UNMIG, Directorate-General for Safety of Mining and Energy Activities - National Mining Office for Hydrocarbons and Georesources; Ministry of Economic Development On line at: <https://unmig.mise.gov.it/>
- Eurocode 8 (EC8) Design of structures for earthquake resistance. CEN (European Committee for Standardization) EN 1998:2004
- Fico R., De Martino G., Marra A., Pecci D., Sabino A., Di Ludovico M., Mannella A., Speranza E., Prota A., Dolce M., (2019) Building aggregates of historical centers: damage analysis and preliminary remarks on reconstruction costs of the Municipalities of the Crater affected by the 2009 L’Aquila earthquake. In: XVIII Anidis conference, Ascoli Piceno, Italy, 15-19 September 2019 (in Italian)
- Galli P. and Camassi R., (2009) Report on the effects of the Aquilano earthquake of 6 April 2009. Quick Earthquake Survey Team—Final Report (in Italian). Istituto Nazionale di Geofisica e Vulcanologia. Web report available at [www.mi.ingv.it](http://www.mi.ingv.it)
- Grünthal G. (editor), (1998) European Macroseismic Scale 1998 (EMS-98). European Seismological Commission, sub commission on Engineering Seismology, working Group Macroseismic Scales. Conseil de l’Europe, Cahiers du Centre Européen de Géodynamique et de Séismologie, volume 15, Luxembourg
- ISTAT, (2011) Italian National Institute of Statistics. Italian population and housing census. On line at: [www.istat.it](http://www.istat.it)
- ISTAT (2017) Censimento generale della popolazione e delle abitazioni 31 dicembre 2017. On line at: <http://www.istat.it/>
- Jaiswal K.S, and Wald D.J., (2010) An Empirical Model for Global Earthquake Fatality Estimation Earthquake Spectra, 26(4):1017-1037
- Klose C.D., (2013) Mechanical and statistical evidence of the causality of human-made mass shifts on the Earth’s upper crust and the occurrence of earthquakes. J Seismol 17(1):109–135
- Lagomarsino S. and Cattari S., (2014) Fragility functions of masonry buildings. In: Pitilakis K., Crowley H., Kaynia A. (editors). SYNER-G: Typology definition and fragility functions for physical elements at seismic risk. Springer Science+Business Media Dordrecht, 2014.
- Locati M., Camassi R., Rovida A., Ercolani E., Bernardini F., Castelli V., Caracciolo C.H., Tertulliani A., Rossi A., Azzaro R., D’Amico S., Conte S., Rocchetti E., Antonucci A. (2019). Database Macrosismico Italiano (DBMI15), versione 2.0. Istituto Nazionale di Geofisica e Vulcanologia (INGV). <https://doi.org/10.13127/DBMI/DBMI15.2>
- Mannella A., Di Ludovico M., Sabino A., Prota A., Dolce M., Manfredi G., (2017) Analysis of the population assistance and returning home in the reconstruction process of the 2009 L’Aquila earthquake, Sustainability,9 (8), 1395.
- Masi A., Samela C., Santarsiero G., Vona M., (2007) Scenari di danno sismico per l’esercitazione nazionale di Protezione civile “Terremoto Val d’Agri 2006”, 12th ANIDIS conference, Pisa, Italy, 10-14 June 2007
- Masi A., Chiauuzzi L., Braga F., Mucciarelli M., Vona M., Ditommaso R., (2011) Peak and integral seismic parameters of L’Aquila 2009 ground motions: observed versus code provision values. Bull. Earthquake Eng., 9, 139-156.
- Masi A., Chiauuzzi L., Samela C., Tosco L., Vona M., (2014) Survey of dwelling buildings for seismic loss assessment at urban scale: the case study of 18 villages in Val D’Agri, Italy. Environmental Engineering and Management Journal, February 2014, Vol.13, No. 2, 471-486.

- Masi A., Digrisolo A., Manfredi V., (2015) Fragility curves of gravity-load designed RC buildings with regularity in plan. *Earthquakes and Structures*, Vol. 9, No. 1 (2015) 1-27
- Masi A., Santarsiero G., Digrisolo A., Chiauzzi L., Manfredi V., (2016) Procedures and experiences in the post-earthquake usability evaluation of ordinary buildings. *Bollettino di Geofisica Teorica ed Applicata* Volume 57, Issue 2, 1 June 2016, Pages199-200
- McGarr A., Simpson D., Seeber L., (2002) Case histories of induced and triggered seismicity. *International Handbook of Earthquake and Engineering Seismology*, eds. W.H.K. Lee, H. Kanamori, P.C. Jennings & C. Kisslinger, Academic Press, vol. 81A, 647–661
- MS-BAS, Microzonazione sismica dei comuni della Basilicata. Ufficio difesa del suolo del Dipartimento Infrastrutture, Opere Pubbliche e Mobilità – Regione Basilicata. Available at web site <http://microzonazione.regione.basilicata.it/Microzonazione>
- Mucciarelli et al., (2005) Progetto di monitoraggio geofisico e di amplificazione sismica di sito di aree vulnerabili del territorio regionale. Convenzione tra Regione Basilicata e Università della Basilicata. On line at: <http://www.crisbasilicata.it/microzonazione/home.html>
- NTC18 (2018), D.M. 17 gennaio 2018 - Norme tecniche per le costruzioni. Ministero delle Infrastrutture.
- OPCM 3274, (2003) Ordinanza del Consiglio dei Ministri n. 3274. Primi elementi in materia di criteri generali per la classificazione sismica del territorio nazionale e di normative tecniche per le costruzioni in zona sismica. GU n. 72 giugno 2003. Available at web site <http://www.cslp.it>
- OPCM, 3519 (28/04/2006) Ordinanza del Consiglio dei Ministri n. 3519. Criteri generali per l'individuazione delle zone sismiche e per la formazione e l'aggiornamento degli elenchi delle medesime zone. GU n.108 11/05/2006). Available at web site <http://www.cslp.it>
- Rovida A., Locati M., Camassi R., Lolli B., Gasperini P. (2019). Catalogo Parametrico dei Terremoti Italiani (CPTI15), versione 2.0. Istituto Nazionale di Geofisica e Vulcanologia (INGV). <https://doi.org/10.13127/CPTI/CPTI15.2>
- SM Working Group (2015) Guidelines for Seismic Microzonation, Conference of Regions and Autonomous Provinces of Italy-Civil Protection Department, Rome. Eds: Bramerini F., Castenetto S., Naso G. On line at:[http://www.protezionecivile.gov.it/httpdocs/cms/attach\\_extra/GuidelinesForSeismicMicrozonation.pdf](http://www.protezionecivile.gov.it/httpdocs/cms/attach_extra/GuidelinesForSeismicMicrozonation.pdf)
- So E., Spence R., (2013) “Estimating shaking-induced casualties and building damage for global earthquake events: a proposed modelling approach,” *Bulletin of Earthquake Engineering*, 11, 347-363
- Tertulliani A., Arcoraci L., Berardi M., Bernardini F., Camassi R., Castellano C., Del Mese S., Ercolani M., Graziani L., Leschiutta I., Rossi A., Vecchi M., (2010) An application of EMS 98 in a medium size city: the case of L’Aquila (Italy) after the April 6, 2009 Mw 6.3 earthquake. *Bull Earthq Eng*. doi:10.1007/s10518-010-9188-4
- Yakut A., Sucuoğlu H., Akkar, S., (2012) Seismic risk prioritization of residential buildings in Istanbul. *Earthquake Engineering and Structural Dynamics* 41:11, 1533-1547
- Zuccaro, G., Cacace, F., (2011) Seismic Casualty Evaluation: The Italian Model, an Application to the L’Aquila 2009 Event. In R Spence, E So, & C Scawthorn, *Human Casualties in Earthquakes Progress in Modelling and Mitigation* (pp. 171-184), Springer.



## CHAPTER VII

### Final remarks and future developments

The estimation of expected losses due to future earthquakes and the definition of sustainable risk reduction plans are crucial for medium-long term seismic mitigation strategies. The biggest challenge of the scientific community is represented by the availability and reliability of analysis tools able to provide a variety of information on future seismic events and their impact on the urban systems. In this framework, innovative methods aimed at supporting seismic risk assessment and reduction have been proposed in the present PhD thesis. Particular focus has been dedicated to the definition of the seismic hazard, the characterization of the building exposure and the estimation of the seismic losses. Firstly, after a literature review of the main approaches to estimate the expected consequences due to future earthquakes, a new model aimed at estimating the direct economic losses (i.e., building repair costs) has been proposed. In order to better represent the seismic behavior of buildings with different structural characteristics, the proposed model allows to explicitly consider both damage severity (i.e., maximum damage level) and damage extension (i.e., distribution along the building height). Specifically, the model has been implemented for existing Reinforced Concrete (RC) building types, by performing an extensive campaign of Non-Linear Dynamic Analyses (NLDAs) to determine the expected damage distributions across the building based on a correlation function between seismic response (i.e., interstorey drift) and damage levels according to the EMS-98 scale.

Subsequently, correlations between macroseismic intensity scales and ground motion parameters have been derived based on a database containing 179 ground-motion records related to 32 earthquake events occurred in Italy in the last 40 years. Peak Ground Acceleration (PGA), Peak Ground Velocity (PGV) and Housner Intensity ( $I_H$ ) as instrumental measures, and European Macroseismic Scale (EMS-98) and Mercalli-Cancani-Sieberg (MCS) as macroseismic measures, have been considered.

With respect to other relationships available in the literature, reversible correlations (i.e., instrumental vs macroseismic intensity and vice versa) have been provided considering both peak (i.e., PGA and PGV) and integral (i.e.,  $I_H$ ) intensity measures and both macroseismic scales, MCS (adopted in Italy) and EMS-98 (used in all European countries). The relationships can be used to both adopt empirical damage estimation methods (e.g., Damage Probability Matrices) and convert the macroseismic data of historical earthquakes into instrumental intensity measures more suitable to risk analyses and design practice.

Concerning the characterization of exposure component, two approaches aimed at describing residential building inventories have been proposed. Firstly, an innovative methodology has been developed to convert the information on the typological characteristics collected through the post-

earthquake survey form (AeDES, used currently in Italy), into recognized international standard formats. The first step of the proposed approach entails the description of the information on the typological characteristics in terms of the faceted taxonomic description proposed by Global Earthquake Model (GEM). This allows to define the exposure information in terms of a taxonomy independent from the vulnerability component and that could be also employed for the consideration of multi-hazard modelling approaches. In a following step, a methodology based on the concept of fuzzy compatibility score has been employed in order to assign to each inspected building a risk-oriented class (i.e., the EMS-98 typologies). Through this step, a model in terms of risk-oriented classes associated to specific fragility models can be obtained and used for large-scale risk assessments. The fuzzy formulation helps mitigating the impact of subjective, expert-based judgment to the class assignment and provides a transparent and sound characterization of the underlying uncertainties, by ensuring the reproducibility of the results.

Furthermore, an approach based on the integration of data collected with the CARTIS procedure (a protocol used in Italy for the typological-structural characterization of buildings at regional scale) and using the RRVS web-based platform (i.e., for a remote visual screening based on satellite images) has been proposed and exemplified in the village of Calvello (Basilicata region, Southern Italy).

The obtained results show that the proposed approach allows to realize an inventory of typological features of residential buildings more efficiently (both in terms of time and resources) with respect to conventional building-by-building surveys and providing significantly better data than the housing census. Such methodology would prove particularly useful tool for large-area assessment, especially in data-poor and economically developing countries.

Within the applications described in this PhD thesis, a comparative analysis of different Casualty Estimation Models (CEMs) available in literature has been carried out in the L'Aquila urban area using the 2009 earthquake data. The findings highlight how the casualty estimation can be significantly influenced by the different parameters associated to the considered CEMs (e.g., damage levels, occupancy rate, building classification).

Subsequently, an exposure model has been implemented in terms of GEM taxonomy and EMS-98 building types, basing on the 2009 L'Aquila post-earthquake data available in the Observed Damage Database (Da.D.O.) platform. The resulting model has been validated based on observed damage data from the same platform and the macroseismic intensity values officially estimated by the National Institute of Geophysics and Volcanology (INGV). Albeit limited to a single-event dataset, with relatively homogeneous building typologies (mainly masonry structures), the results underline the great potential of the proposed methodology to thoroughly exploit the data surveyed after the

earthquakes occurred in Italy over the last 50 years and harmonized in the Da.D.O. platform, and provide relevant information for large-scale seismic risk assessments.

As last application, earthquake damage scenarios have been prepared for the residential building stock of 19 different villages located in the Agri valley, a part of the Basilicata region (Southern Italy) particularly important for its oil extraction activities. Considering a seismic event with an exceedance probability of 10% in 50 years (i.e., 475 years return period) and a vulnerability distribution based on an accurate building-by-building inventory and information collected with CARTIS and RRVS approaches on Calvello village, significant expected consequences in terms of human, social and economic losses have been estimated. Based on these findings, an action plan for the seismic risk mitigation based on the reduction of vulnerability of residential buildings through a structural strengthening program has been proposed and applied to the village of Viggiano. The results show that a significant reduction of losses would derive from the proposed retrofit program and the related costs could be largely compensated by the incoming royalties from oil extraction activities. Although this preliminary application focused on a small village, the proposed strategy can be extended to larger areas.

While the specific results have been reported in the discussion of each chapter, it is worth emphasizing once more that the proposed methodologies can be very useful in the scope of seismic risk assessment and reduction. However, several aspects should be further explored and improved, as described in the following overview of future developments.

Regarding the estimation of the direct economic losses, the methodology should be extended to other building types (e.g., masonry) also by considering different methods to determine the damage distributions while further studies related to the storey repair cost estimation are necessary.

In order to improve the methodology based on the concept of fuzzy compatibility score and further explore the impact of subjective judgment in the class assignment, a participatory review of the class definition schema could be carried out with the collaboration of a panel of experts. Furthermore, a more detailed geospatial analysis of the resulting exposure information could provide better insights for optimizing the sampling and selection procedure during the survey and seeking a trade-off between data quality, coverage and completeness and the available resources.

Finally, in the framework of seismic risk assessment and mitigation of Val d'Agri area, some aspects need to be better addressed, such as the definition of the strengthening costs, the consideration of the uncertainties in the risk components and the evaluation of site effects. As for the latter, microzonation studies for all the villages under study will be available in the near future and therefore could be employed for a more reliable estimation of potential site amplification.

# APPENDIX

## CHAPTER IV

**Table 4A** Macroseismic and instrumental data of the considered events

<i>Data</i>	<i>Epicentral area</i>	<i>Station name</i>	<i>Village</i>	<i>Instrumental parameters</i>			<i>Macroseismic intensity</i>	
				<i>I<sub>H</sub></i> <i>(m)</i>	<i>PGA</i> <i>(g)</i>	<i>PGV</i> <i>(cm/s)</i>	<i>EMS-98</i>	<i>MCS</i>
1980/11/23	Irpinia	ARN	Arienzo	0.13	0.035	3.15	6 <sup>(1)</sup>	6.5 <sup>(1)</sup>
		BRN	Brienza	0.43	0.218	12.68	6.5 <sup>(1)</sup>	7 <sup>(1)</sup>
		BSC	Bisaccia	0.78	0.096	21.44	6 <sup>(1)</sup>	6.5 <sup>(1)</sup>
		BVN	Bovino	0.14	0.048	6.34	5 <sup>(1)</sup>	6 <sup>(1)</sup>
		CLT	Calitri	1.17	0.175	29.06	7.5 <sup>(1)</sup>	8 <sup>(1)</sup>
		MRT	M. San Severino	0.45	0.141	13.29	6.5 <sup>(1)</sup>	7.5 <sup>(1)</sup>
		RNR	Rionero in vulture	0.57	0.099	15.01	7 <sup>(1)</sup>	7.5 <sup>(1)</sup>
		STR	Sturno	1.73	0.316	70.31	7.5 <sup>(1)</sup>	8 <sup>(1)</sup>
		TDG	Torre del greco	0.25	0.060	8.06	5.5 <sup>(1)</sup>	6 <sup>(1)</sup>
		TRR	Tricarico	0.30	0.046	6.58	5.5 <sup>(1)</sup>	6 <sup>(1)</sup>
		BGI	Bagnoli Irpino	1.21	0.187	34.42	7 <sup>(1)</sup>	7 <sup>(1)</sup>
		ALT	Auletta	0.22	0.057	6.28	6 <sup>(1)</sup>	6.5 <sup>(1)</sup>
		BNV	Benevento	0.42	0.046	9.29	6 <sup>(1)</sup>	6 <sup>(1)</sup>
1983/11/09	Parma	FRN	Fornovo di T.	0.05	0.034	1.59	6 <sup>(1)</sup>	6 <sup>(1)</sup>
1984/04/29	Gubbio	PTL	Pietralunga	0.21	0.178	7.96	6 <sup>(1)</sup>	6 <sup>(1)</sup>
		UMB	Umbertide	0.03	0.032	1.13	6 <sup>(1)</sup>	6 <sup>(1)</sup>
		PGL	Peglio	0.04	0.052	2.19	5 <sup>(1)</sup>	5 <sup>(1)</sup>
		CTC	Città di Castello	0.16	0.050	3.59	5 <sup>(1)</sup>	5.5 <sup>(1)</sup>
		CGL	Cagli	0.01	0.007	0.53	5 <sup>(1)</sup>	5 <sup>(1)</sup>
		NCR	Nocera Umbra	0.09	0.204	5.90	6 <sup>(1)</sup>	6 <sup>(1)</sup>
1984/05/07	Lazio-Abruzzo	ATN	Atina	0.15	0.112	3.78	7 <sup>(1)</sup>	7 <sup>(1)</sup>
		PNT	Pontecorvo	0.15	0.068	5.63	5 <sup>(1)</sup>	5 <sup>(1)</sup>
		RCC	Roccamonfina	0.15	0.044	4.40	6 <sup>(1)</sup>	6 <sup>(1)</sup>
		ORT	Ortucchio	0.11	0.087	4.05	5 <sup>(1)</sup>	5 <sup>(1)</sup>
		BRS	Barisciano	0.01	0.013	0.41	4.5 <sup>(1)</sup>	4.5 <sup>(1)</sup>
		CSV	Castelnuovo	0.07	0.028	1.82	5 <sup>(1)</sup>	5 <sup>(1)</sup>
		LPD1	Lama dei pel.	0.15	0.077	5.23	6 <sup>(1)</sup>	6 <sup>(1)</sup>
		SCF	Scafa	0.26	0.133	10.05	6 <sup>(1)</sup>	6.5 <sup>(1)</sup>
		PGG	Poggio Picenze	0.03	0.017	0.76	5 <sup>(1)</sup>	5 <sup>(1)</sup>
		RIP	Ripa Fagn.	0.04	0.017	0.99	5 <sup>(1)</sup>	5 <sup>(1)</sup>
1984/05/11	Lazio-Abruzzo	VLB	V. Barrea	0.24	0.201	8.48	6 <sup>(1)</sup>	6.5 <sup>(1)</sup>
		ATN	Atina	0.04	0.025	1.20	6 <sup>(1)</sup>	6 <sup>(1)</sup>
		LPD1	Lama dei pel.	0.04	0.042	1.63	5.5 <sup>(1)</sup>	5.5 <sup>(1)</sup>
		SCF	Scafa	0.05	0.040	1.99	5 <sup>(1)</sup>	5 <sup>(1)</sup>

Appendix

1985/01/23	Garfagnana	VGL	Vagli paese	0.02	0.031	1.23	4 <sup>(1)</sup>	4 <sup>(1)</sup>
		SST	Sestola	0.02	0.031	1.18	5 <sup>(1)</sup>	5 <sup>(1)</sup>
		BRG	Barga	0.03	0.043	1.12	5 <sup>(1)</sup>	5.5 <sup>(1)</sup>
1985/05/20	L' Aquila	BRS	Barisciano	0.04	0.033	1.59	5 <sup>(1)</sup>	5.5 <sup>(1)</sup>
		CSV	Castelnuovo	0.02	0.050	1.17	5 <sup>(1)</sup>	5 <sup>(1)</sup>
		PGG	Poggio Pic.	0.04	0.050	2.21	6 <sup>(1)</sup>	6 <sup>(1)</sup>
		SDM	S. Dometrio V.	0.02	0.020	1.20	4 <sup>(1)</sup>	4 <sup>(1)</sup>
1987/04/24	Reggio Emilia	SRB	Sorbolo	0.01	0.013	0.34	5 <sup>(1)</sup>	5 <sup>(1)</sup>
		NVL	Novellara	0.04	0.039	2.26	5 <sup>(1)</sup>	5 <sup>(1)</sup>
1987/05/02	Reggio Emilia	SRB	Sorbolo	0.01	0.037	1.11	5 <sup>(1)</sup>	5.5 <sup>(1)</sup>
		NVL	Novellara	0.15	0.077	7.24	5 <sup>(1)</sup>	5 <sup>(1)</sup>
1997/09/26	Umbria-Marche	CLF	Colfiorito	0.74	0.227	17.05	7.5 <sup>(2)</sup>	7.5 <sup>(2)</sup>
		NCR	Nocera-Umbra	0.79	0.502	32.57	7 <sup>(2)</sup>	7.5 <sup>(2)</sup>
		ASS	Assisi	0.23	0.188	10.22	/	6.5 <sup>(2)</sup>
		CSA	Cannara	0.60	0.172	13.41	/	6.5 <sup>(2)</sup>
		MTL	Matelica	0.27	0.116	8.35	/	6 <sup>(2)</sup>
		GBP	Gubbio (GBP)	0.94	0.098	18.06	/	6 <sup>(2)</sup>
		GBB	Gubbio (GBB)	0.09	0.083	2.87	/	6 <sup>(2)</sup>
		BVG	Bevagna	0.31	0.079	8.95	/	6.5 <sup>(2)</sup>
		PGL	Peglio	0.08	0.069	2.63	/	6 <sup>(2)</sup>
		SNG	Senigallia	0.14	0.045	3.85	/	5.5 <sup>(2)</sup>
		LNS	Leonessa	0.04	0.033	1.30	/	5.5 <sup>(2)</sup>
		FHC	Arquata del Tronto	0.03	0.033	1.14	/	5.5 <sup>(2)</sup>
		CSC	Cascia	0.05	0.022	1.39	/	5.5 <sup>(2)</sup>
		CGL	Cagli	0.03	0.020	1.26	/	6 <sup>(2)</sup>
		RTI	Rieti	0.10	0.019	1.80	/	5.5 <sup>(2)</sup>
		PNN	Pennabilli	0.05	0.015	1.08	/	5.5 <sup>(2)</sup>
		AQG	L' Aquila (AQG)	0.02	0.007	0.39	/	5.5 <sup>(2)</sup>
		AQK	L' Aquila (AQK)	0.03	0.004	0.62	/	5.5 <sup>(2)</sup>
		AQI	L' Aquila (AQI)	0.03	0.004	0.65	/	5.5 <sup>(2)</sup>
		1998/09/09	Basilicata	GRM	Grumento	0.12	0.041	2.98
LRG	Lauria-Galdo			0.28	0.242	11.72	6 <sup>(3)</sup>	6 <sup>(3)</sup>
LRS	Lauria San Giovanni			0.30	0.165	12.52	6 <sup>(3)</sup>	6 <sup>(3)</sup>
SCL	Scalea			0.22	0.044	5.03	5 <sup>(3)</sup>	5 <sup>(3)</sup>
VGG	Viggianello			0.15	0.073	3.81	5.5 <sup>(3)</sup>	6 <sup>(3)</sup>
2002/09/06	Palermo	CDI	Castel di Iudica	0.02	0.005	0.49	4 <sup>(4)</sup>	4 <sup>(4)</sup>
		CLG	Caltagirone	0.02	0.007	0.55	4 <sup>(4)</sup>	4 <sup>(4)</sup>
		PTT	Patti	0.05	0.010	1.12	4.5 <sup>(4)</sup>	4.5 <sup>(4)</sup>
2003/01/26	Forlì	STS	Santa Sofia	0.04	0.095	2.46	/	6 <sup>(5)</sup>

Appendix

2003/09/14	Appennino Bolognese	FRE	Firenzuola	0.04	0.026	1.47	5 <sup>(6)</sup>	5.5 <sup>(7)</sup>
		BSZ	Borgo San Lorenzo	0.02	0.010	0.60	4.5 <sup>(6)</sup>	5 <sup>(6)</sup>
		FAZ	Faenza	0.02	0.008	0.60	4.5 <sup>(6)</sup>	4.5 <sup>(6)</sup>
		BRB	Barberino di Mugello	0.02	0.007	0.39	5 <sup>(6)</sup>	5 <sup>(6)</sup>
2004/11/24	Lago di Garda	GVD	Gavardo	0.06	0.073	3.29	/	5.5 <sup>(7)</sup>
2008/01/03	Mugello	FRE	Firenzuola	0.06	0.048	2.90	/	4.5 <sup>(8)</sup>
		BSZ	Borgo San Lorenzo	0.01	0.019	0.43	/	5 <sup>(8)</sup>
		BRB	Barberino di Mugello	0.02	0.015	0.80	/	5 <sup>(8)</sup>
2008/12/23	Emilia Romagna	AUL	Aulla	0.03	0.022	1.44	/	5 <sup>(9)</sup>
		PNM	Pontremoli	0.02	0.015	0.67	/	5 <sup>(9)</sup>
		SSU	Sassuolo	0.02	0.012	0.53	/	4.5 <sup>(9)</sup>
		MDN	Modena	0.03	0.012	0.80	/	4.5 <sup>(9)</sup>
		MIL	Milano	0.01	0.005	0.33	/	4.5 <sup>(9)</sup>
		GNV	Genova	0.01	0.003	0.29	/	4 <sup>(9)</sup>
		LSP	La Spezia	0.005	0.002	0.16	/	4 <sup>(9)</sup>
2009/04/06	L' Aquila	AQV	L' Aquila (AQV)	1.32	0.657	42.66	8.5 <sup>(10)</sup>	9 <sup>(11)</sup>
		AQG	L' Aquila (AQG)	1.15	0.489	35.72	8.5 <sup>(10)</sup>	9 <sup>(11)</sup>
		AQA	L' Aquila (AQA)	0.89	0.444	31.85	8.5 <sup>(10)</sup>	9 <sup>(11)</sup>
		AQK	L' Aquila (AQK)	1.42	0.362	35.77	8.5 <sup>(10)</sup>	9 <sup>(11)</sup>
		CLN	Celano	0.22	0.090	7.04	/	5.5 <sup>(11)</sup>
		AVZ	Avezzano	0.47	0.069	11.29	/	5 <sup>(11)</sup>
		MTR	Monte reale	0.15	0.063	3.54	/	5 <sup>(11)</sup>
		FMG	Fiamignano	0.10	0.027	2.58	/	5.5 <sup>(11)</sup>
		ANT	Antrodoco	0.10	0.026	2.47	/	5 <sup>(11)</sup>
		SUL	Sulmona	0.13	0.034	3.65	/	5 <sup>(11)</sup>
CHT	Chieti	0.30	0.030	7.87	/	5 <sup>(11)</sup>		
2009/12/15	Valle del Tevere	PRG	Perugia	0.01	0.007	0.25	4 <sup>(12)</sup>	/
2011/06/24	Sicilia	NAS	Naso	0.02	0.037	1.05	4 <sup>(13)</sup>	/
		TOR	Tortorici	0.03	0.034	1.36	5 <sup>(13)</sup>	/
		PTT	Patti	0.03	0.021	1.29	4 <sup>(13)</sup>	/
		BCL	Barcellona P. Gotto	0.01	0.006	0.25	4 <sup>(13)</sup>	/
		MZZ	Milazzo	0.00	0.004	0.18	4 <sup>(13)</sup>	/
		GSM	Gioiosa Marea	0.01	0.004	0.19	4.5 <sup>(13)</sup>	/
		NSA	Nicosia	0.01	0.003	0.25	4 <sup>(13)</sup>	/
2011/07/17	Pianura Padana	MRN	Mirandola	0.03	0.026	0.93	4 <sup>(14)</sup>	/
2011/07/25	Torino	SUS	Susa	0.00	0.057	0.52	4 <sup>(15)</sup>	/
		PNR	Pinerolo	0.01	0.022	0.53	5 <sup>(15)</sup>	/
		SLZ	Saluzzo	0.00	0.003	0.10	4 <sup>(15)</sup>	/

Appendix

2012/01/25	Pianura Padana	SRP	Sorbolo	0.15	0.117	7.02	5.5 <sup>(16)</sup>	6 <sup>(16)</sup>		
		NVL	Novellara	0.09	0.074	3.75	4.5 <sup>(16)</sup>	4.5 <sup>(16)</sup>		
		PAR	Parma	0.02	0.027	0.89	5 <sup>(16)</sup>	5.5 <sup>(16)</sup>		
		BRR	Berceto	0.01	0.011	0.64	4.5 <sup>(16)</sup>	4.5 <sup>(16)</sup>		
2012/05/20	Emilia	MRN	Mirandola	1.58	0.303	46.31	6.5 <sup>(17)</sup>	6.5 <sup>(17)</sup>		
2012/05/29	Emilia	MRN.	Mirandola	1.86	0.857	57.49	7.5 <sup>(17)</sup>	7.5 <sup>(17)</sup>		
		CNT	Cento	0.64	0.300	16.87	6 <sup>(17)</sup>	6 <sup>(17)</sup>		
		MOG0	Moglia	0.95	0.240	26.58	7.5 <sup>(17)</sup>	7.5 <sup>(17)</sup>		
		T0814	Carpi	0.86	0.505	23.64	6 <sup>(17)</sup>	6 <sup>(17)</sup>		
		SAN0	San Felice sul Panaro	1.18	0.314	35.24	7 <sup>(17)</sup>	7 <sup>(17)</sup>		
		T0818	Concordia sulla Secchia	1.25	0.280	39.25	7.5 <sup>(17)</sup>	7.5 <sup>(17)</sup>		
		RAV0	Crevalcore	0.31	0.084	9.76	6.5 <sup>(17)</sup>	6.5 <sup>(17)</sup>		
		SAG0	Sant' Agostino	0.27	0.081	7.73	6 <sup>(17)</sup>	6 <sup>(17)</sup>		
		BON0	Bondeno	0.08	0.036	2.89	6 <sup>(17)</sup>	6 <sup>(17)</sup>		
		FIN0	Finale Emilia	0.50	0.239	17.55	7 <sup>(17)</sup>	7 <sup>(17)</sup>		
		2012/10/26	Pollino	0PAP	Papasidero	0.23	0.239	11.64	5 <sup>(18)</sup>	5 <sup>(18)</sup>
				MRM	Mormanno	0.31	0.186	11.24	6 <sup>(18)</sup>	6 <sup>(18)</sup>
				0MOR	Morano Calabro	0.19	0.179	8.42	5 <sup>(18)</sup>	5 <sup>(18)</sup>
VGG	Viggianello			0.17	0.126	5.17	5 <sup>(18)</sup>	5 <sup>(18)</sup>		
0LAI	Laino Borgo			0.13	0.116	5.95	5.5 <sup>(18)</sup>	5.5 <sup>(18)</sup>		
ORS	Orsomarso			0.06	0.072	2.34	5 <sup>(18)</sup>	5 <sup>(18)</sup>		
PRA	Praia a Mare			0.05	0.049	1.96	4.5 <sup>(18)</sup>	4.5 <sup>(18)</sup>		
CVL	Castrovillari			0.05	0.047	1.35	5 <sup>(18)</sup>	5 <sup>(18)</sup>		
LRG	Lauria			0.04	0.037	1.62	4.5 <sup>(18)</sup>	4.5 <sup>(18)</sup>		
SCL	Scalea			0.13	0.033	2.50	4 <sup>(18)</sup>	4 <sup>(18)</sup>		
SDN	San Donato di Ninea			0.03	0.020	0.89	4 <sup>(18)</sup>	4 <sup>(18)</sup>		
0FRA	Frascineto			0.06	0.017	1.50	4 <sup>(18)</sup>	4 <sup>(18)</sup>		
LTR	Latronico			0.05	0.012	1.14	4 <sup>(18)</sup>	4 <sup>(18)</sup>		
2013/06/21	Fivizzano			FVZ	Fivizzano	0.16	0.232	6.58	5 <sup>(19)</sup>	5.5 <sup>(19)</sup>
				PZS	Piazza al Serchio	0.12	0.090	4.81	5 <sup>(19)</sup>	5 <sup>(19)</sup>
2016/02/08	Monti Iblei	PLZ	Palazzolo Acreide	0.01	0.025	0.51	4.5 <sup>(20)</sup>	/		
		NTE	Noto	0.01	0.005	0.16	4 <sup>(20)</sup>	/		
		ISI	Ispica	0.00	0.005	0.19	4 <sup>(20)</sup>	/		
		VZZ	Vizzini	0.01	0.017	0.51	4 <sup>(20)</sup>	/		
		SRT	Sortino	0.01	0.016	0.62	4 <sup>(20)</sup>	/		
		VTT	Vittoria	0.01	0.006	0.20	4 <sup>(20)</sup>	/		
		SCR	Santa Croce Camerina	0.00	0.003	0.10	4 <sup>(20)</sup>	/		
		LNT	Lentini	0.00	0.004	0.17	4 <sup>(20)</sup>	/		
		SRC	Siracusa	0.00	0.002	0.10	4 <sup>(20)</sup>	/		

Appendix

2016/08/24	Accumoli	AMT	Amatrice	1.10	0.878	45.01	10 <sup>(21)</sup>	10.5 <sup>(22)</sup>
		RQT	Arquata del Tronto	0.29	0.424	15.03	8.5 <sup>(21)</sup>	8.5 <sup>(22)</sup>
		PCB	Poggio Cancelli	0.42	0.309	13.30	5 <sup>(21)</sup>	/
		CSC	Cascia	0.19	0.106	5.56	/	5 <sup>(22)</sup>
		MTR	Monte Reale	0.40	0.090	9.70	5.5 <sup>(21)</sup>	6 <sup>(22)</sup>
		LSS	Leonessa	0.06	0.020	2.15	5 <sup>(21)</sup>	5 <sup>(22)</sup>
		SNO	Sarnano	0.16	0.092	6.02	5.5 <sup>(21)</sup>	5 <sup>(22)</sup>
		ASP	Ascoli Piceno	0.10	0.088	2.92	5 <sup>(21)</sup>	5 <sup>(22)</sup>
		ANT	Antrodoco	0.14	0.022	3.18	/	5 <sup>(22)</sup>
		PZI	Pizzoli	0.22	0.051	5.26	/	5 <sup>(22)</sup>
		TLN	Tolentino	0.30	0.120	6.35	/	5 <sup>(22)</sup>
2016/10/26	Ussita	CNE	Castel Santangelo sul Nera	0.97	0.556	37.29	8 <sup>(23)</sup>	8 <sup>(23)</sup>
		PRE	Preci	0.26	0.262	10.22	7 <sup>(23)</sup>	6.5 <sup>(23)</sup>
		CLO	Castelluccio	0.54	0.220	13.42	6.5 <sup>(23)</sup>	6 <sup>(23)</sup>
		FOC	Foligno Colfiorito	0.31	0.613	20.13	5 <sup>(23)</sup>	5 <sup>(23)</sup>
2016/10/30	Norcia	NOR	Norcia (NOR)	2.53	0.320	54.13	8.5 <sup>(23)</sup>	8.5 <sup>(23)</sup>
		NRC	Norcia (NRC)	2.05	0.447	46.14	8.5 <sup>(23)</sup>	8.5 <sup>(23)</sup>
		CNE	Castel Santangelo sul Nera	1.28	0.500	43.01	9 <sup>(23)</sup>	9 <sup>(23)</sup>
		PRE	Preci	0.48	0.324	16.31	7.5 <sup>(23)</sup>	7.5 <sup>(23)</sup>
		CSC	Cascia	0.37	0.165	11.95	6.5 <sup>(23)</sup>	6.5 <sup>(23)</sup>
		FOC	Foligno Colfiorito	0.28	0.382	12.43	5 <sup>(23)</sup>	5.5 <sup>(23)</sup>
		SNO	Sarnano	0.21	0.121	6.72	5 <sup>(23)</sup>	5.5 <sup>(23)</sup>
2017/01/18	Capitignano	TLN	Tolentino	0.31	0.120	7.62	7 <sup>(23)</sup>	7 <sup>(23)</sup>
		MSC	Mascioni (MSC)	0.32	0.241	13.89	5 <sup>(24)</sup>	5.5 <sup>(24)</sup>
		MSCT	Mascioni (MSCT)	0.34	0.253	14.45	5 <sup>(24)</sup>	5.5 <sup>(24)</sup>
		PCB	Poggio Cancelli	0.49	0.566	22.37	7 <sup>(24)</sup>	7.5 <sup>(24)</sup>
		PZI	Pizzoli	0.13	0.105	5.07	5 <sup>(24)</sup>	5.5 <sup>(24)</sup>
		TER	Teramo	0.08	0.090	2.50	5.5 <sup>(24)</sup>	5.5 <sup>(24)</sup>
ASP	Ascoli Piceno	0.08	0.105	2.84	5.5 <sup>(24)</sup>	5.5 <sup>(24)</sup>		

<sup>(1)</sup>Margottini et al., 1992; <sup>(2)</sup>Stucchi et al., 1998; <sup>(3)</sup>Galli et al., 2001; <sup>(4)</sup>Azzaro et al., 2004; <sup>(5)</sup>Camassi et al., 2003a; <sup>(6)</sup>Camassi et al., 2003b; <sup>(7)</sup>Gruppo di Lavoro INGV, 2004; <sup>(8)</sup>Camassi et al., 2008; <sup>(9)</sup>Camassi et al., 2009; <sup>(10)</sup>Tertulliani et al., 2010; <sup>(11)</sup>Galli and Camassi, 2009; <sup>(12)</sup>Arcoraci et al., 2009; <sup>(13)</sup>Azzaro et al., 2011; <sup>(14)</sup>Bernardini et al., 2011a; <sup>(15)</sup>Bernardini et al., 2011b; <sup>(16)</sup>Arcoraci et al., 2012a; <sup>(17)</sup>Arcoraci et al., 2012b; <sup>(18)</sup>Azzaro et al., 2012; <sup>(19)</sup>Arcoraci et al., 2013; <sup>(20)</sup>Azzaro et al., 2016; <sup>(21)</sup>Tertulliani et al., 2016a; <sup>(22)</sup>Galli et al., 2016; <sup>(23)</sup>Tertulliani et al., 2016b; <sup>(24)</sup>Tertulliani et al., 2017



## CHAPTER V

**Table 5A** Attribute values in terms of AeDES form and GEM taxonomy related to building position

AeDES form	GEM taxonomy
AeDES section	GEM attribute
Building Identification	Building Position within a Block
AeDES attribute	GEM attribute level
Building position	<i>POSITION</i>
Isolated	BPD
Internal	BP3
Extreme	BP1
Corner	BP2
Not surveyed	BP99

**Table 5B** Attribute values in terms of AeDES form and GEM taxonomy related to building use

AeDES form	GEM taxonomy	
AeDES section	GEM attribute	
Building Description	Occupancy	
AeDES attribute	GEM attribute level	
Use	<i>Level1: OCCUPCY</i>	<i>Level2: OCCUPCY_DT</i>
Residential	RES	RES99
Production	AGR	AGR99
Business	COM	COM99
Offices	COM	COM3
Public services	COM	COM6
Warehouse	COM	COM2
Strategic services	GOV	GOV99
Not surveyed	OC99	-

**Table 5C** Attribute values in terms of AeDES form and GEM taxonomy related to masonry buildings

AeDES form	GEM taxonomy					
AeDES section	GEM attribute					
Building Typology	Material of the Lateral Load Resisting System and Floor					
AeDES attribute	GEM attribute level					
Masonry building	<i>Level1: Mat_type</i>	<i>Level2: Mat_tech</i>	<i>Level3: Mat_prop</i>	<i>Level1: Floor_mat</i>	<i>Level2: Floor_type</i>	<i>Level3: Floor_conn</i>
A1	MAT99	MUN99	MO99	F99	FM99	FWC99
A2	MAT99	MUN99	MO99	FM	FM1	FWCN
A3	MAT99	MUN99	MO99	FM	FM1	FWCP
A4	MAT99	MUN99	MO99	FM	FM2	FWCN
A5	MAT99	MUN99	MO99	FW	FW1	FWCN
A6	MAT99	MUN99	MO99	FC	FC3	FWCN
B1	MUR	STRUB	MOL	F99	FM99	FWC99
B2	MUR	STRUB	MOL	FM	FM1	FWCN
B3	MUR	STRUB	MOL	FM	FM1	FWCP
B4	MUR	STRUB	MOL	FM	FM2	FWCN
B5	MUR	STRUB	MOL	FW	FW1	FWCN
B6	MUR	STRUB	MOL	FC	FC3	FWCN
C1	MUR	STRUB	MOL	F99	FM99	FWC99
C2	MUR	STRUB	MOL	FM	FM1	FWCP

C3	MUR	STRUB	MOL	FM	FM1	FWCP
C4	MUR	STRUB	MOL	FM	FM2	FWCP
C5	MUR	STRUB	MOL	FW	FW1	FWCP
C6	MUR	STRUB	MOL	FC	FC3	FWCP
D1	MUR	STDRE	MOC	F99	FM99	FWC99
D2	MUR	STDRE	MOC	FM	FM1	FWCN
D3	MUR	STDRE	MOC	FM	FM1	FWCP
D4	MUR	STDRE	MOC	FM	FM2	FWCN
D5	MUR	STDRE	MOC	FW	FW1	FWCN
D6	MUR	STDRE	MOC	FC	FC3	FWCN
E1	MUR	STDRE	MOC	F99	FM99	FWC99
E2	MUR	STDRE	MOC	FM	FM1	FWCP
E3	MUR	STDRE	MOC	FM	FM1	FWCP
E4	MUR	STDRE	MOC	FM	FM2	FWCP
E5	MUR	STDRE	MOC	FW	FW1	FWCP
E6	MUR	STDRE	MOC	FC	FC3	FWCP
Not surveyed	MAT99	L99	MO99	F99	FM99	FWC99

In Table 5C, the masonry building typologies according to AeDES form are identified by means of an alphanumeric code composed of a letter related to the vertical structural type and a number related to the horizontal structural type, as specified below. It is also worth noting that, in the case of multiple information (i.e., double answer) relating to the masonry typology, the most vulnerable one has been selected on the basis of the seismic behavior defined by the different shades of grey color (i.e., darker tones as the expected vulnerability increases).

### Legend

#### Vertical structures:

A, Unknown

B, Irregular layout or bad quality (rubble stones, pebbles) without tie rods or tie beams

C, Irregular layout or bad quality (rubble stones, pebbles) with tie rods or tie beams

D, Regular layout and good quality (blocks, bricks, squared stone) without tie rods or tie beams

E, Regular layout and good quality (blocks, bricks, squared stone) with tie rods or tie beams

#### Horizontal structures:

1, Not identified

2, Vaults without tie rods

3, Vaults with tie rods

4, Beams with flexible slab (wooden beams with a single layer of wooden planks, beams and shallow arch vaults)

5, Beams with semirigid slab (wooden beams with a double layer of wooden planks, beams and hollow flat blocks)

6, Beams with rigid slab (R.C. floors, beams well connected to R.C. slabs)

See Brzev et al. (2013) for a detailed description of the attribute values of GEM taxonomy.

**Table 5D** Attribute values in terms of AeDES form and GEM taxonomy related to other structures

AeDES form	GEM taxonomy	
AeDES section Building typology	GEM attribute Material of the Lateral Load Resisting System and Lateral Load-Resisting System	
AeDES attribute Other structures	GEM attribute level	
	<i>Level1: Mat_type</i>	<i>Level1: LLRS</i>
R.C. frames	CR	LFM
R.C. shear walls	CR	LWAL
Steel frames	S	L99

**Table 5E** Attribute values in terms of AeDES form and GEM taxonomy related to building regularity

AeDES form	GEM taxonomy
AeDES section Building typology	GEM attribute Structural Irregularity
AeDES attribute Regularity-Plan and elevation	GEM attribute level <i>Level1: STR_IRREG</i>
Irregular	IRIR
Regular	IRRE
Not surveyed	IR99

**Table 5F** Attribute values in terms of AeDES form and GEM taxonomy related to roof

AeDES form	GEM taxonomy	
AeDES section Building typology	GEM attribute Roof	
AeDES attribute Roof	GEM attribute level	
	<i>Level3: ROOFSYSMAT</i>	<i>Level5: ROOF_CONN</i>
Thrusting heavy	RC	RWCN
Not thrusting heavy	RC	RWCP
Thrusting light	RWO	RWCN
Not thrusting light	RWO	RWCP
Not surveyed	R99	RWC99

## CHAPTER VI

### Masonry building classes (Lagomarsino and Cattari, 2014)

In the following, the description of the ten classes of masonry buildings according to the SYNER-G taxonomy (Lagomasino and Cattari, 2014) has been reported. Each class is described by a string of codes, separated by slashes and hyphens. Slashes indicate the main categories of the taxonomy: Force Resisting Mechanism (FRM); Force Resisting Mechanism Material (FRMM); Plan (P); Elevation (E); Cladding & Openings (CO); Detailing & Maintenance (DM); Floor System (FS); Roof System (RS); Height Level (HL) and Code Level (CL). Within each category, the list of possible options is defined by proper acronyms and, for some category options, a more detailed classification is defined and indicated by separating the list of codes by hyphens.

1) **URM1-L:** BW-IP/URM-HS-RU-LM/R/R/x/LQD-WoT-WoRB/F-T/P-T/L/PC

Bearing Walls - In plane / Unreinforced Masonry - Hard Stone - Rubble - Lime mortar / Regular (plan) / Regular (elevation) / x / Low quality details - Without tie rods - Without ring beams / Flexible - Timber / Peaked - Timber / Low-rise / Pre-code

2) **URM2-L:** BW-IP/URM-HS-UC-LM/R/R/x/LQD-WT/F-T/P-T/L/PC

Bearing Walls - In plane / Unreinforced Masonry - Hard Stone - Uncut - Lime mortar / Regular (plan) / Regular (elevation) / x / Low quality details - With tie rods / Flexible - Timber / Peaked - Timber / Low-rise / Pre-code

3) **URM2-M:** BW-IP/URM-HS-UC-LM/R/R/x/LQD-WT/F-T/P-T/M/PC

Bearing Walls - In plane / Unreinforced Masonry - Hard Stone - Uncut - Lime mortar / Regular (plan) / Regular (elevation) / x / Low quality details - With tie rods / Flexible - Timber / Peaked - Timber / Mid-rise / Pre-code

4) **URM3-M:** BW-IP/URM-FB-LM/R/R/x/LQD-WT/R-S/P-RC/M/PC

Bearing Walls - In plane / Unreinforced Masonry - Fired brick - Lime mortar / Regular (plan) / Regular (elevation) / x / Low quality details - With tie rods / Rigid - Steel / Peaked - Reinforced Concrete / Mid-rise / Pre-code

5) **URM3-H:** BW-IP/URM-FB-LM/R/R/x/LQD-WT/R-S/P-RC/H/PC

Bearing Walls - In plane / Unreinforced Masonry - Fired brick - Lime mortar / Regular (plan) / Regular (elevation) / x / Low quality details - With tie rods / Rigid - Steel / Peaked - Reinforced Concrete / High-rise / Pre-code

6) **URM3-M-IR:** BW-IP/URM-FB-LM/IR/R/R/x/LQD-WT/R-S/P-RC/M/PC

Bearing Walls - In plane / Unreinforced Masonry - Fired brick - Lime mortar / Irregular (plan) / Regular (elevation) / x / Low quality details - With tie rods / Rigid - Steel / Peaked - Reinforced Concrete / Mid-rise / Pre-code

7) **URM3-H-IR:** BW-IP/URM-FB-LM/IR/R/x/LQD-WT/R-S/P-RC/H/PC

Bearing Walls - In plane / Unreinforced Masonry - Fired brick - Lime mortar / Irregular (plan) / Regular (elevation) / x / Low quality details - With tie rods / Rigid - Steel / Peaked - Reinforced Concrete / High-rise / Pre-code

8) **URM4-M:** BW-IP/URM-FB-LM/R/R/x/HQD-WRB/R-RC/P-RC/M/PC

Bearing Walls - In plane / Unreinforced Masonry - Fired brick - Lime mortar / Regular (plan) / Regular (elevation) / x / High quality details - With ring beams / Rigid - Reinforced Concrete / Peaked - Reinforced Concrete / Mid-rise / Pre-code

9) **URM4-H:** BW-IP/URM-FB-LM/R/R/x/HQD-WRB/R-RC/P-RC/H/PC

Bearing Walls - In plane / Unreinforced Masonry - Fired brick - Lime mortar / Regular (plan) / Regular (elevation) / x / High quality details - With ring beams / Rigid - Reinforced Concrete / Peaked - Reinforced Concrete / High-rise / Pre-code

10) **URM5-M:** BW-IP/URM-HC-CM/R/R/x/HQD-WRB/R-RC/P-RC/M/MC

Bearing Walls - In plane / Unreinforced Masonry - Hollow clay tile - Cement mortar / Regular (plan) / Regular (elevation) / x / High quality details - With ring beams / Rigid - Reinforced Concrete / Peaked - Reinforced Concrete / Mid-rise / Moderate (0.1-0.3g)

## References

- Arcoraci L, Berardi M, Castellano C, Leschiutta I, Maramai A, Rossi A, Tertulliani A, Vecchi M (2009) Rilievo macrosismico del terremoto del 15 dicembre 2009 nella Valle del Tevere e considerazioni sull'applicazione della scala EMS98. Available at website <http://quest.ingv.it>
- Arcoraci L, Berardi M, Brizuela B, Castellano C, Del Mese S, Graziani L, Maramai A, Rossi A, Sbarra M, Tertulliani A, Vecchi M, Vecchi S, Bernardini F, Ercolani E (2012a) Rilievo macrosismico degli effetti del terremoto del 25 gennaio 2012 (Pianura Padana). Available at website <http://quest.ingv.it>
- Arcoraci L, Berardi M, Bernardini F, Brizuela B, Caracciolo CH, Castellano C, Castelli V, Cavaliere A, Del Mese S, Ercolani E, Graziani L, Maramai A, Massucci A, Rossi A, Sbarra M, Tertulliani A, Vecchi M, Vecchi S (2012b) Rapporto macrosismico sui terremoti del 20 (MI 5.9) e del 29 maggio 2012 (MI 5.8 E 5.3) nella Pianura Padana-Emiliana. Available at website <http://quest.ingv.it>
- Arcoraci L, Bernardini F, Brizuela B, Ercolani E, Graziani L, Leschiutta I, Maramai A, Tertulliani A, Vecchi M (2013) Rapporto macrosismico sul terremoto del 21 giugno 2013 (ML 5.2) in Lunigiana e Garfagnana (province di Massa-Carrara e di Lucca). Available at website <http://quest.ingv.it>
- Azzaro R, Barbano MS, Camassi R, D'Amico S, Mostaccio A, Piangiamore G, Scarfi L (2004) The earthquake of 6 September 2002 and the seismic history of Palermo (Northern Sicily, Italy): Implications for the seismic hazard assessment of the city. *Journal of Seismology* 8, 525–543.
- Azzaro R, Mostaccio A, Scarfi L, Tuvè T (2011) Rapporto macrosismico sul terremoto dei Nebrodi del 24/06/2011. Available at website <http://quest.ingv.it>
- Azzaro R, D'Amico S, Scarfi L, Tuvè T (2012) Aggiornamento al rilievo macrosismico degli effetti prodotti dal terremoto del Pollino del 26 ottobre 2012. Available at website <http://quest.ingv.it>
- Azzaro R, D'Amico S, Mostaccio A, Scarfi L, Tuvè T (2016) Rilievo macrosismico del terremoto Ibleo dell'8 febbraio 2016. Available at website <http://quest.ingv.it>
- Bernardini F, Ercolani E (2011a) Rilievo macrosismico degli effetti prodotti dal terremoto del 17 luglio 2011 nella Pianura Padana lombardo-veneta (province di Rovigo, Mantova, Modena e Ferrara). Available at website <http://quest.ingv.it>
- Bernardini F, Ercolani E, Del Mese S (2011b) Rapporto macrosismico sul terremoto torinese del 25 luglio 2011. Available at website <http://quest.ingv.it>
- Brzev S., Scawthorn C., Charleson A.W., Allen L., Greene M., Jaiswal K.S., et al. (2013) GEM Building Taxonomy Version 2.0. GEM Technical Report 2013-02 v1.0.0, GEM.
- Camassi R, Ercolani E (2003a) Rilievo macrosismico del terremoto del 26/01/2003 (Forlivese). Available at website <http://quest.ingv.it>
- Camassi R, Bernardini F, Ercolani E (2003b) Rilievo macrosismico degli effetti prodotti dalla sequenza sismica iniziata il 14 settembre 2003 (Appennino Bolognese). Available at website <http://quest.ingv.it>
- Camassi R, Bernardini F, Del Mese S (2008) Rilievo macrosismico degli effetti prodotti dalla sequenza sismica del 1 marzo 2008 (Appennino Bolognese, Mugello). Available at website <http://quest.ingv.it>
- Camassi R, Ercolani E, Bernardini F, Pondrelli S, Tertulliani A, Rossi A, Del Mese S, Vecchi M (2009) Rapporto sugli effetti del terremoto emiliano del 23 dicembre 2008. Available at website <http://quest.ingv.it>.
- Galli P, Molin D, Camassi R, Castelli V (2001). Il terremoto del 9 settembre 1998 nel quadro della sismicità storica del confine calabro-lucano. Possibili implicazioni sismotettoniche. *Il Quaternario - Italian Journal of Quaternary Sciences*, 14, 31-40.
- Galli P, Camassi R (2009) Rapporto sugli effetti del terremoto aquilano del 6 aprile 2009. Available at website <http://quest.ingv.it>
- Galli P, Peronace E, Tertulliani A (2016) Rapporto sugli effetti macrosismici del terremoto del 24 agosto 2016 di Amatrice in scala MCS. Available at website <http://quest.ingv.it>

## Appendix

Gruppo di Lavoro INGV (2004) Rapporto preliminare sugli effetti del terremoto bresciano del 24 novembre 2004. Available at website <http://quest.ingv.it>

Lagomarsino S. and Cattari S., (2014) Fragility functions of masonry buildings. In: Ptilakis K., Crowley H., Kaynia A. (editors). SYNER-G: Typology definition and fragility functions for physical elements at seismic risk. Springer Science+Business Media Dordrecht, 2014.

Margottini C, Molin D, Serva L (1992) Intensity versus ground motion: a new approach using Italian data. *Engineering Geology* 33:45–58

Stucchi M, Galadini F, Monachesi G (1998) The earthquakes of September/October 1997 in the frame of tectonics and long-term seismicity of the Umbria-Marche (Central Italy) Apennines. Available at website [http://emidius.mi.ingv.it/GNDT/T19970926\\_eng/](http://emidius.mi.ingv.it/GNDT/T19970926_eng/)

Tertulliani A, Arcoraci L, Berardi M, Bernardini F, Camassi R, Castellano C, Del Mese S, Ercolani M, Graziani L, Leschiutta I, Rossi A, Vecchi M (2010) An application of EMS 98 in a medium size city: the case of L'Aquila (Italy) after the April 6, 2009 Mw 6.3 earthquake. *Bulletin of Earthquake Engineering*. DOI: 10.1007/s10518-010-9188-4.

Tertulliani A, Azzaro R (2016a) Sequenza della provincia di Rieti. QUEST – Rilievo macrosismico in EMS98 per il terremoto di Amatrice del 24 agosto 2016. Available at website <http://quest.ingv.it>

Tertulliani A, Azzaro R (2016b) QUEST - Rilievo macrosismico per i terremoti nell'Italia centrale. Aggiornamento dopo le scosse del 26 e 30 ottobre 2016. Available at website <http://quest.ingv.it>

Tertulliani A, Azzaro R (2017) QUEST -Rilievo macrosismico in EMS98 per la sequenza sismica in Italia Centrale: aggiornamento dopo il 18 gennaio 2017. Available at website <http://quest.ingv.it>